

Material/energy conversion processes and methodology for their optimal integration in a territory

Gisèle Abi Chahla

▶ **To cite this version:**

Gisèle Abi Chahla. Material/energy conversion processes and methodology for their optimal integration in a territory. Chemical and Process Engineering. Université Paris sciences et lettres, 2017. English. NNT : 2017PSLEM082 . tel-02476577

HAL Id: tel-02476577
https://pastel.hal.science/tel-02476577

Submitted on 12 Feb 2020

HAL is a multi-disciplinary open access archive for the deposit and dissemination of scientific research documents, whether they are published or not. The documents may come from teaching and research institutions in France or abroad, or from public or private research centers.

L'archive ouverte pluridisciplinaire **HAL**, est destinée au dépôt et à la diffusion de documents scientifiques de niveau recherche, publiés ou non, émanant des établissements d'enseignement et de recherche français ou étrangers, des laboratoires publics ou privés.

THÈSE DE DOCTORAT

de l'Université de recherche Paris Sciences et Lettres
PSL Research University

Préparée à Mines ParisTech

Procédés de conversion matière/ énergie et méthodologie de leur intégration optimale dans un territoire

Material /energy conversion processes and methodology for their optimal integration in a territory

Ecole doctorale n°432

SCIENCES ET METIERS DE L'INGENIEUR

Spécialité ÉNERGÉTIQUE ET PROCÉDÉS

COMPOSITION DU JURY :

Mme. AZZARO-PANTEL Catherine
INP-ENSIACET, Présidente du jury

M. EL HALWAGI Mahmoud
Texas A&M, Rapporteur

Mme. ARLABOSSE Patricia
Mines d'Albi-Carmaux, Rapporteur

M. FAREL Romain
CEA, Membre du jury

M. TRAN Cong-Toan
Mines ParisTech, Membre du jury

M. ZOUGHAIB Assaad
Mines ParisTech, Membre du jury

Soutenue par Gisèle ABI CHAHLA
le 27 Octobre 2017

Dirigée par **Assaad ZOUGHAIB**

MINES ParisTech

PSL RESEARCH UNIVERSITY PARIS

"The world we have created today as a result of our thinking thus far has problems which cannot be solved by thinking the way we thought when we created them."

Albert Einstein

Table of Contents

List of Figures vii
List of Tables xi
Nomenclature xiii

General Introduction 1

Chapitre 1. Contexte et défis (résumé) 5

Chapter 1. Background and Challenges 9
1.1. Unsustainable anthropogenic pressure 10
1.2. The challenge of the Energy Sector 12
1.3. Imperative Precedence for Action 14
1.4. Industrial Ecology towards Sustainable development 15
1.5. Eco-Industrial Park 16
1.6. Process Integration techniques 18

1.6.1. Energy Integration 19
1.6.2. Material Integration 21

1.7. Motivation for this scientific research 22
1.8. State of the art of Process Design methodologies 23
1.9. Scientific ambitions and methodology presentation 29

Chapitre 2. Cadres méthodologiques pour l'intégration des procédés de conversion dans un territoire (résumé) 31

Chapter 2. Methodological Frameworks for Conversion Systems Integration in a Territory 37
2.1. Problem Statement 38
2.2. The Energy and Mass Integration Methodological Bricks 39

2.2.1. Process Heat Integration 39
2.2.2. Process Material Integration 42
2.2.3. Coupled Material and Heat Integration at the process scale 44
2.2.4. Territorial Heat Integration and Material Integration 46

2.3. Integration of Conversion Systems in a Territory with Cooperative Scheme Governance 52
2.4. Integration of Conversion Systems in a Territory with Non-Cooperative Scheme 57

2.4.1. Game Theory − exchanging preferences 60
2.4.2. Coordination techniques 61
2.4.3. Proposed interaction for the non-cooperative scheme 65

2.5. Conclusions 71

Chapitre 3. Étude de cas: Modélisation des systèmes de conversion du bois pour leur intégration dans le parc industriel étudié (résumé) 73

Chapter 3. Case Study: Wood Conversion Systems Modeling for their Integration in the studied Industrial Park 79
3.1. Studied industrial park 80
3.2. Wood Conversion systems overview 82
3.3. Wood to hydrogen conversion system 83

3.3.1. Steam Gasifier 84
3.3.2. Steam reformer 89
3.3.3. Water Gas-Shift reactor 92
3.3.4. Combustion chamber model 95
3.3.5. Water separation model 96

3.4. Wood to methane conversion system 98

3.4.1. Methanation unit 98
3.4.2. Compressor model 100
3.4.3. Carbon dioxide separation model 101

3.5. Wood to electricity and heat conversion system 102

3.5.1. Furnace model 102
3.5.2. Steam turbine model 103
3.5.3. Splitter and mixer models 104

3.6. Process scale up 104
3.7. Conversion System Economic model 105

3.7.1. Conversion System Fixed Cost 105
3.7.2. Conversion System Variable Cost 107

3.8. Conclusions 108

Chapitre 4. Application des cadres méthodologiques pour l'intégration des procédés de conversion dans un territoire (résumé) 109

Chapter 4. Application of the methodological frameworks for Conversion System integration in a territory....119
4.1. Economic data Hypotheses....120
4.2. Reference Scenario Establishment....120
4.3. Conversion routes design and process degree of freedom....123

4.3.1. Wood to hydrogen conversion route....124
4.3.2. Wood to methane conversion route....126
4.3.3. Wood to energy conversion route....129

4.4. CS integration in a territory with cooperative scheme....131

4.4.1. Problem Statement....131
4.4.2. Results of CS1wood implementation in the territory....132
4.4.3. Results of CS2wood implementation in the territory....135
4.4.4. Results of CS3wood implementation in the territory....139
4.4.5. Comparison of the three wood conversion pathways....141
4.4.6. Further assessment of the best Scenarios....142
4.4.7. EIP configuration of the best adjudicated Scenario....149

4.5. CS integration in a territory with non-cooperative Scheme....150

4.5.1. Problem Statement....150
4.5.2. Results for long term investment strategies....151
4.5.3. Sensitivity Analysis....156

4.6. Conclusions....162

Conclusions and Perspectives....165

References....169

List of Figures

Figure 1: The evolution of the term "process integration" as a term (Gundersen, 2013) 2
Figure 2. Conversion Process relationship with process integration techniques 2

Figure 1.1. World population since the industrial revolution including the projections till 2100 10
Figure 1.2. Annual carbon dioxide emissions by world region from 1751 to 2015 11
Figure 1.3. World total primary energy supply from 1971 to 2014 by fuel (Mtoe) (IEA, 2016) 12
Figure 1.4. World final energy consumption projections by fuel 13
Figure 1.5. Avoided emissions from energy efficiency improvements in IEA countries (IEA, 2016) 13
Figure 1.6. Total avoided fossil fuel import costs with share of savings by country/region (IEA, 2016) 14
Figure 1.7. Kalundborg Eco-Industrial park, Denmark 16
Figure 1.8. Eco-industrial network in the Tianjin TEDA (Shi, et al., 2009) 17
Figure 1.9. Hot and cold composite curves representation 19
Figure 1.10. Grande composite curve 19
Figure 1.11. Tertiary heat network between three sites (Farhat, et al., 2015) 20
Figure 1.12. Limiting composite curves- water pinch 21
Figure 1.13. Source/sink composite curves 21
Figure 1.14. The model superstructure of Hugo & Pistikopoulos, 2005 23
Figure 1.15. Optimization procedure scheme of Palazzi, et al., 2007 24
Figure 1.16. Superstructure model of the developed methodology by Palazzi, et al., 2007 24
Figure 1.17. Overview of the developed methodology by Gassner & Maréchal, 2009 25
Figure 1.18. Overview of the developed methodology by Gerber, et al., 2011 26
Figure 1.19. Overview of the developed methodology by Gerber, et al., 2013 27
Figure 1.20. Industrial actors exchange in cooperative and non-cooperative schemes 29

Figure 2.1. Basic scheme of the transshipment model (Barbaro & Bagajewicz, 2005) 40
Figure 2.2. Schematic representation of interactions between the MAN and HEN 44
Figure 2.3. Superstructure of the heat integration through non-isothermal mixing 46
Figure 2.4. The building blocks of the problem required for the waste streams definition and their conversion processes identification 53
Figure 2.5. Master Problem superstructure of the conversion pathways 54
Figure 2.6. Potential generated scenarios of Territory presenting two waste streams 55

Figure 2.7. Computational framework of the Master-slave problem for integrating conversion systems in a territory with cooperative scheme governance 55
Figure 2.8. Agents act and react with their environments 57
Figure 2.9. Agent principled negotiation (Wangermann & Stengel, 1999) 58
Figure 2.10. Agent structure (Romero & Ruiz, 2014) 59
Figure 2.11. The prisoner's dilemma: a) normal form, b) extensive form 61
Figure 2.12. Agent interactions work flow framework for the territorial integration of conversion systems in a non-cooperative scheme 66
Figure 2.13. The potential agents' population 68

Figure 3.1. Geographical distance between the industrial actors of the virtual park 80
Figure 3.2. Grand Composite Curves of each actor of the territory (a) Site 1, (b) Site 2, (c) Site 3 81
Figure 3.3. Overview of the main conversion pathways of woody biomass 82
Figure 3.4. Block flow diagram of wood waste conversion to hydrogen 83
Figure 3.5. Fixed bed gasifier: 84
Figure 3.6. Fluidized bed gasifier: 84
Figure 3.7. Entrained flow gasifier 84
Figure 3.8: The chemical reactions taking place in the gasifier 86
Figure 3.9: Dynamic variation of the primary pyrolysis product composition 86
Figure 3.10. Gas composition profile along the gasifier length 88
Figure 3.11. Steam to biomass effect on gas composition 88
Figure 3.12. Steam to biomass effect on the tar content of the gasifier's output 88
Figure 3.13. Stream reformer geometric form 90
Figure 3.14. Gas composition profile along the steam reformer 91
Figure 3.15. Water Gas-Shift membrane reactor 93
Figure 3.16. Combustion chamber on Aspen Plus® 96
Figure 3.17. Water separation unit 97
Figure 3.18. Separation unit on Aspen plus® 97
Figure 3.19. Block flow diagram of wood waste conversion to methane 98
Figure 3.20. Methanation unit 99
Figure 3.21. Gas composition profile in the methanation unit 100
Figure 3.22. Block flow diagram of wood waste conversion to electricity and heat 102
Figure 3.23. Adiabatic furnace block diagram 102
Figure 3.24. Furnace assembly on Aspen plus® 103
Figure 3.25. (a) Splitter unit, (b) mixer unit 104

Figure 4.1. HEN of Site 1 as an isolated industrial actor 121
Figure 4.2. HEN of Site 2 as an isolated industrial actor 122
Figure 4.3. HEN of Site 3 as an isolated industrial actor 122
Figure 4.4. Bio-refinery placement relative to the existing industrial actors 123
Figure 4.5. Wood to hydrogen conversion process flow sheet 124
Figure 4.6. Wood to methane conversion process flow sheet 126
Figure 4.7. Wood cogeneration process flow sheet 129
Figure 4.8. Superstructure of W_1^{wood} conversion pathways 131
Figure 4.9. Sample of the territory's prospective generated scenarios 132
Figure 4.10. Economic statuses of EIP configurations induced from integrating CS_1^{wood} in the park. 133
Figure 4.11. Net present values over ten years of selected scenarios integrating CS_1^{wood} in the park. 134

Figure 4.12. Hydrogen yield from $CS_{1,\,set\,q}^{wood}$ 135
Figure 4.13. MER_{hot} and MER_{cold} of $CS_{1,\,set\,q}^{wood}$ 135
Figure 4.14. Economic statuses of EIP configurations induced from integrating CS_2^{wood} in the park .136
Figure 4.15. Net present values over ten years of selected scenarios integrating CS_2^{wood} in the park..137
Figure 4.16. Methane yield from $CS_{2,\,set\,q}^{wood}$ 138
Figure 4.17. MER_{hot} and MER_{cold} of $CS_{2,\,set\,q}^{wood}$ 138
Figure 4.18. Economic statuses of EIP configurations induced from integrating CS_3^{wood} in the park..139
Figure 4.19. Net present values over ten years of selected scenarios integrating CS_3^{wood} in the park..140
Figure 4.20. Electric power generation from $CS_{3,\,set\,q}^{wood}$ 140
Figure 4.21. Heat generation of $CS_{3,\,set\,q}^{wood}$ 140
Figure 4.22. Economic status for the three investigated wood conversion routes combined..... 141
Figure 4.23. Comparison of the NPV over ten year period for the best scenario of each pathway..... 143
Figure 4.24. Economic statuses of the best scenarios for each pathway with a varying reference 144
Figure 4.25. NPV over ten years for the best scenario of each pathway with 20€ the ton of wood..... 144
Figure 4.26. NPV over ten years for the best scenario of each pathway with 40€ the ton of wood..... 145
Figure 4.27. NPV over ten years for the best scenario of each pathway with 41€ the ton of wood..... 145
Figure 4.28. NPV over ten years for the best scenario of each pathway with 80€ the ton of wood..... 146
Figure 4.29. NPV over ten years for the best scenario of each pathway with 100€ the ton of wood... 146
Figure 4.30. NPV over ten years for the best scenario of each pathway with 154€ the ton of wood... 147
Figure 4.31. NPV over ten years for the best scenario of each pathway with a low gas market price. 148
Figure 4.32. NPV over ten years for the best scenario of each pathway with a high gas market price 148
Figure 4.33. EIP configuration of the best adjudicated scenario in cooperative scheme 149
Figure 4.34. NPV at 100 months of operation of IA_1 152
Figure 4.35. NPV at 100 months of IA_2 152
Figure 4.36. NPV at 100 months of operation of IA_3 153
Figure 4.37. NPV at 100 months of IA_4 153
Figure 4.38. NPV at 100 months of the NI..... 153
Figure 4.39.The equilibrium states social welfare..... 153
Figure 4.40. EIP configuration of the most adequate equilibrium state in non-cooperative scheme ... 154
Figure 4.41. Bidding potentials of $PA_{1,1}$ population 155
Figure 4.42. $PA_{1,3}$ population bidding potentials 155
Figure 4.43. $PA_{1,2}$ population's bidding potentials 156
Figure 4.44. Bidding potential and final bid variation with the investment strategy 157
Figure 4.45. NPV at 100 months of IA_1 158
Figure 4.46. NPV at 100 months of IA_2 158
Figure 4.47. NPV at 100 months of IA_3 159
Figure 4.48. NPV at 100 months of IA_4 159
Figure 4.49. NPV at 100 months of the NI..... 160
Figure 4.50.The equilibrium states social welfare..... 160
Figure 4.51. EIP configuration of the upmost welfare equilibrium state for the high gas market price 160
Figure 4.52. Overall heat synergies for the studied gas market prices:(a) low, (b) medium, (c) high .161

Fig. 1. Cadre de calcul du problème Maître-Esclave pour l'intégration des systèmes de conversion dans un territoire régi d'une gouvernance coopérative.....XXXIII
Fig. 2. Le workflow d'interaction des agents pour l'intégration des systèmes de conversion dans un schéma non-coopératif..... 35
Fig. 3. Diagramme fonctionnel de la conversion du bois en hydrogène 75
Fig. 4. Diagramme fonctionnel de la conversion du bois en méthane..... 76
Fig. 5. Diagramme fonctionnel de la conversion du bois en énergie..... 77
Fig. 6. Statuts économiques des trois voies étudiées de conversion du bois 111
Fig. 7. Comparaison des VAN sur dix ans pour le meilleur scénario de chaque voie..... 112
Fig. 8. Configuration de l'éco-parc pour le meilleur scénario du territoire en gouvernance coopérative 113
Fig. 9. VAN à 100 mois d'opération de IA_1..... 115
Fig. 10. VAN à 100 mois d'opération de IA_2..... 115
Fig. 11. VAN à 100 mois d'opération de IA_3..... 116
Fig. 12. VAN à 100 mois d'opération de IA_4..... 116
Fig. 13. VAN à 100 mois d'opération du NI..... 116
Fig. 14. Le *social welfare* des états d'équilibres..... 116
Fig. 15. Configuration de l'éco-parc pour l'état d'équilibre le plus adéquat du schéma non-coopératif 117

List of Tables

Table 1.1. State of the art summary table of the conversion system integration in a territory 28

Table 3.1. Data of the energy streams for the three sites of the park 80
Table 3.2. Recovery and utility demand found by the territorial Energy integration.....81
Table 3.3. Kinetic parameters.....86
Table 3.4. Kinetic model of the heterogeneous zone 87
Table 3.5. Kinetic model of the homogenous zone 87
Table 3.6. Gasifier operating and design parameters 88
Table 3.7. Steam reformer kinetic model 91
Table 3.8. Steam reformer operating and design parameters 91
Table 3.9. Kinetic models of both high and low temperature water gas-shift reactions 93
Table 3.10. Molar and Energy balance of the WGS membrane reactor.....94
Table 3.11. HWGS and LWGS developed models validation 94
Table 3.12. Operating and design parameters 95
Table 3.13. WGS membrane reactor validation 95
Table 3.14. The gas mixture combustion reactions.....95
Table 3.15. Dymola® model results comparison with Aspen's.....96
Table 3.16. Dymola® model results comparison with Aspen Plus® results.....97
Table 3.17. Methanation unit kinetic model.....99
Table 3.18. Coefficients of the methanation kinetic model.....100
Table 3.19. Operating and design parameters 100
Table 3.20. Operating parameters 101
Table 3.21. Dymola® model results comparison with Aspen Plus® results for the compressor.....101
Table 3.22. Biomass secondary pyrolysis reactions.....102
Table 3.23. Comparison of Dymola® model results with those of Aspen Plus® 103
Table 3.24. Operating parameters 104
Table 3.25. Dymola® model results comparison with Aspen Plus® results for the steam turbine.....104
Table 3.26. Reference investment cost of the conversion system units 106
Table 3.27. Correlation coefficients for the investment of the cogeneration units.....106
Table 3.28. Price of the conversion systems resources and products.....107

Table 4.1. Economic status of the territory's sites as isolated actors 123
Table 4.2. Heat streams data of the wood to hydrogen conversion system.....125
Table 4.3. The generated sets of parameters for the hydrogen route.....126

Table 4.4. Heat streams data of the wood to methane conversion system 127
Table 4.5. The generated sets of parameters for the methane route 128
Table 4.6. Heat streams data of the wood to electricity and heat conversion system..... 129
Table 4.7. The generated sets of parameters for the cogeneration route 130
Table 4.8. Economic status of the territory for best judged prospect scenarios 142
Table 4.9. Economic status of the reference scenario for each gas market price 147
Table 4.10. Bidding potential of the three PA for the investigated gas market prices 158

Tableau 1. Statuts économiques du territoire pour les meilleurs scénarios 111

Nomenclature

Latin letters

A	cross section area of the gasifier	m^2
a_r	Steam reformer cross sectional area	m^2
a_{H2}	H_2 membrane area per unit length of the reactor	$m^2.m^{-1}$
Capex	Capital cost	€
C_{he}	Fixed cost for a utility heat exchanger	€
C_{hu}	Fixed cost for a utility heat stream hu	€
C_i	Molar concentration of component i	$mol.m^{-3}$
C_i^w	Nominal cost for mass flow rate sent to waste sink i	€
C_j^f	Nominal cost for mass flow rate provided by fresh source j	€
C_{pi}	heat capacity of component i	$J.mol^{-1}.K^{-1}$
C_S	Nominal cost for heat exchanger area	$€.m^{-2}$
CS^z_k	The k^{th} conversion system of material z	-
C_t	Annual net inflow	€
Cu_p	Default cold utility load at plant p	kW
C_0	Total initial investment	€
d	Gasifier diameter	m
D	Reactor's diameter	m
DRate	Discount rate	-
E_i	apparent activation energy for component i	$kJ.mol^{-1}$
Ex	Exergy consumption	kW
F_i	Molar flow rate of component i	$mol.s^{-1}$
F_{i0}	Initial molar flow rate of component i	$mol.s^{-1}$
$Gain_{syn}$	Generated gain from the established synergies	€
G_i	Mass flow rate required by sink i	$kg.s^{-1}$
G_i^w	Total mass flow rate sent to sink i	$kg.s^{-1}$
ΔG	Gibbs free energy	$J.mol^{-1}$
h	Enthalpy	$J.mol^{-1}$
H	Head loss	M
Hu_p	Default hot utility load at plant p	kW
HXA	Heat exchanger surface are	m^2
HXCost	Heat exchanger cost	$€.m^{-2}$

ΔH_R	heat of reaction	$J.mol^{-1}$
I	Investment cost	€
I_p	Process Sinks	-
I_w	Waste sinks	-
J_f	Fresh sources	-
k_0	Pre-exponential factor	s^{-1}
K	Contaminants	-
K_{eq}	Equilibrium constant	-
k_w	Thermal conductivity of the steam reformer wall	$J.m^{-1}.s^{-1}.K^{-1}$
L	Reactor axial length	M
L_{fresh}	Total mass flow rate provided by the entire fresh sources	$kg.s^{-1}$
L_{ij}	Mass flow rate from source j allocated to sink i	$kg.s^{-1}$
$L_{ij}^{mu/su}$	Mass flow rate from splitter unit su associated to source j allocated to mixer unit mu associated to sink i	$kg.s^{-1}$
L_j	Total mass flow rate of source j	$kg.s^{-1}$
L_j^f	Total mass flow rate provided by fresh source j	$kg.s^{-1}$
L_j^{su}	Mass flow rate from source j allocated to splitter unit su	$kg.s^{-1}$
$\dot{m}$	Mass flow rate	$kg.s^{-1}$
$\dot{m}_{p,net}$	Mass flow rate transferred from plant p to network net	$kg.s^{-1}$
$\dot{m}_{net,p}$	Mass flow rate transferred from network net to plant p	$kg.s^{-1}$
M_m	Molar mass	$kg.mol^{-1}$
m_z	Number of potential conversion systems of material z	-
n_{h_1,h_2}	Number of heat exchanger between h_1 and h_2 which is either 1 or 0	-
N	Number of components in the reactor	-
N_R	number of reactions	-
N_{H2}	hydrogen permeation rate through the membrane	$mol.m^{-2}.s^{-1}$
Opex	Operating cost	€
P	Operating pressure of the reactor	bar
P_i	Partial pressure of component i	bar
$P_{H_2}^{high}$	partial pressure of hydrogen in the catalytic bed channel	bar
$P_{H_2}^{low}$	partial pressure of hydrogen in the non reaction channel	bar
P_j^b	Buying price of heat at the network temperature j	€/kW
P_j^s	Selling price of heat at the network temperature j	€/kW
PO	Pumping power	kW
q	Heat transferred to the steam reformer per reactor length	$J.m^{-1}.s^{-1}$
$q_{gazeifieur}$	heat flux transferred to the gasifier per unit length of the reactor	$J.m^{-1}.s^{-1}$
q_{hu}	Heat required or provided by utility heat stream hu	kW
Q	Heat load	kW
$Qc_{net\ i,\ p}$	Heat transferred from plant p to network net at interval i	kW
Q_{ij}	Heat transferred from industrial agent i to the network temperature j	kW
Q_{ji}	Heat transferred from the network temperature j to the industrial agent i	kW
$Qh_{net\ i,\ p}$	Heat transferred from network net to plant p at interval i	kW
$Q_{p,i}$	Sum of streams enthalpies in plant p at interval i	kW
r	Discount rate	

r_k	reaction rate of k reaction	$mol.m^{-3}.s^{-1}$
R	gas constant	$J.mol^{-1}.K^{-1}$
$R_{p,i}$	Cascaded energy in plant p at interval i	kW
S	Surface longitudinale par longueur du vapo-reformeur	$m^2.m^{-1}$
S_{h_1,h_2}	Heat exchanger area between heat stream h_1 and cold stream h_2	m^2
SV^z_k	Sovereign variable of the k^{th} conversion system of material z	-
ΔS	Entropy variation	$J.mol^{-1}.K^{-1}$
T	Temperature	K
T_a	Ambient temperature	K
T_b	biomass temperature	K
$T_{Cu,\ p}$	Temperature at the sink of plant p	K
$T_{Hu,\ p}$	Temperature at the source of plant p	K
T_m	membrane operating temperature	K
ΔT	Minimum temperature difference in the heat exchangers	K
V	Velocity	$m.s^{-1}$
V_i	Instantaneous yield of component i	$kg.\,kg^{-1}_{biomass}$
V_i^*	Ultimately attainable yield of component i	$kg.\,kg^{-1}_{biomass}$
V_{new}	The scaled-up reactor volume	m^3
V_{old}	The reference reactor volume	m^3
w	Catalyst mass	kg
W	Power	kW
X	Scale-up factor	-
x_i	Molar fraction of component i	-
$y_{j,k}$	Composition of source j for contaminant k	ppm
z	axial reactor coordinate	m
$z_{i,k}^{max}$	Maximum allowable composition of sink i for contaminant k	ppm
$z_{i,k}^{min}$	Minimum allowable composition of sink i for contaminant k	ppm

Greek letters

β_k	Maximum bidding potential	€/unit
υ_{ik}	Stoichiometric coefficient of component i of reaction k	-
δ_w	Steam methane reformer wall thickness	m
δ_{H_2}	hydrogen membrane thickness	m
ρ	Density	$kg.m^{-3}$
η	Efficiency	-
ξ_k	Extent of reaction	$mol.s^{-1}$

Subscripts and superscripts

0	Reference value
in	Inlet
is	Isentropic
mu	Mixer unit

net	Network
nr	Non-reaction channel of the membrane reactor
out	Outlet
Pa	palladium
r	Catalytic bed channel of the membrane reactor
su	Splitter unit

Acronyms

Bin	Defines a binary variable associated to a continuous variable
EIP	Eco-industrial park
GHG	Greenhouse gases
HEN	Heat exchanger network
HENS	Heat exchanger network synthesis
HWGS	High temperature water gas shift
LWGS	Low temperature water gas shift
MAN	Mass allocation network
MAHEN	Mass allocation and heat exchanger network
NOH	Number of operating hours
NPV	Net present value
SMR	Steam methane reformer
WGS	Water gas shift

General Introduction

With the unsustainable anthropogenic greenhouse gases (GHG) emissions pressure, stemming from the intense demographic and economic growth since the industrial revolution, intertwining with the prevailing linear production and consumption model, the planet is attaining its limit of natural resources and its capacity to intake waste and pollution. Corollary to being consumed faster than they can be replenished at the current demand, resources are becoming scarcer and thus more expensive. The challenges the world is facing today enjoin an imperative for alteration from the linear economic model towards a sustainable paradigm that ensures meeting the present energy and material demands without jeopardizing the ability of future generations to meet their proper needs.

A global response on global warming was translated in restrictive political regulations on anthropogenic GHG emissions to contend climate change and halt temperature rise through better energy and resource management. The daunting challenge of industries being to cope and comply with the current and upcoming ecological regulations inevitably impacts their economic performances. Nonetheless, by migrating towards circular economy, which is regenerative by design as opposed to the extractive linear model, an industrial entity can meet modern ecological standards while jointly cutting down its operating costs as well as its dependency on the fluctuating resources markets. This is achieved through the reuse and recycling of its useless rendered products for them to be reintroduced back into the production cycle and thus majorly curb both its primary resource demand and waste emissions. On greater scope, partnerships can be made between neighboring industries through resource and waste exchange; one's waste thus becomes another's raw material and thereby evolving towards becoming an eco-industrial park (EIP) that drives economic development for its participating parties while minifying their environmental footprint. Therefore the prime purpose of this doctoral work is to assist geographically neighboring industries to migrate towards becoming an EIP in the aim of shifting to a sustainable production and consumption model more adaptable to modern ecological standards.

To achieve strongly viable EIP structures, potential synergies that decrease resource usage or waste emission should be assessed to ensure their veritable physical feasibility. However, a company is improbably to adopt an identified synergy incurring additional investment costs unless it proves major cut down in operating expenses. Therefore modeling and optimizing industrial park networks in which energy and material flows circulates entail systematic integrated process design techniques which aggregate the sub-systems components for an overarching functionality. With their emphasis on the efficient use of resources, process integration techniques have resulted in significant benefits to the industrial sector in terms of process improvements, increased productivity, resource management, pollution prevention, and operating cost reductions (Morar & Agachi, 2010).

The tangible economic and environmental performances ensuing from this technique, led process integration to becoming a scientific research field very tackled in recent years as illustrated in Figure 1. Indeed, process integration, which was initiated in the late 1970s, has two main objectives; the first of which is to integrate the use of material (e.g., hydrogen and water) and energy to reduce their consumption, and the second corollary to the first, is to minimize the production of waste and harmful emissions to the environment.

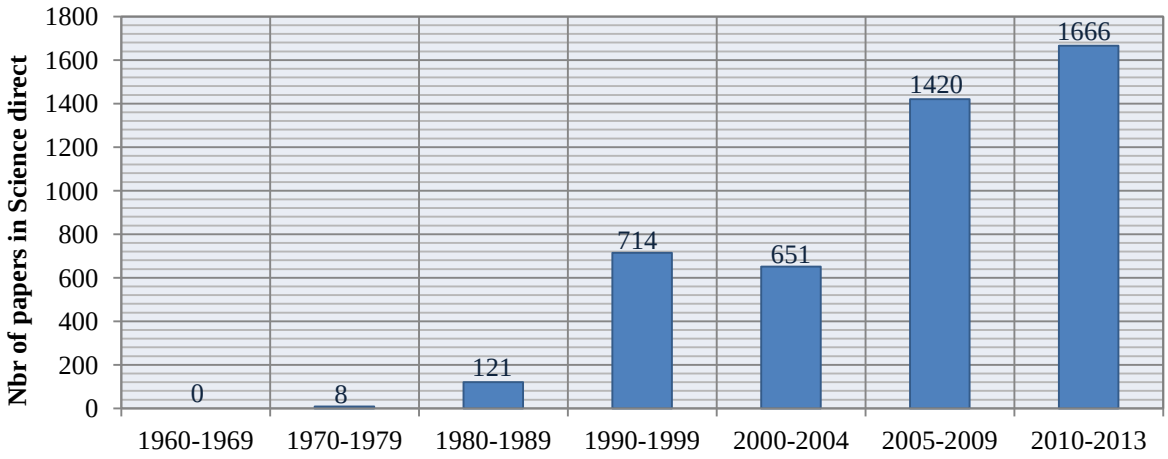


Figure 1: The evolution of the term "process integration" as a term (Gundersen, 2013)

The energy integration and the material integration methodologies, investigate using a holistic approach the potential synergies between the resources demand and waste discharge of different process units. The untapped opportunities of the remainders from the local integration to be recovered by geographically proximate industrial sites could be assessed through the territorial energy and material integration. However, maximizing on-site and inter-sites synergies using exclusively process integration methods implies considering the component valorization in its original form and corollary missing the reuse opportunities of useless rendered components in another form. The conversion brings the possibility of turning the non-recoverable streams from their initial form into another usable energy or material product through chemical processes reintroducing it back into the cycle and thus inducing substantial economic revenues. Consequently, bridging the gap between the mass and heat integration methods by incorporating conversion systems for the non-recoverable streams in their initial form ensues a giant step towards closing the energy and material loops, Figure 2.

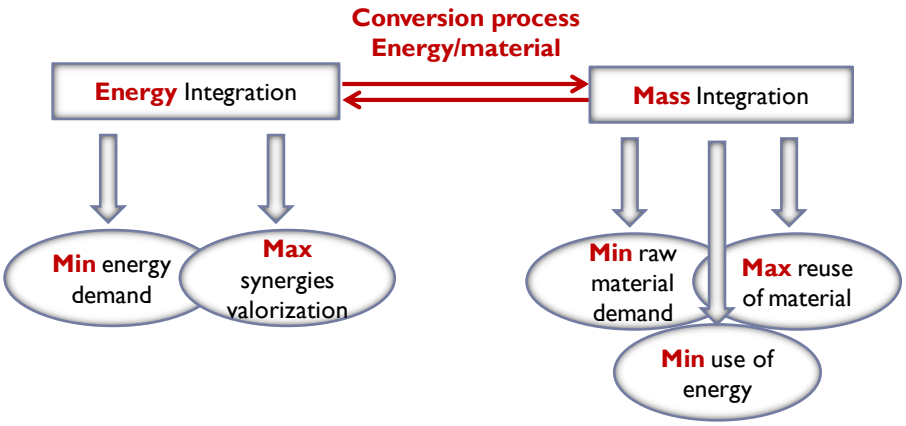


Figure 2. Conversion Process relationship with process integration techniques

In this context, the integration of conversion systems in an industrial territory, as an extension of conventional process integration techniques for EIP design, delimits the perimeter of this doctoral work. The state of the art territorial energy and mass integration methods are mostly built considering cooperative partners that exchange the established synergies for no price. However the more realistic version is for EIP industrial actors to trade their energy and material streams through monetary transactions. The existing process integration models could be amended to account for the costs and/or benefits of non-cooperative actors from participating in an identified exchange. This thesis thus aims on contributing to the development of methodologies for designing cost-effective conversion pathways, for the unrecoverable waste from mainstream integration methods, to be implemented in an industrial territory either with cooperative or non-cooperative economic scheme governance.

This manuscript exhibits the led doctoral work to achieve the aforementioned objective. It revolves around four chapters. The first consists on raising the issue of EIP configurations design. It details the motivation for exploring such configurations and explains the existing state of the art limitations in closing the energy and material loops. By dint of the novelty of incorporating conversion systems to the integration problems which consolidates circular economy the scientific objectives and challenges will as well be addressed in the first chapter.

In this context, the second chapter presents the methodological bricks required to construct the intended conceptual frameworks. On the basis of these building blocks, two distinct methodological frameworks for integrating conversion systems in a territory are proposed. The first, being for cooperative neighboring industries, serves to determine the best EIP pattern with the most profitable conversion routes for the non-recoverable streams. As the second is developed for self-interested actors and thus enables determining the inter-sites energy and material equilibrium transaction trades based on the individual objectives of each participating industry.

The third chapter describes the virtual industrial zone employed for the application of the proposed methodologies. This chapter also presents the process units models of the non-recoverable stream conversion pathways judged most suitable for the investigated park.

The fourth and final chapter illustrates the approach of incorporating conversion systems to the energy and material integration techniques through its application on the intended case study.

At the end of this manuscript, the contributions, but also the present limitations of the proposed approach, which have emerged from the application of the methodological frameworks, enable to suggest a conclusion on the undertaken work and sketch some perspectives.

Chapitre 1 (résumé)

Contexte et défis

Dans le cadre de la Convention-cadre des Nations Unies sur les changements climatiques, les pays ont promis de réduire leur empreinte environnementale provenant des activités humaines grâce à une meilleure gestion de l'énergie et des ressources. En effet, en comptabilisant les déchets comme des ressources plutôt que des handicaps, ils peuvent être réintroduits dans le cycle de production par des opportunités de réutilisation et de recyclage conduisant à une réduction importante des émissions de déchets ainsi qu'à la demande en ressources primaires. Lorsque c'est mis en œuvre, ça permet de créer de nouvelles ressources internes et réduit la demande de ressources externe, pliant ainsi le flux d'économie linéaire et potentiellement le ferme. L'économie circulaire et plus particulièrement l'écologie industrielle tournent principalement autour de ce concept qui est aussi le cadre prédominant de cette thèse.

Contrairement au modèle linéaire extractif, l'économie circulaire est régénératrice par conception puisqu'elle s'efforce de créer des processus en boucle fermée pour l'ensemble des activités humaines. Elle vise ainsi à conserver la valeur maximale de ses flux circulants en cours d'utilisation pour éventuellement recycler ou remettre à neuf les déchets et sous-produits générés afin de les réintroduire dans le cycle de production. L'UE en entrain de s'approcher rapidement de faire de l'économie circulaire une réalité dans sa région. La Commission européenne a en effet adopté en 2015 le dossier sur l'économie circulaire[1] qui englobe des propositions législatives sur la prévention, la réutilisation et le recyclage des déchets et des produits usés. Ils restent pleinement engagés à mettre en œuvre ce plan d'action vers la durabilité comme en témoigne la plate-forme d'appui au financement de l'économie circulaire qu'ils ont créée début 2017 pour stimuler l'adoption des projets d'économie circulaire par les investisseurs (European Commission, 2017).

Le cadre de l'économie circulaire a émergé des principes fondamentaux de l'écologie industrielle. Ce dernier est un ensemble d'approches systémiques multidisciplinaires fondées sur l'étude des flux de matières et d'énergie à travers les systèmes industriels dans le but de favoriser une conception optimale des procédés et une gestion efficace des ressources. La vision globale de l'écologie industrielle est, comme son nom l'indique, la reconnaissance que les systèmes industriels sont intégrés dans les écosystèmes mondiaux, ce qui exige un comportement intégré complexe pour permettre leur coexistence durable. Dans le cadre de cette notion, un acteur industriel s'efforce de réutiliser et de recycler ses sous-produits ou de valoriser ses déchets afin de réduire à la fois ses apports de ressources primaires et ses émissions de déchets de et vers la nature. Sur une plus grande échelle, des partenariats sont établis entre les industries voisines grâce à l'échange de ressources et de

[1] Directive 2008/98/EC - Directive 1999/31/EC

déchets; de ce fait, les déchets d'un deviennent la matière première de l'autre. Non seulement ces relations synergiques stimulent le bien-être environnemental et économique, mais elles forgent également des liens importants entre les industries. Les éco-parcs industriels offrent une démonstration prometteuse de l'écologie industrielle. Ils surviennent de groupes industriels consentant au commerce de leurs déchets et ressources.

En effet, un domaine zoné et destiné au développement industriel est désigné comme un parc industriel. Pour évoluer vers un éco-parcs, il doit justifier et encourager la durabilité environnementale par le biais des criteres de responsabilité sociale et environnementale plus strictes, de stratégies efficaces de gestion des ressources et de l'énergie et de partage collaboratif de produits et de services. L'objectif principal des éco-parcs industriels est donc de stimuler le développement économique de ses parties participantes par le biais de transactions mutuellement profitables tout en minimisant leur empreinte environnementale.

La conception d'éco-parc industriel se fait principalement avec des processus d'essais et d'erreurs et non avec des stratégies de conception systématiques et optimales. Le grand nombre d'initiatives infructueuses des implémentations des éco-parcs aux Etats-Unis et en Europe, témoigne du défi que représente la construction des relations d'échange de sous-produits. Les multiples participants industriels impliqués dans l'éco-parc jouent un rôle majeur en empêchant éventuellement sa mise en place. Cependant, les avantages tangibles des éco-parcs existants l'emportent sur les difficultés et incitent à l'étude et à l'optimisation de la symbiose industrielle dans le but de mettre en œuvre des structures analogues optimales à travers le monde. Ceci manifeste la nécessité de méthodologies et d'outils systématiques pour leur conception générant des scénarios de synergies optimales. Les performances économiques et environnementales tangibles qui découlent de ces résultats encouragent les échanges entre les acteurs industriels potentiels qui se chargent de mettre en place des structures d'éco-parc fortement viables.

L'échange entre-usines d'énergie et de matière résultant de la collaboration des occupants du éco-parc, réduit le fardeau des décharges locales et réduit l'impact environnemental tout en augmentant ou en préservant la rentabilité des parties engagées. Pour créer ces avantages, il faut évaluer les synergies potentielles qui réduisent l'utilisation des ressources ou les émissions de déchets afin d'assurer leur véritable faisabilité physique. Cependant, il est improbable qu'une entreprise adopte une synergie identifiée entraînant des coûts d'investissement supplémentaires à moins qu'elle ne prouve une réduction des charges d'exploitation. Par conséquent, la modélisation et l'optimisation des réseaux de parcs industriels, dans lesquels circulent ces flux, impliquent des techniques systématiques de conception de procédé intégrée qui regroupent les composants des sous-systèmes pour une fonctionnalité globale.

Traditionnellement, les techniques d'intégration de procédé adhèrent à l'énergie et à la matière (par exemple, l'eau et l'hydrogène) séparément puisqu'elles forment les deux catégories de flux principales des réseaux industriels. Les méthodologies d'intégration de l'énergie, tant au niveau du procédé que du territoire, permettent de minimiser la demande énergétique du système en maximisant les synergies internes et en générant ainsi une utilisation efficace de l'énergie. Ces méthodes peuvent également être utilisées pour intégrer de façon optimale, via l'analyse exergétique, des systèmes de récupération de chaleur à basse température qui améliorent la qualité de l'énergie non exploitée en élevant sa température ou en la convertissant en énergie électrique; recréant alors des nouvelles opportunités d'exploitation. De même, les techniques d'intégration de matière visent à minimiser le besoin de matières premières en recherchant des opportunités optimales de réutilisation et de recyclage des déchets dans des procédés tolérant des niveaux de pureté plus faibles. L'utilisation de ces techniques classiques d'intégration des procédé engendre l'efficacité énergétique et l'utilisation optimale des ressources. Par la suite, les utilités d'énergie et de matière première nécessaires pour

répondre aux demandes locales et territoriale sont significativement diminuées avec la mise en œuvre des scénarios de synergies identifiés.

Les deux techniques précédemment vues, qui sont intégrées dans la famille d'intégration de procédé, permettent l'identification de scénarios de synergie potentiels, que ce soit à l'échelle du procédé ou au niveau entre-sites. Par la suite, ils conçoivent des réseaux pour redistribuer intelligemment l'énergie et la matière entre différentes sources et puits afin d'assurer l'échange entre les participants industriels. Cependant, il se peut que ces méthodes ratent des possibles synergies à cause de la forme constante des flux dans le système. Pour une gestion plus efficace des ressources et une réduction de la pression environnementale, la modification de la forme des déchets irrécupérables est obligatoire pour les réintroduire dans le système.

Comme exposé précédemment, pour obtenir des structures d'éco-parc fortement viables avec une utilisation efficace des ressources, les synergies devraient être générées par des outils systémiques. Cependant, maximiser les synergies sur site et entre-sites en utilisant exclusivement des méthodes d'intégration de procédé est limitée à la valorisation des composants dans leurs formes originales, résultant alors à manquer les opportunités de réutilisation du composant sous une autre forme.

Par conséquent, l'objectif scientifique de cette thèse est de proposer une méthodologie d'intégration des procédé de conversion énergie/matière basée sur une approche entrelacée entre conception de procédé et intégration de procédé permettant d'explorer de nouvelles voies de récupération des flux de déchets. La méthodologie vise à maximiser l'économie circulaire d'un territoire en recherchant la meilleure voie de valorisation des flux non-utilisables en les convertissant à d'autre forme de flux qui répondent le mieux aux besoins du parc et entraînant ainsi leur réinsertion dans le système. Par conséquent, une meilleure efficacité du système et une réutilisation plus rationnelle des ressources peuvent être obtenues.

La mise en place de systèmes de conversion des déchets pour fermer les boucles de matière et d'énergie vise à reconvertir les déchets et les sous-produits non récupérables en ressources pour d'autres procédés ou industries. La conception et la synthèse de ces synergies ne peuvent être réalisées qu'après l'application de techniques de conception de procédé permettant d'identifier systématiquement les flux optimaux du système.

De l'état de l'art étudié, les méthodologies développées dans la littérature sont limitées sur plusieurs aspects. Soit qu'ils ne prennent pas en compte l'intégration de masse ou ne considèrent que l'optimisation d'une voie prédéfinie à l'échelle locale, ou même ne tiennent pas compte des réseaux de transport. N'ayant pas la possibilité d'identifier des voies de conversion économiquement réalisables pour les déchets d'un territoire, le besoin d'une méthodologie pour aller plus loin pour fermer la boucle vers l'écologie industrielle est convaincant. Cette méthodologie innovante devrait permettre de traiter la récupération de l'énergie et des rejets de matière au moyen de procédé de conversion. Il devrait intégrer à la fois la conception des procédés et les techniques d'intégration des procédés au niveau local et entre-sites dans le but d'évaluer les voies de conversion multiples pour les déchets irrécupérables; générant alors des configurations optimales de symbiose industrielle avec la conception de système de conversion la plus appropriée. La réalisation des objectifs scientifiques de cette thèse fait face à trois essentiels défis méthodologiques:

- Premièrement, la conception du procédé doit prendre en compte plusieurs systèmes de conversion d'un déchet défini avec différentes options de produit. Non seulement le potentiel de conversion énergétique de la matière est étudié, mais d'autres alternatives de conversion apporteraient également la possibilité de transformer les déchets non utilisables grâce à des procédés chimiques en une autre forme de matière utilisable.

- Deuxièmement, l'intégration du procédé devrait être étroitement liée à la conception du procédé pour des synergies optimales des flux d'énergie et de matières à l'échelle du système de conversion. Au niveau entre-sites, l'intégration de procédé territoriale doit être réalisée en tenant compte des réseaux de transport des flux échangés.
- Troisièmement, la méthodologie développée devrait traiter deux scénarios économiques: le premier est l'intégration du système de conversion dans un parc régi d'une gouvernance coopérative dans lequel les acteurs industriels troquent les déchets et les sous-produits; et le second est le cas d'un territoire avec un régime non-coopératif dans lequel les acteurs explorent constamment des stratégies pour trouver leurs propres intérêts et, par conséquent, l'échange de déchets et de sous-produits est accompli par des transactions d'achat et de vente.

La méthodologie développée sera en mesure de générer des configurations de synergies optimales pour un éco-parc industriel incluant la modification des déchets irrécupérables via des systèmes de conversion. Pour relever le premier défi scientifique, les procédés de conversion sont sélectionnés à partir d'une base de données diverse créée pour chaque type de déchet tout en tenant compte de la topologie et des activités du territoire et donc de différentes voies de conversion des déchets non exploités.

La méthodologie est basée sur trois briques méthodologiques primordiales qui sont la conception de procédé et l'intégration de procédé au niveau du système et à l'échelle du territoire. Par conséquent, pour pouvoir l'implémenter, chacune de ces briques a été sélectionnés pour être utilisés à partir de l'état de l'art. L'approche méthodologique consiste à assembler les briques de l'intégration énergétique et de matière avec les procédés de conversion pour la résolution globale du problème visant à identifier la voie optimale des déchets irrécupérables qui seront en concurrence avec d'autres conversions alternatives.

Même si les régimes coopératifs et non coopératifs sont fondés sur les mêmes briques méthodologiques mentionnées ci-dessus, ils consistent en des cadres entièrement différents. Celui proposé pour le schéma coopératif consiste principalement d'un problème Maître qui gère via une analyse combinatoire les paramètres de fonctionnement et les options de conception technologique des procédés de conversion pour lui permettre d'examiner simultanément les conditions de faisabilité ainsi que la pertinence économique et énergétique des possibilités de conversion . Ce problème maître gère les deux problèmes esclaves de l'intégration des procédés local et territorial. Par conséquent, ce modèle maître-esclave assure l'aspect imbriqué soulevé dans le deuxième défi scientifique.

Cependant, dans un environnement où les acteurs industriels manifestent des intérêts individuels, un mécanisme centralisé de haut en bas n'est plus valide. Par conséquent, l'intégration de systèmes de conversion dans un territoire avec des acteurs cherchant leurs propres intérêts nécessite un autre cadre méthodologique. Un modèle basé sur la formulation agent est donc proposé pour formuler le problème dans lequel la technique de coordination choisie est la négociation. Le flux de travail de ce dernier a été développé pour assurer la création de synergies optimales pour des états d'équilibre de transaction d'achat et de vente.

La démonstration des deux cadres méthodologies développées a été réalisée sur une étude de cas constituée d'un parc industriel virtuel. Suite à la définition de l'étude de cas, les procédé de conversion des déchets irrécupérables identifiés ont été recensés puis formulés dans leurs modèles physiques et économiques. Pour respecter le périmètre de cette thèse, le bois est désigné comme étant le type des déchets irrécupérable du territoire.

Chapter 1

Background and Challenges

In this chapter, an overview of the unsustainable pressure originating from human activities is first presented to evince the alarming environmental issues and resources consumption humanity is facing with the current demographic and economic growth. The resulting consequences in particularly on the energy and industrial sector are then examined in the aim of exhibiting the reasons behind the prevailing linear economic model not being fit for the future. Afterwards, the political actions that have been conducted to face this alarming situation are discussed. The translation of those actions led countries to pledge under the UNFCCC ambitious targets to curb resources depletion and environmental footprint origination from human activities.

Circular economy is gaining momentum as an answer for shifting towards a new sustainable paradigm more convenient to modern society and which enables reaching the set goals. Thereafter, the industrial ecology, of which circular economy emerged fundamental principles, is evoked for its direct implications in the industrial world and for it being chiefly dominating the framework of this thesis. Eco-industrial parks (EIP), which arise from industrial clusters consenting on trading waste and resources, adduce a promising demonstration of industrial ecology. The most iconic example of EIP is illustrated along with another success story of governmental EIP planning.

The complexity tied together with the multiple industrial participants inter-sites synergies, manifest the need for systematic and systemic methodologies to achieve strongly viable EIP structures. Process integration techniques with their emphasis on the efficient use of energy and resources through maximizing internal synergies are great tools for modeling and optimizing EIP. Therefore, the state of the art of both energy integration and material integration are explored. Subsequently, this doctoral thesis motivation are presented showing the limitation of exclusively employing process integration for maximizing on-site and inter-sites synergies.

Following the explanation of this thesis prime objective which lies on developing a systematic methodology for integrating energy/material conversion systems in a territory based on an intertwined approach between process design and process integration to explore new reuse paths of unrecoverable waste, the state of art of process design methodologies in the context of industrial ecology are scouted. Finally, based on the analysis of the available and latest work tackling tools and techniques for closing the energy and material loops, the scientific challenges of this research are explored and the vision of the methodology to be developed for addressing these challenges is presented.

1.1. Unsustainable anthropogenic pressure

The Industrial Revolution is the time when the world shifted from the old manual laboring to the new machinery age by dint of technological inventions mainly powered by fossil fuels. The invented machinery aided in speeding up the production and enabled mass manufacturing. Subsequently, Humanity began to exhibit unprecedented economic prosperity. This time marked a major turning point in global history; it drastically altered human lifestyles and thus their relationship with their environment. Since then, the living standards and medical knowledge were profoundly advanced resulting in health improvements and life longevity. Consequently, the world population propelled towards an exponential growth; numbering 7.5 billion living human beings today, yet 200 years ago only 1 billion person were alive, as it can be visualized in Figure 1.1. The two most populated countries, China and India, comprise jointly more than one third of the population.

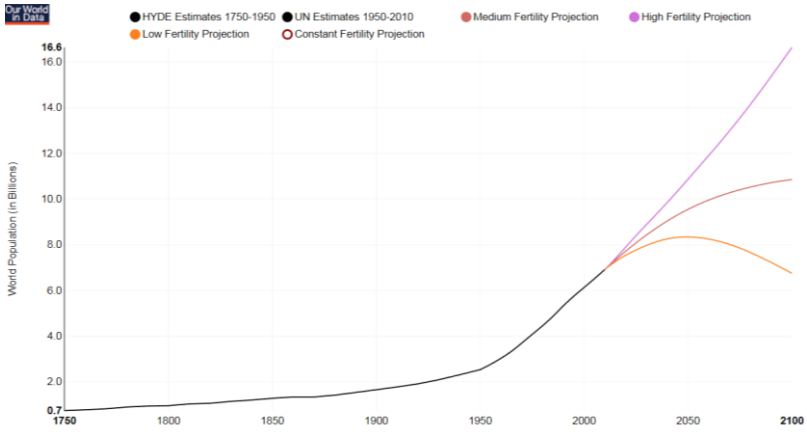


Figure 1.1. World population since the industrial revolution including the projections till 2100[2]

However, the global economic blooming and demographic growth came at the environment expense. The natural resources requisite to make the increasing production possible were under enormous demand showing the implications of limited available resources. While prior to the Industrial Revolution these resources were taken for granted as being inexhaustible since there had always been higher available amounts than the demand for them. Furthermore, the prevailing manufacturing paradigm was dominated by linear economy which is a 'take, make, use, dispose' model of production. Consequently with such model, great production is indelibly tied together with increased wastes generation which are disposed of to decompose or pollute.

Industrialization and population growth led to a steep increase in migration and urbanization. Migrants flocked from rural to urban areas while other countryside regions were transformed to urbanism. As a corollary to the increasing population, landmass scarcity arises since industry, housing and agriculture manifest to occupy a place for their activities. Urbanization is widely spread particularly in developing countries where rural communities tend to adopt urban culture in search of acquiring higher social and economic standards to ultimately become cities. This brings about the need of infrastructure development, transportation and communication improvements and quality medical facilities to ease the access to food, medicine and energy; subsequently yielding to greater natural resources consumption to ensure the community growing requirements.

[2] https://ourworldindata.org/future-world-population-growth/

Another unintended consequence attributable to the production expansion driven by fossil fuel consumption is the rapid increase of greenhouse gas emissions and pollution leading to a planetary warming impact. The increase in energy stored in the atmosphere severely disrupt the global climate leading to extreme weather events such like floods, violent storms and intense summer heat waves. In order to halt temperature rise, carbon dioxide emissions must be cut down since it is responsible for four-fifths of the global warming increase by greenhouse gases. The visualization in Figure 1.2 depicts the dramatic increase of the global carbon dioxide emissions from half a billion tons in 1815 to over 36 billion tons 200 years later. Bearing in mind the long residence time of anthropogenic greenhouse gases in the atmosphere, their cumulative build-up is of ultimate significance. The Intergovernmental Panel on Climate Change (IPCC) actually estimated that to preserve the opportunity to restrain global warming to 2 °C relative to pre-industrial levels, carbon dioxide emissions is not ought to surpass 3000 billion tons of which two thirds have already been emitted before 2014 (IEA, 2015). Consequently, the prevailing linear economic model is detriment to the path towards this goal and exhibits no sustainability for humanity nor for Earth.

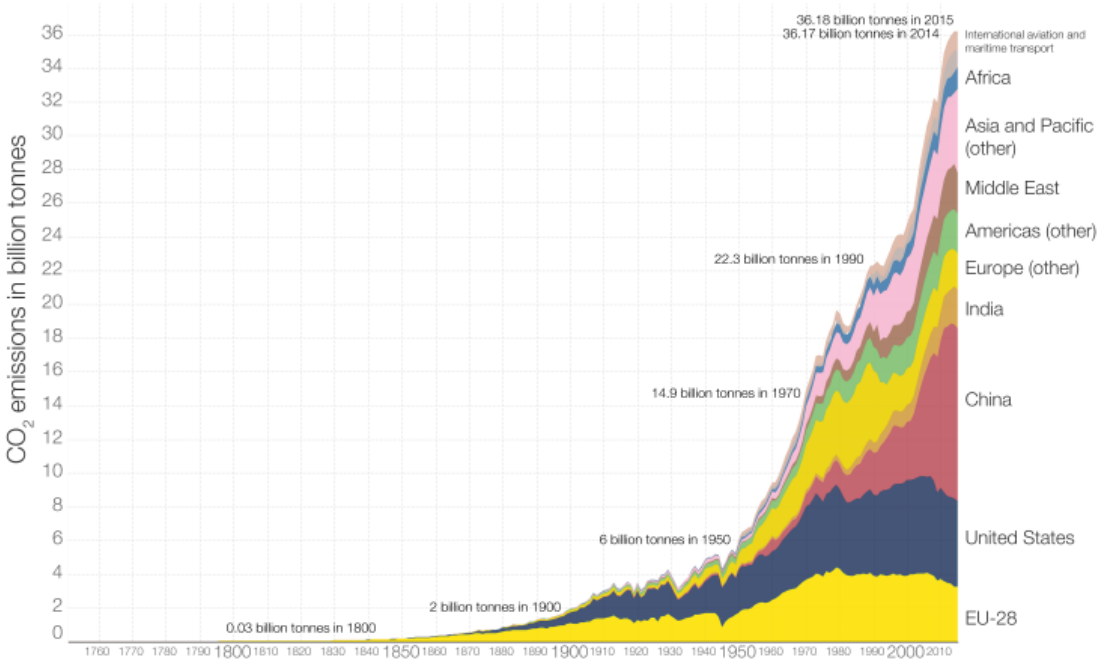


Figure 1.2. Annual carbon dioxide emissions by world region from 1751 to 2015[3]

Furthermore, according to the United Nations prospects (UN, 2017), the world population is expected to increase by approximately 20% and attain 9 billion by 2040. Every country is affected by this growth, though the 47 least developed countries (LDCs) designated by the United Nations maintain their relatively high fertility level ensuing their population size to nearly double in 2050. This calls for an increase demand for food, water, commodities, energy, education and health care. Hence with resources being consumed faster than they can be replenished at the current demand, the economic model of the past is not fit for the future. New sustainable paradigm of production and consumption must be implemented to curb resources depletion and climate change in the face of population expansion and its requirements accretion.

[3] https://ourworldindata.org/co2-and-other-greenhouse-gas-emissions/

1.2. The challenge of the Energy Sector

The daunting challenge lies within the energy sector as it accounts for the majority of the anthropogenic greenhouse gas emissions today (i.e., 32 Gt out of 36 Gt in 2014). Over the past four decades the world primary energy supply has more than doubled, Figure 1.3, reflecting an exacerbation of human pressure on the planet. In 2014, it amounted to 13 700 Mtoe which is equivalent to approximately 160 000 TWh. Inevitably, fossil fuels (coal, oil and Natural gas) account for the dominant energy source making up four-fifth of the planetary energy supply in 2014, substantially contributing to the greenhouse gas emissions. The primary energy supply differs from the final energy consumption. This latter refers to the fraction of the primary energy supply acquired by consumers in its final form. The industrial sector accounts for the largest share of the world final energy consumption (37%), followed by the transport (28%) and residential sectors (23%) (IEA, 2016) mainly fueled by a continued reliance on fossil fuels.

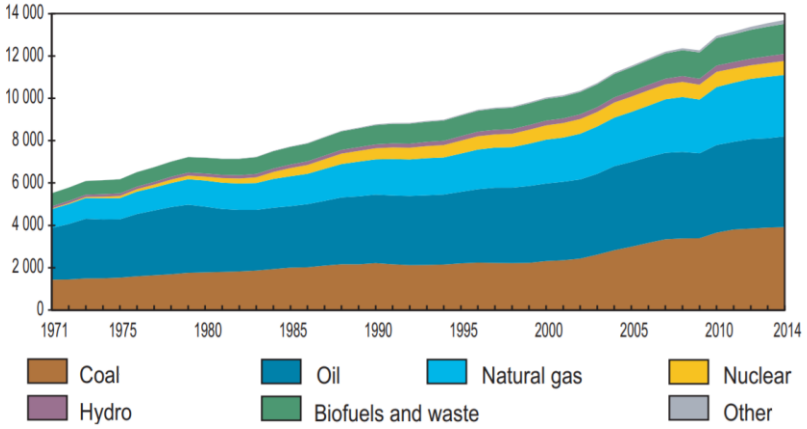


Figure 1.3. World total primary energy supply from 1971 to 2014 by fuel (Mtoe) (IEA, 2016)

In two decades, the global gross domestic product (GDP) will double going up to 145 trillion US dollars (OECD, 2015). This massive economic growth will strongly influence the world energy consumption to meet the demand of industry, transportation and residential sectors. A large share of energy-related greenhouse gas emissions actually comes from the three nations with the largest economy in purchasing power parity (PPP) terms – China, United States and India. In 2015, they were responsible for more than half of global carbon dioxide emissions, Figure 1.2. Based on current policies and regulations governing fossil fuel use, the global energy consumption is projected to continue on climbing reaching 20 537 Mtoe in 2040 (eia, 2016), a 50% increase from 2014.

Concerns about the anthropogenic pressure effects led in the 21st century the use expansion of non-fossil renewable energy sources and nuclear power. Although renewable energy and nuclear power are growing with a steep ascent of 2.6% and 2.3% each year respectively, fossil fuels will continue on providing the greatest part of the world energy demand throughout the foreseeable future, Figure 1.4. Not only for the aforementioned reasons renewable energy adoption was boosted, clean energy made strides also by dint of the fluctuating crude oil market. Those wild swings in oil prices are driven by global variations in demand and supply, and are also greatly influenced by natural disasters (e.g., Hurricane Katrina in 2005 or the Mississippi River flood in 2011), by political instabilities (e.g., wars in Iraq, Afghanistan, Syria and Libya) and by economic crisis (e.g., subprime mortgage crisis in 2008). The energy challenge is thus dual: to mutually reduce the fossil fuels share in the energy mix and to mitigate global energy consumption.

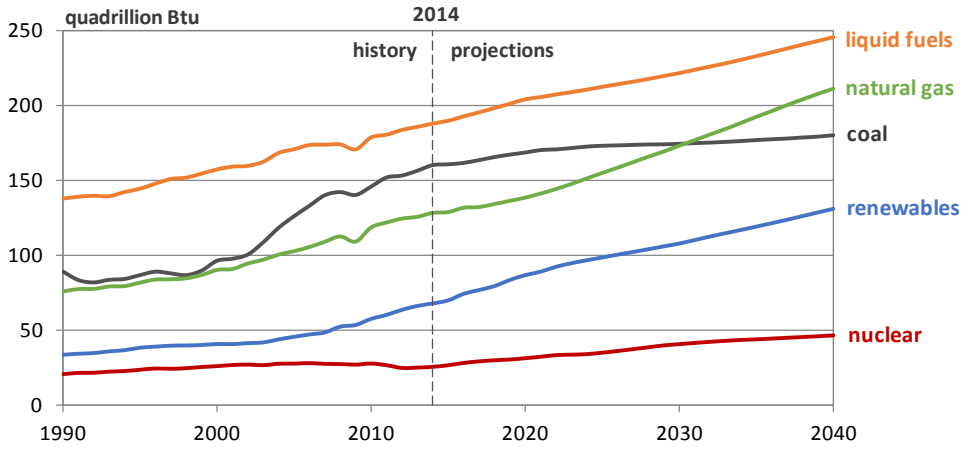


Figure 1.4. World final energy consumption projections by fuel

Energy efficiency plays a leading role in addressing the second part of this challenge. By definition, it intents on using less energy to provide the same output. Therefore improving a system energy efficiency will directly lead to its energy consumption decrease. Avoided fossil fuel consumptions from energy efficiency improvements, avert greenhouse gas emissions. This was perceived in IEA[4] countries which scored in 15 years a cumulative savings of carbon dioxide emissions greater than their 2015 mutual emissions, Figure 1.5. This effect emphasizes the importance of even seemingly small efficiency measurements which together accumulate to make a difference.

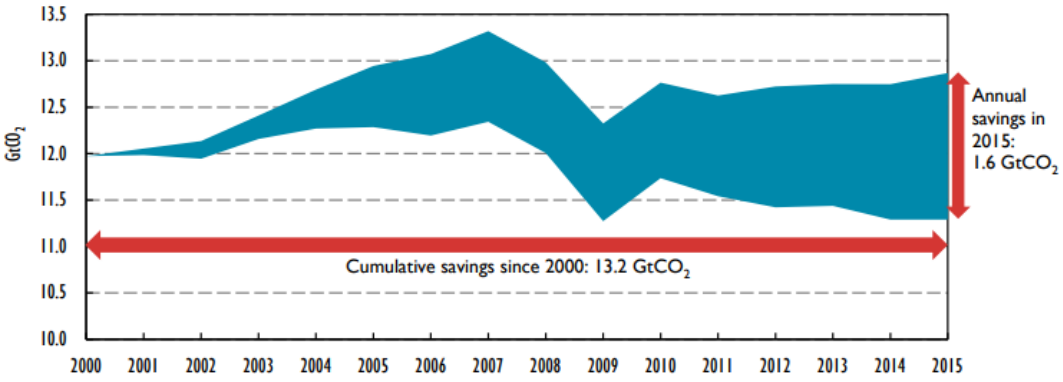


Figure 1.5. Avoided emissions from energy efficiency improvements in IEA countries (IEA, 2016)

There are significant economic benefits associated with implementing energy efficiency measures which extend far beyond lowering energy bills for households. By reducing their energy demand companies can raise their products profitability and lower the risk exposure stemming from volatile energy prices and thus operate their businesses more efficiently. This economic pillar also contributes in shrinking a nation dependency on foreign energy imports and could lower the depletion rate of domestic energy resources. From 2000 to 2015, IEA countries managed to avoid 7% of their total energy imports by dint of energy efficiency enhancements, Figure 1.6. Half of the energy import savings were recorded by the European Union (EU) which manifests as the largest energy importing region in the world.

[4] The International Energy Agency is an autonomous organization with 29 member countries

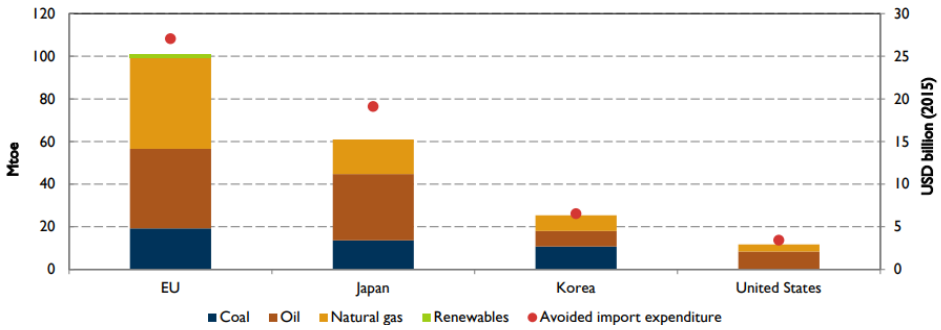


Figure 1.6. Total avoided fossil fuel import costs with share of savings by country/region (IEA, 2016)

1.3. Imperative Precedence for Action

Faced with the unsustainable anthropogenic pressure, which manifests louder with daily growing awareness, the imperative for action enjoins mandatory. Our decision-making patterns are ought to be fundamentally reappraised in order to redirect towards sustainable society development. The construction of a new model for global governance, capable of managing the entirety of the problem is thus awaited. With the goal of mitigating climate change, political actions have been taken to handle the adverse effects of human activities which brought about environment and natural resources deterioration. It started in 1983 when the United Nations became aware of the heavily declining situation. It therefore established the Brundtland Commission in order to rally countries in pursuing "Sustainable Development". The aforementioned term was coined and defined in the commission issued report as "Meeting the needs of present generations, while not compromising the ability of future generations to meet their own needs"[5].

Based on the scientific consensus that global warming is occurring, an international treaty, the United Nations Framework Convention on Climate Change (UNFCCC), was opened for signature at the Earth Summit in Rio de Janeiro in 1992. The framework depicts the outlines for international cooperation to contend climate change in which the definition of sustainability was reiterated. The pledged parties convened annually in Conferences of the Parties (COP) since 1995 to assess the advancement in dealing with environmental impact cut down and communities' social conditions enhancement in the aim of strengthening the global response to climate change. In 1997, the Kyoto Protocol, which implements the UNFCCC objective, was coined and adopted. The protocol legally set binding obligations for pledged developed countries to minify their greenhouse emissions to attain defined targets. A first commitment period was from 2008 to 2012 and a second period was initiated to bridge the gap between the end of the previous one and the start of the new global agreement in 2020. In 2007, the EU countries have agreed to jointly reach by the year 2020[6] a set of three environmental targets: 20% greenhouse emission reduction, 20% renewable sources share in the energy mix and 20% energy cut through energy efficiency enhancement compared to 1990 levels. The latest step marking the international effort to combat climate change is the 21st yearly COP which was held in Paris in late 2015. During the Paris agreement, each of the 196 parties' representatives reported their country's contribution targets in the aim of limiting average global temperature increase to less than 2 °C. The proposed plans implementation was discussed last year during the COP22 in Marrakech.

[5] Report of the World Commission on Environment and Development: Our common future, 1987
[6] https://ec.europa.eu/clima/policies/strategies/2020

For instance, France committed to cut down three-fourth of its greenhouse emissions by 2050. To meet this international engagement, it has resolved to raise the renewable share of its energy mix to 32% by the end of the next decade and to reduce by half its energy consumption by 2050[7]. To implement this transition, France national sustainable development strategy encompass lowering one-fourth of the industry sector emissions and one-third from the waste management emissions. This will be translated by considerable challenges on the three sustainable development pillars of the industrial sector (i.e., ecological, social and economic). Therefore industrial actors must be prepared to cope and comply with the current and upcoming ecological regulations inevitably impacting their economic performances. However, through innovative work on technical cost-effective solutions such as process efficiency enhancements and resources use optimization, industries can meet modern ecological standards with the least economic detriment. By accounting wastes (heat or material) as resources with great potential instead of liabilities, reusing and recycling opportunities conspicuously beget. When put into effect, it creates new internal resources and reduces external supply demand thus bending the linear economy flow and potentially closing it. Circular economy and more particularly industrial ecology chiefly revolve around this concept which is also the predominant framework of this thesis.

1.4. Industrial Ecology towards Sustainable development

With the prevailing linear production and consumption model, the planet is attaining its limit of natural resources and its capacity to intake waste and pollution. Circular economy is gaining momentum as an answer for shifting towards a new sustainable paradigm more convenient to modern economy. As opposed to the extractive linear model, circular economy is regenerative by design since it endeavors creating closed loop processes for the entire human activities. It thus aims at retaining the maximum possible value of its circulating flows whilst in use to eventually recycle or refurbish the generated waste and byproducts for them to be reintroduced back into the production cycle. The EU is fast approaching making circular economy a reality in its region. The European Commission actually adopted in 2015 the Circular Economy Package[8] which encompasses legislative proposals on waste prevention, reuse and recycling of useless rendered products. They remain fully committed to implementing this Action Plan towards sustainability as was reflected in the Circular Economy Finance Support Platform they established in early 2017 to boost circular economy projects uptake by investors (European Commission, 2017).

The circular economy framework emerged fundamental principles from Industrial Ecology. This latter is a set of multidisciplinary systemic approaches founded on examining material and energy flows through industrial systems in the furtherance of optimal process design and effective resource management. The overarching insight of industrial ecology is, as the name implies, the recognition that industrial systems are embedded within the global ecosystems which enjoins complex integrated behavior to enable their sustainable coexistence. Within this notion, an industrial actor endeavors to reuse and recycle its by-products or upgrade its waste to cut down both its primary resource intake and waste emissions from and to the nature. On greater scope, partnerships are made between neighboring industries through resource and waste exchange; thereby one's waste becomes another's raw material. Not only do these synergistic relationships prompt environmental and economic welfare, they equally forge prominent bonds amongst industries. Eco-industrial parks adduce a promising demonstration of industrial ecology. They supervene from industrial clusters consenting on trading waste and resources.

[7] http://www.gouvernement.fr/en/cop21-france-s-national-commitments
[8] Directive 2008/98/EC - Directive 1999/31/EC

1.5. Eco-Industrial Park

The most sited definition of an Eco-Industrial Park (EIP) states that it is, 'a community of manufacturing and service businesses located together on a common property. Members seek enhanced environmental, economic, and social performance through collaboration in managing environmental and resource issues' (Lowe, 2001). Actually, an estate zoned and intended for industrial development is designated as an industrial park. For it to evolve towards becoming an EIP, it must substantiate and foster environmental sustainability by the means of greater social and environmental responsibility standards, efficient resource and energy management strategies and collaborative products and services sharing. The prime purpose of EIP is thus to drive economic development for its participating parties through mutually proftibale transactions while minifying their environmental footprint. The synergistic manner by which an EIP community is connected mimics natural ecosystem. By that discarded by-products (energy, material and water) from one industrial party are recovered and reused as resources by another, traditionally separate, party which lead to improving their competitive advantage, a process referred to as industrial symbiosis (Chertow, 2000). In conjunction with the generated revenues, turning waste into vendible product instill proactive social relationships via new business opportunities and embed environmental stewardship by nourishing energy efficiency and diverting waste from landfill.

A historical first and canonical example of EIP is Kalundborg in Denmark, Figure 1.7. It encompasses eight private and public actors, among which the largest Danish power Station (Asnæs) and the biggest Oil Company in the Baltic Region (Statoil). Roughly five decades ago, the first collaboration came into being when Statoil agreed to provide its surplus gas to Gyproc, a local gypsum supplier. Since then and as opposed to governmental EIP planning, partnerships were formed and negotiated gradually by private initiatives with no political intevention.

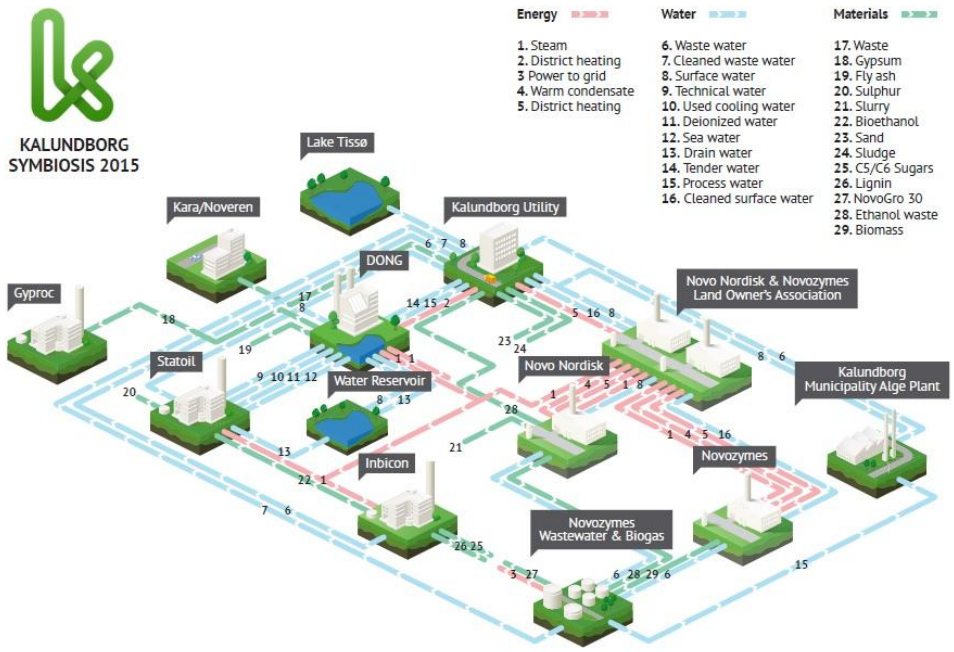


Figure 1.7. Kalundborg Eco-Industrial park, Denmark[9]

[9] http://www.symbiosis.dk /en

Eventhough originally they rose out of necessity and for purely economic reasons, some of subsequently arranged bargains were made for environmental reasons. It wasn't until 1989 that the Kalundborg collaboration was appointed as industrial symbiosis. The established interchanges jointly contributed to significant water, fuel and energy savings. Considerable waste volume was as well avoided through the developed complex symbiosis network. Over and above the 80 million US dollars of annual economy[10], the physical linkages averts the emission of 275 thousand tons of CO_2 each year avoided by the reduction of oil use in the heat and power generation.

Many countries throughout the world have been trying to develop industrial symbiosis, such as Styria in Austria, Brownsville in the USA, Ulsan in South Korea and Tianjin Park in China. The Tianjin Economic-Technological Development Area (TEDA) exhibits an epitome of governmental EIP planning. One of the pioneers in EIP development in China, it was established in 1984 with the State Council approval in compliance with international standards and regulations. It aimed to becoming a leading green manufacturing zone which attracts prime foreign corporations. With the new adopted national laws of international certifications in the beginning of the 21st century, TEDA was compelled to start incorporating circular economy principles for what the certification offers whether elevating the environmental management or enticing investors by improving the public image of TEDA. Staying loyal to its pursuit, TEDA was officially nominated as an EIP in 2005 and become one of the first state-sponsored pilot demonstrations in China. Water and landmass scarcity initially drove TEDA to make efficient use of these critical natural resources. The prompt economic growth it witnessed made vital reducing and recycling energy and resources since their demand grew immensely. Subsequently, various industrial symbioses were established progressively with potent governmental involvement, Figure 1.8.

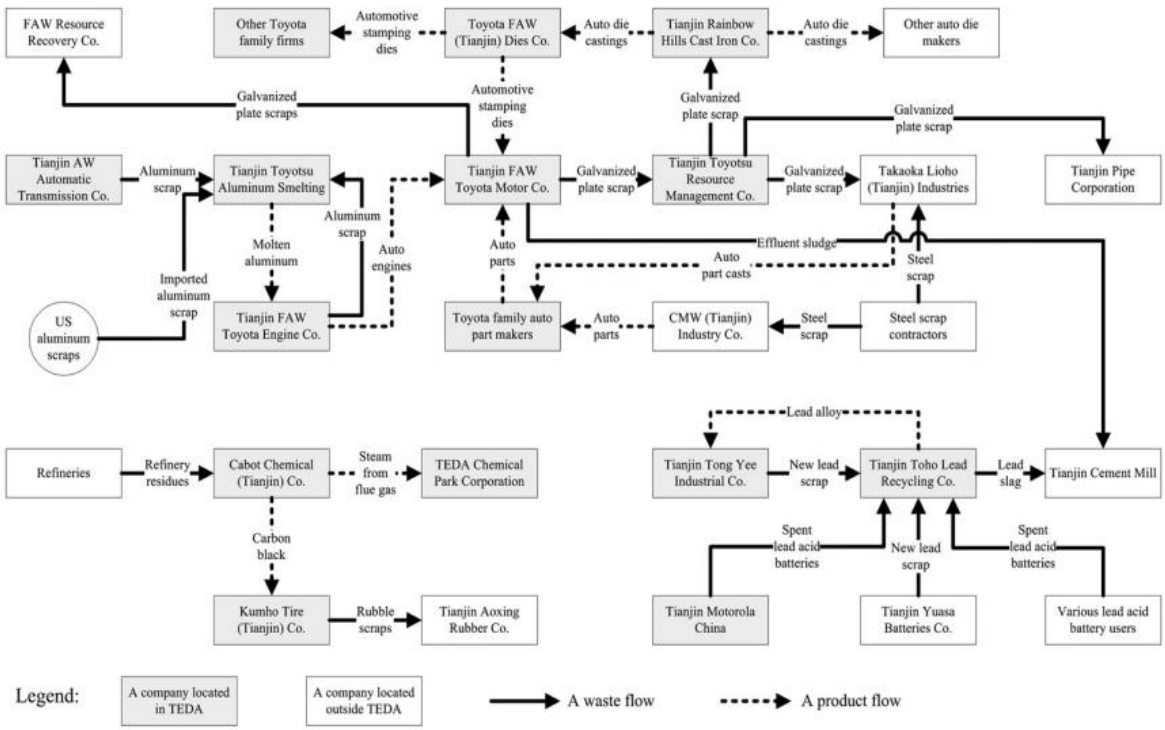


Figure 1.8. Eco-industrial network in the Tianjin TEDA (Shi, et al., 2009)

[10] http://www.euronews.com/2015/06/26/industrial-symbiosis-in-kalundborg-turning-waste-into-a-resource

By 2013, its GDP exceeded 250 billion Renminbi and above 80 inter-firm symbiotic activities were reckoned[11] covering infrastructure sharing, waste recovery, water and energy cascading, and by-products exchanges. TEDA has been ranked as the most attractive economic development zone for foreign investment by China's Ministry of Commerce for a decade since 1998. However, its industrial symbiosis outreach remains modest, deeming the 10,000 companies of this huge industrial park. This shows the untapped potential that is yet to be unleashed through new symbiotic relationships.

As exhibit the two aforementioned examples, designing EIP is mostly done with trial and error processes and not with systematic and optimal design strategies. The large number of unfruitfull initiatives of EIP implementations in the USA and in Europe, evince the challenge required for constructing by-products exchange relationships. The multiple industrial participants involved in the EIP, play a major role in possibly impeding its establishment. However, the tangible advantages of existing EIP prevail over the difficulties and incite the study and optimization of industrial symbiosis in the aim of implementing optimal analogous structures throughout the world. This manifest the need for systematic methodologies and tools for EIP design which generate optimal synergies scenarios. The tangible economic and environmental performances ensuing from those results encourage the interchange between potential industrial actors helming to achieve strongly viable EIP structures.

1.6. Process Integration techniques

Inter-plant energy and materials exchange resulting from EIP occupants' collaboration, curb the burden of local landfills and reduce the environmental impact whilst raising or preserving the profitability of engaged parties. To give rise for those advantages, potential synergies that decrease resource usage or waste emission should be evaluated to ensure their veritable physical feasibility. However, a company is improbably to adopt an identified synergy incurring additional investment costs unless it proves a cut down in operating expenses. Therefore modeling and optimizing industrial park networks, in which these flows circulates, entail systematic integrated process design techniques which aggregate the sub-systems components for an overarching functionality. With their emphasis on the efficient use of resources, process integration techniques have resulted in significant benefits to the industrial sector in terms of process improvements, increased productivity, resource management, pollution prevention, and operating cost reductions (Morar & Agachi, 2010).

Traditionally, process integration techniques adheres to energy and material (e.g., water and hydrogen) seperatly since they form the two main flow categories of the industrial networks. The methodologies of energy integration, on both process and territorial levels, enable the minimization of the system energy demand by maximizing internal synergies and thereby engendering efficient use of energy. These methods can also be employed to optimally integrate, via the exergy analysis, low temperature heat recovery systems which upgrade the quality of the untapped energy by elevating its temperature or by converting it into electric power; recreating by that new harnessing opportunities. Similarly, material integration techniques aim at minimizing the need for raw material by looking for optimal reuse and recycling of waste material in processes tolerating lower purity levels. Employing these mainstream techniques of process integration begets energy efficiency and optimal resource usage. Subsequently, the energy utilities and the raw materials required to meet the local and territorial demands are significantly decreased with the implementation of the identified synergies scenarios.

[11] http://www.isige.mines-paristech.fr/institut-superieur-ingenierie-gestion-environnement/news/envim/circular-economy-workshop

1.6.1. Energy Integration

Linhoff and Flower (Linnhoff & Flower, 1978) introduced the concept of energy integration for the first time by the pinch method in 1978. Their technique enables the identification, for a defined minimum temperature difference in the heat exchangers (ΔT_{min}), of the potential recoverable amount of heat jointly with the minimum required energy utility resulting in a decrease of the process energy demand. The minimum allowed temperature difference is mainly an economic parameter which indicates a nearly optimal balance between investment (the cost of heat exchangers) and operating costs (energy utilities) (Klemeš, et al., 2013). In parallel to the thermodynamic pinch analysis approach developed for energy integration, another alternative approach based on superstructure optimization was developed (Papoulias & Grossmann, 1983a) (Papoulias & Grossmann, 1983b). This technique, solved using numerical models, is based on the mathematical formulation of the problem which consists on developing a superstructure that encompasses all the possibilities for operations and connections which form potential candidates of the optimal design. First, the minimum utility targeting method was modeled using a linear programming (LP). Then the descendants of the LP, the mixed integer linear programming (MILP), allowed having the minimum number of heat exchangers units assembly resulting in an optimal utility target.

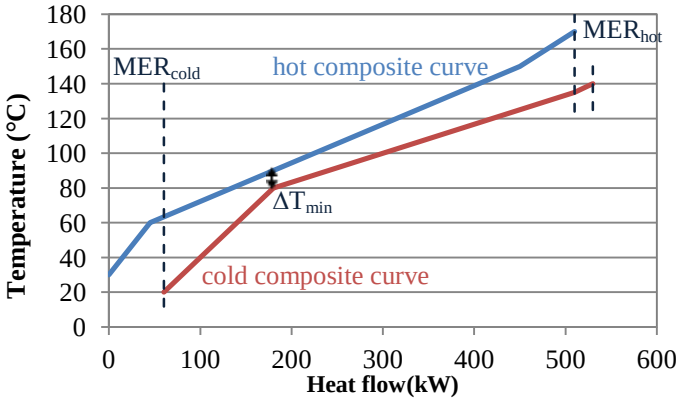


Figure 1.9. Hot and cold composite curves representation

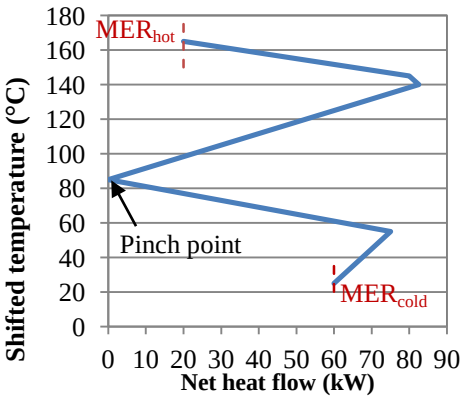


Figure 1.10. Grand composite curve

The main employed tool in the pinch analysis is the composite curves, a single curve for all the process hot streams appointed as the "hot composite curve" (releasing heat) and another for the cold ones, termed the "cold composite curve" (requiring heat), Figure 1.9. The overlap between the two composite curves represents a target for potential heat recovery in a process (Kemp, 2007). The residual heating and cooling in the composite curves represent the external minimum energy supply required for heating (MER_{hot}) and for cooling (MER_{cold}). The point of the smallest vertical distance between the two composite curves, which is equivalent to ΔT_{min} account for the recovery bottleneck and is considered to be the heat recovery pinch (Klemeš, et al., 2013).

The pinch method led to the development of the grand composite curve (GCC) (Townsend & Linnhoff, 1983), Figure 1.10. This latter depicts the temperature profile as a function of the net enthalpy difference between heating and cooling energies. It is plotted using the shifted temperatures obtained by translating down the hot composite curve and up the cold composite curve by $\Delta T_{min}/2$. The temperature corresponding to the null net heat is appointed to as the pinch point of the process. The zone above the pinch presents a heat deficit and that below the pinch is an exothermic zone with cooling demand. The GCC shows the interface between the process and utility system and allows the most suitable utilities combination which must be selected prior to the heat exchangers design.

Extending the thermodynamic approach enabled the synthesis of the heat exchanger network (HEN) which in turn introduced the idea of "downstream paths" illustrating the way disruption propagates in the network (Kotjabasakis & Linhoff, 1986). The HEN synthesis was also developed following the mathematical formulation method, in which the network is generated by the energy cascade model based on LP and MILP (Floudas, et al., 1986). The need to achieve flexibility under variable and uncertain operating conditions has led to the introduction of multi-period operations. This concept allowed altering the designed model pinch point and utility demand periodically (Floudas & Grossmann, 1986). One example of recent developments in multi-period HEN synthesis is a deterministic and stochastic MINLP that accounts for future variability in the utilities price. This study showed that utility consumption could be significantly reduced if future utility prices were to be considered rather than current prices (Nemet, et al., 2012).

Even though these entire considerations are concerned for local integration of processes, the grand composite curve can be easily extended to the site wide scale. Linhoff and Dhole (Dhole & Linnhoff, 1993) introduced the total site analysis method (TSA) to handle energy integration between multiple plants. This method consists in drawing the sources and sinks profiles based on the GCC of each actor participating in the energy exchange and thus subject to energy integration. These profiles are used to determine each industrial site energy requirements prior to the HEN design. Similarly further published studies dealt with energy integration of multiple plants but were based on mathematical programming techniques (MILP) (Maréchal & Kalitventzeff, 1998) (Bagajewicz & Rodera, 2002).

When multiple industrial sites are involved in the energy integration, the total site analysis (TSA), may encounter complexity imposed by the direct energy integration between the streams of each site. Tertiary heating networks provides the means to accomplish the inter-sites heat recovery. Figure 1.11 illustrates an example of a tertiary network developed by Farhat et al. (Farhat, et al., 2014). These authors proposed a methodology for optimal network synthesis while considering the thermodynamic conversion systems. Their work points out the benefit of including such systems, in fact those consolidate energy recovery. Then this work was further elaborated with the proposition of a HEN optimization model (Farhat, et al., 2015) which accounts for both exergy and economic aspects of the heat transfer system. Their economic analysis encompasses the pipelines serving for synergies transportation and thus the sites geographical locations relative to each others.

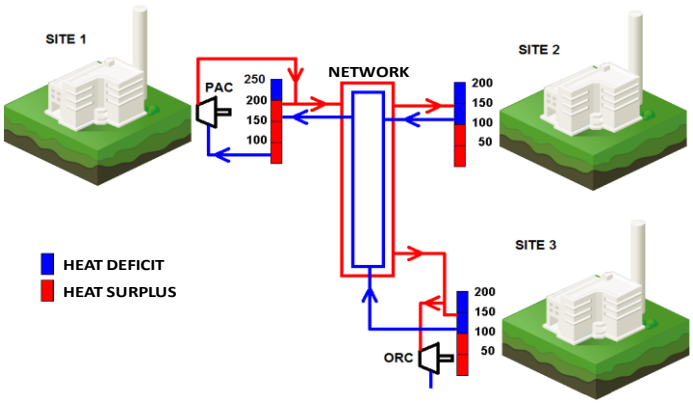


Figure 1.11. Tertiary heat network between three sites (Farhat, et al., 2015)

The composite curves representation can be used whenever a "quantity" (e.g., heat or mass) has a "quality" (e.g., temperature or concentration) (Gundersen, 2013), this fact enables to extend the pinch method to material streams.

1.6.2. Material Integration

Material exchange is the most apparent analogy for energy exchange. Consequently, the developed techniques for energy integration underwent extension towards the optimization of the process material exchange. The basic ideas of the thermodynamic HEN analysis were used to introduce the concept of material allocation networks, in which material rich and poor flow (in contaminants) form the composite curves resulting in a material pinch by analogy to the heat pinch (El-Halwagi & Manousiouthakis, 1989). This two steps systematic methodology is designed to transfer material from a rich stream set to a poor stream set in order to reach the required contaminants concentrations while minimizing waste production and fresh resource demand. In the first step, the pinch points (Material Pinch) which limits the mass exchange between process streams are identified, allowing the preliminary networks generation. The design of this latter is enhanced in the second step in the aim of developing a final network configuration satisfying the affected material synergies at a minimal cost. A significant change in the methodologies of the mass allocation networks synthesis and wastewater discharge minimization was introduced in 1994 (Wang & Smith, 1994).

A graphical approach was proposed for targeting the minimum fresh water consumption and consequently the waste water production, through contaminants transfer from the material flow to the fresh water source, Figure 1.12. This method relies on the principle that concentration is the synergies driving force (El-Halwagi, et al., 2003). The limitations of mass allocation network methods which are developed for minimizing the discharged and the fresh resources have led to a new way for treating the problem through the source and sinks representation (Dhole, et al., 1996). This representation is appointed by the recycling/reuse problem and it consists on assigning different sources (supply) to sinks (demand) so the fresh source consumption is minimized (El-Halwagi & Spriggs, 1998). The graphical representation of this problem is illustrated by two curves of concentration versus flow rate: the first is the source composite curve and the second is that of sinks whose intersection point forms the Material Pinch, Figure 1.13.

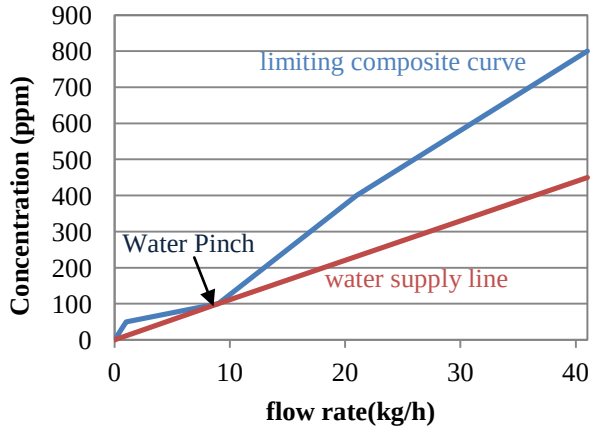


Figure 1.12. Limiting composite curves- water pinch

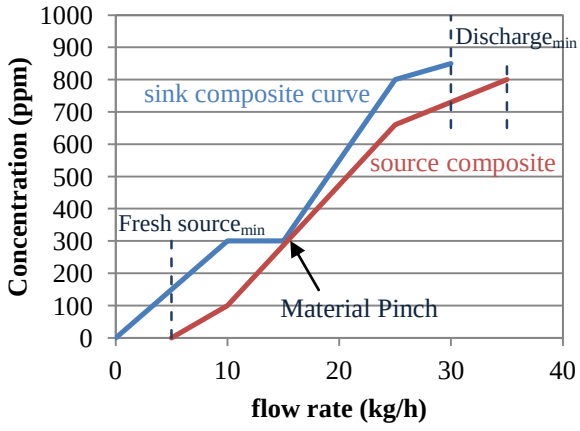


Figure 1.13. Source/sink composite curves

The recycling/reuse based mass integration techniques are limited to the problem governed by the material flows compositions. However process units are not confined just to this criterion but also to the material stream properties such as pH, density and viscosity. Hence the development of a new generic approach based on the key properties evolution in addition to the essential components is presented in (Shelley & M. El-Halwagi, 2000). Unlike chemical components, properties are not maintained and thus cannot be traced throughout the process without conducting material balances for

each component. Therefore to overcome this limitation, properties tracing is carried out through the development of conservative quantities, called 'clusters' which substitute the non-conservative properties. These clusters are designed to maintain two basic rules for conservation within and between streams. This new technique of material exchange network design was subsequently generalized to tackle the properties integration problem (El-Halwagi, et al., 2004). For systems with a single key property, a graph technique based on the pinch method determines the material exchange for minimal use of fresh source, maximum recycling and minimum waste discharge (Kazantzi & El-Halwagi, 2005). The developed work for the material networks and that of the properties have often neglected the temperature effect on the properties. Given the different temperature levels in the process units it becomes primordial to consider this factor since it results in the variation of these levels for material flows (Jiménez-Gutiérrez, et al., 2014) and links both energy and material integration problems.

Alternative approaches to that of the material pinch have been developed to formulate network synthesis methods based on mathematical programming techniques. These studies usually consider the contaminants concentration in the material streams as the main limit to be dealt with for the network design. However, these models are applicable to moderate size problems as combinatorial complexity increases exponentially with the number of material flows (Klemeš, et al., 2013). The first mathematical optimization program based on properties tracing for the mass integration networks synthesis was reported in 2009 (Ponce-Ortega, et al., 2009). For the recycling / reuse problems, mathematical programs which consider several components were also developed (Savelski & Bagajewicz, 2001). One of the recent studies of the material allocation networks design which uses mathematical programming is the approach presented by Ghazouani, et al. (Ghazouani, et al., 2015). The network design problem is formulated by a MILP model whose objective function includes fresh resources, waste streams and utilities leading to the minimization of the annual cost. The sources and sinks composite curves were used to determine the allocation restrictions between the material streams and thus inducing a reduction of the solution's search space. The heat integration of the material streams is conducted simultaneously using an energy cascading model, wherein the temperature scale is discretized in order to linearize the problem. By building a defined temperature scale for the energy cascade model, it become possible to split the main flow into several streams that will first exchange heat through the heat exchanger network and then through their mixture.

The two previously overviewed techniques, which are embedded in the process integration family, allow the identification of potential synergy scenarios whether on the process scale or at the inter-sites level. Subsequently, they design networks to intelligently redistribute energy and material between different sources and sinks to ensure the interchange between the industrial participants. However, these methods may be missing out on prospect synergies as a consequence to the abiding form of the system flows. For further efficient resource management and environmental burden reduction, the alteration of unrecoverable waste is mandatory to introduce them back into the system.

1.7. Motivation for this scientific research

As exhibited earlier, to achieve strongly viable EIP structures with efficient use of resources, the synergistic relationships should be generated by systemic methodologies and tools such as process integration. However, maximizing on-site and inter-sites synergies using exclusively process integration methods implies considering the component valorization in its original form, corollary resulting in missing the reuse opportunities of the component in another form.

Therefore, the scientific objective of this doctoral dissertation is to propose a methodology for integrating energy/material conversion processes based on an intertwined approach between process design and process integration which enables exploring new paths for the recovery of waste streams and bridging the gap between the mass and heat integration methods. The methodology aims on maximizing the circular economy of a territory by searching for the best valorization pathway of non-usable streams and thus converting them to streams which most suit the system's needs. The originality of this work lies within the conversion that brings the possibility of turning the non-usable waste into another usable energy or material through chemical processes resulting in its reinsertion in the system. Therefore higher system efficiency and more rational reuse of resources can be achieved.

1.8. State of the art of Process Design methodologies

The implementation of waste conversion systems to close the material and energy loops aims at reconverting unrecoverable waste and by-products to becoming resources for other processes or industries. The design and synthesis of these synergies can only be achieved after applying process design techniques to systematically identify the optimal flows of the system. Within the context of process design, Hugo, et al. (Hugo & Pistikopoulos, 2005) presented a strategy for optimizing the design of supply chain networks based on a multi-objective mathematical programming enabling the compromise between economic objectives and environmental impact.

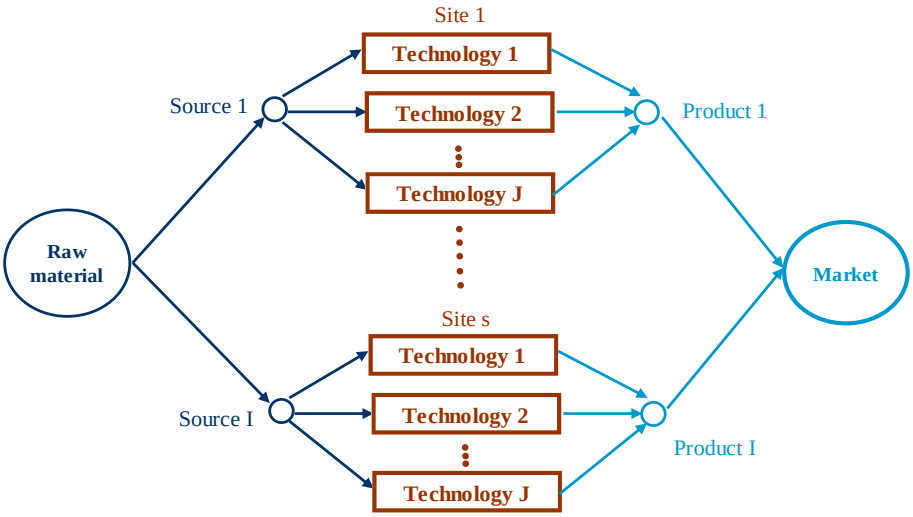


Figure 1.14. The model superstructure of Hugo & Pistikopoulos, 2005

Their proposed methodology, serving as a decision-support tool for environmentally conscious strategic planning and design of supply chain networks, is based on a superstructure. This latter is formed by markets requesting I products with J technologies candidates for the production of these products. Their problem takes into consideration 's' geographical sites locations where the processes are installed, Figure 1.14. After the superstructure construction by the definition of its variables, the multi-objective optimization algorithm generates a set of supply chain solutions. From this set of alternative solutions, a chain is selected based on a compromise between the defined objectives. They illustrated their model capabilities by a case study consisting of two markets both demanding vinyl chloride monomer (VCM) and ethylene glycol (EG). Those are considered to be produced from the raw materials ethylene and chlorine with six potential technology candidates. Their case study showed

how compromise solutions can achieve environmentally conscious supply chain with strategic investment, since an improvement in the environmental performance is only attainable if the decision-maker is willing to compromise the net present value of the investment. Although this approach optimizes the process design while considering several products and several sources, it does not take into account the energy and material integration on both local and territorial scale.

In a similar context, Palazzi, et al. (Palazzi, et al., 2007) have developed a systematic method for the identification of the optimal configuration of an integrated energy system. The heat flows are compiled first using conventional process simulation programs which are based on the system's mass and energy balances. Then, energy integration is conducted on the system level using the Pinch method which generates the heat exchanger network after identifying the minimum energy required by the system. Finally, in order to assess the performance, size and the cost of the system, a thermo-economic model is employed. They applied their developed method to design an optimal fuel cell model (SOFC) using a multi-objective optimization that minimizes the investment cost while maximizing the system efficiency. The search space for this optimization is defined by the decision variables and their limits, Figure 1.15. Their model thus involves a number of state variables consisting of two groups: the decision variables which are set by the user, and the dependent variables that are calculated by solving the model equations. For an optimal system design, the methodology developed by Palazzi, et al. is served by a superstructure formed by multiple alternative choices for each step of the system. This superstructure is constructed subsequently to defining the process steps and conducting a survey of the possible technology options for each of those. However these options consider converting a source into a defined product, Figure 1.16, thus for any chosen pathway the end product is the same. Therefore, the scope of this method is limited to the optimization of a conversion system design which generates a beforehand selected product.

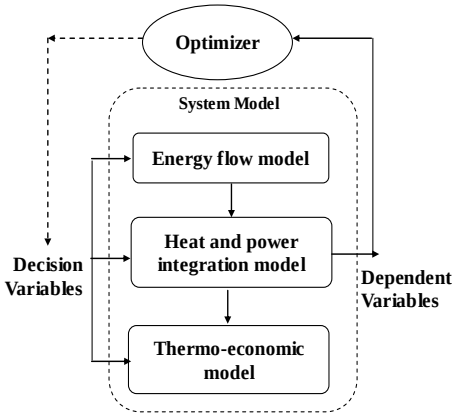


Figure 1.15. Optimization procedure scheme of Palazzi, et al., 2007

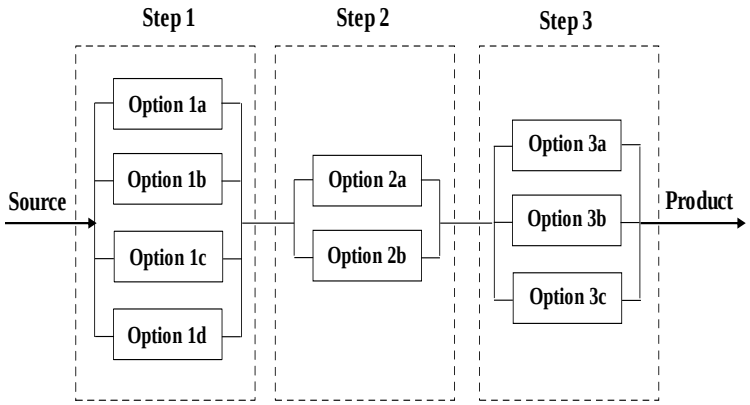


Figure 1.16. Superstructure model of the developed methodology by Palazzi, et al., 2007

Gassner and Maréchal (Gassner & Maréchal, 2009) developed a method based on splitting the problem into several parts, Figure 1.17. First, and after establishing the conversion process block flow diagram, the adapted technologies for each conversion step are identified. Then a set of optimal process configuration is evaluated, while taking into account the design goals, by a multi-objective optimization which evaluates energy flows, energy integration and economic models. Finally, the results are assessed in respect to environmental criteria enabling the identification of the most promising process design.

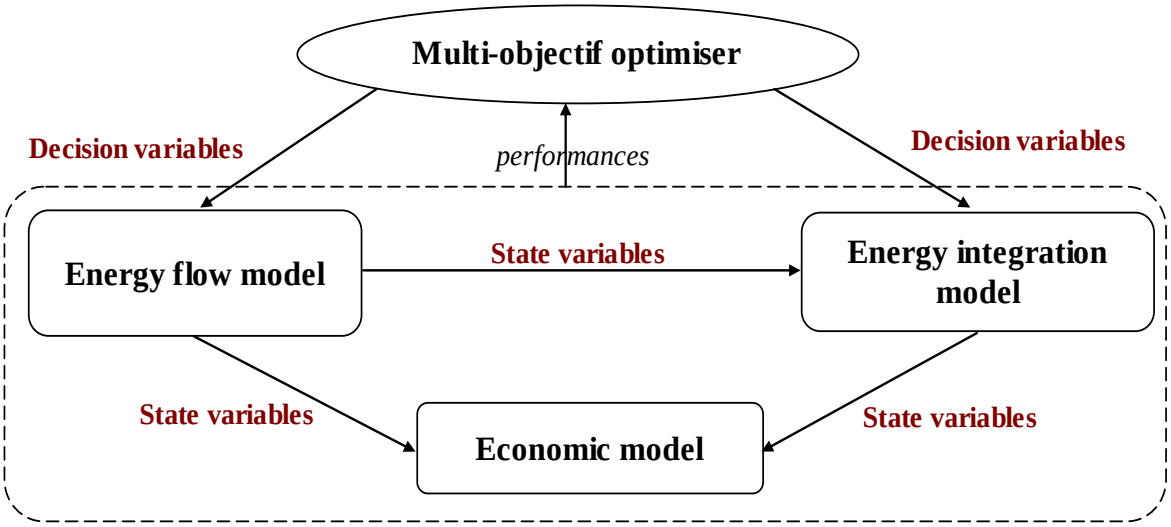


Figure 1.17. Overview of the developed methodology by Gassner & Maréchal, 2009

In their methodology, the construction of the process block flow diagram comes after defining the characteristics of the desired product as well as the available raw material. The definition of the material flow possible pathways and the operating condition intervals, for which the chemical transformations are thermodynamically and technically feasible, allow the identification of the possible technologies for each step resulting in the problem superstructure construction. The technologies operating conditions, set as decision variables, are managed by a genetic algorithm. These decision variables define the energy flow model characteristics which the authors developed using a commercial flow sheeting tool based on an equation solver formulation that does not require a resolution sequence definition. The purpose of the aforementioned model, which is established for every technology forming the superstructure, is to simulate the conversion process units in the aim of determining their heat excess and demand. Once these are defined, the authors employ the heat cascade to design the heat exchanger network (HEN) in the energy integration model.

This latter is formulated as a MILP with constraints imposed by the heat cascade and considers a minimum approach temperature ΔT_{min}. Its resolution allows the optimization of the heat recovery by minimizing either the total exergy variation or the operating costs based on energy integration. Using the composite curves computed from the energy integration model, the cost of the HEN is evaluated in the their developed economic model. As for the equipments costs, they are estimated by size and not capacity based correlations. The multi-objective optimization generates a set of Pareto optimal process configurations based on the performance indicators evaluation. Although this method enables the design of a conversion system optimal configurations, but it addresses the problem on a local system level. Moreover, not only the integration step is limited to the energy aspect and does not include the material integration, but also this approach is intended for the optimal design of a single product conversion process. Therefore this method as elaborated cannot be used in the context of industrial ecology but only at the process design level.

Gerber, et al. (Gerber, et al., 2011) proposed a methodology for integrating life-cycle assessment (LCA) in a thermo-economic model for energy conversion systems optimal design. To perform this approach, they added a new layer to the methodology developed by Gassner and Marshal (Gassner & Maréchal, 2009). In its original form, the performance evaluation was limited to an economic model. Yet, in order to include environmental indicators they have developed a life-cycle analysis model with which they amended the previously developed method, Figure 1.18.

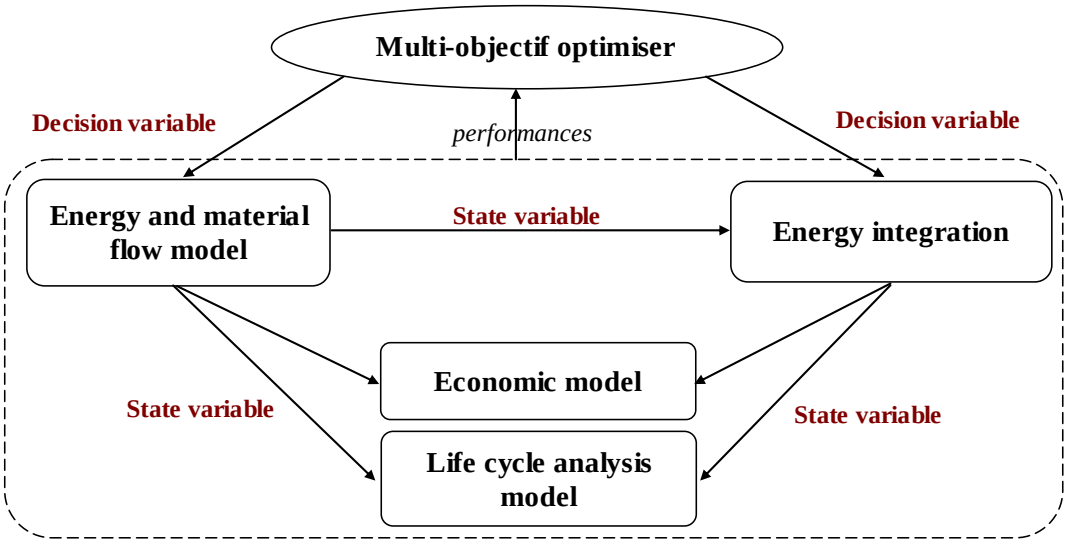


Figure 1.18. Overview of the developed methodology by Gerber, et al., 2011

More specifically, this approach allows the integration of performance indicators which analyzes the life cycle for a multi-objective optimization in order to guarantee the simultaneous inclusion of the thermo-economic and the environmental performance to the designed process. They demonstrated their methodology on a thermo-chemical process generation of SNG (synthesis gas) from biomass, emphasizing the large environmental effect of process integration. In contrast to previously developed methodologies, this methodology considers systems converting a resource to several products and not just into a single one. However it is limited to the energy demand with no regard to materials product. Moreover, this approach does not consider the integration problem at the material scale.

Founded on the same principles, Fazlollahi and Maréchal (Fazlollahi & Maréchal, 2013) have developed process design method with economic and environmental objectives including multi-period energy integration. The aim of this approach is to provide the process energy requirements at minimal cost. Therefore, multi-objective optimization techniques are used to evaluate the design and CO2 emissions of a poly-generation technology. Similarly to previous work, this methodology is based on problem decomposition. It is formulated by a MINLP problem solved by two optimization algorithms. The first algorithm, which controls the second slave problem, encloses the decision variables including the type and optimal dimensions of the available and alternative technologies. These variables are used to define the superstructure of an urban system. The thermodynamic and economic states of the superstructure are then evaluated using a thermo-economic simulation model with the aim of which is to assess the cost, the heat transfer and energy requirements of the selected equipments. These latter along with the available energy sources and the energy consumption profiles are the input data of the second algorithm which solves an energy integration problem formulated as a MILP model. It determines the optimal superstructure technology usage while jointly fulfilling the requirements of the system and minimizing its total cost. Their proposed approach neglects material integration and is applied in the context of energy service production.

Based on previously developed methodologies, Gerber, et al. (Gerber, et al., 2013) worked on developing a new approach of process design while considering industrial ecology, process integration as well as life-cycle assessment. This methodology allows the identification of optimal conversion systems configurations. The followed calculation pattern is illustrated in Figure 1.19. The multi-objective optimization problem attempt to simultaneously minimize costs and environmental impacts

whilst sizing the potential technological units in the superstructure using the decision variables. It is solved with a genetic algorithm (step 1). The processes material and energy flows are generated based on the decision variables defined by a process simulation software and the LCI (life cycle inventory) databases (step 2). The optimization algorithm controls another MILP program which combines mass and energy integration and takes as inputs the flows generated in step 2. This MILP objective is to minimize the operation costs of the system and/or the environmental impacts (step 3). The economic performances are evaluated with a thermo-economic model developed for each process unit (step 4) and the environmental impacts result from the emissions or extractions to or from the environment. In the final step, the optimization objectives are computed over each period, after which they are combined to form the total system performance (step 5). The authors applied their methodology to design of productive system for energy distribution in urban areas. The waste treatment is ensured by different conversion technologies considering both the economic and environmental aspects. While the methodology is promising and enables preliminary system design, but it is not suited for industrial eco-parks. This consists in representing the involved actors' multiplicity.

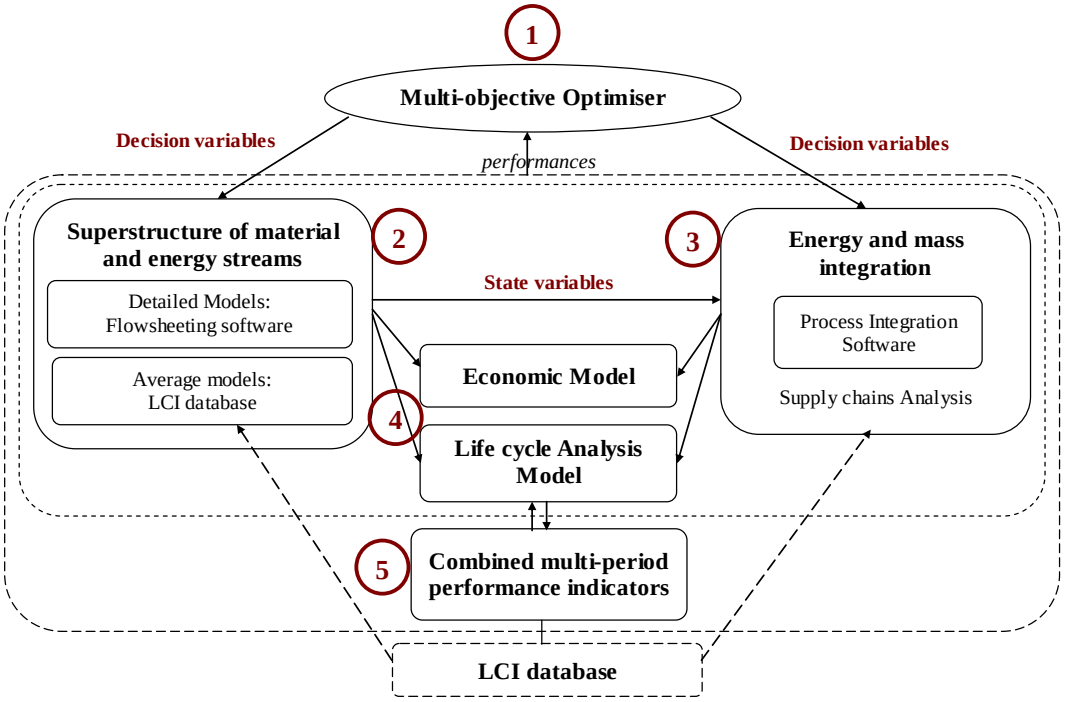


Figure 1.19. Overview of the developed methodology by Gerber, et al., 2013

Table 1.1 summaries the previously investigated methodologies chiefly by their objectives and limitations. From the reviewed state of the art, the developed methodologies in the literature are limited on several aspects. They either do not take into account mass integration and consider only the optimization of one predefined pathway on a local scale, or do not consider the heat transportation networks. Lacking the possibility of identifying economically feasible conversion pathways for the disposed waste of a territory, a need for a methodology to go one step further in closing the loop towards industrial ecology is compelling. This innovative methodology should be capable of addressing energy and material discharge recovery through conversion processes. It should incorporate both process design and process integration techniques on the local and inter-sites levels in the aim of assessing multiple conversion pathways for the unrecoverable wastes; subsequently generating optimal industrial symbiosis configurations with the most suitable conversion system design.

Table 1.1. State of the art summary table of the conversion system integration in a territory

Authors	**Objectives**	**Optimization**	**Scale**	**Limitations**
(Hugo & Pistikopoulos, 2005)	Supply chain design	- minimize environmental impacts - minimize fixed costs	Territorial	Do not consider process integration
(Palazzi, et al., 2007)	Process design from different technologies	- maximize system efficiency - minimize fixed costs	Local	Preselected single product system
(Gassner & Maréchal, 2009)	Thermo-economic process design	Multi-objectives: - maximize electricity production - minimize fixed costs	Local	- Do not consider material integration - Single product system
(Gerber, et al., 2011)	Thermo-economic and environmental process design	- thermodynamic goals - economic objective - environmental goals	Local	Do not consider material integration
(Fazlollahi & Maréchal, 2013)	Multi period Thermo-economic process design	- minimize fixed costs - minimize operating costs - minimize CO_2 emissions	Local	- Do not consider material integration - Targeted products : energy services
(Gerber, et al., 2013)	Process design in industrial ecology and life cycle analysis	- minimize environmental impacts - minimize investment and operating costs	Territorial	Do not consider the energy and material transportation networks

1.9. Scientific ambitions and methodology presentation

The analysis of process integration techniques aiming at finding the optimal synergies between industrial actors revealed the missed reuse opportunities of unrecoverable waste in another form. Furthermore, the state of the art of process design in the industrial ecology context is quite recent and limited. Therefore the main objective of this thesis is to provide a systemic and systematic methodology aiming at closing the energy and material loops by integrating energy/material conversion system in the territory. This methodology should be capable of designing cost-effective conversion pathways for the undesirable waste for them to be reintroduced in the territory and thus mitigate waste generation and resource intake. The achievement of this thesis scientific objectives encounter three prime methodological challenges:

- First, the process design must append multiple conversion systems of a defined waste with different product options. Not only the energy conversion potential of material is investigated, but other conversion alternatives would as well bring the possibility of turning the non-usable waste into another usable material through chemical processes.
- Secondly, process integration should be intertwined with process design for optimal synergies of both energy and material flows at the conversion system scale. At the inter-sites level, territorial process integration is ought to be carried out while accounting for exchanged streams transport networks.
- Third, the developed methodology should deal with two economic scenarios: the first is the conversion system integration in a EIP with cooperative scheme wherein industrial actors barter waste and by-products; and the second is the case of an EIP with non-cooperative scheme in which actors constantly explore strategies to find their own individual interests and hence waste and by-products exchange is accomplished through purchase and selling transactions, Figure 1.20.

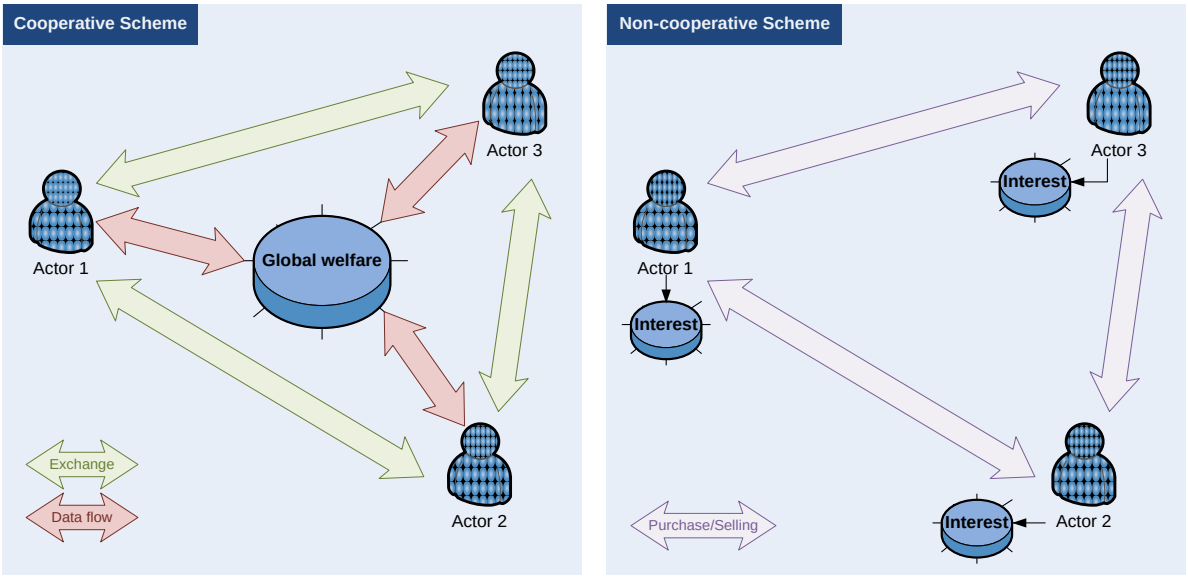


Figure 1.20. Industrial actors exchange in cooperative and non-cooperative schemes

The developed methodology will be able to generate optimal synergies configurations for an EIP encompassing the alteration of unrecoverable waste via conversion systems. To address the first scientific challenge, the conversion processes are selected from a diverse database created for each type of waste while accounting for the territory's topology and activities and thus includes different conversion pathways for the untapped waste.

The methodology is based on three primordial methodological bricks which are process design and both process integration on the system level and on the territorial scale. Consequently, to be able to implement it, each of these bricks must be at disposal. Therefore the first part of Chapter 2 presents the local energy integration and the TSA models selected to be employed from the previously explored state of the art. The methodological approach consists in assembling the bricks of the energy and material integration with the conversion processes for the global problem resolution aiming to identify the optimal pathway of the unrecoverable waste which will be in competition with other alternative conversion.

Even though both cooperative and non-cooperative schemes are founded on the same aforementioned methodological bricks, they consist of entirely different frameworks. That proposed for the cooperative scheme mainly consists of a Master Problem that handles via a combinatorial analysis the operating parameters and technological design options of the conversion processes for it to ensure examining simultaneously the feasibility conditions as well as the economic and energetic relevance of the conversion possibilities. This Master Problem manages the two slave problems of local and territorial process integration. Consequently this Master-slave model ensures the intertwined aspect raised in the second scientific challenge.

However in an environment wherein industrial actors exhibit individual interests, a top-down centralized mechanism is no longer valid. Therefore, the integration of conversion systems in a territory with self-interested actors requires a different framework. An agent based model is thus proposed to formulate the problem in which the chosen coordination technique is negotiation. This latter work flow is developed to ensure optimal synergies creation for an equilibrium purchase and selling transactions. The methodological frameworks for integrating conversion systems in a territory in both cooperative and non-cooperative economic schemes are introduced in the second part of the following chapter.

Subsequent to the definition of the case study that will serve for the demonstration of the developed methodologies, the conversion processes of the identified unrecoverable waste are censused and then formulated in their physical and economical models. The case study presentation and the conversion systems modeling are presented in Chapter 3.

The last chapter serves as the demonstration of the two developed methodologies framework. This is carried out by applying the two proposed frameworks on a case study consisting of a virtual industrial park. Building the database for a defined waste entails process modeling for each conversion system which is burdenly time consuming, whereof for the scope of this thesis woody biomass effluent is appointed to be the unrecoverable waste of the territory. Consequently, the elaborated conversion processes in Chapter 3 correspond to wood conversion systems.

Chapitre 2 (résumé)

Cadres méthodologiques pour l'intégration des procédés de conversion dans un territoire

Un système de conversion est un ensemble de processus réactifs et/ou non-réactifs qui consistent à convertir une matière première en un produit désiré. Dans les procédés non-réactifs, la composition chimique de l'ensemble du système est considérée comme inchangée. Les pompes à chaleur, par exemple, transfèrent la chaleur thermique en l'absorbant à partir d'une source de chaleur et en la libérant dans un puits de chaleur en utilisant une source d'énergie externe sans l'occurrence de réactions chimiques. C'est également le cas des unités de régénération et de mélange au cours desquelles de nouveaux flux sont formés par mélange homogène ou séparation physique en absence de toute transformation chimique. Cependant, les processus réactifs impliquent la destruction et la formation de liaisons chimiques entraînant un changement de composition chimique.

Les techniques d'intégration d'énergie consistent à limiter la demande de chaleur du procédé ou du territoire par la maximisation des synergies internes. Ces techniques renforcées par l'analyse exergétique peuvent encore améliorer l'efficacité énergétique globale en employant des systèmes de conversion de chaleur tels que les pompes à chaleur, le cycle de Rankine organique et les systèmes de réfrigération par absorption. Ceux-ci améliorent la qualité du flux de chaleur inexploitée en élevant sa température ou en la convertissant en énergie électrique pour qu'elle soit réutilisée dans d'autres procédés. De façon analogue, les techniques d'intégration matière visant à réduire la demande de ressources en maximisant l'échange interne des déchets peuvent intégrer des systèmes de traitement des flux matières (e.g., des unités de régénération et des unités de mélange) pour étendre les possibilités de synergies. Par conséquent, les techniques d'intégration d'énergie et de matière tentent de rechercher la valorisation de l'énergie, des coproduits et des déchets simplement dans leur composition d'origine.

En absence de la demande d'un coproduit ou d'un déchet (e.g., les eaux usées) pour pouvoir être réutilisé dans le territoire, même s'il passe par des systèmes de traitement, aucune intégration possible de ces déchets n'est possible. Cependant, changer sa composition chimique grâce à des procédés réactifs (e.g., des photo-bioréacteurs) lui offre de nouvelles possibilités de récupération dans une nouvelle composition (e.g., la biomasse des algues). Par conséquent, l'optimisation des synergies sur site et entre sites en utilisant exclusivement des méthodes d'intégration de processus implique de manquer les opportunités de réutilisation du composant sous une autre forme. L'intégration de procédés réactifs au problème initial étend les possibilités de synergies en intégrant des flux non utilisables dans une nouvelle composition dans le système. Par la suite, avec la réutilisation rationnelle

des ressources et de l'énergie, l'économie circulaire d'un territoire est stimulée, ce qui peut directement améliorer les performances économiques et environnementales.

La méthodologie proposée traite spécifiquement l'intégration des systèmes de conversion réactifs dans un territoire en utilisant une approche imbriquée entre la conception des procédés et l'intégration du procédé. Pour mettre en œuvre cette méthodologie, deux régimes économiques sont distingués: coopératif et non coopératif. Dans un territoire régi par un régime coopératif, les acteurs industriels sont censés travailler ensemble pour le bien-être global. Ainsi, l'exécution de chaque synergie identifiée est assurée en communiquant les flux d'énergie et de matériaux associés et génère une facture économique unique pour l'ensemble du parc. Cependant, dans un schéma non-coopératif, les participants industriels du parc manifestent des intérêts individuels et n'acceptent donc pas l'échange de leurs flux sauf s'ils croient qu'il sera plus rentable pour eux de s'engager dans la synergie que sans d'y participer. Les variabilités significatifs entre les deux schémas expliquent la nécessité de deux cadres méthodologiques différents. Alors que l'intégration du schéma coopératif est formulée en utilisant une approche maître-esclave, le schéma non coopératif peut être difficile à contrôler avec un mécanisme top-down centralisé. La modélisation orientée agents est donc utilisée pour développer la méthodologie d'intégration des procédés de conversion dans un territoire à schéma non-coopératif. Même si deux cadres distincts sont développés pour chaque système, ils sont tous deux basés sur la conception de procédé, l'intégration de procédé local et l'intégration territoriale. Les modèles utilisés dans cette thèse en tant que briques méthodologiques d'intégration ont été sélectionnés en se basant sur une étude de l'état de l'art.

Intégration des systèmes de conversion dans un territoire régi d'une gouvernance coopérative

Dans un territoire régi par une gouvernance coopérative, les acteurs industriels dans une proximité géographique essaient de réaliser un objectif commun en coopération. Ils participent mutuellement à créer et favoriser des synergies potentielles en partageant également les frais de leurs mise en place ainsi que les bénéfices générés. Une telle gouvernance peut être le cas d'un territoire idéal dans lequel un seul investisseur (i.e., le Gouvernement) prend en charge les coûts d'installation des réseaux et les gains sont distribués aux acteurs qui ont participé à la récupération ou à la réorientation des ressources pour réutilisation. Le cas de figure qui est plus réaliste pourrait être le cas d'une entité industrielle avec plusieurs unités impliquées; l'industrie met ainsi en œuvre les synergies identifiées entre ses unités pour améliorer ses activités ou ses procédés. Par conséquent, l'intégration des procédés de conversion dans un territoire à gouvernance coopérative nécessite une structure de contrôle centralisée qui régit le comportement du système.

Le premier élément constitutif du problème est l'identification des acteurs localisés dans les limites géographiques du territoire et qui recherchent des performances améliorées par collaboration. En utilisant les données des acteurs industriels, une intégration énergétique territoriale et une intégration de matière sont lancées pour trouver la configuration d'échange potentielle entre les acteurs collaboratifs. Le schéma d'échange qui en résulte révèle les possibilités limitées de récupération d'un flux de matière O_i^z de $Site_i$. Les flux de matières inutilisables dans leur forme initiale sont les flux déchets W du territoire. Les flux déchets identifiés dans l'ensemble W sont ensuite ciblés dans le but d'élaborer un inventaire constitué des éventuels procédés de conversion de ces flux qui permettront de les réintroduire dans le territoire sous une nouvelle forme. A partir de cet inventaire, les systèmes de conversion jugés d'intérêt et les plus adaptés aux besoins de chaleur et de matière du Territoire sont sélectionnés et introduits dans un nouvel ensemble CS.

Chaque CS^z_k est formulé par un modèle physique basé sur les bilans énergétique et massique de ses unités de procédés et par un modèle économique dépendant des paramètres de conception des composants du système. L'évaluation de ces modèles permet de définir le degré de liberté des systèmes de conversion en termes de paramètres de fonctionnement et d'options de conception technique. Par la suite, un ensemble de variables souveraines SV^z_k est introduit pour tout CS^z_k formé par les variables $SV^z_{k,l}$ qui définit son degré de liberté et dont chacune est délimitée par des limites inférieure et supérieure. La collection des variables souveraines pour l'ensemble des éléments CS est manipulée par un problème maître pour créer la superstructure du problème constituée de tout les chemins potentiels de conversion des flux non-utilisables et de chaque voie ses propres variables souveraines se ramifient.

Le problème maître manipule la superstructure pour créer des scénarios potentiels du territoire réel avec une voie de conversion possible pour chaque flux de déchets identifié. Il choisit une voie pour transformer le flux de matière z en choisissant d'abord un système thermodynamique CS^z_k de CS puis en agissant sur l'une de ses variables souveraines $SV^z_{k,l}$ en respectant ses limites supérieure et inférieure pour créer le $q^{ème}$ ensemble de paramètres pour le $k^{ème}$ système de conversion de matériel z, set_q. Une fois que toutes les variables du $k^{ème}$ système de conversion et leurs plages sont adoptées et prises en compte dans une génération de scénario antérieure, le problème maître passe à une nouvelle voie de conversion pour le flux de matière z, CS^z_{k+1} et maintient cette configuration jusqu'à ce qu'il ne reste plus de chemin.

Lorsque l'ensemble des scénarios prospectifs est généré par les combinaisons créées à l'aide de la superstructure des chemins de conversion, la tâche du problème maître consiste désormais à évaluer un objectif commun défini pour chacun de ces scénarios à travers une intégration simultanée d'énergie et de matière. Ce qui permettra d'identifier les configurations de synergies optimales et les paramètres de fonctionnement et de conception des meilleurs systèmes de conversion à implanter sur le territoire.

Le problème maître gère deux problèmes esclaves dans le but d'atteindre l'objectif visé. Le premier est le problème d'intégration locale et le second est le problème d'intégration au niveau territorial. La conception des échangeurs de chaleur des deux problèmes sont effectuées simultanément pour assurer la convergence vers un compromis optimal entre les synergies locales des flux du procédé et les opportunités d'échange entre-sites. La Fig. 1 illustre le cadre de calcul du problème maître-esclave pour l'intégration de procédés de conversion dans un territoire régi d'une schéma coopératif.

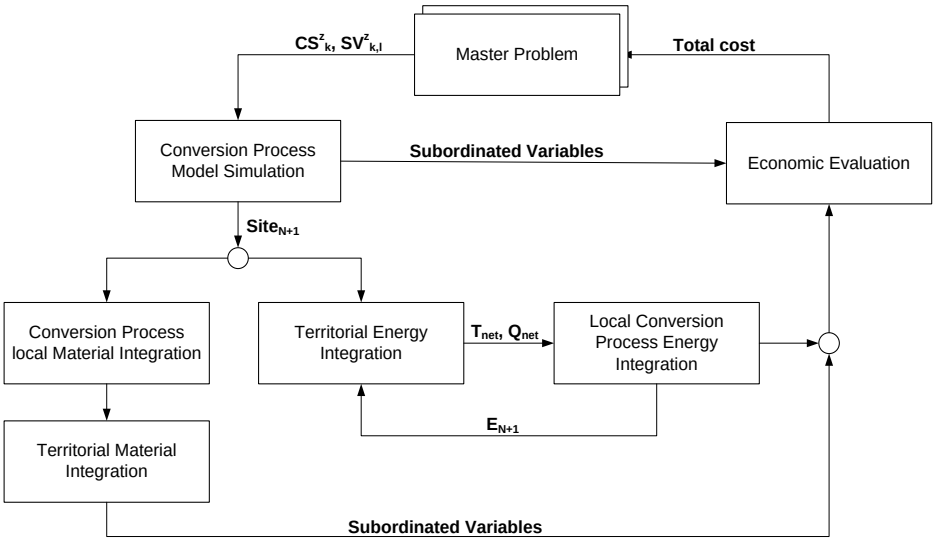


Fig. 1. Cadre de calcul du problème Maître-Esclave pour l'intégration des systèmes de conversion dans un territoire régi d'une gouvernance coopérative

Le cadre méthodologique proposé pour un schéma coopératif génère les coûts globaux fixes et variables induits des configurations de synergies optimales de plusieurs scénarios prospectifs du territoire réel avec les voies de conversion mises en œuvre. Par conséquent, il permet l'identification de la meilleure conception ainsi que les spécifications techniques des scénarios de conversion des flux non-utilisables.

Intégration des systèmes de conversion dans un territoire régi d'une gouvernance non-coopérative

Le deuxième cadre méthodologique a été proposé pour la conception d'éco-parc industriel régi par une gouvernance non-coopérative. Contrairement au schéma coopératif où l'intérêt global du territoire est recherché par les acteurs industriels du parc, dans la gouvernance non-coopérative, chaque acteur cherche à maximiser ses intérêts individuels. Par conséquent, la non-linéarité des activités agrégées des différents acteurs, entraîne la complexité de la formulation du problème en utilisant un mécanisme centralisé avec un seul objectif. La modélisation à base d'agents a donc été choisie pour modéliser et simuler le problème dans le but de prendre en compte plusieurs agents hétérogènes ayant chacun sa propre fonction objective et agissant et réagissant au comportement de l'autre. L'interaction entre les agents a été établie en utilisant les mécanismes de négociation pour assurer la coordination entre leurs actions, Fig. 2.

Trois types d'agents ont été définis: agent investisseur réseau (NI), agent industriel (IA), agent potentiel (PA). Ces agents sont capables de contrôler leur propre comportement, chacun agissant dans la poursuite de ses propres objectifs tout en interagissant les uns avec les autres dans un territoire partagé. L'agent investisseur du réseau négocie avec les deux autres agents pour échanger des flux d'énergie et de matières par le biais de négociations bilatérales, conformément au protocole d'offres alternées. Il prend en charge l'investissement et les coûts d'installation des pipelines qui assurent le transport des flux de matières et d'énergie intersites. Chaque industrie dans les limites prédéfinies du territoire est un agent industriel IA_i qui appartient à l'ensemble d'agents industriels IA. Le nombre total de sites existants est noté n. Le troisième type d'agent est l'agent potentiel PA_{ik} qui est un élément de PA contenant l'ensemble des agents potentiels. Comme son nom l'indique, PA_{ik} est un acheteur potentiel des déchets W_i de IA_i. Ce type d'agents n'existe pas sur le territoire.

Pour chaque déchet non-utilisable qu'un agent industriel rejette, une vente aux enchères unilatérale basée sur l'enchère anglaise est tenue avec l'agent industriel étant le commissaire-priseur et les agents potentiels comme la collection des soumissionnaires dans le but d'attribuer les déchets au soumissionnaire avec l'offre la plus élevée. Les agents potentiels font référence aux systèmes thermodynamiques réactifs possibles qui peuvent modifier la composition initiale des flux déchets et les convertir en nouveaux produits qu'ils pourraient ensuite vendre à d'autres acteurs industriels du parc. Les agents potentiels du même déchet se font d'abord concurrence pour échanger W_i avec IA_i et ensuite le gagnant identifié investit dans un système de conversion pour transformer la forme originale de W_i en un nouveau produit à vendre dans le parc. Donc ce gagnant, comme il est ajouté au territoire, devient un agent industriel IA_{n+1}. L'investisseur du système de conversion peut également communiquer avec l'investisseur du réseau pour acheter ou vendre de la chaleur ou de la matière à partir du réseau.

La méthodologie proposée permet l'établissement des décisions stratégiques à mettre en œuvre par chaque agent cherchant son propre intérêt dans un territoire à gouvernance non-coopérative en identifiant les prix d'équilibre des flux d'achat et de vente entre agents.

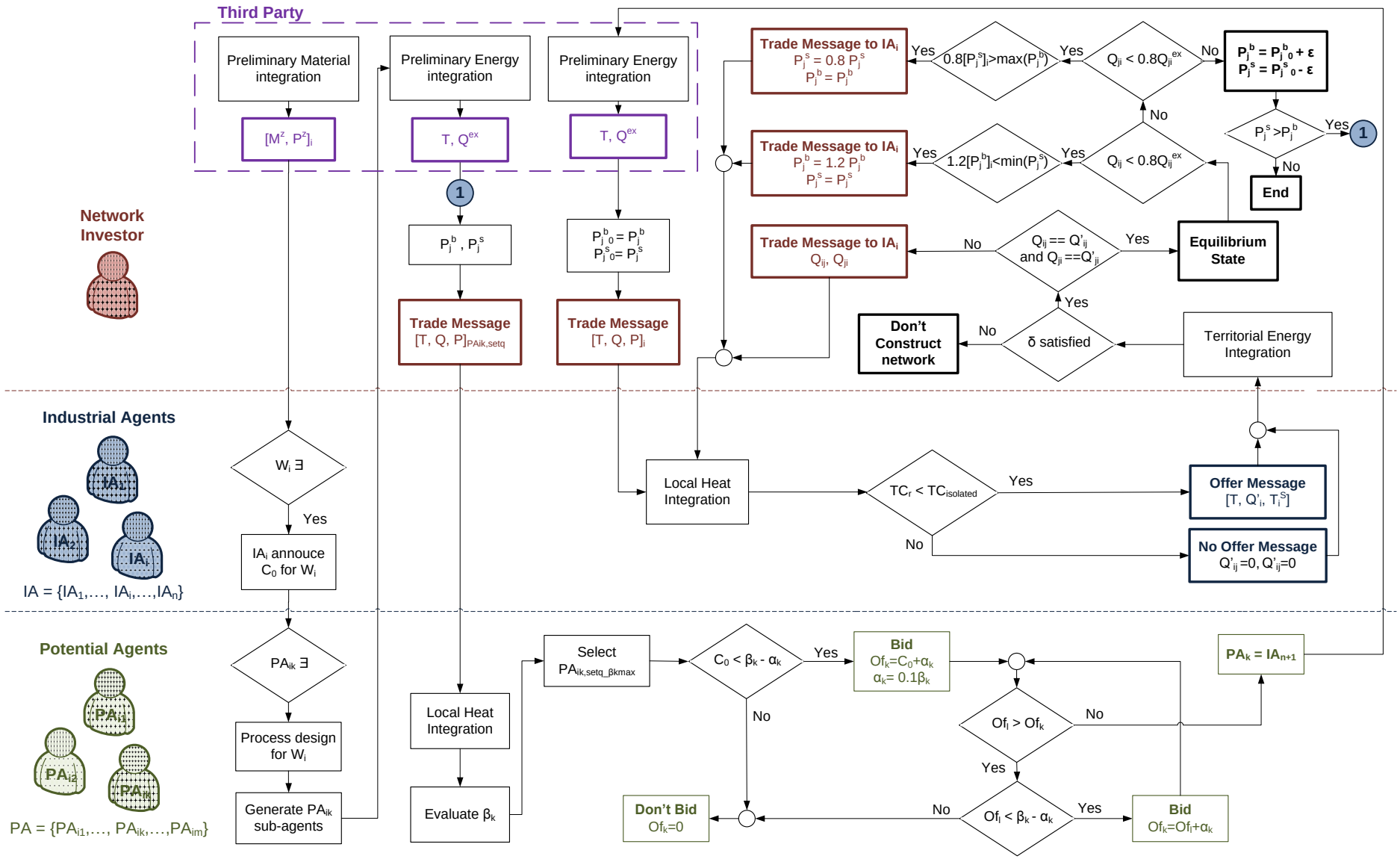


Fig. 2. Le workflow d'interaction des agents pour l'intégration des systèmes de conversion dans un schéma non-coopératif

Pour explorer les résultats potentiels qui pourraient découler des deux méthodologies, le chapitre suivant présentera l'étude de cas sur laquelle les cadres méthodologiques proposés seront appliqués. A partir de l'évaluation préliminaire du territoire étudié, les flux irrécupérables seront identifiés. Par la suite, le chapitre 3 explorera les systèmes de conversion des déchets identifiés et présentera les modèles physiques et économiques des unités de processus de chaque voie de conversion sélectionnée.

Chapter 2

Methodological Frameworks for Conversion Systems Integration in a Territory

In the preceding chapter, the contextual components behind the motivation of this thesis were presented. The state of the art investigated in the previous chapter has shown to be lacking a systematic methodology for the integration of conversion systems in a territory to closing the energy and material loops. This result motivated the work done in this thesis. Subsequently, it helped defining the scientific ambitions of this work as being to develop a systematic methodology for guiding the design of cost-effective conversion pathway for the non-usable waste of a territory in its original form which make up the topic of this chapter.

First, the definition of conversion systems is introduced to unravel the type of processes this thesis aims to integrate in a territory. Three methodological bricks are judged to form the basis for the intended methodology development. Those are process design, process integration and inter-sites integration. The models to be employed for material integration and energy integration on both process and inter-sites levels are selected from the state of the art research work. Their overarching philosophies are explored before attacking the methodology construction. This latter is carried out by distinguishing cooperative and non-cooperative governing economic schemes.

With collaborative scheme governance, industrial actors seek to achieve cooperatively a shared common goal. Even though each actor may have different individual targets, their primary motivation is the social welfare maximization which consists of the sum of the entire individual profits associated to a given objective. In contrast, in a territory with non-cooperative scheme industrial actors are self-interested. They search to maximize their individual interests irrelevantly of the welfare of the territory and thus they only participate in implementing an agreement if it contributes in increasing their individual interests.

The substantial differences between a territory governed by a cooperative or a non-cooperative economic schemes entail the necessity of distinct methodological frameworks to integrate conversion processes. Consequently, for each type of those governance schemes a methodology is proposed in the aim of accomplishing the main objective of this thesis. For a cooperative scheme, the problem is formulated as a Master-slave mechanism. The complexity tied to self-interested actors is explored and the utilization of multi-agent system modeling for non-cooperative scheme is justified. The possible coordination techniques that enable the agents to mutually achieve their goals are then presented. The negotiation technique is furtherly detailed since it is selected as the agents' coordination mechanism.

2.1. Problem Statement

A conversion system is a set of reacting and/or non-reacting thermodynamic processes that consist in converting a raw material into a desired product. In non-reacting thermodynamic processes, the chemical composition of the entire system is considered unchanged. Heat pumps for instance transfer thermal heat by absorbing it from a heat source and releasing it to a heat sink using an external power source without the occurrence of chemical reactions. This is also the case of regeneration and mixing units during which new streams are formed by homogeneous mixing or physical separation in the absence of any chemical transformation. Whereas reacting thermodynamic processes involve the destruction and formation of chemical bonds ensuing a chemical composition change.

Energy integration techniques consist in limiting process or territory heat demand through internal synergies maximization. These techniques reinforced with the exergy analysis can further improve the overall energy efficiency by employing heat conversion systems such that heat pumps, Organic Rankine Cycle and absorption refrigeration systems. Those upgrade the untapped heat flow value through elevating its temperature or converting it into electric power for it to be reused in other processes. Analogically, material integration techniques aiming to reduce resource intake by maximizing internal waste exchange may integrate material treatment systems (e.g., regeneration and mixing units) to extend the synergies possibilities. Consequently, both energy and material integration techniques attempt to search for valorizing energy, by-products and waste merely in their original composition.

When no demand of a by-product or a waste (e.g., wastewater) exist for it to be reused, even with it going through treatment systems, no possible integration of that waste is feasible. However, changing its chemical composition through reacting thermodynamic processes (e.g., photo-bioreactors) offers new opportunities for it to be recovered in a new composition (e.g., algae biomass). Therefore, maximizing on-site and inter-sites synergies using exclusively process integration methods implies missing the reuse opportunities of the component in another form. Integrating reacting thermodynamic systems to the initial problem extends the synergies possibilities by embedding non-usable streams in a new composition into the system. Subsequently, with the rational reuse of resources and energy the circular economy of a territory is boosted which can directly improve economic and environmental performances.

The proposed methodology specifically deals with integrating reacting conversion systems in a territory using an intertwined approach between process design and process integration. In order to implement this methodology, two governing economic schemes are distinguished: cooperative and non-cooperative. In a territory governed by a cooperative scheme, industrial actors are supposed to work together in the furtherance of the global welfare. Hence, the execution of each identified synergy is ensured by imparting the associated energy and material streams and generates one economic bill for the entire park. However, in a non-cooperative scheme, the industrial participants of the park manifest individual interests and thus only accept trading their streams if they believe that it will be more profitable for them to engage in the synergy than it would be without participating. The significant interspaces between the two schemes explain the need for two different methodological frameworks. While the cooperative scheme integration is formulated using a Master-slave approach, the non-cooperative scheme can be difficult to control with a top-down centralized mechanism. Agent-based modeling is thus employed to develop the methodology for integrating conversion processes in a territory with non-cooperative scheme. Even though two distinct frameworks are developed for each scheme, they are both based on process design, local process integration and inter-sites integration. The employed models in this thesis as the integration methodological bricks were selected from the state of the art and they are explored and detailed in the following section.

2.2. The Energy and Mass Integration Methodological Bricks

2.2.1. Process Heat Integration

Local process integration aims at achieving optimal synergies for both energy and material flows at the process scale. Local energy integration is a holistic approach that takes advantage of potential interactions amongst the process units to maximize heat recovery and thus minimize energy consumption. The heat exchanger network synthesis (HENS) manifests as the key step to implement the identified synergies for a given process. It ensures economically optimal design that enables reaching the minimum energy targets computed by the pinch analysis (cf §1.6.1). The limitations tied to the manual calculation procedure that employs the well-known HENS methodologies based on the pinch analysis led to the development of mathematical programming alternatives.

These latter can either be formulated using sequential or simultaneous solving strategies. While sequential techniques consist on partitioning the HENS problem, simultaneous methods search for optimal design by solving the entire problem at once. Not decomposing the problem might require using non-linear formulations which may lead to numerical resolution difficulties and for a non-convex problem the resulting solution is probably the local and not the global optimum. Nonetheless, linearizing the problem mainly by creating a discrete temperature scale and approximating the heat exchangers area computation enables employing linear programming optimization techniques to perform a simultaneous resolution of the problem without encountering the non-linear numerical difficulties.

Many models using the linearization techniques have been developed in the aim of designing realistic heat exchanger network. Among recent works, the mixed-integer linear (MILP) model that have been proposed by Barbaro & Bagajewicz and which enables the approximation of the heat exchanger areas while handling stream splitting, non-isothermal mixing and permitting multiple matches between two streams (Barbaro & Bagajewicz, 2005). The extension of this MILP was carried out by the research work lead by Zoughaib (Zoughaib, 2017) to additionally feature the incorporation of multiple heat exchanger technologies. Their model was selected to be employed as the local energy integration model in this thesis and is presented thereafter.

Mathematical formulation of the selected energy integration model for HENS

To outline the general philosophy of the HENS, the employed sets throughout the model are first explored. A set of heat transfer zone is established, that is $Z= \{z \mid z \text{ is a heat transfer zone}\}$, to enable handling imposed heat transfer restrictions by the designer from certain intervals to others. Moreover this set allows separating the design in multiple sub-networks thus simplifying the problem complexity. Streams are distinguished between process and utility stream. While a process stream have its inlet and outlet temperature and the mass flow rate fixed, only the temperatures of a utility stream are fixed and its flow rate varies to satisfy the energy demands of the process streams. In order to identify hot, cold streams, and heating, cooling utilities, the following listed sets are employed.

$H^z=\{i|i \text{ is a hot stream in zone z}\}$

$C^z=\{j|j \text{ is a cold stream in zone z}\}$

$HU^z=\{i|i \text{ is a heating utility present in zone z}\}$ $(HU^z \subset H^z)$

$CU^z=\{i|i \text{ is a cooling utility present in zone z}\}$ $(CU^z \subset C^z)$

The temperature scale is partitioned into several intervals in each zone to ensure the linearity of the problem. It is constructed by first considering the angular points of the GCC (grand composite curve), because using the shifted temperatures is equivalent to imposing that no exchange is possible unless the hot stream's temperature is higher than that of the cold stream by ΔT_{min}. Then the temperature partition is submitted to the three following steps:

- The designer sets a maximal temperature step $\Delta T_{max}^{partition}$ which implies halving any higher temperature interval until the entire sub-intervals respect this parameter.
- Following the first partition step, if a stream does not have at least one internal interval, it is divided into three equally distributed intervals.
- After these two steps, if the total intervals number is less than a minimum value set by the designer, the biggest intervals are halved until reaching the desired number.

The upper and lower temperatures of interval m are appointed to respectively as T_m^U and T_m^L. Furthermore, different sets of the problem related to the temperature intervals are defined as follow:

M^z={m | m is a temperature interval in zone z}
M_i^z={m | m is a temperature interval belonging to zone z, in which hot stream i is present}
N_i^z={n | n is a temperature interval belonging to zone z, in which cold stream i is present}
H_m^z={i | i is a hot stream present in temperature interval m in zone z}
C_n^z={i | i is a cold stream present in temperature interval n in zone z}

Moreover, a number of sets is introduced for the designer to fix the permitted heat transfer connections between the defined cold and hot streams:

P={(i , j) | a heat exchange match between hot stream i and cold stream j is permitted}
P_{im}^H={i | heat transfer from hot stream i at interval m to cold stream j is permitted}
P_{im}^C={j | heat transfer from hot stream i to cold stream j at interval n is permitted}

Using the temperature intervals, the model, which is actually based on the transshipment-transportation paradigm, is able to generate the energy and flow balances. The heat exchange between a hot stream i and a cold stream j in zone z is adduced in Figure 2.1, in which at each interval in z $q_{im,jn}^z$ accounts for the heat transferred from interval m of i to interval n of j.

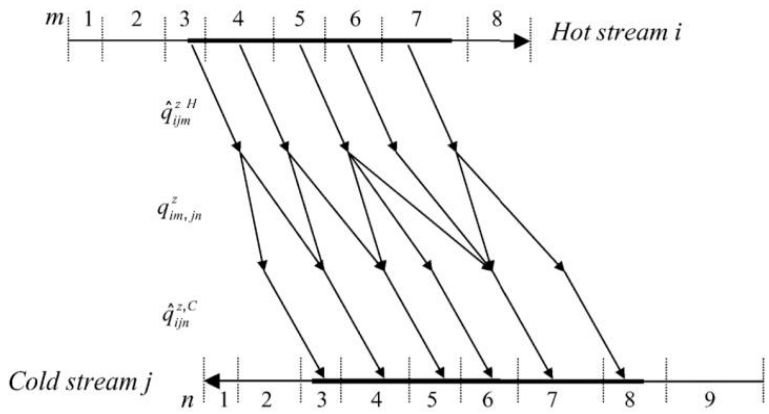


Figure 2.1. Basic scheme of the transshipment model (Barbaro & Bagajewicz, 2005)

The heat balance equations for hot utilities and hot process streams are expressed respectively in Eq.(2.1) and Eq.(2.2); wherein F_i^H denotes for the flow rate of the hot utility stream i and $\Delta H_{im}^{z,H}$ is the enthalpy variation for hot stream i at interval m in zone z. By analogy, the heat balances of the cold utility and cold process streams can be easily acquired. Notice that for process streams the enthalpy variations are accounted as parameters since they are easily computed with their temperature intervals and flow rate which are fixed with the definition of the problem. However, the flow rates of the utility streams are variable as mentioned earlier and will be optimally determined by the model.

$$F_i^H\left(T_m^U - T_m^L\right) = \sum_{\substack{n\in M^z \\ T_n^L < T_m^U}} \sum_{\substack{j\in C_n^z \\ j\in P_{im}^H \\ i\in P_{jn}^C}} q_{im,jn}^z \qquad z\in Z;\ m\in M^z;\ i\in H_m^z;\ i\in HU^z \tag{2.1}$$

$$\Delta H_{im}^{z,H} = \sum_{\substack{n\in M^z \\ T_n^L < T_m^U}} \sum_{\substack{j\in C_n^z \\ j\in P_{im}^H \\ i\in P_{jn}^C}} q_{im,jn}^z \qquad z\in Z;\ m\in M^z;\ i\in H_m^z;\ i\notin HU^z;\ i\notin NI^H \tag{2.2}$$

To account for multiple heat exchanger technologies a new set is defined, namely $T=\{t \mid t \text{ is an available technology}\}$. A correlation factor $FHEX_t$ representing the efficiency of technology t compared to the counter-current reference heat exchanger is introduced for a more realistic design. The required heat exchanger area that enables the heat transfer between hot stream i and cold stream j is computed according to Eq.(2.3); in which h_{im} and h_{jn} are respectively the film heat transfer coefficients for hot stream i at interval m and cold stream j at interval n, and the ΔT_{mn}^{ML} is the mean logarithmic temperature difference between intervals m and n (pre-calculated parameter since the temperature boundaries of the intervals are known).

Practically, a single exchanger shell can encompass a limited heat transfer area. In order to take this constraint into consideration, a maximal area $A_{ijt\,max}^z$ is set by the designer for each pair of streams i and j. An integer variable U_{ijt}^z is employed to define the existence or not of the appropriate heat exchanger following the relation: $A_{ijt}^z \le A_{ijt\,max}^z U_{ijt}^z$.

$$\sum_{t\in T_{ij}} A_{ijt}^z FHEX_t = \sum_{m\in M_i^z} \sum_{\substack{n\in N_j^z;\ T_n^L < T_m^U \\ j\in P_{im}^H; i\in P_{jn}^C}} \frac{q_{im,jn}^z (h_{im}+h_{jn})}{\Delta T_{mn}^{ML} h_{im} h_{jn}} \qquad z\in Z;\ i\in H^z;\ j\in C^z;\ (i,j)\in P \tag{2.3}$$

A new set P_t is introduced to allow or forbid, for each heat exchanger technology, a heat transfer matching between two streams. It is defined as: $P_t = \{(i,j) \mid \text{a heat exchange match between hot stream i and cold stream j via technology t is permitted}\}$. By that the heat exchanger area A_{ijt}^z is either null if $(i,j) \notin P_t$ or has a positive value if (i,j) are included in P_t.

The objective function of the local heat integration problem is to minimize the total cost engendered from the installation of the identified synergies in the process. The total cost, which is expressed in Eq.(2.4), includes the heat exchanger costs and the employed utilities to cover the remaining surplus heat and energy deficit after the synergies establishment.

$$\min: \text{cost} = \sum_{z\in Z}\sum_{i\in HU^z}(c_i^{HF}B_i^z + c_i^H F_i^H \Delta T_i) + \sum_{z\in Z}\sum_{j\in CU^z}(c_j^{CF}B_j^z + c_j^C F_j^C \Delta T_j) + \sum_{z\in Z}\sum_{i\in H^z}\sum_{j\in C^z}\sum_{t\in T_{ij}}(c_{ijt}^F U_{ijt}^z + c_{ijt}^A A_{ijt}^z) \quad (2.4)$$

The hot and cold utility costs are represented by c_i^H and c_j^C respectively which are cost parameters proportional to the utility power and by a fixed cost c_i^{HF} for the installation of a utility i. A linear expression is employed to approximate the cost of the heat exchanger which consists of both fixed and variable costs. The fixed cost related to the number of shells of technology t is expressed by c_{ijt}^F while that related the heat exchanger surface is c_{ijt}^A . ΔT_i and ΔT_j account for the temperature range of hot stream i and cold stream j.

2.2.2. Process Material Integration

By analogy to energy integration, material integration methods search for internal synergies possibilities between the process units aiming to decrease resources usage and reducing the burden of landfills. By examining particular features of the waste such as its composition, it could be allocated towards processes requiring such properties. Nonetheless, waste streams could be regenerated to upgrade their quality for further recovery opportunities using regeneration units. The reuse/recycle problem is either formulated supposing fixed pollutant load or fixed flow rate. Constructing the material integration problem based on the first hypothesis entails a major drawback tied with the process units' definition. This latter is carried out through characterizing each process unit by a fixed pollutant mass load to be removed, missing out on recovery possibilities by not accounting for other type of units such as reactors which can generate or consume materials. However material integration problems with fixed flow rate are not confined to certain types of processes, but instead each process producing or consuming any material may be taken into consideration in designing the synergies topology and identifying the required amount of fresh resource. In such problems, the produced or discharged streams of a process are denoted as sources with a fixed flow rate and composition and the required materials are designated as sinks having a range of acceptable composition.

Even though graphical approaches were employed to optimize fresh water consumption, those are limited to single contaminant and small sized problems. Consequently, mathematical programming techniques have been developed to systematically deal with more complex problems. While non-linear optimization might be of an easier setup to write than linearizing the problem's equations, the resulting solutions might be stuck in a local optimum. Therefore, the selected methodology to be employed in this thesis for designing the local material allocation network (MAN), which is reported in the work of El-Halawgi (El-Halwagi, 2012), is formulated as a mixed-integer linear problem (MILP) based on the fixed flow rate hypothesis that ensures better flexibility on the sources and sinks quality specifications. This MILP mathematical formulation is presented below.

Mathematical formulation of the selected local material integration model for MAN design

The effluents of the studied process units are denoted as Process Sources ($j \in J_p$) having a fixed flow rate L_j and a composition ($y_{j,k}$), whereas the Process Sinks ($i \in I_p$) must be supplied by a flow rate G_i with contaminants composition bounded by ($z_{i,k}^{min}, z_{i,k}^{max}$). The none reusable effluents in the Process Sinks are sent to Waste Sinks ($i \in I_w$) that can intake a flow rate G_i^w whose value results from the optimization problem.

The Fresh Sources ($j \in J_f$) put at disposal to answer the need of the process sinks are also characterized by a specific composition $y_{j,k}$ for every contaminant k and each source j has a mass flow rate L_j^f to be determined. This latter is evaluated as expressed in Eq. (2.5) by the sum of the distributed mass flow rates to the Process and Waste sinks from Fresh source j.

$$\forall\, j \in J_f, \sum_{i \in (I_p \cup I_w)} L_{ij} = L_j^f \tag{2.5}$$

As expressed in Eq.(2.6), the global consumption of fresh resources L_{fresh} is defined as the aggregation of the entire utilized Fresh sources flow rates. To design an optimal material allocation pattern, L_{fresh} must be minimized while complying with the mass balances of the sinks and sources components of the material network.

$$L_{fresh} = \sum_{j \in J_f} L_j^f \tag{2.6}$$

Consequently, the mass flow rate required by each sink i must be equivalent to the combined flow rates it receives from the Process Sources and the Fresh Sources, Eq.(2.7), while respecting the allowable contaminants limits, Eq.(2.8).

$$\forall\ i \in I_p, \sum_{j \in (J_p \cup J_f)} L_{ij} = G_i \tag{2.7}$$

$$\forall\, k \in K,\ G_i \times z_{i,k}^{min} \leq \sum_{j \in (J_p \cup J_f)} L_{ij} \times y_{j,k} \leq G_i \times z_{i,k}^{max} \tag{2.8}$$

By analogy, the total flow rate G_i^w received by every Waste Sink i is ought to be equal to the linear combination of the total treated Process Sources flow as expressed in Eq.(2.9), and the relationship of the quality range limits represented in Eq.(2.10) must be satisfied.

$$\forall\ i \in I_w, \sum_{j \in (J_p \cup J_f)} L_{ij} = G_i^w \tag{2.9}$$

$$\forall\, k \in K,\ G_i^w \times z_{i,k}^{min} \leq \sum_{j \in (J_p \cup J_f)} L_{ij} \times y_{j,k} \leq G_i^w \times z_{i,k}^{max} \tag{2.10}$$

As for Process Sources mass balance, the flow rates sum of the entire allocated streams to every sink have to be equal to the fixed mass flow rate L_j of Process Source j as denoted in Eq.(2.6).

$$\forall\, j \in J_p, \sum_{i \in (I_p \cup I_w)} L_{ij} = L_j \tag{2.11}$$

2.2.3. Coupled Material and Heat Integration at the process scale

When the energy streams of a process are directly related to its material sources and sinks, material streams are characterized by a temperature determined according to the process unit from which a stream is generated or in which it is inputted; they are hence designated as either hot or cold streams. The recovery or reuse of material involve the identification of the flow rate for each allocated stream entailing the need for also establishing the heat load transported by this mass or the required quantity to be evacuated from it. Thereby heat exchange can take place between the material streams in a similar manner as in a heat integration problem.

Subsequently in such situations, the MAN design must be carried out simultaneously with the HENS. Therefore an alternative model which couples energy and material integration could be employed to replace the two integration steps when waste material streams are considered as both mass and energy resources. The opted algorithm for simultaneously designing the MAN and HEN at the process units scale, referred to as the mass allocation and heat exchanger networks (MAHEN), is the developed MILP by Ghazouani, et al. (Ghazouani, et al., 2017) which is also founded on the sources/sinks representation and is explored in the following paragraphs.

Mathematical formulation of the selected model for the local MAHEN synthesis

The mass flow going from a source towards a sink could either be a hot or a cold stream with a variable heat load in the energy integration problem depending on the temperature of its starting and ending points. In addition to the heating and cooling requirements created by mass streams, process heat streams with fixed heat demands are also taken into consideration in the HEN synthesis. Mixer and splitter units are introduced to enhance the energy integration of mass streams. The mixer units can be placed before the indirect heat exchange between material flows to combine streams heading to the same sink in the aim of reducing the energy requirements or lowering the HEN complexity. Each mixer is thus associated to a single sink and is defined by a fixed temperature. As for the splitter units, each is also characterized by a specific temperature however its input comes from one defined source. This latter can be connected to multiple splitters at once and heat exchangers could either be placed downstream or upstream from the splitter. Figure 2.2 depicts the problem components' interactions.

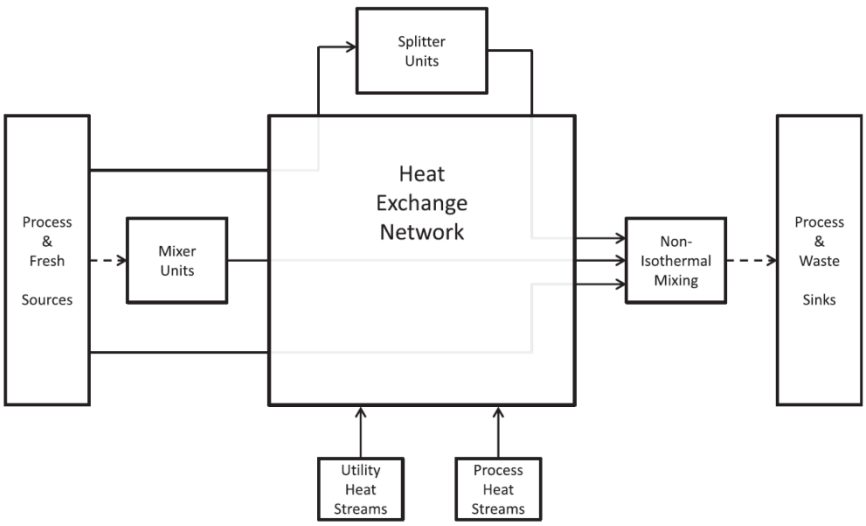


Figure 2.2. Schematic representation of interactions between the MAN and HEN

The introduced mass balances for every component of the previously described material integration problem (cf. §2.2.2) are amended to include the newly appended units. Subsequently, the required mass flow rate G_i of every Process sink i must be equivalent to the sum of the entire received streams from Process and Fresh Sources in addition to the flow rates sent from the splitter L_{ij}^{su} and mixer L_{ij}^{mu} units, Eq.(2.12). The contaminant content of sink i is bounded by an upper limit $z_{i,k}^{max}$. This constraints the mass balance as expressed in Eq.(2.13) and it thus must be satisfied.

$$\forall\ i \in I_p,\ \sum_{j \in (J_p \cup J_f)} L_{ij} + \sum_{su \in SU(j)} \sum_{j \in (J_p \cup J_f)} L_{ij}^{su} + \sum_{mu \in MU(i)} \sum_{j \in (J_p \cup J_f)} L_{ij}^{mu} = G_i \tag{2.12}$$

$$\forall\ k \in K,\ \sum_{j \in (J_p \cup J_f)} L_{ij} \times y_{j,k} + \sum_{su \in SU(j)} \sum_{j \in (J_p \cup J_f)} L_{ij}^{su} \times y_{j,k} + \sum_{mu \in MU(i)} \sum_{j \in (J_p \cup J_f)} L_{ij}^{mu} \times y_{j,k} \leq G_i \times z_{i,k}^{max} \tag{2.13}$$

The computed mass flow rate G_i^w of each Waste Sink i have to be equivalent to the total treated amount of sources and of the associated mixer units flow rate as expressed in Eq.(2.14), while restricting the contaminant transmitted to the sink by an upper limit according to Eq.(2.15).

$$\forall\ i \in I_w,\ \sum_{j \in (J_p \cup J_f)} L_{ij} = G_i^w \tag{2.14}$$

$$\forall\ k \in K,\ \sum_{j \in (J_p \cup J_f)} L_{ij} \times y_{j,k} + \sum_{su \in SU(j)} \sum_{j \in (J_p \cup J_f)} L_{ij}^{su} \times y_{j,k} + \sum_{mu \in MU(i)} \sum_{j \in (J_p \cup J_f)} L_{ij}^{mu} \times y_{j,k} \leq G_i^w \times z_{i,k}^{max} \tag{2.15}$$

Further, the mass flow rate of each Process Source $j \in J_p$ constitutes the aggregate of the allocated streams to the Process and Waste sinks as well as those sent to the splitters and mixers. The mass balance of these components is depicted in Eq.(2.16). The total mass flow rate L_j^f of every Fresh Source $j \in J_f$ presents the same expression as the aforementioned source type. Those flow rates are not however of fixed values as the flow rates of Process sources, but instead they are the outcome of the allocation optimization problem.

$$\forall\ j \in J_p,\ \sum_{i \in (I_p \cup I_w)} L_{ij} + \sum_{su \in SU(j)} L_j^{su} + \sum_{i \in (I_p \cup I_w)} \sum_{mu \in MU(i)} L_{ij}^{mu} = L_j \tag{2.16}$$

The additional system components' mass balances are expressed respectively in Eq.(2.17) and Eq.(2.18) for the splitter and mixer units. The mass flow rate transferred to a splitter $su \in SU(j)$ from its associated source j is denoted by L_j^{su} and that allocated from su to a mixer unit $mu \in MU(i)$ associated to sink i is represented by the term $L_{ij}^{su/mu}$. Moreover, L_i^{mu} appoints the amount of mass sent from a mixer unit mu to its sink i, knowing that mu could be supplied by another mixer or splitter.

$$\forall\ j \in (J_p \cup J_f),\ \forall\ su \in SU(j),\ \sum_{i \in (I_p \cup I_w)} L_{ij}^{su} + \sum_{i \in (I_p \cup I_w)} L_{ij}^{su/mu} = L_j^{su} \tag{2.17}$$

$$\forall\ i \in (I_p \cup I_w),\ \forall\ mu \in MU(i),\ \sum_{j \in (J_p \cup J_f)} L_{ij}^{mu} + \sum_{j \in (J_p \cup J_f)} \sum_{su \in SU(j)} L_{ij}^{su} = L_i^{mu} \tag{2.18}$$

A temperature scale is built in the aim of maintaining a linear formulation for the energy balance equations. The temperature partition is carried out following the same steps as in the heat integration model described in §2.2.1. For every source type of the mass problem that interacts in the HEN, two variables are introduced. The first being $L_{ij,n}$ which represents the mass flow rate extracted from L_{ij} at the temperature T'^{*}_{n} to be sent to sink i and with n being the temperature index on the predefined scale referred to with N_{ij}^{out}. The second defined variable is $\widetilde{L}_{ij,n}$ denoting the remaining flow rate of L_{ij} that goes into the HEN at the n^{th} temperature interval. It is hence equal to $(L_{ij} - \sum_{k=n+1}^{N_{ij}^{max}} L_{ij,k})$ for a hot stream, and to $(L_{ij} - \sum_{k=N_{ij}^{min}}^{n} L_{ij,k})$ for a cold stream. The heat/mass integration superstructure created from the introduced variables is represented in Figure 2.3, and noting that the extracted flow rate at each temperature level $L_{ij,n}$ is bounded by the total allocated mass flow rate L_{ij}.

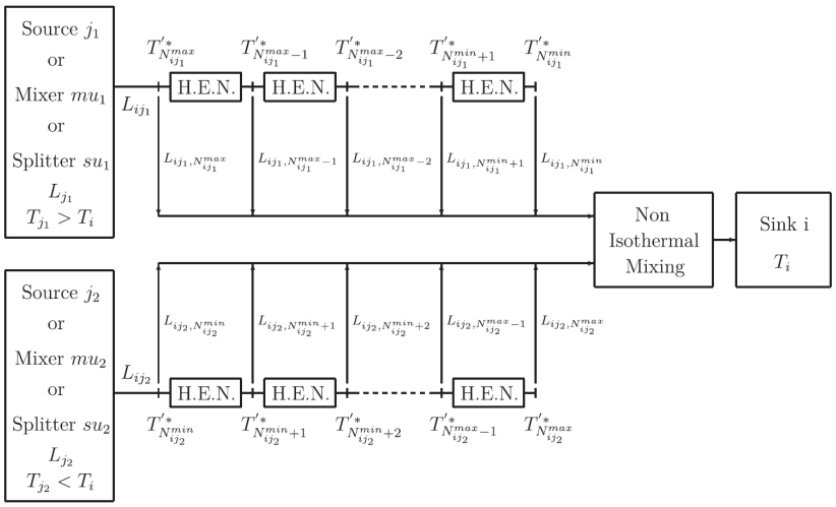


Figure 2.3. Superstructure of the heat integration through non-isothermal mixing

Based on the transshipment model, the overall heating and cooling requirements of the HEN network are computed. The MILP objective function consists on minimizing the total cost to achieve an economically optimal MAHEN configuration. This cost consists of the annual operating and capital costs of the networks. It is evaluated as expressed in Eq. (2.19) considering a nominal cost for the fresh sources, waste sinks and hot utilities. The heat exchangers' investment is computed as for the HEN model described is section 2.2.1 according to their required quantities and relative to their surface area assuming a unit cost for each item.

$$\text{Cost}= \sum_{h_1 \in H_{hot}} \sum_{h_2 \in H_{cold}} (C_{he} \times n_{h1,h2} + C_S \times S_{h1,h2}) + \text{NOH} \times \sum_{n=1}^{IP} \frac{1}{(1+ir)^n} \left[\sum_{j \in J_f} C_j^f \times L_j^f + \sum_{i \in I_w} C_i^w \times G_i^w + \sum_{h_u \in H_u} C_{h_u} \times q_{hu} \right] \quad (2.19)$$

2.2.4. Territorial Heat Integration and Material Integration

2.2.4.1. Territorial Heat Integration or Total Site Analysis

Additional utilities are mostly still required to fulfill the process residual heating and cooling demands even after local heat integration techniques. The problem was therefore expanded to TSA (cf §1.6.1) also called total site heat integration to include the possibilities of heat exchange between plants within a geographical proximity.

TSA actually enables the exploration of potential inter-sites heat transfer, engendering further energy savings to on-site energy integration for industrial actors. Mixed-integer and linear programming for the synthesis of heat exchange through transport networks were issued from the TSA. Even though using tertiary networks for the inter-sites heat exchange may have an energy penalty by dint of the additional required heat exchanger compared to direct integration, it prevents any potential leakage and thus reduces control issues. Steam was proposed in literature as the transport medium due to its great heat capacity enabling smaller diameter pipes compared to other fluids. Amongst the state of the art of territorial heat integration, the novel methodology that was proposed by Farhat, et al. for hydraulic networks and heat exchangers optimization considering exergy and economic aspects (Farhat, et al., 2015).

It consists of two MILP models which can be resolved either sequentially or simultaneously. The first is based on coupling TSA and exergy analysis in the aim of enhancing the territorial exergy efficiency through optimal heat transfer networks and thermodynamic conversion systems. For a sequential resolution, the networks capacities and temperatures from the first MILP make the input for the second MILP that evaluates the proposed heat exchange economically. It employs an economic objective function considering the network investment that takes account of the industrial sites' geographical positioning to specify the routing, sizes of pipes and the areas of heat exchangers and utilities' operating costs. The developed models by Farhat, et al. were chosen to be used in this thesis for the territorial energy integration and they are overviewed in the following paragraphs.

Mathematical formulation of the selected territorial energy integration models

Temperature partition is carried out to ensure the linearity of the models. This is achieved using the shifted temperatures of the process streams. Sub-divisions are added in each interval for enabling different network temperatures exploration. However to avoid getting multiple temperature sets, the temperature intervals generated from each site are combined to form one temperature scale for the entire territory. The temperature indices are set in ascending order where the highest temperature index is zero and the lowest is N. The transshipment model is applied for each site in the territory using the constructed temperature scale.

Assuming that streams in the same temperature interval i and belonging to the same site p are already integrated, thus i is formed by the enthalpies' sum $Q_{p,i}$ of the streams within the interval. Hot streams enthalpies are supposed positive and those of cold streams are negative. Therefore when $Q_{p,i}$ has a positive value, the interval i presents a heat surplus which can be cascaded as a remainder R_i to lower temperature intervals, whereas a negative of $Q_{p,i}$ value corresponds to a heat deficit. In order to meet heating or cooling demands, two types of default utilities are introduced. The default hot utility is at the highest temperature interval (i=0) and is supposed to be generated from a combustion source. Its exergy consumption is evaluated according to Eq.(2.20), where T_{hup} represents the temperature at the source, T_a the ambient temperature and η account for the exergy efficiency. The default cold utility in the other hand could either be cooling processes using ambient sources, thus assumed with no exergy consumption, or refrigeration systems for sub-ambient cooling temperatures. This latter have an exergy consumption expressed in Eq.(2.21), wherein $T_{Cu,p}$ account for the temperature at the sink and Cu_p the load of the cold utility of plant p.

$$Ex = \eta \times \left(\frac{1 - T_a}{T_{hu,p}}\right) \times Hu_p \tag{2.20}$$

$$Ex = \eta \times \left(\frac{1 - T_{Cu,p}}{T_a}\right) \times Cu_p \tag{2.21}$$

Heat exchange between sites is carried out using tertiary networks with steam or liquid (pressurized water or oil) as the carrying medium. A separate formulation for both steam and liquid networks is written in the models. However, since it is most commonly used in industry, steam networks formulation is detailed here.

Since steam networks have constant operating temperatures, the built temperature scale is employed to identify the potential operating temperatures of the networks. These latter are constrained by the minimum temperature difference they make with the operating temperature of a process stream. Hence, this difference should be valid at the plant providing heat to the network at interval i according to Eq.(2.22), and at the plant receiving heat from the network following Eq.(2.23).

$$T_i \geq T_{net} + \Delta T_{net,i} \tag{2.22}$$

$$T_{net} \geq T_i + \Delta T_{net,i} \tag{2.23}$$

Once the definition of the heat exchange between a site and multiple networks are established, the energy balance in each plant at every interval can be elaborated according to Eq.(2.24), where NET denotes the total number of networks. This means that the heat load $Q_{p,i}$ at the temperature interval i in plant p is equivalent to the difference between the received heat from network net $Qh_{net,i,p}$ and the transferred heat from plant p to network net, adding to that the cascaded heat from the above temperature $R_{p,i-1}$ and abstracting the transferred remainder to the below temperature $R_{p,i.}$ However for the highest temperature interval (i=0) of plant p, the injected default hot utility load Hu_p is appended. Similarly for the lowest temperature interval (i=N), the cold utility load Cu_p is subtracted from the energy balance of plant p.

$$Q_{p,i} = \sum_{net=0}^{NET} Qh_{net,i,p} - \sum_{net=0}^{NET} Qc_{net,i,p} + R_{p,i-1} - R_{p,i} \tag{2.24}$$

As for the energy balance within a network, it is considered that no storage is permitted; thus the total gained heat by the network "net" from the sites at interval i must be equal to the total distributed heat load from the network "net" to the entire plants at that temperature interval. This relationship is expressed in Eq.(2.25) with the total number of sites denoted as ns.

$$\sum_{p=1}^{ns} Qh_{net,i,p} = \sum_{p=1}^{ns} Qc_{net,i,p} \tag{2.25}$$

The above mathematical formulations enable determining the heat exchange characteristics such as networks capacities and operating conditions. They are computed in the first MILP model with the objective function in its simplified form in Eq. (2.26) as the core criterion (when thermodynamic conversion systems are used their exergy consumption and generation are also included). This actually consists on minimizing the exergy consumption of the heat integration system and thus the hot and cold utility utilization.

$$\min: \quad \text{exergy} = \sum_{p=1}^{ns} \eta \times \left(\frac{1\text{-}T_a}{T_{hu,p}}\right) \times Hu_p + \sum_{p=1}^{ns} \eta \times \left(\frac{1\text{-}T_{Cu,p}}{T_a}\right) \times Cu_p \tag{2.26}$$

The resulting heat exchange solution of the first MILP model is inputted to a second MILP in the aim of economically optimizing the hydraulic networks according to their preselected operating temperatures and capacities for inter-sites heat exchange. The second algorithm requires the geographic positioning of the participating sites relative to one another to being able of establishing available pipe routing, junction locations and costs.

The intersection between paths that serves for laying down the needed pipes form nodes which could potentially be pipe junctions. Different pipe diameters are supposed passing through each path to enable the selection of the one with the best economic performance, considering their length formed by the individual paths extent defined by two nodes. In order to guarantee mass conservation throughout the network, the nodes law is applied on every node n as expressed in Eq.(2.27); in which plants is a new defined set, namely plants={p | p is a plant in the problem connected to the node n}.

$$\dot{m}_{net,plants} = \sum_{p=1}^{ns} \dot{m}_{p,net} - \sum_{p=1}^{ns} \dot{m}_{net,p} \tag{2.27}$$

The pressure losses in the pipes are as well taken into account; and since pressure drop is a non-linear function of the velocity, this function is linearized piecewise leading to the introduction of a number of velocity intervals.

For each pipe diameter, different flow velocities can be encountered. A binary variable $Vbin_{net,v,d,m\rightarrow n}$ is therefore introduced for each velocity interval v that bounds the velocity $V_{net,v,d,m\rightarrow n}$ of a pipe with diameter d connecting node m to node n in network net. This is expressed as in Eq.(2.28), in which $Vmin_v$ and $Vmax_v$ represent the lower and upper bounds velocities of interval v. By that a pipe exists when this binary variable is equal to a unit and thus its velocity could take up any value ranging between the upper and lower bounds. However in order to limit the selection for each path to a single pipe diameter, the constraint in Eq.(2.29) must be satisfied.

$$Vbin_{net,v,d,m\rightarrow n} \times Vmin_v \leq V_{net,v,d,m\rightarrow n} \leq Vbin_{net,v,d,m\rightarrow n} \times Vmax_v \tag{2.28}$$

$$\sum_d \sum_v Vbin_{net,v,d,m\rightarrow n} \leq 1 \tag{2.29}$$

The pressure drop in the hydraulic pipe connecting node m to node n is evaluated through the linearized pressure losses equation as depicted in Eq.(2.30) in which LA and LB represent the linearization coefficients. The previously defined binary variable is also included in the expression to account for the existence or not of pipe with velocity $V_{net,v,d,m\rightarrow n}$. Consequently, the pumping power serving for the medium transportation can also be assessed in the same manner, Eq.(2.31), where LC and LD are the coefficients of linearization.

$$H_{net,v,d,m\rightarrow n} = \left(LA_{v,d} \times V_{net,v,d,m\rightarrow n} + LB_{v,d} \times Vbin_{net,v,d,m\rightarrow n}\right) \times l_{m\rightarrow n} \tag{2.30}$$

$$PO_{net,v,d,m\rightarrow n} = \left(LC_{v,d} \times V_{net,v,d,m\rightarrow n} + LD_{v,d} \times Vbin_{net,v,d,m\rightarrow n}\right) \times l_{m\rightarrow n} \tag{2.31}$$

The objective function of the second MILP, which consists on determining the economic feasibility of the predefined networks operating temperatures, is the total cost of the synergy network. It is expressed in Eq.(2.32) where NOH denotes the yearly operating hours, ir the actualization rate, y the year and IP represents the integration period. The goal is to minimize the cost function to achieve an economically optimal heat exchange configuration with the networks temperatures and capacities specified on exergy basis by the first MILP.

$$\min: \quad \text{cost} = \text{Capex} + \sum_{t=1}^{IP} \text{NOH} \times \text{Opex}_y \times \left(\frac{1}{1+\text{ir}}\right)^y \tag{2.32}$$

Capex accounts for the investment costs required to implement the pipelines and the heat exchangers that ensure the synergies between the industrial sites. The piping system installation costs are evaluated according to the chosen pipes costs using the previously defined binary variable, Eq.(2.33). The $\text{pipeCost}_{d,m\to n}$ corresponds to the pipe cost of diameter d connecting node m to n, it thus depends on the physical properties of the pipeline.

$$\text{Capex}_{piping} = \sum_{net,v,d,m,n} \text{Vbin}_{net,v,d,m\to n} \times \text{PipeCost}_{d,m\to n} \tag{2.33}$$

With a non-linear cost function, heat exchanger costs are written piecewise with respect to their surface area in order to ensure linearity. The same method employed for the linearization of pressure loss is conducted by bounding an interval e of heat exchanger's surface area by upper and lower limits defined by HXAmin_e and HXAmax_e respectively. The heat exchanger cost function form consists of a fixed cost FC and a variable cost VC depending on its area. A new binary variable $\text{HXAbin}_{net,p,s,i,j,e}$ is introduced to prevent fixed costs from being added to the cost function when the heat exchanger does not exist, Eq.(2.34). The cost function of a heat exchanger set for an exchange among stream s of plant p and network net between the temperature interval i and j is thus expressed in Eq.(2.35). The total heat exchangers investment is its sum over the entire temperature intervals for each plant and every network.

$$\text{HXAmin}_e \times \text{HXAbin}_{net,p,s,i,j,e} \leq \text{HXA}_{net,p,s,i,j,e} \leq \text{HXAmax}_e \times \text{HXAbin}_{net,p,s,i,j,e} \tag{2.34}$$

$$\text{HXCost}_{net,p,s,i,j,e} = \text{VC} \times \text{HXA}_{net,p,s,i,j,e} + \text{FC} \times \text{HXAbin}_{net,p,s,i,j,e} \tag{2.35}$$

As for Opex, it represents the yearly operating costs of the network which includes the electricity required for pumping the circulating medium and the hot and cold utilities costs. The total pumping power is deduced from summing $\text{PO}_{net,v,d,m\to n}$ over each path for every defined velocity interval and for the number of networks. This power is multiplied by the electric energy cost to obtain the annual operating cost of the pipelines, Eq.(2.36). The Opex generated from the utilized utilities is computed using Eq.(2.37).

$$\text{Opex}_{pumping} = \text{Cost}_{elec} \times \sum_{net,v,d,m,n} \text{PO}_{net,v,d,m\to n} \tag{2.36}$$

$$\text{Opex}_{utilities} = \sum_{p=1}^{ns} \text{Cost}_{heat,p} \times \text{Hu}_p + \sum_{p=1}^{ns} \text{Cost}_{elec,p} \times \left[\eta \times \left(\frac{T_a}{T_{Cu,p}} - 1\right) \text{Cu}_p\right] \tag{2.37}$$

2.2.4.2. Territorial Material Integration

Subsequent to designing optimal recovery networks at the process scale, an industrial site might still have waste discharge and resource demand. Looking at implementing inter-sites synergies to exchange these material streams, leads jointly towards higher rationality in resource consumption and lower burden on landfills. To design the material transport network between the suppliers and the demanders, the model of Ghazouani, et al. (Ghazouani, 2016) was selected to be employed in this thesis and is therefore explored in the following section. The author actually extended its previously proposed process material integration models to the territorial wide scale aiming to design cost-effective transport network ensuring material allocation between industrial sites. This model is partially inspired from Farhat's model (Farhat, et al., 2015).

Mathematical formulation of the selected territorial material allocation network model

The network in which recovered materials circulate to be transferred from a provider plant to another consumer is considered to have defined starting and ending points manifested by these entities respectively. The aforementioned points are modeled as waste sinks for the network inlet and as fresh sources to represent the outlet material at disposal. Waste sinks are considered to have no predefined mass flow rate G_i^w. They do however have a limitation on the material composition for each contaminant k in the waste sink i feeding streams denoted by $(z_{i,k}^{min}, z_{i,k}^{max})$ and the proprieties of sink i are also bounded by $(p_{i,m}^{min}, p_{i,m}^{max})$ for every propriety m. A fresh source j on the other hand has a flow rate L_j^f to be determined and is characterized by a specific composition $y_{j,k}$ for every contaminant k and by a set of proprieties $p_m = \{ p_{j,m} \mid p_{j,m}$ value of the propriety m of stream j$\}$.

The entire material networks existing in the studied territory are defined in the set M_{net}, namely: $M_{net}=\{(j , i) \mid$ a material network with fresh resource j and waste sink i$\}$. Those are included in the mass balance of each site of the territory through duplicating the fresh resource j and waste sink i. Assuming no mass loss within the network, every entering material stream must be sent back to a consumer site. Further, knowing that multiple inputs for a similar waste sink can be received from different actors by the network and that this latter can then redistribute the fresh source to several industrial sites, the mass balance of every network is expressed as in Eq.(2.38) wherein s is an element of the set of sites S, namely: $S=\{s \mid$ s an industrial site in the territory$\}$.

$$\sum_{s \in S} G_{i\,s}^{w} = \sum_{s \in S} L_{j\,s}^{f} \quad , \forall\, (j,i) \in M_{net} \tag{2.38}$$

The network specifications are defined by the fresh source characteristics in terms of composition and proprieties. Subsequently the range of the composition and proprieties of the network's feeding streams must be determined in such way to have the selected network specifications centered in the intervals boundaries of the waste sink. To design the material allocation network, first the possible paths on which pipelines could be installed to transport material streams are defined. Each path is formed by two nodes which could either designate an industrial site or an intermediate point. The material network design is established by minimizing the total cost of the network assuming no variable costs related to the streams mass flow rate, it thus only consists of the pipeline investment required to ensure the material allocation. The capital cost of the network is evaluated according to the distance between the two nodes of the path wherein a pipeline is installed.

2.3. Integration of Conversion Systems in a Territory with Cooperative Scheme Governance

In a territory with cooperative scheme, actors within geographic proximity try to achieve a shared common goal cooperatively. They mutually participate to create and foster potential synergies by equally bearing the expenses for putting them in place while sharing the generated earnings. Such scheme may be the case of an ideal territory wherein a single investor (i.e. the government) takes in charge the cost for the networks installation and the gains are distributed to the actors who took part in recovering or redirecting resources for reuse. Or more realistically, it could be the case of one industrial organization with several involved units; thus it implements the newly identified synergies between the units to improve its business or technical processes. Hence, the integration of conversion systems in a territory with cooperative scheme entails a centralized control structure that governs system behavior. The first building block of the problem, Figure 2.4, is identifying the actors located in the defined geographic premises of the territory and that seek enhanced performance through collaboration in managing resource and energy consumption and waste discharge of the territory. An industrial actor, denoted as $Site_i$, is defined by its geographic coordinates C_i, the energy streams list of its entire units E_i, the current available utilities U_i for its heat and cold requirements, and the set of its material demand M_i and material discharge O_i. The aforementioned sets are defined as follow and in which $i \in \{1,..N\}$, N being the number of Sites:

$Territory=\{Site_i \mid Site_i$ is an industrial actor located in the geographic boundary of the territory$\}$
$C_i=\{(x,y) \mid (x,y)$ are the geographic coordinates of $Site_i\}$
$E_i=\{(T_{in},T_{out},Q) \mid$stream of $Site_i$with inlet temperatureT_{in} and outlet temperature T_{out} of fixed heat load Q$\}$
$U_i=\{(T_{in},T_{out},Q, P) \mid$utility of $Site_i$with inlet and outlet temperatures T_{in},T_{out} of variable heat load Q at price P$\}$
$M_i=\{(M_i^z, C_i^z) \mid$ material z of flow rate M_i^z and quality C_i^z required by the process units of $Site_i\}$
$O_i=\{(O_i^z, C_i^z) \mid$ material z of flow rate O_i^z and quality C_i^z released by the process units of $Site_i\}$

These data serve as inputs for the territorial energy integration and material integration problems which consist on finding the optimal synergies patterns between the collaborative actors' streams. The assessment of the resulting exchange amongst the industrial actors of Territory reveals any limited opportunities of recovering a material stream O_i^z of $Site_i$ ensuing from the non-existent demand of material z. The non-usable material streams in their initial form are the waste streams W of the territory. This set is introduced below, wherein $z \in Z = \{$material z, .., material v$\}$.

$W=\{W_i^z \mid W_i^z$ is the mass flow rate of material z discharged by $Site_i$ and has no reuse opportunity as z$\}$

Adapted reacting systems convert the initial composition of the non-usable stream into a new form. By searching to transform them into usable products that answer the local demand of Territory, further economy can be achieved since the utility cost of such products will be avoided thus leading to the increase of the territory's welfare. The identified waste streams in the set W are targeted in the aim of elaborating an inventory consisting of the possible reacting conversion processes of these materials. From this inventory, the conversion systems which are judged to be of interest and most suited for the heat and material requirements of Territory are selected and introduced in a new set CS.

$CS=\{CS^z{}_k \mid CS^z{}_k$ is the k^{th} reacting thermodynamic conversion system of material z$\}$

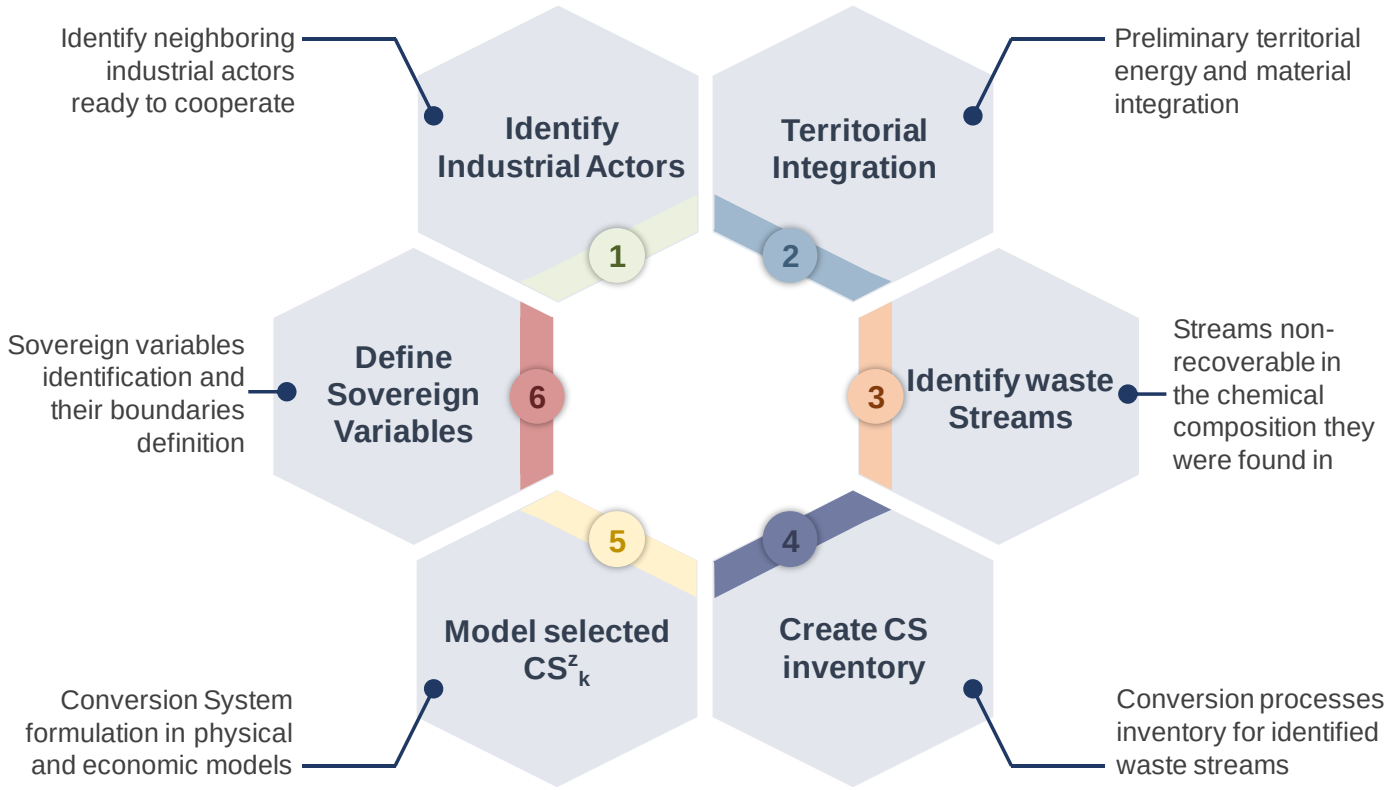


Figure 2.4. The building blocks of the problem required for the waste streams definition and their conversion processes identification

Since m_z is defined as the number of the potential conversion systems of material z, CS thus consists of $\sum_{z\in Z} m_z$ components. Each CS^z_k is formulated in a physical model based on the energy and material balances of its process units and in an economic model contingent on the design parameters of the system's components. The appraisal of these models enables the definition of the conversion systems' degree of freedom in terms of operating parameters and technical design options, DOF^z_k denoting that of CS^z_k. Subsequently, a set of sovereign variables SV^z_k is introduced for every CS^z_k formed by the variables $SV^z_{k,l}$ that depicts its degree of freedom and each of which is bounded by lower and upper limits; noting that $l \in \{1, .., DOF^z_k\}$. A sovereign variable can take up any value ranging between its fixed intervals bounds which are established according to the technological operation constraints. The collection of the sovereign variables for the entire CS elements is listed in a single set SV.

$SV^z_k = \{(SV^z_{k,l}, SV^{min}, SV^{max}) | (SV^{min}, SV^{max})$ are the lower and upper limits respectively of $SV^z_{k,l}\}$

$SV = \{SV^z_k \mid SV^z_k$ is the sovereign variables of the k^{th} conversion system of material $z\}$

A Master problem handles the SV set and first creates the problem superstructure consisting of the entire potential conversion pathways of the non-usable streams and from every single system its own sovereign variables branch out. A sample of this superstructure is depicted in Figure 2.5.

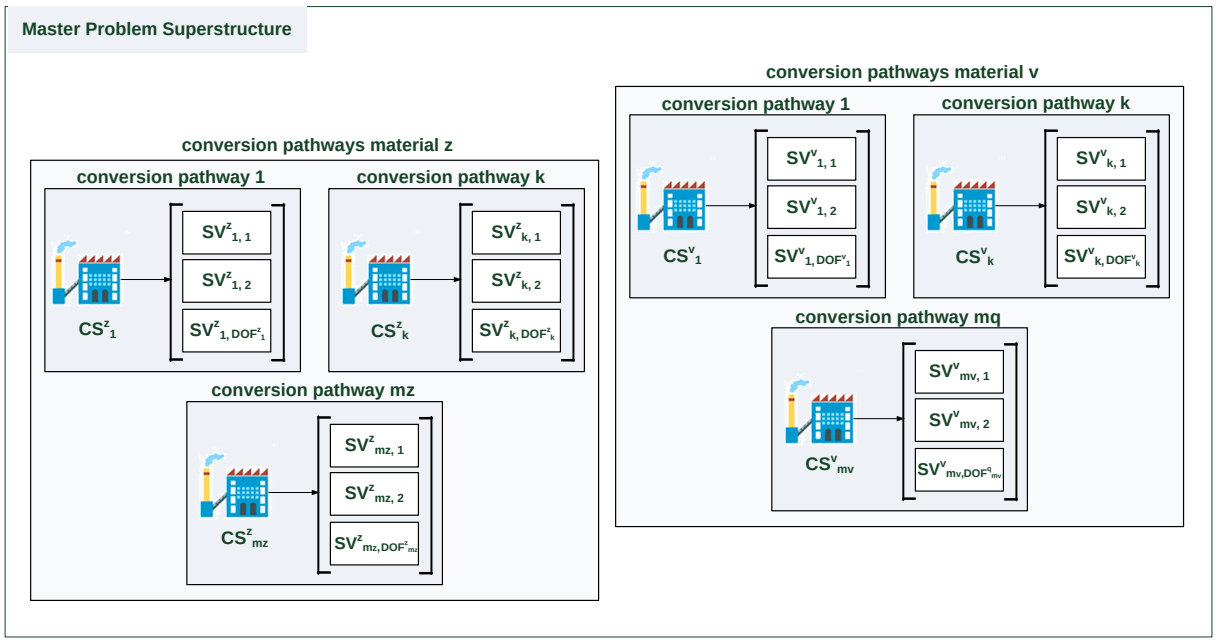


Figure 2.5. Master Problem superstructure of the conversion pathways

The Master problem manipulates the superstructure to create potential scenarios of the actual territory with one possible conversion pathway for every non-usable material found in the beforehand identified set W, Figure 2.6. It selects a pathway for transforming material z by primary choosing a reacting thermodynamic system CS^z_k from CS and then acting on one of its sovereign variables $SV^z_{k,l}$ with respect to its upper and lower boundaries to create the q^{th} set of parameters for the k^{th} conversion system of material z, set_q. Once the entire variables of the k^{th} conversion system and their ranges are adopted and considered in a prior scenario generation, the Master problem switches to a new conversion pathway for material z, CS^z_{k+1} and maintain this pattern until no pathways are left.

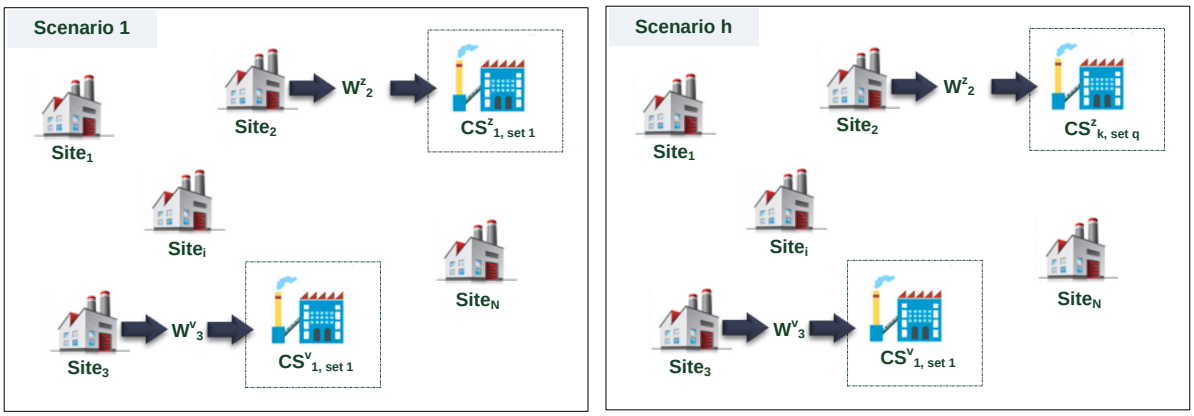


Figure 2.6. Potential generated scenarios of Territory presenting two waste streams

When the set of the entire prospective scenarios is generated by the combinations created using the conversion pathways superstructure, the task of the Master problem consists henceforth on assessing a common defined objective for each of these scenarios through a simultaneously energy and material integration. In order to eventually pick out the optimal synergies configurations and the operating and design parameters of the best conversion systems to be implemented in the territory.

The Master problem manages two slave problems for the purpose of achieving the aimed goal. The first is the local integration problem and the second is the integration problem at the territorial level. The heat exchanger design syntheses of both problems are carried out simultaneously to ensure convergence towards an optimal trade-off between the local synergies amongst the process streams and the inter-sites exchange opportunities. Figure 2.7 depicts the computational framework of the Master-slave problem for integrating conversion systems in a territory with cooperative scheme.

As a first step, the Master problem launches the simulation platform Dymola® in order to compute the physical and economic models of the selected conversion systems for the appropriate set of operating and design parameters. The resulting energy and material streams are employed to define the conversion system as an industrial actor $Site_{N+1}$ appended to the Territory set. The waste stream is thus reintroduced into the territory by dint of its conversion to a new usable product whether in the form of energy or in a new material composition.

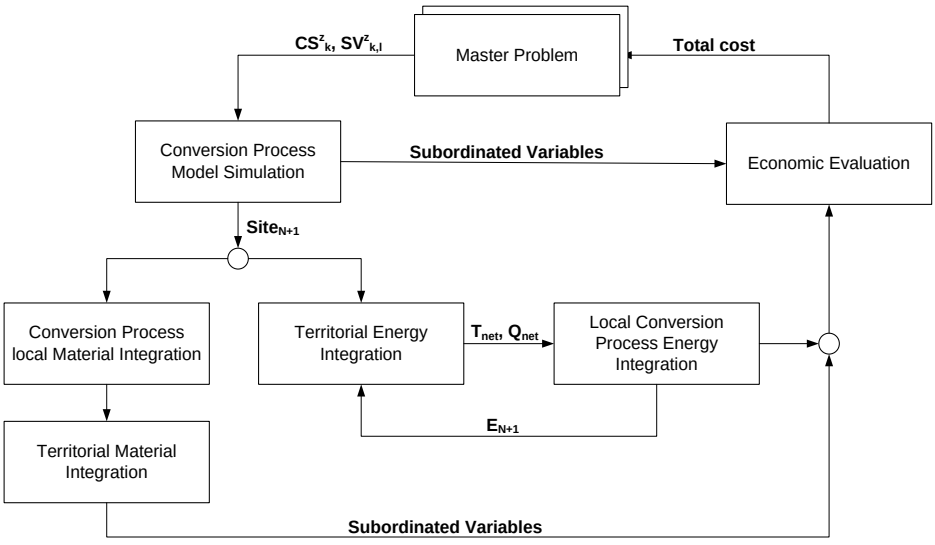


Figure 2.7. Computational framework of the Master-slave problem for integrating conversion systems in a territory with cooperative scheme governance

The local material integration of $Site_{N+1}$ is carried out to evaluate the opportunities for internal material recovery amongst the conversion system units. Afterwards, an inter-sites material integration is ran in order to design the allocation networks that will serve for the material transport from one site to another if any synergies are detected. The territorial heat integration problem is conducted with the updated Territory set to establish the optimal steam network temperatures to be implemented. The ensuing networks temperatures T_{net} and the corresponding exchanged heat load with each $Site_i$ are transmitted to the (N+1) local integration problems. Those are defined as sets T_{net} and Q_{net}:

$$T_{net}=\{T_j \mid T_j \text{ is the temperature number j of the steam network}\}$$

$$Q_{net}=\left\{(Q_{ij},Q_{ji}) \mid Q_{ij}/Q_{ji} \text{ is the heat load transferred/received from/by agent i to/from the network at } T_j\right\}$$

The heat loads Q_{ji} and Q_{ij} are incorporated respectively in $Site_i$ integration problem as a hot utility T_j available at the Market heat price and as a free cold utility. The heat exchangers connected to these utilities are supposed with no charges in the local problem since their installation costs are accounted for in the territorial problem. After the internal synergies establishment, the remainder streams that do exchange heat with the network are used to modify the energy stream list E_i of each $Site_i$ to only consist of those streams and thus the territorial problem is repeated with the amended sites. The local and territorial integration are iterated until both problems generate the same heat loads outcome each $Site_i$ exchange with the network. It is supposed that no external heat (i.e. centralized utility) can be supplied to the network; hence the heat networks only serve to ensure synergies between the industrial actors. A way to assess a centralized utility is to introduce it as a new Site among the elements of Territory.

Once the heat loads converge, the subordinated variables formed by the economic data that result from the integration problems and from the economic model simulation of the conversion process are retrieved and then injected into the economic evaluation function. This latter consists of the territory's total cost which is the sum of its variable and fixed costs and is expressed in Eq.(2.39).

$$\text{TotalCost} = \sum_{i=1}^{N+1} \text{Capex}_{\text{Site}_i} + \text{Capex}_{\text{HEN}} + \text{Capex}_{\text{pipe}} + \sum_{y=1}^{\text{Nbr}_{\text{year}}} \frac{1}{(1+\text{ir})^y} \times \left[\sum_{i=1}^{N+1} \text{Opex}_{\text{Site}_i} - \text{Gain}_{\text{syn}} - \text{Revenue}_{\text{CS}}\right] \quad (2.39)$$

The fixed costs of the territory are generated from the investments of the conversion system units and its heat exchangers, in addition to the inter-sites heat exchangers installation costs and those of the pipelines that ensure the heat and material transport. The fixed costs also account for the expenses each industrial site requires for the implementation of its local heat exchangers. As for the variable cost, it is the resources expenses required to maintain the systems operation. It thus entails the resources required by each site of the park and the potentially introduced utilities by the conversion system as well as the profits from sales of surplus commodities generated by the conversion process and from the established synergies. The gain from this latter are manifested in the territorial problem by the heat or material that an industrial actor pays to get from the network and the energy or waste that is sent to the network for no fees. The cycle is repeated by passing through the Master Problem to test alternative configurations of Territory to eventually cover the whole prospective scenarios and generate a set of the best synergy patterns for the studied territory defined in terms of its variable and fixed costs. It is noteworthy that for conversion systems with a high number of sovereign variables, the prospective scenarios generation might become of great complexity. In such case, the Master problem could incorporate a meta-heuristic genetic algorithm that manages the conversion pathways superstructure to beget more effectively potential territory's scenarios. The objective function of this algorithm would consist on the minimization of the territory's total cost.

2.4. Integration of Conversion Systems in a Territory with Non-Cooperative Scheme

As opposed to cooperative scheme, in non-cooperative scheme actors constantly explore strategies to find their own individual interests at the expense of the whole territory, i.e., the industrial park. These systems can be difficult to control with a top-down centralized mechanism owing to the autonomy that each actor exhibits; thus the integration of the conversion system in a territory with self-interested actors requires a different framework. With the need to partition the analysis or synthesis of the system into sub-problems, this system can be defined as a complex system (Bakule, 2008). The aforementioned consists of many components acting and reacting to each other's behavior and whose aggregate activity is nonlinear. To model and simulate complex systems, agent-based models (ABMs) form arguably a generalized framework for this purpose (Sayama, 2015).

Actually ABMs derived from distributed artificial intelligence; the objective shifted from reproducing the knowledge and reasoning of one intelligent agent to several heterogeneous agents each with its own goal and thus need to coordinate actions to meet these goals (Bousquet & Le Page, 2004). They were successfully applied for solving problems that require distributed reasoning, decentralization and coordination. ABMs, also called multi-agent systems (MAS), are systems composed of a collection of interacting computational components known as agents (Bogg, et al., 2008). These agents are capable of controlling their own behavior, i.e., have autonomy of action, with each acting in the furtherance of their own goals while interacting with each other in a shared environment. They are able to achieve this by perceiving their environment through sensors and acting upon that environment through their actuators (or effectors) (Russell & Norvig, 1995), Figure 2.8.

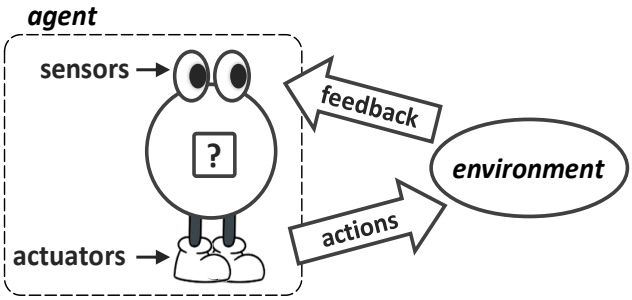


Figure 2.8. Agents act and react with their environments

Typically agents can only intercept, process and react to their environment but cannot control it. They choose whether to cooperate or to compete based on the payoffs and costs for choosing one of either options. Those payoffs may vary depending on the game they are engaged in with other agents. Some scenarios have very low incentive for cooperation while favoring competition; these are called zero-sum game, while others have much lower costs and higher payoffs for cooperation.

Wangermann and Stengel proposed a novel method for coordination in MAS using principled negotiation (Wangermann & Stengel, 1999). This negotiation technique is based on the book "Getting to Yes" by Roger Fisher and William Ury. It focuses on the negotiating parties' interests not positions, generates options for mutual gain and uses objective criteria to evaluate them. This means negotiators should propose new solutions allowing gains for both parties, not fight over the original positions which assume a zero-sum game with only one winner.

Using this technique Wangermann and Stengel (Wangermann & Stengel, 1999) developed an iterative optimization method for MAS where an initial master plan formulates each agent's actions before the agents repeatedly search for alternative plans that ensure mutual gain, Figure 2.9.

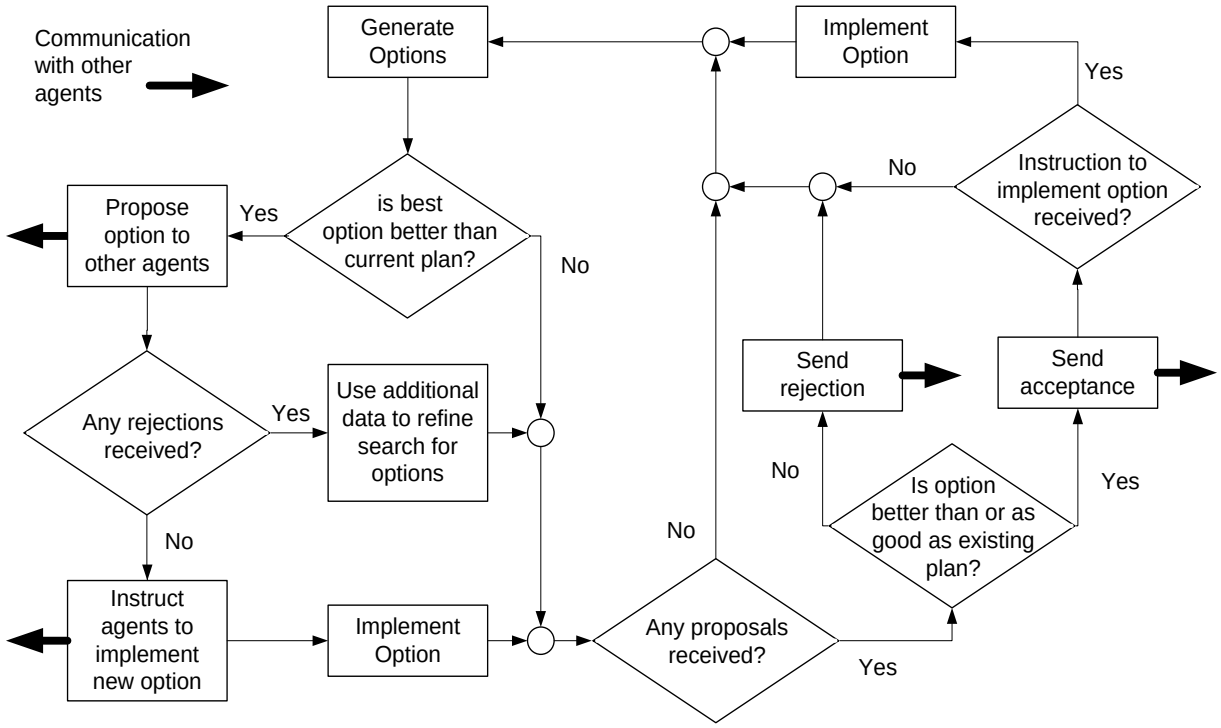


Figure 2.9. Agent principled negotiation (Wangermann & Stengel, 1999)

An agent proposes the option which it finds in the furtherance of its interests and then the others accept or reject it after evaluation. With no rejections the proposed option is implemented. However if one agent does reject it, it transmits a message with the reasons for rejection to the proposer. This latter enhances its search based on this information.

In the MAS formulation problem proposed by Wangermann and Stengel (Wangermann & Stengel, 1999) agents are either *maximizers* or *satisfciers* agents. While the former seeks to maximize its utility function, the latter ensures that the proposed action plan is satisfactory. A maximizer agent does not propose an option except if it estimates that the action plan could be beneficial to other agents or does not affect them.

Depending on an agent knowledge about other agents, its options search space could be limited to its own feasible set of plans or may extend to include others action plans. There is no guarantee that its proposed option would not decrease other maximizers' utility functions when it has no knowledge about other agents. Moreover agent actions are not necessarily affected by every proposed option plan. Therefore to prevent needless communication between agents while ensuring good coordination when no knowledge is possessed about other agents, the authors proposed the use of a coordinating agent that evaluates proposals and passes them on to the concerned agents. This coordinator only requires the information to be able to assess the agents' interactions and not optimize their actions. The principled negotiation technique is particularly interesting since it does not require any agent to have a global knowledge of the other agents' utility functions.

Romero and Ruiz (Romero & Ruiz, 2014) have put forward an analytical model based on ABMs for the assessment of cooperative relationships among actors in eco-industrial parks (EIPs). They defined the object of the simulation by five indexes that measures the overall system evolution based on environmental and economic criteria. They formulated the agents' structure according to their proprieties and behaviors rules, Figure 2.10. The aforementioned considers agents with goal-directed behaviors and thus the satisfaction level of their objectives is the criterion conditioning their actions. Hence the satisfaction level of employing the strategy q_x is exhibited with the utility function $P(q_x)$ which is the sum of four indexes evaluating economic profit, social benefit, environmental impact and the advantage strategy degree. Those indexes asses the improvement gained by applying the strategy q_x relative to the situation where no exchange with other agents is performed. Each index is assigned with a weighting coefficient to adjust its contribution in the utility function.

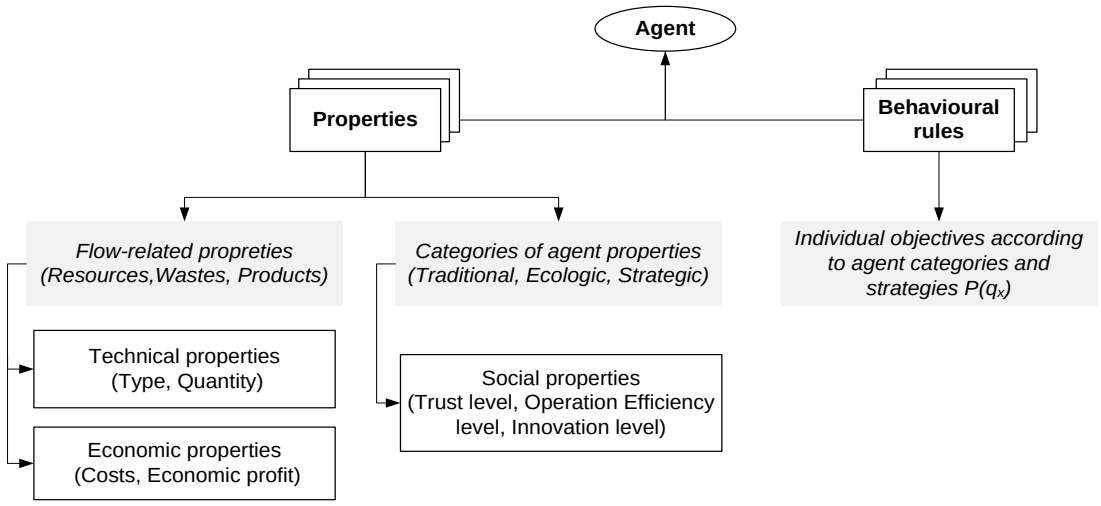


Figure 2.10. Agent structure (Romero & Ruiz, 2014)

The authors proposed three categories of agents: *traditional agent*, *ecologic agent* and *strategic agent*. While a traditional agent is mainly motivated economically to employ environmental-projects, an ecologic agent is rather concerned by the environmental impacts of its activities. As for a strategic agent, it represents proactive companies that promote innovation and actively participate in such projects. In their problem formulation the authors gave the agents four possible modes of actions. The first is production wherein each actor consumes resources and generates wastes to manufacture certain products. The second is adaptation that gives the agent the possibility to react to other agents interactions or to a change in its surroundings. This reaction is defined as the internal mechanism in an agent to update its properties. To allow synergies between agents and thus flow exchange, the third agents mode of action is cooperation. The last action an agent can perform according to the authors is disappearance. An agent disappears when its operation generates no economic profits.

Romero and Ruiz (Romero & Ruiz, 2014) defined the agents surroundings as three subsystems: natural, social and economic surroundings. The natural surroundings engender resources and take in wastes of other systems. Consequently it influences the economic properties of resource flows. However changes in social surroundings generate an impact on the waste flow economic properties since this system defines the norms governing the operation of technologies, i.e., waste management taxes. As for the economic surroundings, it is represented by the economic market governed by the demanded products. Therefore a variation in these surroundings acts directly on the resources and wastes quantities.

The authors considered the interaction between agents to be conditioned first by the possible substitution of agents flows and then by agents behavioral rules. Therefore they established a knowledge database including different flow substitutions that matches resources with wastes that could substitute them. Once the wastes are determined, they serve as searching parameters to identify agents generating such wastes or byproducts and thus may be interested in material exchange. An agreement about the quantity to be exchanged should be settled between seller and buyer agents where the payoffs of each strategy is computed by the utility function $P(q_x)$. Based on non-cooperative game theory, each agent proposes four strategies build upon the quantity of exchanged waste q_x relative to either resources quantity rq_j for the buyer agent, Eq.(2.40), or wastes quantity wq_k for the seller agent, Eq.(2.41). Nash equilibrium served to define the best strategy of which both parties would not deviate.

$$\text{Buyer} : q_{A_i} = \{q^1_{A_i} : q_x > rq_j \ , \ q^2_{A_i} : q_x = rq_j \ , \ q^3_{A_i} : q_x < rq_j \ , \ q^4_{A_i} : q_x = 0\} \tag{2.40}$$

$$\text{Seller} : q_{A_{i'}} = \{q^1_{A_{i'}} : q_x > wq_k \ , \ q^2_{A_{i'}} : q_x = wq_k \ , \ q^3_{A_{i'}} : q_x < wq_k \ , \ q^4_{A_{i'}} : q_x = 0\} \tag{2.41}$$

From the above exhibited literature work, it can be induced that two main techniques could be employed for self-interested agent strategies establishment: Game theory and coordination techniques. Both of these techniques are further explored in the following sections.

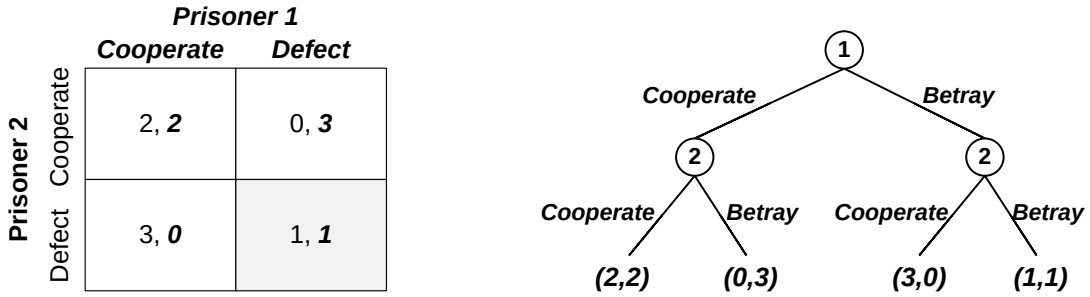
2.4.1. Game Theory – exchanging preferences

Game theory is the discipline of studying strategic interactions between self-interested actors with respect to their preferences. Its foundation traces back to 1944 to the work of Neumann and Morgenstern (Von Neumann & Morgenstern, 1944). Their analysis was restricted to zero-sum games and was expanded by Nash (Nash, 1951) in the 50s to include wider variety of games.

A game is defined by n players each with a finite set of strategies (i.e., actions) and a payoff function that calculates the utility against each strategy. The action profile $a = (a_1, a_2, \ldots, a_n)$ is a set of n items formed by the actions of all the players with a_i denoting that of player $i \in \{1, 2, \ldots, n\}$ and a_{-i} that of all the others except player i. The payoff of player i depends not only on the action he undertakes but also on that chosen by the other players, thus it is function of the action profile and is denoted by $u_i(a)$. The action profile a^* is a Nash equilibrium if no player has in interest changing its strategy when the others actions are held fixed, Eq.(2.42) wherein a^*_i is the best action of player i. A deterministic strategy in which a player performs an exact action is a game with pure strategies. However when at least one player randomly select a strategy to implement by assigning a probability to each pure strategy, they are playing mixed strategies. By introducing mixed strategies Nash (Nash, 1951) proved that every game with n players having a finite pure strategies to choose from can have at least one Nash equilibrium.

$$\text{for every player } i : u_i\left(a^*_i, a^*_{-i}\right) \geq u_i\left(a_i, a^*_{-i}\right) \ \forall \ a_i \tag{2.42}$$

A strategic game is when players act simultaneously or when they are not aware of the other players previous actions. Normal form is used to represent strategic interactions of players in a matrix form which shows the players, their strategies and payoffs. Whereas extensive form is employed to represent sequential games in a tree structure where each vertex contains the player's number and from which the possibilities of its actions branch out. The tuples at the end of each action sequence (i.e., each path through the tree) corresponds to the players' payoff for the respective action sequence.



(a) (b)

Figure 2.11. The prisoner's dilemma: a) normal form, b) extensive form

Figure 2.11 represents the prisoner's dilemma in both normal (where the row player's payoff is listed first) and extensive forms. This standard example was formalized to illustrate why intelligent agents might not cooperate even though it is in their best interest to do so. Two prisoners, with no means of communications between them, are offered a bargain by the prosecutors to reduce their sentence. They both have two options: either testify that the other committed the crime and thus defect, or remain silent and cooperate with the other prisoner. Both prisoners are fully aware of the potential strategies the other could undertake since they are offered the same deal. Knowing that the best strategy of the other prisoner is to defect, each prisoner will prefer confessing that the other committed the crime. Therefore the Nash equilibrium in this game is when both players choose to defect. What is interesting in this equilibrium is that the prisoners could have achieved better outcome if they both cooperate instead of both defecting. However, by breaking the mutual cooperation each of them could enhance his payoff.

The two main problems in applying Nash equilibrium is, first that this equilibrium may not exist in some games and second that other games could have multiple Nash equilibrium thus the players will be bewildered on which action to take (Weiss, 1999). The second drawback of Nash equilibrium is that sometimes efficiency goals and stability goals conflicts as exhibited in the prisoner's dilemma.

2.4.2. Coordination techniques

Agent dynamics are functions of positive and negative feedback loops. Consequently the actions of one agent in turn have an influence on the future behavior of another. Therefore agents must coordinate their actions to meet their individual goals mutually. To formalize the coordination strategies among agents three main issues should be addressed: decision-making, control structures and communication (Bousquet & Le Page, 2004). Agents could either have centralized or decentralized control structures that define their hierarchical relationships while a coordinating agent could also be employed to avoid conflicts or needless communication. The aforementioned can be carried out through passing different sorts of information like data, solutions, constraints and preferences among agents. Different classifications of coordination mechanisms have been proposed in literature for MAS. Shaw and Fox (Shaw & Fox, 1993) proposed a set of coordination mechanisms of which coordination by revising actions, by synchronization, by negotiation, by exchanging preferences (using game theory approach), by structured group mediation, by opportunistic goal satisfaction and by constraints reasoning. Whereas Jennings (Jennings, 1996) considered that the most common mechanisms for managing coordination are confined to three mechanisms: organizational structuring,

meta-level information exchange and multi agent planning. Mariano and al. (Mariano, et al., 2001) added contracting approach and reactive tuple spaces (also known as Blackboard) to the classification of Jennings.

In the context of a non-cooperative scheme of the industrial park the most appropriate and realistic mechanism for agents' coordination takes shape in negotiation. Therefore following Jennings classification (Jennings, 1996), we briefly explore in the following sections organizational structure and multi-agent planning and we go more in depth into the coordination by negotiations.

2.4.2.1. Organizational structure

This coordination approach consists of organizing agents in a hierarchical community which specifies information and control relationships amongst them. Those control relationships shape the interaction between agents and thus help their coordination. The higher level informs the lower level of the actions to undertake, in contrast to flat structure where this is attainable exclusively by negotiation.

2.4.2.2. Multi-agent Planning

The coordination by multi-agent planning consists of agents specifying their future actions and interactions in plans to achieve certain objectives. In this approach agents are fully aware of each action they will conduct, and other agents' activities that they will undertake and the interactions that will occur. The required information involved to constantly reconstruct the plans demand more computational and communication resource than the other two coordination mechanisms.

2.4.2.3. Negotiation mechanisms

The joint agreement reached by two or more agents each trying to attain its individual goal is called negotiation. The preference of agent i of agreement α over an alternative agreement α' is represented by the preference relation $\alpha \preceq_i \alpha'$. Employing utility theory helps mapping an agent interests over a set of available alternatives by real numbers and thus quantifies the agent degree of preference (Shoham & Leyton-Brown, 2009). Hence a utility function u_i representing the preference relation $\preceq_i$ is such that: $\alpha \preceq_i \alpha' <=> u_i(\alpha) \leq u_i(\alpha')$.

The negotiation is a strategic interaction that follows certain protocols defined by a set of rules such that the available actions for each negotiator and the sequence of their interaction. These protocols can be evaluated according to many criteria governing the choice of the negotiation mechanism according to the desired properties of the system (Weiss, 1999).

- Pareto efficiency: An agreement α is Pareto Optimal or Pareto efficient if there is no other agreement α' that would be better for at least one agent without being worse for any other. This criterion has a global perspective and is used to compare the solutions reached by the negotiation protocol.
- Social Welfare: This criterion is employed to evaluate alternative solutions reached by measuring the global good of agents. The sum of all agents' utilities associated to a given agreement is the social welfare. This property forms a subset of Pareto efficiency.
- Rationality: A self-interested agent would not participate in a negotiation if the payoff of the negotiated agreement is not higher than the payoff it would get without participating in the negotiation.

- Stability: Negotiation mechanisms are stable when agents have no incentive deviating from the desired agreement.
- Computational efficiency: Negotiation protocols should be designed with a limited computational burden.

Negotiations can be distinguished in three types according to the number of parties involved in the negotiations: One-to-one, one-to-many and many-to-many negotiators. Some examples of popular negotiation protocols are discussed below according to the aforementioned classification.

a) One-to-one negotiation – Bilateral bargaining

Bilateral bargaining is a socioeconomic problem involving two agents with a common interest to cooperate but with conflicting solutions to achieve this cooperation. The negotiation protocols of non-cooperative bargaining games with complete information can be used by two players to divide a given surplus resulting from the profit of reaching an agreement. Li and al. (Li, et al., 2003) discussed three protocols for such negotiation:

- The ultimatum game: One agent proposes a split of the surplus while the other can either accept or reject the offer. Both players end up with nothing in the case of refusal.
- Monotonic concession protocol: The protocol proceeds in rounds; in each both agents simultaneously make an offer. An agreement is reach when the offer of one player scores at least as high as the counter player current proposal. In the case where both offers hold, the proposal is selected by tossing a coin. If no agreement is reached the players can either concede by proposing a better offer or stand firm.
- Alternating offers: one player offers a fraction of surplus to the other player. This latter can either accept, reject or propose a counter offer. If the player does propose a counter offer, the initial proposal maker can either accept, reject or propose another counter offer. The loop goes on until one player accepts the proposal of its opponent.

Bilateral Bargaining with one sided incomplete information is when the buyer is informed about the seller (the buyer knows the seller's cost price) while the seller has no information about the other party (Li, et al., 2003). Three negotiations protocols for this type of games are the seller-offer game, the buyer-offer game and the alternating-offer game. In the first game the seller makes an offer that the buyer can either accept or reject. Whereas in a buyer-offer game, the buyer proposes an offer considering the seller's cost since the seller will only accept it if it is higher than its cost. As its name points out, in an alternating-offer game the players keep alternating between proposing and responding until an agreement is reached.

b) One-to-many negotiation – Single sided Auctions

Auction mechanisms provide easily implemented protocols for one-to-many negotiation. They are popularly employed for allocation of tasks, resources and goods. A single sided auction setting is made up of an auctioneer agent (the seller) and a collection of bidders agents (the buyers) with the goal for the auctioneer to allocate an item to one of the bidders (Wooldridge, 2002). The agents are self-interested thus the auctioneer plays to maximize the allocating item price while the bidders try to get it at the lowest price. Auction mechanisms may vary along with three main dimensions (Wooldridge, 2002). The first is the determination of the winner bidder and the price he pays for the allocated item. Protocols where the bidder with the highest bid wins and pays the bid amount for the item are known

as first-price auctions. However there is another type known as second-price auction where the highest bidder wins but pays the amount of the second highest bid. Another dimension is the visibility of bids between bidders. When bidders know each other bids the auction is said open-cry conversely when they are not able to know bids made by other agents it is said sealed-bid auction. The third dimension is how bidding proceeds. If the bidding goes only for one round after which the winner is allocated the item, the auction is a one shot auction. The second option is for the bidding price to start low and increase in successive rounds, this is an ascending auction. Alternatively descending auction is when the auctioneer starts with a high price and decrease in successive rounds. Some of the widely known auction protocols are:

- English Auctions: The auctioneer starts with a low reservation price which could be zero. Then in each round agents must bid more than the highest current bid. The auction ends when no agent is willing to raise the bid and the item is awarded to the highest bidder that pays that amount. English auctions are thus first-price, open cry, ascending auctions.
- Dutch Auctions: The auctioneer starts offering the item for a very high price and lowers it a little bit in each round; first bidder to accept the current offer is allocated the auctioned item. These auctions are open-cry, descending.
- First-price Sealed-Bid Auctions: These are an example of one round auctions where bidders submit an offer privately for the item to the auctioneer. This latter award the item to the highest bidder.

c) Many-to-many negotiation – Markets

The business definition of a market is where forces of demand and supply interact to trade goods or services for money. Unlike conventional one sided auctions with a single, centralized auctioneer and many buyers, double auction markets (two sided auction) consist of multiple buyers entering in competitive bids to purchase commodities offered by competing sellers that submit simultaneously their ‘ask price’ to the market. Hence double auction markets balance demand and supply efficiently in a decentralized system (Vytelingum, et al., 2008). In a continuous double auction (CDA), bids and asks are matched immediately if possible, otherwise orders are recorded in the order book. A CDA lasts for a certain period of time known as trading period during which offers and orders are continuously accepted.

Another well-known negotiation mechanism based on market structure is the Contract Net protocol (CNP) defined by Smith and Davis (Smith & Davis, 1981) for task allocation. This protocol enables the coordination amongst agents to carry out complex tasks that cannot be performed by a single agent. Each agent is a node in the network that can either take the role of a manager (buyer) or a contractor (seller). Those nodes are interconnected in such that every node can send messages to every other node (Smith & Davis, 1981). In the CNP, when an agent has a complex task unsolvable in isolation, it takes the role of a manager, breaks down the problem into sub-tasks and announces to the network the need of contractors to achieve it. Then contractor agents evaluate the task according to their ability and place bids for it. After assessing the received bids, the manager agent selects the contractor to whom he awards the contract and communicates the result to the task bidders. Finally the assigned contractor transmits the results of the tasks to the manager. Aknine and al. (Aknine, et al., 2004) extended the CNP for contractors to be able to manage several negotiation processes simultaneously. In the extended version (Aknine, et al., 2004), tasks are assigned to bidders proposing consecutively two best offers in the 'PreAccept' and 'DefinitiveAccept' phases and bidders are rejected when having two consecutive offer failures in 'PreReject' and 'DefinitiveReject'.

2.4.3. Proposed interaction for the non-cooperative scheme

The non-cooperative scheme of an industrial park is supposed to be in this research study the situation when industries, geographically located in the predefined boundaries, search to increase their personal gain instead of that of the park. This personal interest pursuit associated with a lack of communication engenders a detriment on synergies that eventually could be more beneficial for the park's industrial actor's economy if put in place and could thus directly influence their environmental footprint. To avoid this, we propose a MAS that enables the interaction between actors in the aim of executing potential synergies that are in favor of each of the industries.

Based on the previously explored strategy establishment techniques, game theory is found to be inapplicable in the displayed context in which agents must coordinate their actions to meet their individual goals mutually. Nevertheless the coordination through the negotiation mechanism is more adapted for self-interested agents, while organizational structure and multi-agent planning suits more non-antagonistic agents (Weiss, 1999).

Consequently the selected interaction model is based on the negotiation mechanisms with three types of agents involved: network investor, industrial agent, potential agent. The network investor agent negotiates with the other two agents to trade energy and material streams through bilateral bargaining following the alternating offers protocol. It takes in charge the investment and the installation costs of the pipelines that ensure the inter-sites material and energy streams transportation.

Each industry in the predefined boundaries is accounted for as an industrial agent IA_i which belongs to the industrial agents set IA defined below. The total number of existing sites is denoted by n. The third type of agents is the potential agent PA_{ik} which is an element of the set PA containing the entire potential agents. As its name states, PA_{ik} is a potential buyer of IA_i's waste W_i. This type of agents is none-existing in the territory.

$IA=\{IA_i \mid IA_i$ is an industrial site i located in the predefined boundaries of the park$\}$

$PA=\{PA_{ik} \mid PA_{ik}$ is a potential conversion system investor k for waste W_i of $IA_i\}$

The potential agents of the same waste first compete to trade W_i with IA_i and then the identified winner invests in a conversion system to transform the original form of W_i into a new product to be sold in the park. Therefore this winner, as it is appended to the territory, becomes an industrial agent IA_{n+1}. The conversion system investor can also communicate with the network investor to either buy or sell heat or matter from the network. To identify a CS_s as a PA_{ik}, a CS database containing the resources required by different conversion systems and their products is went through to find resource matches for each W_i. The interaction work flow between these agents for the non-cooperative scheme is illustrated in Figure 2.12.

In addition to the three aforementioned types of agents, a Third Party intervenes to conduct the preliminary studies of the territory ensuring that no agent possesses an overall knowledge of the circulating energy and material flows in the park. The Third Party collects the industrial agents' energy flow temperatures and heat flux. It then carries out the total site analysis based on exergetic evaluation of optimal heat exchanges possibilities between the agents included in the problem. Afterwards, the Third Party transmits to the Network investor the identified steam network temperatures T and the possible heat to be transferred to and from the network Q^{ex}. The aforementioned sets are defined hereafter along with two other sets of the problem, Q and P. Those are related to the Network Investor trading messages sent to the involved agents and are introduced in the following paragraph.

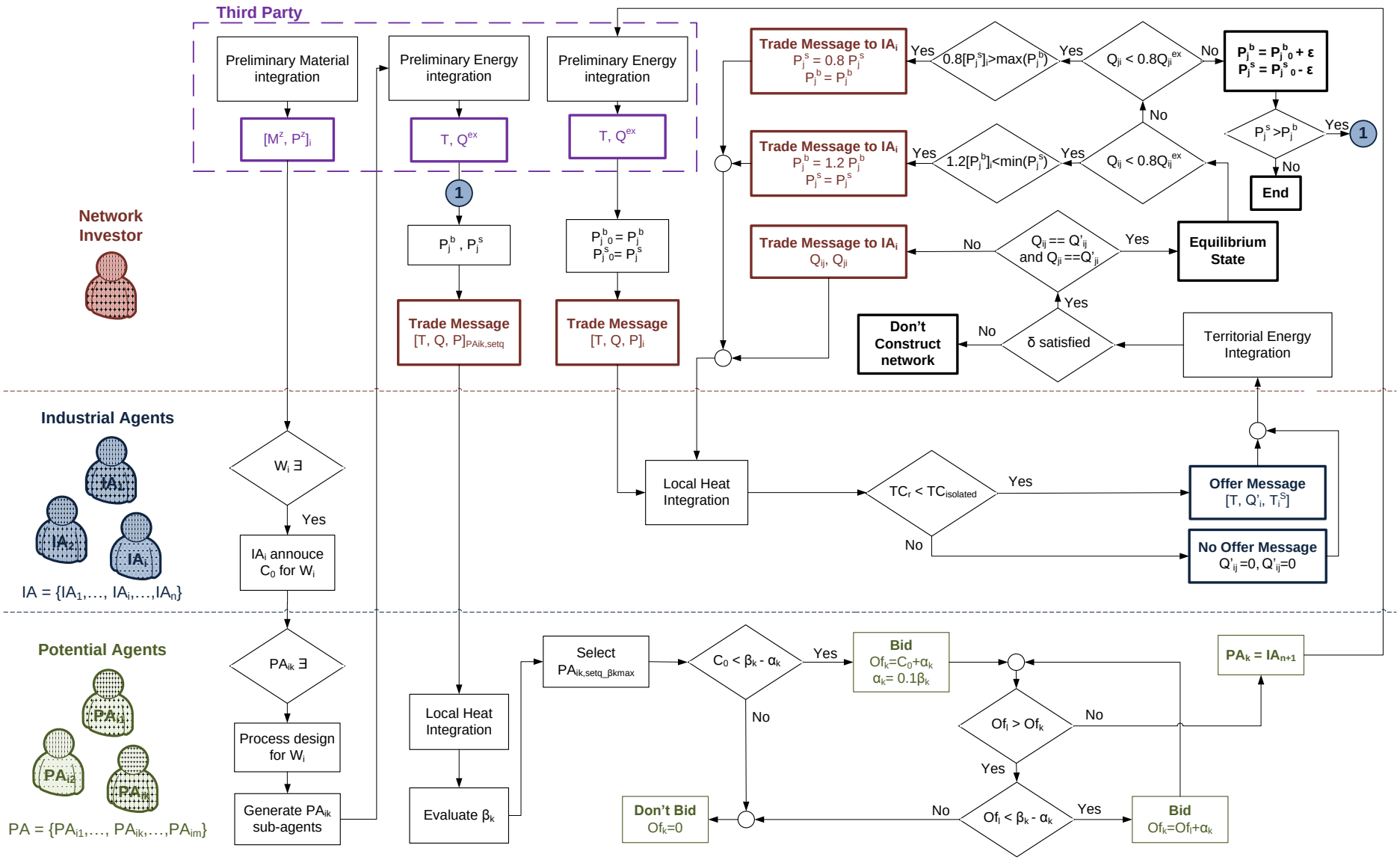


Figure 2.12. Agent interactions work flow framework for the territorial integration of conversion systems in a non-cooperative scheme

$T=\{T_j \mid T_j$ is the temperature number j of the steam network$\}$
$Q^{ex}=\{Q_{ij}{}^{ex} \mid Q_{ij}{}^{ex}$ is the maximal heat transferred/received from/by agent i to/from the network at $T_j\}$
$Q=\{(Q_{ij},Q_{ji}) \mid Q_{ij}/Q_{ji}$ is the heat load transferred/received from/by agent i to/from the network at $T_j\}$
$P=\left\{(P_j^b, P_j^s) \mid P_j^b \text{ is the buying price for heat at } T_j \text{ and } P_j^s \text{ is its selling price proposed by the Network Investor}\right\}$

According to the received evaluation from the third party, the network investor generates a specific Trade Message for each IA_i consisting of the network temperatures T it will construct, the amount of energy Q_{ij} and Q_{ji} the Network Investor will buy or sell to Industrial agent i at the buying and selling prices P_j^b and P_j^s respectively. The specific Trade Message sent to IA_i is therefore constructed using the three sets: $[T, Q, P]_i$. At the network temperature T_j, IA_i can either transfer Q_{ij} to the network or receives Q_{ji} from it. Consequently at each network temperature only one of these two quantities can have a positive value. As for the P set, it is created relative to the Market heat utility price that varies according to the utility's temperature which is in this case T_j.

The selling and buying prices are reevaluated at each iteration of the entire problem according to the heat utility price and supposing a linear variation slopes formed by a new introduced parameter Cost%. The P_j^b is assumed to be a fraction represented by Cost% of the utility price. Since this parameter is defined as being directly proportional to the problem's number of iterations with a 10% step (a parameter that could be altered), the buying price starts from zero and increases progressively in each iteration. As for the selling offer P_j^s, the network investor proposes to supply heat at the heat utility price and then this offer decreases in the following iterations in function of $(1-$ Cost%).

Simultaneously to the preliminary energy integration evaluation, the Third Party conducts a preliminary territorial material integration by assessing the resources demand and waste discharge of the IA. It subsequently informs each concerned agent i with whom it can trade to get its resources or give its wastes through the Material Message $[M^z, P^z]_i$. This latter is formed by the amount M^z of the exchanged material z and by the price of z which is assumed equal to its Market price for both buying and selling agents when both of these $\in$ IA. The newly introduced sets are defined as follow:

$M^z = \{M_{ip} \mid M_{ip}$ is the mass flow of material z transferred from agent i to agent p$\}$
$P^z = \{(P^{z,b}, P^{z,s}) \mid$ the buying and selling prices respectively for material z $\}$

However when a network is required to transport material z to establish an identified synergy, the Network Investor takes in charge putting in place the pipeline and becomes the intermediate agent for exchanging material z between two Industrial agents. Therefore it charges the Market price for selling z and pays less for the agent from whom it is buying z in order to achieve a return on its investment. By evaluating the received Material Message and its waste discharge, each IA_i is able to identify whether or not it has a waste W_i that has no possible synergy in the territory in its existing form. If that is the case, IA_i announces the start of a single sided auction for its non-usable amount of W_i at an initial price $C_0 \in R^+$.

The auction's participants are the potential agents which are identified by running through the CS database searching for the possible W_i conversion systems. This database consists of physical and economic processes models formulated based on their energy and material balances. According to the auctioned annual quantity of W_i, PA_{ik} evaluates its system design parameters and size it for the complete use of W_i since the auction is based on the concept of 'Take it or leave it'; meaning that the auction's participants can only place their bids for the entire auctioned quantity of W_i.

Once the potential agent PA_{ik} sizes its conversion system, it generates different sub-potential agents by modifying the operating parameters of its process units, thus creating multiple $PA_{ik,set\ q}$, namely:$PA_{ik} = \{PA_{ik,set\ q} \mid PA_{ik,set\ q}$ is a sub-agent of PA_{ik} with the operating parameters set number q$\}$. For every created sub-agent in the potential agents' population, which is depicted in Figure 2.13, the Third Party takes on the energy entailed from the conversion system in order to conduct a territorial exergetic energy integration supposing in its problem $PA_{ik,set\ q}$ an industrial site of the territory along with the existing IA. It also evaluates the territorial opportunity usage of $PA_{ik,set\ q}$ produced material streams through the territorial material integration. Then the Network Investor employs the transmitted results from the Third Party to generate the specific Trade Message for $PA_{ik,set\ q}$: $[T, Q, P]_{PA_{ik,set\ q}}$ and its Material Message$[M^z, P^z]_{PA_{ik,set\ q}}$.

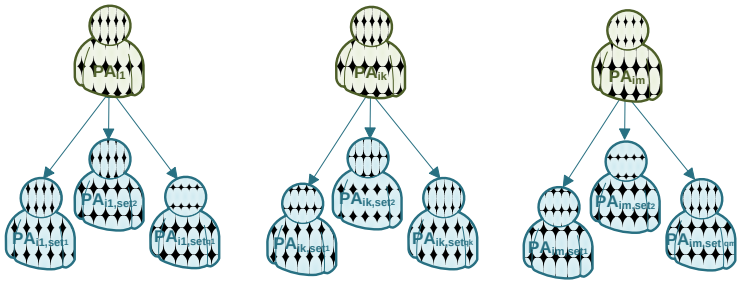


Figure 2.13. The potential agents' population

Accounting for the received Trade Message, $PA_{ik,set\ q}$ carries out its local heat integration problem. Actually each time an agent receives a Trade Message from the Network Investor, it creates new utilities with the proposed network temperatures aiming to incorporate the offered trade in its problem and to eventually evaluate it. When the offered trade at T_j refers to the amount of heat Q_{ij} the Network Investor wants to buy from IA_i, this latter appends this proposition to its problem as a cold utility at T_j with a negative cost equal to the price P_j^b; whereas for an offer from the Network Investor of selling Q_{ij} at T_j, a hot utility is created with a cost of P_j^s.

The sub-potential agents use the results from their local integration to evaluate the highest price they can bid at to get W_i and reach the return on investment goals. A new set is introduced, namely: $\beta_k = \left\{\beta_{k\,PA_{ik,set\ q}} \;\middle|\; \beta_{k\,PA_{ik,set\ q}}\right.$ is the maximum amount PA_{ik} is willing to bid for $\left.W_i\right\}$. To assess its bidding limit, $PA_{ik,set\ q}$ accounts for its entire investment and operating costs according to Eq.(2.43) and considering a number of operating years manifested in the parameter 'Nbr_{year}'.

$$\beta_{k\,PA_{ik,set\ q}} = -\left[Opex_{HEN} + Opex_{CS} - Revenue_{CS} + \frac{Capex_{HEN} + Capex_{CS}}{\sum_{y=1}^{Nbr_{year}} (1 + DRate)^{-y}}\right] \tag{2.43}$$

The operating costs of $PA_{ik,set\ q}$ cover the resources expenses required to maintain the conversion system operation as well as the local heat utility demands which are assessed during its local energy integration. As for the capital cost, it embeds the investment needed to implement the conversion system and those to install the heat exchangers needed to establish synergies between its internal heat streams. After evaluating the maximum bidding potentials of its entire sub-agents population, PA_{ik} selects the agent with the best operating parameters set that results in the uppermost β_k. It hence enters the auction for W_i with this sub-agent, meaning that $P_{ik,set\ q_\beta kmax}$ becomes PA_{ik}.

The agents' interaction during the auction course is based on the one-to-many negotiation based on the English auction protocol. To decide if it is possible for it to place a bid in the auction, PA_{ik} first examines its β_k compared to the initial announced price C_0 for W_i. If it manifests as profitable, PA_{ik} places a bid Of_k higher than C_0 by α_k which is defined as ten percent of its β_k. Each potential agent participating in the auction keeps on proposing greater bids than the others' previous offers until it reaches its bidding limit and thus gets out of the auction. This latter ends when no agent is willing to raise the bid and W_i is awarded to the highest bidder. The winning potential agent becomes a new industrial agent; hence the industrial agents' number increases by the addition of the conversion system agent to the initial n sites, by that IA tallies N elements: IA = {IA_1, IA_2,.., IA_n, IA_{n+1}}. The trade the auction's winner is going to establish with IA_i for its waste is incorporated at the end of the auction in both parties' economic balances. In the first's, this transaction manifests as resource expenses equivalent to the winning bid it made to get W_i, while it generates a new income source for the second via selling its previously none-usable waste.

When a new agent is appended to the territory, the exergy optimal networks might vary with the introduced streams of that agent. Subsequently, the Network Investor issues a new Trade Message specific for each agent accounting for the updated IA set. Each industrial agent then carries out a local heat integration for its own streams considering the proposed networks in the Trade Message received from the Network Investor. This is achieved by calling the local HENS algorithm which seeks to design the optimal synergies configuration that enables the minimization of the total cost. Therefore, the self-interested agent would not exchange heat with the network for the proposed temperatures and prices if the engendered total cost from participating in the network is not lower than the total cost it would get by exclusively using its own utilities. In the case where IA_i does not find it lucrative to exchange heat with the network and thus chooses to act as an isolated agent, it sends a No Offer Message to the Network Investor. In contrast, if it does find it profitable, IA_i transmits an Offer Message to the Network Investor indicating the amount of heat it wants to sell or buy at the network temperature T_j for the proffered prices: [$T_{,}$ Q'_i, T_i^S]. The new sets are introduced as follow:

$$Q'_i = \left\{ (Q_{ij}^s, Q_{ji}^s) \middle| Q_{ij}^s / Q_{ji}^s \text{ are the heat loads } IA_i \text{ wants to sell/buy to the network at } T_j \text{ via stream s} \right\}$$

$$T_i^S = \left\{ (T_{in}^{s,j}, T_{out}^{s,j}) \middle| (T_{in}^{s,j}, T_{out}^{s,j}) \text{ are the inlet and outlet temperatures of } IA_i\text{'s stream s that exchanges with } T_j \right\}$$

Once the network investor receives the Offer Messages from the entire industrial agents, it launches the territorial energy integration. The algorithm used in the cooperative scheme to conduct such integration is amended to be suitable for the non-cooperative governance. The buying and selling energy prices are introduced in the algorithm and are set from the sent Trade Messages. It is supposed that no possible utility can be added on the network; meaning that the network only buys from a site offering heat the amount of energy that it can resell to another site according to the received Offer Messages. The objective function of the problem employed in the cooperative scheme and which consists on minimizing the total cost is amended and written as in Eq.(2.44). It expresses the objective function of the Network Investor which aims at identifying its purchase and sale transactions for an optimal network design. The capital cost is only generated by the pipeline installation costs since the heat exchangers are taken in charge by the industrial agents.

$$\text{min:} \quad \text{totalCost} = \text{Capex}_{\text{pipeline}} + \sum_{y=1}^{\text{Nbr}_{\text{year}}} \frac{1}{(1+\text{DRate}_{\text{NI}})^y} \times \sum_{i=1}^{N} \sum_{j=1}^{\text{Networks}} (P_j^b \times Q_{ij} - P_j^s \times Q_{ji}) \qquad (2.44)$$

In the aim of preventing the territorial integration algorithm from numerically adding utilities on a seller site to increase the quantity the network can buy to supply the entire required heat by other sites, since this path decreases the network's total cost, a buying limit variable Q_{ij}^{limit} is introduced. A buying limit variable Q_{ji}^{limit} is also created to impede transferring heat from a deficit site to a cold utility just to increase the site demand and economically justifying the network's purchase of the complete offered energy of other sites to resell it at a higher price to cover the deficit sites' increment. Both of these variables are set as constraints for the design optimization as expressed in Eq.(2.45).

$$\begin{cases} Q_{ij} \leq Q_{ij}^{limit} = \sum_{s=1}^{NbrStoTj} Q_{ij}^{s} \\ Q_{ji} \leq Q_{ji}^{limit} = \sum_{s=1}^{NbrSfromTj} Q_{ij}^{s} \end{cases} \tag{2.45}$$

If the Network Investor does not meet its set return on investment, no network is constructed. Consequently, the negotiations for heat synergies end after informing the industrial agents through an empty Trade Message sent to the entire elements of IA. Otherwise if the heat exchange network took shape from the proposed offered messages, the Network Investor retransmits a new Trade Message to IA with the actual heat amounts it will buy Q_{ij} or sell Q_{ji} to IA_i at the network temperature T_j. The industrial agents then reevaluate their payoffs from only trading the amount of energy proposed by the Network Investor via the local integration problem. They hence either transfer a new Offer or No Offer Message accordingly to the Network Investor which repeats its network design optimization. The negotiations goes on until the amount of heat each IA_i wants to trade Q'_i is identical to the quantities Q the Network Investor is willing to incorporate in the network. The joint agreement on the energy and material trading reached by the Network Investor and the industrial agents and which contributes in increasing the individual payoffs of the self-interested agents is defined as an equilibrium state. The case in which the territory's agents have no incentive from cooperation and thus none engages in any agreement is also considered as an equilibrium state.

Once an equilibrium point is reached the Network Investor weighs up the resulting exchanged energy amounts in the territory Q to the maximal synergies Q^{ex}. When the heat IA_i offers to buy or sell to the network is lower than four-fifth of the maximal potential offer, the Network Investor reevaluates the buying and selling prices it have proposed resulting in this income. It actually seeks on finding other equilibrium state in which more synergies can be implemented and that might turn out to be more profitable for it. The price at which the Network Investor buys heat from IA_i for T_j is increased by 20% compared to the earlier offer if the energy IA_i have put to sale is lower than four-fifth of its potential. The selling price is also decreased by the same percentage if IA_i haven't bought 80% of Q_{ij}^{ex}. The amended Trade Messages are resent to IA inducing the necessity for IA_i to revisit its local HENS and consequently restarting the equilibrium state search engendered from the upgraded prices. As long as the enhanced heat buying price at T_j does not surpass the lowest selling price, $P_j^b$is increased. And while the altered selling price for IA_i is still higher than the greatest buying heat price at T_j, P_j^s could be reduced. When the limits in Eq. (2.46) are reached and no further adjustment can be made to the specific prices, the entire negotiation problem is reiterated.

$$\begin{cases} [P_j^b]_i \times 1.2 < \min(P_j^s) \\ [P_j^s]_i \times 0.8 > \max(P_j^b) \end{cases} \tag{2.46}$$

Actually in the previous amendment step of the energy selling and buying prices, the changes were carried out specifically for each temperature and for each agent. Meaning, when agent IA_i have indeed exchanged its full potential with the network, its Trade Message $[T, Q, P]_i$ is maintained unchanged; while for another industrial agent IA_p that might offer higher amounts of energy at T_j for a better pricing, the Network Investor proposes a new Trade Message $[T, Q, P]_p$ with higher buying or lower selling prices for heat according to the offer Message of IA_p.

However once the variation limits are reached, the problem is reiterated with new Trade Messages engendered from resetting the buying and selling prices for the entire IA population according to the heat utility prices with the updated Cost% parameter which varies as described earlier with the number of iterations. Subsequently the auction is repeated since the bidding limits of the potential agents will be influenced by the updated Trade Messages and thus the auction outcome might too. Before the auction is relaunched, the winner of the previously conducted auction is removed from the industrial agents set IA so that the waste W_i could be put up again for sale. Nevertheless, if the new auction winner has already won in preceding problem iteration, the Network Investor revises in the same manner the Trade Messages to be issued and the auction is restarted since the resulting equilibrium states will definitely be less favorable for the self-interested Network Investor. The reason behind that is the fact that by integrating the same conversion system in the territory the optimal synergies design will not be affected for the evaluated energy streams remain intact. Consequently, when the Network Investor offers to sell heat at a lower price and to buy it for a higher value for IA, it will be converging towards the similar energy exchange equilibrium state in which its payoff is lower. Therefore resending such Trade Message is contradictory with its objective consisting on increasing its individual interest and thus the Network Investor has no incentive from participating in these negotiations.

The problem number of iterations is restricted to five times limiting the computational burden by dint of the prices amendment method reckoned on the parameter Cost%. This latter attain the value of 0.5 at the fifth iteration with the increment step fixed at 0.1. Consequently the buying P_j^b and selling P_j^s prices of heat at T_j both become half the utility price cost. The Network Investor would not accept to buy and sell heat at the same price with the pipeline installation expenses it has to bear, thus a single equilibrium state exists at the fifth iteration and above. This is the state where no heat network is installed meaning that circular economy does not prevail and considerable synergies opportunities between the territory's agents are omitted. Subsequently, the entire problem halts at the fifth iteration.

2.5. Conclusions

In this chapter two methodological frameworks for integrating reacting thermodynamic conversion systems in a territory were proposed to create new valorization opportunities of the non-usable streams in their original form by converting them into new recoverable products. The methodological bricks of the energy and material integration used in the construction of the proposed methodologies were explored and state of the art models were selected to be employed for that purpose. The first methodology was developed for a territory governed by cooperative scheme. In such governance, industrial actors within a geographic proximity collaborate to establish inter-sites synergies in the aim of improving the global welfare of the territory by searching to reduce its total operating expenses. The ensuing investment bills from implementing the material and energy exchanges are parceled out on the territory's participating actors since they are supposed to share costs and gains as a single entity.

The proposed methodology was formulated as a Master-slave problem, in which the Master problem manipulates the sovereign variables of the non-usable identified streams' conversion processes which are established in the conversion pathways' superstructure to create the potential territory's scenarios. The two slave problems that follow the Master problem are the MILP models of the local and territorial integration. The proposed methodological framework of a cooperative scheme generates the global capital and variable costs induced from the optimal synergies patterns of several prospective scenarios of the actual territory with the implemented conversion pathways. Therefore, it enables the identification of the best design and technical specs of the non-usable streams conversion scenarios.

The second methodological framework was proposed for designing eco-industrial parks with non-cooperative governance. In contrary to cooperative scheme where the global interest of the territory is sought by the park's industrial actors, in non-cooperative governance each actor searches to maximize its individual interests. Hence, the non-linearity of the aggregate activities of the different actors, entails the complexity of formulating the problem using centralized mechanism with a single objective. Agent-based modeling was therefore chosen to model and simulate the problem in the aim of accounting for several heterogeneous agents each with its own objective function and that acts and reacts to each other's behavior. The interaction between agents was established using the negotiation mechanisms to ensure the coordination between their actions. Three types of agents were defined: network investor agent, industrial agent, potential agent. These agents are capable of controlling their own behavior, with each acting in the furtherance of its own goals while interacting with each other in a shared territory.

For each non-usable waste an industrial agent discharges, a single sided auction based on the English Auction is held with the industrial agent being the auctioneer and the potential agents as the collection of bidders in the aim of allocating the waste to the bidder with the highest bid. The potential agents refer to the possible reacting thermodynamic systems which can change the initial composition of waste streams and convert them into new products that it could sell to other industrial actors. The network investor trades heat with industrial agents through buying and selling transactions and takes in charge the installation of the material and energy transport networks. The proposed methodology enables the establishment of the strategic decisions to be implemented by each self-interested agent in a territory with non-cooperative governance by identifying the equilibrium prices for the purchase and sale flows between agents.

To explore the potential results that could be ensued from both methodologies, the following chapter will present the case study on which the proposed methodological frameworks will be applied. From the preliminary assessment of the studied territory, the unrecoverable streams will be identified. Subsequently, Chapter 3 will explore the conversion systems of the identified waste and will exhibit the physical and economic models of the process units of each selected conversion pathways.

Chapitre 3 (résumé)

Étude de cas: Modélisation des systèmes de conversion du bois pour leur intégration dans le parc industriel étudié

L'étude de cas est constituée d'un parc industriel virtuel formé de trois usines dénommées Site 1, Site 2 et Site 3. Le Site 1 présente une demande d'hydrogène de 1,5 t/h et génère 12 t/h de déchets de bois. Le parc étudié n'a aucune synergie initiale et aucun système de valorisation des déchets de bois rejetés. L'étude vise à trouver la meilleure configuration d'éco-parc industriel ayant une configuration de synergie optimale.

Les besoins en énergie du parc sont identifiés en fonction des températures des flux en circulation et des capacités de la charge thermique de chaque site. Avec les acteurs industriels du parc étant bien distingués par leurs demande de ressources, leurs besoins énergétiques et leurs décharge de déchets, les synergies entre-sites pourraient être étudiées à travers les problèmes territoriaux d'intégration de matière et d'énergie. Le réseau d'échangeur de chaleur exergétique est conçu par la minimisation de la consommation d'éxergie du système d'intégration de la chaleur, ce qui entraîne l'utilisation la plus faible des utilités chaude et froide. L'algorithme d'intégration employé calcule les synergies potentielles entre les acteurs du parc en proposant des réseaux de chaleur tertiaires pour éviter la complexité imposée par l'intégration énergétique directe entre les flux de chaque site. Le fluide de transport d'énergie est censé être de la vapeur qui pourrait circuler à différents niveaux de pression; chaque réseau est donc défini par un niveau de température spécifique. Les synergies établies ont permis une récupération totale de la chaleur entre-sites de 22,62 MW.

Étant donné que les deux seuls flux de matière présents sur le territoire sont de composition différente, aucune répartition possible entre les déchets de bois et l'hydrogène n'est possible. L'hydrogène doit donc être acheté des fournisseurs externes pour maintenir le bon fonctionnement du parc. Et même en recherchant des synergies entre les acteurs industriels, 12 t / h de déchets de bois sont encore déversés sans aucune opportunité de valorisation car aucun des sites ne présente une telle demande. Le procédé de conversion offre la possibilité de transformer les déchets de bois non utilisables en d'autres composants utilisables et permet leur réinsertion dans le territoire. Par conséquent, les systèmes de conversion potentiels du bois sont étudiés dans la section suivante et ceux qui se révèlent les plus appropriés pour le territoire étudié sont identifiés pour être ensuite modélisés.

Aperçu des systèmes de conversion du bois

Pour produire divers produits à partir de la biomasse ligneuse déchargée sur le territoire, comme les combustibles, l'énergie et d'autres produits chimiques, une bio-raffinerie intégrant des procédés de conversion de la biomasse est nécessaire. Les procédés qui impliquent la destruction et la formation de liaisons chimiques générant ainsi un changement de composition chimique de la biomasse peuvent être classés en deux catégories principales:

- Conversion thermochimique: pyrolyse, combustion et gazéification.
- Conversion biochimique: hydrolyse, fermentation et digestion anaérobie.

Dans les voies de conversion thermochimique, la combustion directe est la voie la plus évidente pour récupérer le potentiel calorifique de la biomasse en la convertissant en chaleur, des turbines à vapeur pourraient être ajoutées pour co-générer de l'énergie électrique. La gazéification du bois forme une autre voie de conversion thermochimique. Le gaz résultant peut être converti en produits de plus grande valeur que le bois, tels que les biocarburants liquides par Fischer-Tropsch, ou l'hydrogène en couplant un vapo-reformeur de méthane à un réacteur de Water-Gas Shift. Le bois peut être aussi converti en méthane en plaçant une unité de méthanation en aval du gazéifieur. D'autre part, la conversion biochimique de la biomasse consiste en une réaction d'hydrolyse qui décompose la biomasse ligneuse en molécules de sucre qui sont ensuite transformées par fermentation pour produire de l'éthanol.

La valorisation du bois déchets par la production de chaleur et d'électricité, la production d'hydrogène ou de méthane ont été choisis pour être mis en compétition puisque le parc a besoin d'hydrogène et de chaleur et que l'électricité et le méthane peuvent être vendus au réseau électrique national et au réseau de gaz respectivement. Les unités de processus formant chacune de ces voies sont identifiées puis modélisées à l'aide du langage Modelica® dans le logiciel Dymola® par des modèles physiques basés sur leurs bilans d'énergie et de masse tout en tenant compte de la réaction chimique survenant dans les réacteurs. Les hypothèses établies et les modèles développés ont été validés ou comparés aux résultats de la littérature et se sont ainsi révélés fiables. Des modèles économiques sont également proposés sur la base des capacités unitaires en vue de prendre en compte l'impact de l'altération des paramètres de conception lors de la comparaison de différents scénarios de dimensionnement des procédés de conversion. Les modèles servent en fait à simuler plusieurs ensembles de paramètres de fonctionnement et à évaluer les schémas des procédés qui en découlent, à partir desquels les flux d'énergie et de matière seront extraits pour conduire l'intégration selon le schéma économique du territoire.

Système de Conversion du bois en hydrogène

Le chemin de conversion étudié du bois en hydrogène se compose de trois étapes essentielles: la gazéification, le reformage à la vapeur et le transfert de gaz à l'eau (WGS). Deux étapes sont ajoutées pour bénéficier de la sortie de gaz résiduaire du réacteur WGS. L'organigramme de la production d'hydrogène à partir des déchets de bois est illustré à la Fig. 3. Avec de la vapeur comme agent gazéifiant, la biomasse est convertie en un mélange gazeux riche en hydrogène contenant du goudron qui est un mélange complexe d'hydrocarbures condensables. Le produit de gazéification est raffiné dans le réacteur de reformage à la vapeur par la conversion du goudron en hydrogène. La production supplémentaire de ce dernier est réalisée dans le réacteur à membrane de la réaction de gaz

à l'eau, qui est formé d'un lit catalytique où la réaction WGS a lieu et d'un autre canal dans lequel l'hydrogène est séparé progressivement à travers une membrane sélective d'hydrogène. Le gaz sortant du canal de lit du réacteur WGS est constitué d'hydrogène, de monoxyde de carbone et de méthane non converti, formant ainsi un potentiel combustible. Par conséquent, ce dernier est brûlé dans une chambre de combustion avec de l'oxygène pur pour saisir l'opportunité de n'avoir que du dioxyde de carbone et de l'eau comme produits qui sont éventuellement séparés par condensation d'eau.

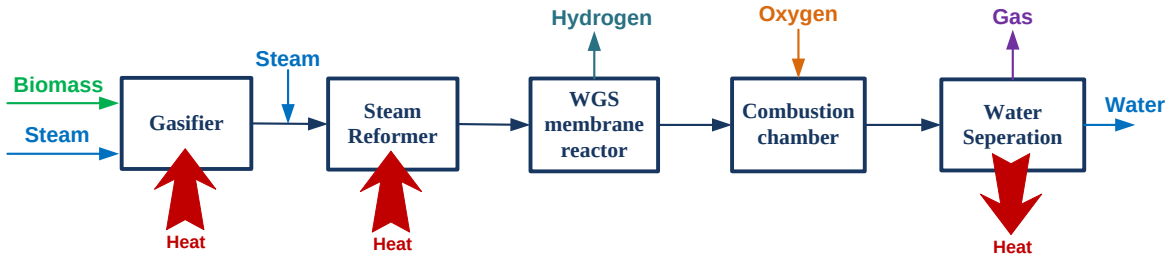


Fig. 3. Diagramme fonctionnel de la conversion du bois en hydrogène

Gazéifieur

Le modèle de gazéifieur développé représente un lit fluidisé fonctionnant à haute température et pression atmosphérique. Il est formé de deux zones: une zone hétérogène qui est la partie inférieure du gazéifieur comportant le lit fluidisé et une zone homogène. Le gazéifieur est modélisé sous la forme d'un réacteur à écoulement piston unidimensionnel dans deux sous-modèles cinétiques formant les deux zones du réacteur.

Vapo-reformage

Dans le but de produire de l'hydrogène de haute pureté, une qualité de gaz de synthèse significative est recherchée. En se basant sur l'état de l'art, un réacteur secondaire placé en aval du gazéifieur a été utilisé pour améliorer le produit de gazéification par reformage du goudron par un catalyseur à base de nickel. Avant d'entrer dans le reformeur à vapeur, les produits de gazéification sont mélangés à de la vapeur pour ajuster leur rapport vapeur / carbone afin d'empêcher le dépôt de carbone sur la paroi du réacteur. Une fois dans le reformeur à vapeur, la vapeur réagit avec le méthane et le goudron à haute température (700-1100 ° C) en présence du catalyseur et produit de l'hydrogène et du monoxyde de carbone. La réaction est formulée par un modèle cinétique utilisant la méthode des différences finies (FDM) du premier ordre. Un modèle unidimensionnel en régime permanent a été développé pour simuler le réacteur de reformage à la vapeur satisfaisant les équilibres molaires et énergétiques d'un réacteur à écoulement piston.

Réacteur à membrane de la réaction du gaz à l'eau

Le réacteur à membrane de la réaction du gaz à l'eau (ou réaction de Dussan) se compose d'un lit catalytique où la réaction chimique a lieu et d'un autre canal dans lequel l'hydrogène est aspiré par un effet de vide à travers une membrane faite d'un alliage riche en palladium (Pd-Ag). Dans le canal du lit, le monoxyde de carbone réagit avec la vapeur pour produire un mélange d'hydrogène et de dioxyde de carbone. En raison de la sous pression dans le canal non-réactif, la sélectivité de la membrane permet la séparation progressive de l'hydrogène au fur et à mesure de sa production dans le mélange.

Chambre de Combustion

Le gaz sortant du canal catalytique du réacteur à membrane WGS a une valeur calorifique significative. Pour tirer parti de cette caractéristique, il est brûlé dans une chambre de combustion avec de l'oxygène pur comme oxydant pour limiter la composition de la sortie à la vapeur d'eau et au dioxyde de carbone. Ce procédé est formulé à l'aide d'un modèle d'équilibre thermochimique basé sur l'équilibre chimique du procédé.

Séparation d'eau

L'étape de séparation de l'eau est accomplie d'abord en refroidissant les gaz de combustion à une température inférieure au point de saturation de l'eau. Cette diminution de température favorise le passage de l'eau du gaz à la phase liquide lorsqu'elle atteint sa température de condensation. Ensuite, le mélange liquide-vapeur passe à travers un ballon de détente où le gaz sort du haut et le liquide du fond du tambour en raison de la différence de densité.

Système de Conversion du bois en méthane

La deuxième voie de valorisation possible est la conversion du bois en méthane dont l'unité principale est celle de la méthanisation qui assure la production de méthane. Néanmoins, une gazéification thermochimique est également essentielle à cette voie compte tenu du besoin de convertir la biomasse en un mélange gazeux avant son introduction dans l'unité de méthanation. La Fig. 4 représente l'organigramme du système de conversion du bois en méthane. La gazéification de la biomasse à la vapeur génère un mélange riche en hydrogène. Le passage de ce dernier dans l'unité de méthanation augmente sa teneur en méthane. Cependant, pour obtenir un méthane de haute pureté, l'eau est d'abord condensée en refroidissant le gaz, puis le mélange est comprimé pour éventuellement séparer le dioxyde de carbone via une membrane sélective. Le modèle de gazéifieur décrit dans la section précédente de la filière de production d'hydrogène est également utilisé pour cette voie de conversion puisqu'il s'agit du même réacteur de gazéification de la biomasse par la vapeur d'eau.

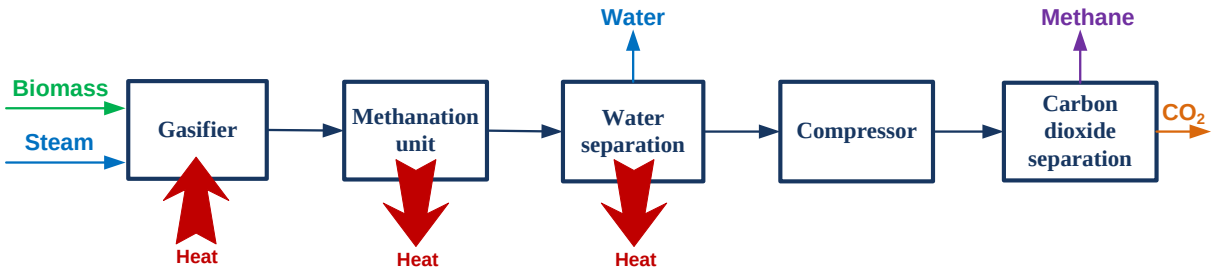


Fig. 4. Diagramme fonctionnel de la conversion du bois en méthane

Unité de méthanation

L'hydrogène contenu dans le gaz de sortie de gazéification réagit avec le monoxyde de carbone sur un catalyseur à base de métal pour produire du méthane et de la vapeur. Cette réaction hautement exothermique se produit simultanément dans l'unité de méthanation avec une réaction secondaire de la réaction du gaz à l'eau. En considérant un processus isotherme, l'évacuation d'énergie du réacteur est égale à celle générée par la réaction chimique qui se produit à l'intérieur.

Compresseur

Comme le montre l'organigramme en bloc de la Fig. 4, un compresseur est nécessaire avant la séparation du dioxyde de carbone puisque la technologie employée à cet effet nécessite un flux sous pression. Le compresseur est modélisé avec un rendement isentropique de η_{is} par ses bilans massique et énergétique dans lequel les enthalpies de chaque composant à différents états sont calculées à l'aide des corrélations intégrées dans Dymola®.

Unité de séparation du dioxyde de carbone

Après avoir récupérer l'eau du gaz à la sortie de la méthanation, le CO_2 reste le seul composant à éliminer pour atteindre un flux très riche en méthane adapté aux spécifications du réseau de gaz. La capture du dioxyde de carbone à l'aide de membranes a été sélectionnée pour récupérer le CO_2 dans le procédé de conversion du bois en méthane. La membrane perméable employée permet la diffusion du dioxyde de carbone et du monoxyde de carbone tandis que le reste du mélange peut être collecté de l'autre côté de la membrane.

Système de Conversion du bois en électricité et chaleur

La conversion du bois en énergie est la troisième voie de valorisation étudiée. En effet, la combustion exothermique de la biomasse libère de la chaleur qui peut être absorbée par l'eau soit lors du changement de phase, soit pour un gradient de température dans un échangeur de chaleur. En ajoutant un cycle de vapeur simple après le four à biomasse, l'électricité est produite par l'expansion de la vapeur dans la turbine et la chaleur latente stockée à l'intérieur peut être libérée à travers le condenseur. En divisant le flux avant qu'il passe par la turbine, la chaleur peut être récupérée à deux niveaux de température différents, comme le montre la Fig. 5. Notant qu'en fonction de la fraction sélectionnée autorisée à traverser la boucle du circuit thermique (Heat path), la quantité d'électricité produite change et donc l'énergie libérée au niveau des condenseurs aussi.

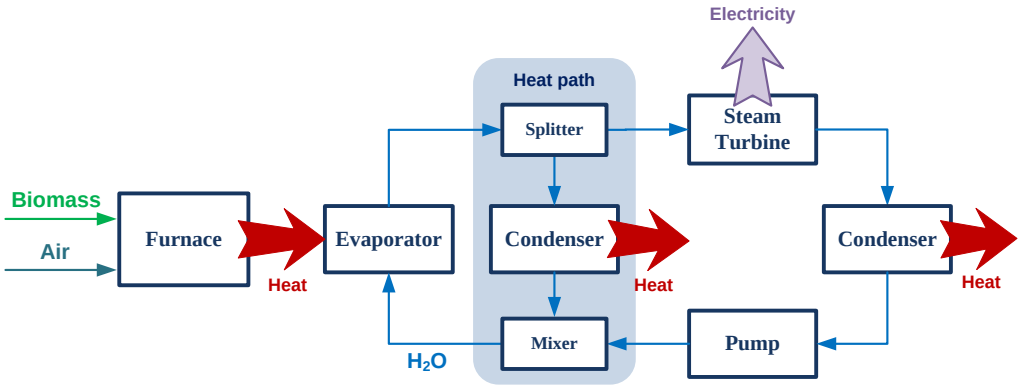


Fig. 5. Diagramme fonctionnel de la conversion du bois en énergie

Four de biomasse

Le modèle du four adiabatique est formé par la chambre de combustion utilisé pour la voie de conversion en hydrogène avec deux étapes supplémentaires pour convertir la biomasse en un mélange gazeux. En entrant dans le four, la biomasse est instantanément transformée en gaz, goudron et coke, sous l'effet de la chaleur, par la réaction de pyrolyse. À 300 ° C, le craquage du goudron ou la pyrolyse secondaire est supposé commencer. Cette étape est formulée comme un modèle d'équilibre thermochimique. L'air est ensuite introduit dans le four qui est à 600 ° C pour déclencher la combustion. La température de l'air d'entrée est définie comme un paramètre du modèle. L'énergie

nécessaire pour chauffer l'air introduit à 600 ° C et celle pour la réaction endothermique de la pyrolyse est couverte par une partie de l'énergie produite par la combustion exothermique, donc le flux de chaleur n'est pas nul dans ce système et est égal à ce transfert énergie. Par conséquent, la température des gaz de combustion est évaluée une fois que ce flux de chaleur est déterminé.

Turbine à vapeur

L'énergie thermique transférée au flux de vapeur provenant des gaz de combustion est convertie en travail mécanique par la turbine. En supposant une efficacité isentropique de η, le travail généré a été évalué. L'enthalpie réelle du courant sortant peut être évaluée à partir de l'enthalpie de sortie réelle trouvée.

Séparateur et mélangeur

Pour permettre la récupération de la chaleur à deux niveaux de températures dans le système de conversion du bois en énergie, un séparateur de flux a été employé. Ce composant permet la division du flux en deux. Le premier traverse la turbine avec une fraction x du débit d'entrée, et le reste du flux (1-x) circule dans la boucle du circuit thermique où la chaleur est récupérée à haute température. Après son expansion dans la turbine, la chaleur latente libérée par son refroidissement peut être récupérée à une température inférieure à celle du chemin de la boucle de chaleur. Pour boucler le cycle, un mélangeur a été ajouté après avoir pompé le flux d'eau à basse température pour atteindre la même pression du flux à haute température.

Modèle économique des systèmes de conversion

Le modèle économique de chacun des systèmes de conversion est formulé par leurs coûts fixes et variables. Le coût fixe d'un procédé est en fait constitué par l'investissement nécessaire à l'installation de chacune de ses unités. Quant au coût variable du procédé, il comprend le coût d'exploitation dont sont déduits les coûts et les revenus évités. Le coût d'exploitation du système correspond aux dépenses associées à la matière première requise pour assurer le fonctionnement efficace du système de conversion. Les coûts évités découlent des frais évités de la taxe sur le dioxyde de carbone, et les revenus proviennent de la vente des sous-produits qui ne sont pas demandés dans le parc (électricité et gaz naturel).

Dans le chapitre suivant, les systèmes de conversion du bois développés seront utilisés comme base de données pour les applications des cadres coopératifs et non-coopératifs. Ces derniers seront démontrés sur le parc industriel exploré dans le but de concevoir une configuration d'éco-parc optimale et d'identifier les schémas de synergie à mettre en œuvre.

Chapter 3

Case Study: Wood Conversion Systems Modeling for their Integration in the studied Industrial Park

In the previous chapter two methodological frameworks were introduced for integrating conversion systems in a territory with cooperative and non-cooperative schemes. To demonstrate the application and the potential results of the proposed methodologies, an industrial park will be investigated by searching to acquire the best on-site and inter-sites synergy patterns. In this chapter, the case study description is presented. It consists of three industrial sites located in the geographically predefined boundaries with energy and material needs and discharge. The preliminary study of this park is carried out based on the territorial energy and material integration in the aim of searching for resources and energy exchange between the industrial participants of the park and to eventually detect any limited opportunity for recovering a discharged energy or material streams ensuing from their non-existing demand in the territory. The preliminary evaluation shows woody biomass as being unrecoverable in its original form in the park. Therefore to create new synergy opportunities, the conversion of the wood initial composition into new usable commodities is investigated.

Three conversion systems are judged to be the most adapted to possibly being implemented in the studied industrial park. The conversion of wood to hydrogen, to methane and to heat and electricity are identified as the most suitable conversion pathways to be explored. Modeling these conversion paths is mandatory to enable designing the process units and to establish the process flowsheet for different operating options to eventually find the optimal operating conditions and technical process design adequate for the territory. Consequently, the block flow diagrams for the selected conversion systems are first established in the aim of identifying the main set of processes for each pathway. Afterwards, the mathematical formulations in terms of energy and material balances of each unit of these conversion systems are detailed based on literature studies. A gasifier, steam reformer, water-gas shift membrane reactor, methanation unit, biomass furnace are the main reactors modeled in this chapter. The economic model is as well elaborated for each wood conversion option to enable evaluating this aspect in the pathways competition for the most cost-effective wood composition transformation.

3.1. Studied industrial park

The case study consists of a virtual industrial park formed by three plants denoted as Site 1, Site 2 and Site 3. They are supposed to be geographically separated as depicted in Figure 3.1. Site 1 presents a hydrogen demand of 1.5 t/h and it is supposed to also generate 12 t/h of wood waste. The studied park has no initial synergies and no valorization systems for the discharged wood waste. The study aims at finding the best eco-industrial park configuration via optimal synergy patterns.

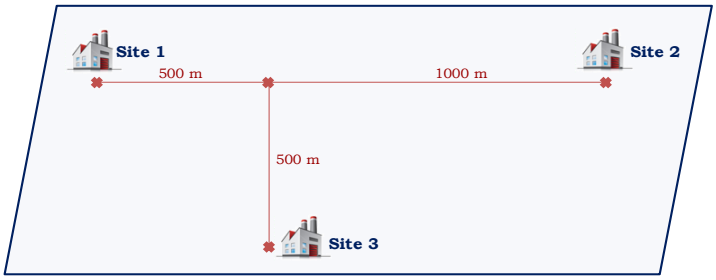


Figure 3.1. Geographical distance between the industrial actors of the virtual park

The energy requirements of the park are identified according to the circulating streams' temperatures and heat load capacities of each site which are listed in Table 3.1. Notably, the highest heat demand temperature is at 270°C and the lowest is at 50°C. Considering an average ambient air temperature of 20°C, the park shows no need of refrigeration systems since the ambient air can be employed to cool down the flows by releasing the excess heat into it. From the energy streams input and output temperatures and their heat flow found in the park, the grand composite curves (GCC) of each site are plotted, Figure 3.2, showing the net heat demands of the industrial actors. Above the pinch point, the net energy represents the heat deficit and below it is the heat surplus.

Table 3.1. Data of the energy streams for the three sites of the park

	Stream	Input Temperature (°C)	Output Temperature (°C)	Net heat load (MW)
Site 1	H1	230	55	35
	H2	155	80	55
	C1	120	270	44.5
	C2	70	150	60
Site 2	H1	240	200	32
	H2	230	70	30
	H3	150	60	40
	C1	50	210	80
	C2	90	250	50
Site 3	H1	250	90	44
	H2	220	80	60
	C1	150	260	43

As illustrated in the GCC, Site 1 has 38 MW of heat deficit above 130°C and releases 23 MW below this temperature. The pinch point of Site 2 is at 100°C and its minimum heating and cooling energy requirements are 38 MW and 10 MW respectively. Site 3 however presents 76 MW of excess heat below 210°C. Promising heat synergies could be foreseen form the analysis of the resulting curves.

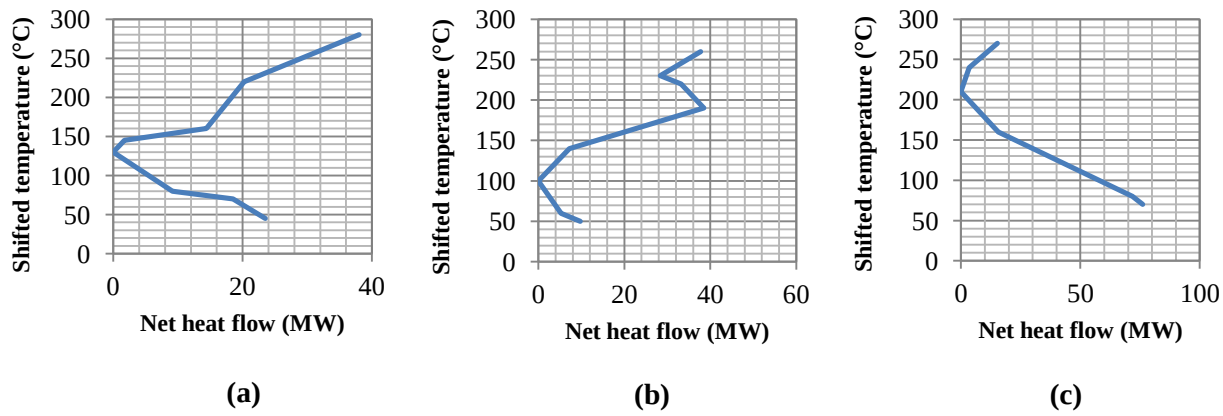


Figure 3.2. Grand Composite Curves of each actor of the territory (a) Site 1, (b) Site 2, (c) Site 3

With the park's participating actors being well distinguished by their resources demand, energy requirements and waste discharge, inter-sites synergies could be investigated through the territorial material and energy integration problems. The exergy optimal HEN is designed by the minimization of the heat integration system's exergy consumption which ensue the lowest hot and cold utilities utilization. The GCC of the three industrial sites form the territorial energy integration data input. The employed integration algorithm computes the potential synergies between the park's actors by proposing tertiary heating networks to avoid the complexity imposed by the direct energy integration between the streams of each site. The energy transport fluid is supposed to be steam that could circulate at different pressure levels; each network is therefore defined by a specific temperature level with a maximum number of networks limited to four. It is supposed that no heat utilities are allowed to be added on the network, and thus this latter can only intake heat surplus from an industrial site when it can retransfer the recovered heat to another site with deficit.

Table 3.2 exhibits the exergy optimal synergies between the sites of the park resulting from the territorial heat integration problem. Three steam networks are proposed, the highest being at 160°C. With the negative sign in the table denoting the heat removed from the corresponding entity, it is noted that the excess heat form Site 3 is collected at the three network levels to be transferred to Site 1 and Site 2. The established synergies enabled a total inter-sites heat recovery of 22.62 MW.

Table 3.2. Recovery and utility demand found by the territorial Energy integration

Network temperature (°C)	Site 1	Site 2	Site3	Network Capacity(MW)
160	4.88	3.13	-8.01	8.01
155	0	6.25	-6.25	6.25
145	1.14	7.22	-8.36	8.36
			Total Recovery(MW)	22.62

Since the only two material streams present in the territory are of different composition, no possible allocation between wood waste and hydrogen is possible. Hydrogen must therefore be purchased from external suppliers to maintain its operation. And even by searching for synergies between the industrial actors, 12 t/h of wood waste are still discharged without any valorization opportunity since none of the sites present such demand. The conversion process brings the possibility of turning the non-usable wood waste into other usable components and allows its reinsertion in the system which is otherwise unattainable. Therefore, the potential conversion systems of woody biomass are investigated in the following section and the ones that are found to be most suitable for the studied territory are identified to be subsequently modeled.

3.2. Wood Conversion systems overview

The discharged woody biomass in the territory has a proximate analysis of 86% volatiles and 14% fixed carbon on a dry molar basis, which matches the composition of lignocellulosic (LC) biomass found in literature (Stahl, et al., 2004), in addition to its 8 wt% moisture content. To produce various commodities from this biomass such as fuels, power, and other chemicals, a bio-refinery that integrates biomass conversion processes is required. The reacting processes that involve the destruction and formation of chemical bonds generating a chemical composition change of the LC biomass can be classified under two main categories:

- Thermochemical conversion: pyrolysis, combustion and gasification.
- Biochemical conversion: hydrolysis, fermentation and anaerobic digestion.

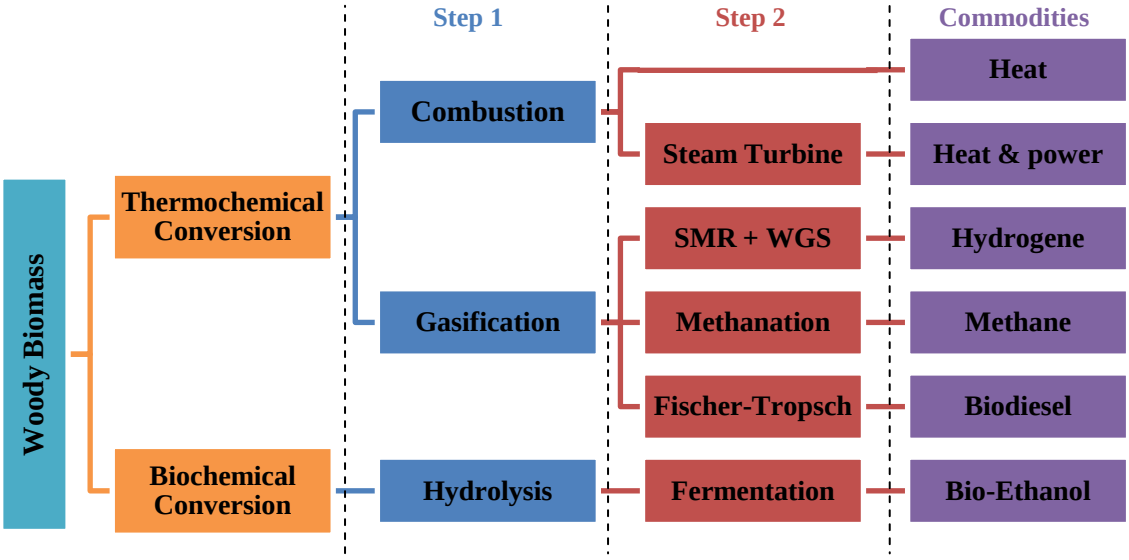


Figure 3.3. Overview of the main conversion pathways of woody biomass

The main conversion pathways of woody biomass are illustrated in Figure 3.3. In thermochemical conversion routes, heat manifests as being the essential ingredient. Direct combustion is the most evident pathway to recover the calorific potential of biomass by converting it into heat. Belt conveyors transport the wood feedstock into a combustion chamber wherein it is burnt in the presence of oxygen. The generated heat from combustion is transferred to a heat transfer medium, which is usually steam, to be then redistributed to feed endothermic processes. Steam could also be converted to electrical power via steam turbines. This path is the process of material conversion into energy. The main difference in the alternative routes of combustion, which are pyrolysis and gasification, lies within the extent to which the chemical reactions are consented to proceed which is typically controlled by the imposed temperature of reaction or by the oxidant accessibility.

Wood gasification forms another thermochemical conversion pathway. In such process the wood is first heated at relatively low temperatures in the absence of oxygen until it is converted into pyrolysis gases and tars. The resulting mixture is gasified at elevated temperatures with a gasifying agent that is selected depending on the subsequent catalytic upgrading of the produced gas. The latter can actually be converted into commodities of higher value than wood, such as liquid biofuels through Fischer-Tropsch synthesis. Other catalytic conversion routes involve the production of hydrogen by coupling a steam methane reformer to a Water-Gas Shift reactor. Further, by placing a methanation unit downstream of the gasifier biomass can be converted to methane.

On the other hand, biochemical conversion of biomass consists of the hydrolysis reaction that breaks down the structural carbohydrates of LC into its component sugar molecules. The resulting sugars are then transformed into organic acids, alcohols or hydrocarbons via fermentation by microorganisms using anaerobic digestion[12]. The fermented mash goes through distillation and dehydration to separate ethanol from the residues. The fermentation being a microbiological process, it typically takes place at atmospheric pressure and temperatures ranging from ambient to 70°C.

Waste wood valorization through heat and power generation, hydrogen or methane generation are challenged since the park has hydrogen and heat demand and assuming that electricity and methane can be sold to the national power grid and to the gas network respectively. Each of these three possible waste wood conversion systems are first formulated in their physical mass and energy balances and then by their economic models. Based on literature studies, the developed models of each unit of the selected conversion routes are described in the rest of this chapter. The aim of the detailed models is to identify the material and the energy streams for each of the conversion units, while being able to model the impact of tuning their operating parameters, in order to generate the superstructures which enable the integration problems resolution for both cooperative and non-cooperative schemes.

3.3. Wood to hydrogen conversion system

The studied conversion path of wood to hydrogen consists of three essential steps: gasification, steam reforming and the water gas-shift (WGS). Two steps are added to benefit from the waste gas output of the WGS reactor. The block flow diagram of the hydrogen production from wood waste is shown in Figure 3.4. Each of these blocks are modeled using Modelica® language in the Dymola® software by their physical equations of mass and energy balance while taking into account the chemical reactions taking place inside each of the reactors.

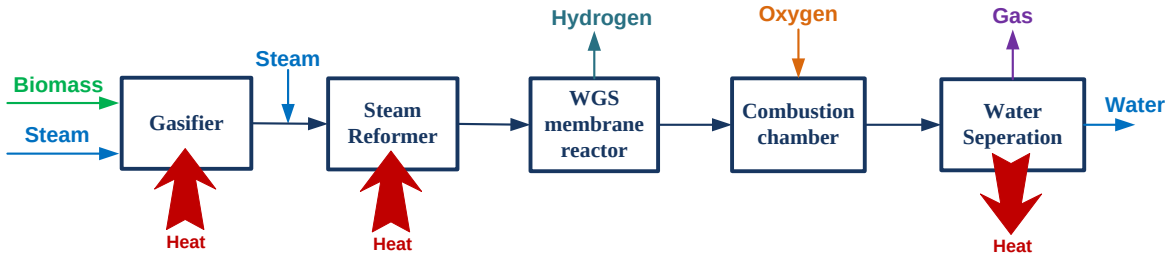


Figure 3.4. Block flow diagram of wood waste conversion to hydrogen

With steam as the gasifying agent, the biomass is converted to a hydrogen rich gaseous mixture containing tar which is a complex mixture of condensable hydrocarbons. The gasification's product is refined in the steam reforming reactor by the conversion of tar to hydrogen. The additional production of this latter is carried out in the water gas-shift (WGS) membrane reactor, which has a catalytic bed where the WGS reaction takes place and another channel wherein hydrogen is separated gradually through a selective hydrogen membrane. The exiting gas from the bed channel of the WGS reactor consists of hydrogen, carbon monoxide and unconverted methane thereby forming a potential fuel. Hence this latter is burned in a combustion chamber with pure oxygen to grasp the opportunity of having only carbon dioxide and water as products which are separated by water condensation.

[12] The processes by which microorganisms break down biodegradable material in an oxygen-starved environment

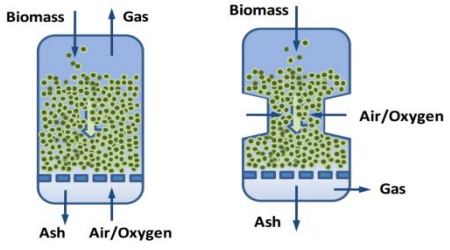
3.3.1. Steam Gasifier

3.3.1.1. Gasifier overview

Thermo-chemical gasification is the conversion by partial oxidation of carbonaceous material such as coal or biomass at elevated temperature (>700°C) into a mixture of hydrogen, carbon monoxide and carbon dioxide. The resulting gas mixture may also contain methane, traces of higher hydrocarbons, water and various contaminants such as char particles, ash, tars and oils. Gasification is performed inside a reactor called a gasifier in the presence of a gasifying medium which can be air, oxygen, steam or carbon dioxide. The gasification downstream value and potential processing is highly dependent on the choice of the oxidizing agent. Air gasification results in the production of a poor heating value gas ($4 - 7$ MJ.m^{-3}) known as "producer gas". It is only suitable for boiler and gas engines operation. The low calorific value of producer gas is ensued from the product gas dilution by the non-combustible Nitrogen gas; whereas oxygen or steam gasification produces synthesis gas or "syngas" which presents better heating value ($12 - 28$ MJ. m^{-3}). Syngas can be converted into synthetic natural gas (methane) or it could also be used as feedstock to a WGS reactor where it is processed into hydrogen or to a Fischer-Tropsch reactor to produce synthetic fuel (diesel or gasoline).

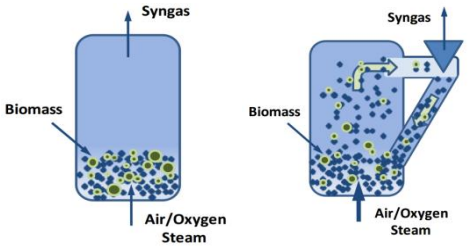
Several sequential processes occur to the carbonaceous material in the gasifier. First at around 100°C the water content in the feed is evaporated. This is the drying process in which the resulting steam is subsequently mixed into the gas flow. Then in the absence of an oxidizing agent and when the solid fuel temperature attain 300 to 500°C, it pyrolyses to solid char, condensable hydrocarbons (tar) and gas (Bridgwater, 1995). This is referred to as the primary pyrolysis and it proceeds faster than the gasification reactions. The aforementioned reactions are the partial oxidation of the solid char, tar pyrolysis (or thermal cracking of tars) and gas pyrolysis. Actually with the provision of additional heat, the solid, liquid and gas products of the primary pyrolysis react with the gasifying agent to produce lighter molecules and eventually permanent gases (H_2, CO, CH_4 and lighter hydrocarbons), therefore resulting in lesser quantities of hydrocarbons and tars. However not all the liquid products are converted in the gasifier due to the physical restriction of the reactor and the chemical reactions limitations. Consequently, remaining tar contaminants are found in the final gasification product.

A range of reactor configurations has been developed for industrial biomass gasification. The main differences between these technologies are essentially in: the contact mode between the feed and the gasifying agent, the heat transfer mode (i.e., whether it is directly heated by partially combusting some biomass or indirectly heated from an external source) and the gasifier operating temperature and pressure. The principal types of gasifiers are briefly described below and for which a recent review can be found in the work of Molinoa et al. (Molinoa, et al., 2016). The schemes of the different gasifier types illustrated in Figure 3.5 to Figure 3.7 are from Taylor et al. (Taylor, et al., 2009).



(a) (b)

Figure 3.5. Fixed bed gasifier: (a) updraft, (b) downdraft



(a) (b)

Figure 3.6. Fluidized bed gasifier: (a) bubbling, (b) circulating

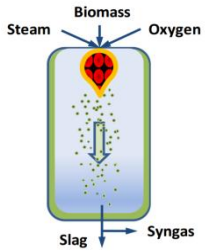


Figure 3.7. Entrained flow gasifier

Fixed bed gasifier

Vertical fixed bed gasifiers are subdivided into updraft and downdraft reactors, Figure 3.6. Updraft is a countercurrent gasifier where the oxidizing agent is introduced from the bottom and the feed from the top of the gasifier. As a consequence of this configuration, the tars generated from the pyrolysis are either condensed by the entering cool feed or are carried upward by the flowing hot product gas resulting in a high tar content gas (Bridgwater, 1995). The produced gas sensible heat is recovered by means of direct heat exchange with the descending fuel. The resulting condensed tars are thus further cracked in the reaction zones where they were recycled back. In the bottom of the reactor, the solid char is partially oxidized by the incoming gasifying agent.

In a downdraft gasifier, solids and gases are in descending concurrent flow where biomass is fed from the top and the oxidant from both sides of the reactor around its throat. This latter is a constriction high temperature region packed bed where the reaction products are mixed ensuing an effective tar thermal cracking. Consequently, the gases feature low content of tar than the products of the updraft gasifier. However, the internal heat exchange is not as efficient as in an updraft gasifier.

Fluidized bed gasifier

A fluidized bed is the physical phenomenon whereby a fixed bed of fine solids placed under appropriate conditions is transformed into a liquid-like state by contact with a flowing gas. Fluidized bed gasification was developed to increase fixed bed efficiency by taking advantage of the mixing characteristics and higher reaction rates related to the gas-solid contact. Reportedly the fluidized bed gasifier efficiency is about five times that of fixed bed gasifier (Bingyan, et al., 1994).

A bubbling fluidized gasifier (Figure 3.6.a) features a bed of fine inert material (usually silica sand) held in fluidization conditions with the oxidizing agent being blown bottom-up through the bed in a sufficient speed to maintain the solid agitation. Even though most of the biomass conversion to product gas occurs within the fluidized bed which regards only the lower part of the gasifier, some conversion reactions continues in the freeboard zone, i.e., the upper part of the gasifier where only the gas phase is present. Currently fluidized bed gasifier stands as the most promising technology for biomass gasification (Molinoa, et al., 2016).

With a high enough velocity of the upward flowing gasifying agent, a large amount of solids is entrained with the product gas forming the circulating fluidized gasifier. Consequently the fluidized bed is expanded to occupy the entire reactor (Figure 3.6.b). The entrained sand or char are captured and recycled back by a cyclone intercepting the gas flow at the top of the reactor. As a result, the carbon conversion efficiency is improved compared to the bubbling fluidized bed.

Entrained flow gasifier

In an entrained flow reactor fine particle fuel ($0.1 - 1$mm) is concurrently fed from the top of the gasifier with a pressurized gasifying agent (usually steam or oxygen), Figure 3.7. The fine feed could be either a dry pulverized solid, a fuel slurry or an atomized liquid fuel. Consequently the fuel particles are entrained in a dense turbulent cloud throughout the gasifier which operates at high temperature and pressure (25 – 30 bar). The turbulent flow results in high reaction rates and enables significant throughput, thus inducing great quality syngas. This type of gasifiers melt the ash into liquid inert slag discharged from the bottom of the reactor.

Plasma reactor

An electric discharge is delivered to a plasma torch inducing a high temperature ionized gas. Untreated waste is fed to the gasifier from the top of the reactor where it is melted, vaporized and then dissociated into smaller molecules by the released energy from the plasma. The organic material is converted into high quality syngas and the inorganic residue is retrieved as a vitrified slag.

3.3.1.2. Steam gasifier modeling and validation

The developed gasifier model represents a bubbling fluidized bed operating at high temperature and atmospheric pressure. It is formed by two zones: a heterogeneous zone of length $L_{heterogeneous}$ which is the lower part of the gasifier wherein the fluidized bed and a homogeneous zone or the freeboard zone of length $L_{homogenous}$, Figure 3.8. In the heterogeneous zone, there is a particle-free bubble phase and an emulsion phase which contains the particles and fraction of gases. However considering the scope of this thesis, the two phases present in the heterogeneous zone were assumed to be as one. This hypothesis was set relying on the results reported by Ji et al. (Ji, et al., 2009) on the gas composition and temperature uniformity in both phases resulted from the mass and energy transfer between the bubble and emulsion phases.

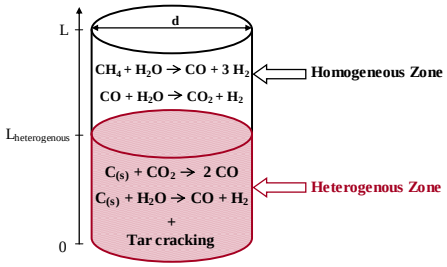


Figure 3.8: The chemical reactions taking place in the gasifier

The biomass is constantly fed into the gasifier along with steam. Under the heat effect, the biomass is converted to a gaseous mixture immediately upon entering the reactor by the primary pyrolysis reaction. This reaction allows the devolatilization of the biomass and thus induces its conversion into three products: gas, tar and char; each having a formation rate given by Eq.(3.1) where the product i has a production V_i (kg per kg biomass) at time t. The kinetic parameters of this equation are listed in Table 3.3 (Ji, et al., 2009). The formation of each of these products through the decomposition of biomass is assumed to take place at the inlet of the gasifier through independent chemical reactions. The primary pyrolysis is instantaneous given the products rate of formation. In fact the reaction reaches the steady state after 0.05 seconds as depicted in Figure 3.9 for a biomass temperature T_b of 450°C. Noting that phenol (C_6H_6O) serves to represent the tar formed by the primary pyrolysis in this work.

$$\frac{dV_i}{dt} = k_{0_i} \exp^{-\left(\frac{E_i}{RT_b}\right)} \left(V_i^* - V_i\right) \qquad (3.1)$$

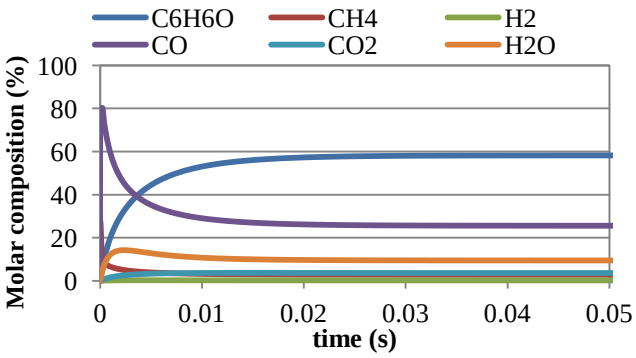


Figure 3.9: Dynamic variation of the primary pyrolysis product composition

Table 3.3. Kinetic parameters

Component	log k_0 (1/s)	E_i (kJ/mol)	V_i^* (kg/$kg_{biomass}$)
C_6H_6O	5.4	83.64	0.493
CH_4	13	251.21	0.0241
H_2	6.17	114.18	0.0016
CO	11.75	220.66	0.2164
CO_2	5.39	97.99	0.0308
H_2O	6.71	103.01	0.0804

The tar cracking reactions as well as the char conversion into carbon monoxide and hydrogen take place simultaneously in the heterogeneous zone where the inert material (silica sand) is deposited. The aforementioned reactions and their kinetics are listed in Table 3.4, where C_i denotes the molar concentration of component i and P_i its partial pressure. In all the kinetic equations the reactor's temperature T is in Kelvin. The phenol thermal cracking influences to a large extent the output gas composition since it forms more than half of the primary pyrolysis products.

Table 3.4. Kinetic model of the heterogeneous zone

Chemical reaction	Reaction Kinetic ($mol.m^{-3}.s^{-1}$)
Thermal tar cracking kinetic model	
$C_6H_6O \rightarrow CO + 0.4C_{10}H_8 + 0.15C_6H_6 + 0.1CH_4 + 0.75H_2$	$r_1=10^7 \exp\left(\frac{-10^5}{RT}\right)C_{C_6H_6O}$
$C_6H_6O+3H_2O \rightarrow 4CO+2CH_4+2H_2$	$r_2=10^7 \exp\left(\frac{-10^5}{RT}\right)C_{C_6H_6O}$
$C_{10}H_8 \rightarrow 7.38C+0.275C_6H_6+0.97CH_4+1.235H_2$	$r_3=1.7\times10^{14} \exp\left(\frac{-3.5\times10^5}{RT}\right)C_{C_{10}H_8}^{1.6}C_{H_2}^{-0.5}$
$C_6H_6+2H_2O \rightarrow 1.5C+2.5CH_4+2CO$	$r_4=2\times10^{16} \exp\left(\frac{-4.43\times10^5}{RT}\right)C_{C_6H_6}^{1.3}C_{H_2}^{-0.4}C_{H_2O}^{0.2}$
Heterogeneous reactions kinetic model	
$C+CO_2 \rightarrow 2CO$	$r_5=4\ 364 \exp\left(\frac{-29844}{T}\right)C_{CO_2}$
$C+H_2O \rightarrow CO+H_2$	$r_6=\frac{4.93\times10^3 \exp\left(\frac{-18522}{T}\right)P_{H_2O}}{1+\ 11.1 \exp\left(\frac{-3548}{T}\right)P_{H_2O}+1.53\times10^{-9} \exp\left(\frac{25161}{T}\right)P_{H_2}}$

In the homogeneous zone of the reactor, the steam reforming reaction converts the produced methane from the first zone to hydrogen and carbon monoxide. The aforementioned is converted into hydrogen and carbon dioxide by the water gas-shift reaction. The chemical reactions and the corresponding reaction kinetics occurring in the gasifier's homogenous zone are listed in Table 3.5.

Table 3.5. Kinetic model of the homogenous zone

Chemical reaction	Reaction Kinetic ($mol.m^{-3}.s^{-1}$)
$CH_4 + H_2O \rightarrow CO + 3H_2$	$r_7=1.65\times10^{11} \exp\left(\frac{-2.4\times10^5}{RT}\right)C_{CH_4}^{1.7}C_{H_2}^{-0.8}$
$CO + H_2O \rightarrow CO_2 + H_2$	$r_8=2.78\times10^6 \exp\left(\frac{-1510}{T}\right)\left(C_{CO}C_{H_2O}-\frac{C_{CO_2}C_{H_2}}{K_{eq}}\right)$

The gasifier is modeled as a one dimensional plug flow reactor in two kinetic sub-models forming the two zones of the reactor where each satisfies the molar and the energy balance described in (3.2) and (3.3), respectively. The molar balance takes into account the chemical reactions of each component in the reactor, where υ_{ik} is the stoichiometric coefficient of component i of reaction k. The sub-models are combined together using a connector model which transfers the material composition and the stream temperature from the output of the first zone to the input parameters of the second.

$$\frac{dF_i}{dz}=A\sum_{k=1}^{N_R}\upsilon_{ik}r_k \tag{3.2}$$

$$\frac{dT}{dz}=\frac{A\sum_{k=1}^{N_R}(-\Delta H_k r_k)+q_{gasifier}}{\sum_{i=1}^{R}(-F_i C_{p_i})} \tag{3.3}$$

The gasifier model was developed in Modelica® language and simulated using Dymola® software. The predicted model results superpose with those of the gasifier model developed by Ji, et al. (Ji, et al., 2009) as depicted in Figure 3.10. This graph illustrates the molar gas composition profile in both heterogeneous and homogenous zones of the reactor. The design and operating parameters employed to carry out the simulation are listed in Table 3.6. The hydrogen production increases throughout the reactor especially in the homogenous zone since it is promoted by the water gas-shift and the steam reforming reactions.

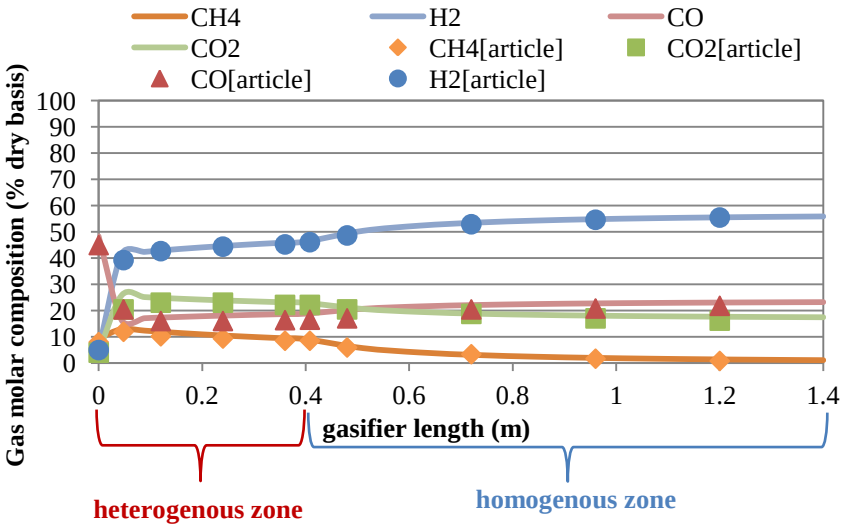


Table 3.6. Gasifier operating and design parameters

Parameter	Value
Pressure	1 bar
$T_{entrance}$	730 K
Steam flow rate	1.85 kg/hr
Steam to biomass ratio	1
$L_{heterogenous}$	0.4 m
$L_{homogenous}$	1 m
d	0.15 m

Figure 3.10. Gas composition profile along the gasifier length

Figure 3.11 shows the effect that has the steam to biomass ratio on the final gas composition. The simulated composition is consistent with the experimental data (Herguido, et al., 1992) indicated by the symbols. The hydrogen and carbon dioxide gas content increase with the steam to biomass ratio, since the increment in the steam flow rate promotes the production of these two components as shown by the chemical reactions of Table 3.5. Moreover the thermal tar cracking is boosted by a large amount of steam thus inducing great decrease in the tar content of the gasifier output, Figure 3.12.

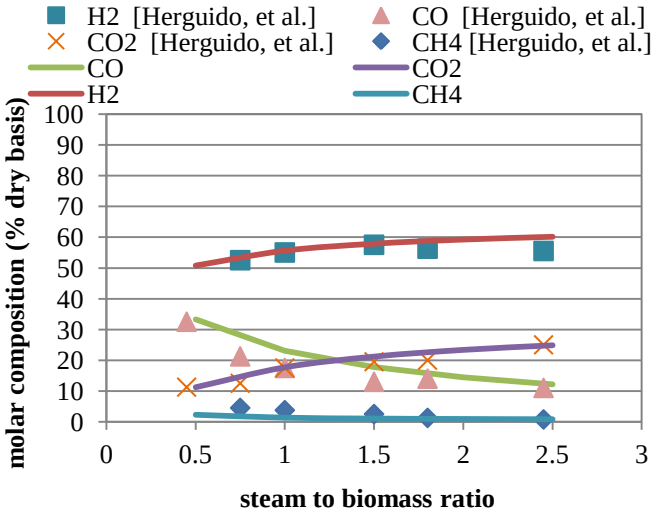


Figure 3.11. Steam to biomass effect on gas composition

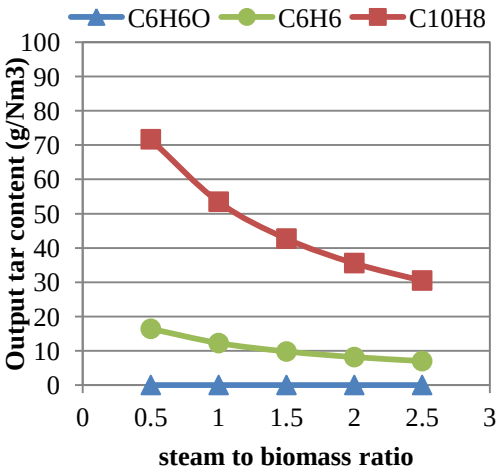


Figure 3.12. Steam to biomass effect on the tar content of the gasifier's output

3.3.2. Steam reformer

3.3.2.1. Tar removal overview

The major challenge of biomass gasification is the formation of tar which leads to unacceptable levels of tar content in the product gas. This complex mixture of condensable hydrocarbons, when resulting from biomass gasification, is formed by different classes of compounds originated under various reaction regimes (Milne & Evans, 1998). It includes single-ring aromatic compounds (benzene, toluene) and two-ring aromatic compound (naphthalene) in addition to other complex polycyclic aromatic hydrocarbon. High concentration of tar can lead to operational problems in downstream processes and quality degradation of the produced gas. At low temperatures, tar condensates into a thick and viscous liquid thus blocking, fouling corrosion, erosion and abrasion of process equipment such as engines, gas coolers, filter elements and turbines (Li & Suzuki, 2009) (Vivanpatarakij, et al., 2014). Therefore, removal of tar components from the biomass gasification product gas is mandatory before the gas use.

Several tar removal techniques have been proposed in literature. Those can be classified into physical method and thermo-chemical conversion techniques. Physical techniques include ceramic candle filters, wet scrubbers, electrostatic precipitators and cooling towers (Vivanpatarakij, et al., 2014), while chemical tar removal methods consist of tar conversion into synthesis gas by either using high temperatures (thermal cracking) or by catalytic material such as nickel-based catalysts, noble metal catalysts, dolomite or olivine (Noichi, et al., 2010) (catalytic cracking and reforming). Unlike physical tar removal that merely separate tar from the gasification product, thermo-chemical methods are way more attractive owing to their effective tar removal while simultaneously converting it into useful gaseous product and thus increasing the gasification overall efficiency (Guana, et al., 2016).

However, non-catalytic thermal tar cracking requires significantly high temperatures (>1100°C) to decompose the large organic molecules to permanent gases and achieve high cleaning efficiency (Sutton, et al., 2001). Catalytic tar conversion in the other hand can reduce the reaction temperature thus presenting less energy demand while converting more effectively tar into useful gases (Guana, et al., 2016). Depending on the catalyst position according to the gasification reactor, two groups are distinguished for catalytic tar conversion. The first is that of primary catalysts which consist on directly adding the catalyst to the biomass feed, thus the tar catalytic cracking takes place inside of the gasifier. The second group, known as secondary catalysts, uses a secondary reactor downstream from the gasifier where the catalyst is placed and where the tar conversion occurs. The secondary reactor runs independently of the gasifer type and therefore it can operate under different conditions than those of the gasification unit.

Several studies were conducted to investigate the potential of different catalysts to decompose tar generated in biomass gasification. Dolomite is found suitable for such use and is mostly employed as a secondary catalyst. While it presents excellent conversion rates for heavy hydrocarbons, Dolomite is not active for methane reforming contained in the gasification product hence requiring further upgrading if syngas is sought (Han & Kim, 2008). Alkali metal catalysts are found to be more efficient when directly added to biomass as primary catalyst. Even though they reduce significantly both tar and methane content while enhancing the gasification rate of reactions (Xu, et al., 2010), Alkali catalysts recovery is difficult and costly (Sutton, et al., 2001). Commercially available Nickel based catalytic material is highly effective for heavy and light reforming and hence the adjustment of the gasification product to syngas quality. To catalytically clean and upgrade the gas from tar, Nickel based catalysts act best as secondary catalysts. It was reported to attain nearly complete decomposition of biomass gasification tar and light hydrocarbons when used in a downstream reactor (Han & Kim, 2008).

3.3.2.2. Steam reformer modeling and validation

In the aim of producing high purity hydrogen, significant syngas quality is sought. Based on the state of the art presented in the preceding section, a secondary reactor placed downstream from the gasifier is employed to upgrade the gasification product through tar reforming by a Nickel based catalyst. Before entering the steam reformer, the gasification products are mixed with steam to adjust their steam to carbon ratio in order to prevent carbon deposit on the reactor's wall. Once in the steam reformer, the steam reacts with methane and tar at high temperature (700 − 1100 °C) in the presence of Nickel based catalyst and produces hydrogen and carbon monoxide. The steam reformer is a tubular reactor of a length L with a diameter d and a cross section area of $\pi d^2/4$, Figure 3.13.

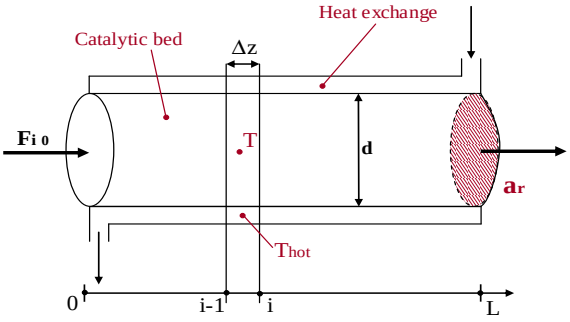


Figure 3.13. Stream reformer geometric form

The reaction is formulated by a kinetic model using the finite-difference method (FDM) of the first order described in (3.4). The discretization is carried out assuming N intervals with a step Δz between each two nodes equal to the reactor length L divided by the number of intervals N. The required heat exchange for the endothermic chemical reactions is transmitted through the walls of the reactor by thermal diffusion, Eq. (3.5). The term q refers to the energy supplied to the flow circulating in the catalytic bed which has a wall thickness of δ_w and a thermal conductivity k_w. The lateral surface S of the reactor is found by $\pi dL/\Delta z$.

$$\frac{dX_i}{dz} = \frac{X_i - X_{i-1}}{\Delta z} \tag{3.4}$$

$$q = S \times \frac{k_w}{\delta_w} \times (T - T_{hot}) \tag{3.5}$$

A one-dimensional steady-state model was developed to simulate the steam reformer reactor satisfying the molar and energy balances of a plug flow reactor. The continuity equation of each component i, Eq. (3.6), and the energy balance of the catalytic bed, Eq. (3.7), are implemented in the model by the length discretizing of the reactor of Δz. Noting that the molar balance takes into account the components chemical transformation, with υ_{ik} denoting the stoichiometric coefficient of component i in reaction k in which it participates. It is negative for reactants and positive for products.

$$\frac{dF_i}{dz} = a_r \sum_{k=1}^{N_R} \upsilon_{ik} r_k \tag{3.6}$$

$$\frac{dT}{dz} = \frac{a_r \sum_{k=1}^{N_R} (-\Delta H_k r_k) - q}{\sum_{i=1}^{R} \left(-F_i C_{p_i}\right)} \tag{3.7}$$

The chemical reactions and their kinetics described in Table 3.7 (Jess, 1996) are used to model the steam reformer. According to the gasifier simulations, the phenol is entirely converted in the gasifier's tar cracking reactions (Figure 3.12). Therefore its conversion is not taken into account in the steam reformer and the tar is modeled by naphthalene $C_{10}H_8$ and benzene C_6H_6. In fact, steam reforming of tars boosts the hydrogen production and thus its molar flow rate.

Table 3.7. Steam reformer kinetic model

Chemical reaction	Reaction Kinetic ($mol.m^{-3}.s^{-1}$)
$CH_4+0.5CO_2+0.5H_2O\rightarrow 1.5CO+2.5H_2$	$r_1=4.5\times10^{10}\exp\left(\frac{-2.5\times10^5}{RT}\right)C_{CH_4}$
$C_6H_6+3CO_2+3H_2O\rightarrow 9CO+6H_2$	$r_2=2\times10^{11}\exp\left(\frac{-1.96\times10^5}{RT}\right)C_{C_6H_6}$
$C_{10}H_8+5CO_2+5H_2O\rightarrow 15CO+9H_2$	$r_3=4.3\times10^{13}\exp\left(\frac{-3.32\times10^5}{RT}\right)C_{C_{10}H_8}^{0,2}C_{H_2}^{0,3}$

To ensure the validity of the developed steam reformer the simulation results were compared to those of Ji, et al. (Ji, et al., 2009) who proved the consistency of their model with the experimental data of Cabellero, et al. (Caballero, et al., 1997). The simulated one meter length reactor has a diameter d of 0.16m. In their model, Ji, et al. (Ji, et al., 2009) considered that the heat to the steam reformer is supplied by a furnace surrounding the reactor. The furnace temperature profile is correlated and integrated in the model in the form of three curves according to the reactor length, Eq. (3.8).

$$T_{hot}(z)=\begin{cases}25778z+700.78 & z<0.025m\\ -5820z+1490.7 & 0.025<z<0.067m\\ 318.16z^4-934.97z^3+1048.9z^2-541.67z+1132.7 & z>0.067m\end{cases} \quad (3.8)$$

The variation of the gas molar content throughout the steam reformer axial length of the model simulation and the results of Ji, and al (Ji, et al., 2009) are illustrated in Figure 3.14, for the operating and design parameters listed in Table 3.8. The hydrocarbons in the reactor are dissociated in the steam presence thus generate a hydrogen rich gas. These dissociation reactions are highly endothermic whence they crave for heat. The molar content of carbon monoxide increases throughout the reactor and goes from 23% at its inlet to 34% at its outlet; whereas that of the carbon dioxide decreases from 17% to 8%. The content variation of the aforementioned components are more apparent on the graph by dint of the larger raise compared to the hydrogen concentration augmentation. Although small differences between the results are noted in the first centimeters of the reactor, the output gas composition is well aligned with the experimentally validated model of Ji, and al (Ji, et al., 2009).

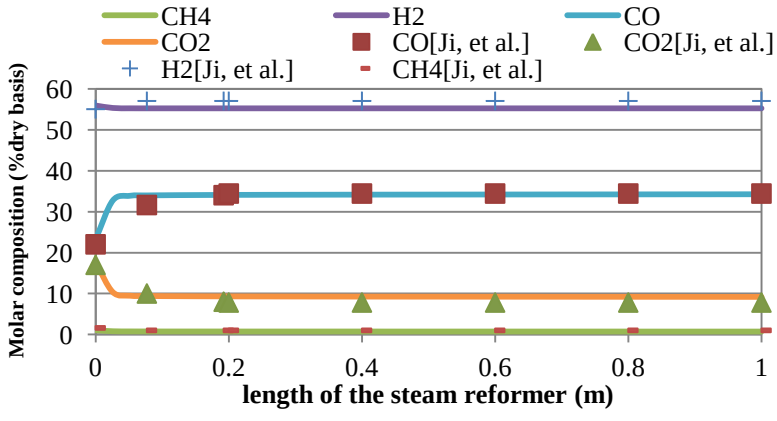


Figure 3.14. Gas composition profile along the steam reformer

Table 3.8. Steam reformer operating and design parameters

Parameter	Value
CH_4	1.5 % $_{dry\ basis}$
tar	3.5 % $_{dry\ basis}$
CO_2	17 % $_{dry\ basis}$
CO	23 % $_{dry\ basis}$
H_2	55 % $_{dry\ basis}$
Tar_0	75 g/Nm^3
P	1.013bar
$T_{0\ entrée}$	1023 K
L	1 m
d	0.16 m

3.3.3. Water Gas-Shift reactor

3.3.3.1. Water Gas-Shift overview

The significant levels of the unwanted carbon monoxide produced by the biomass gasification and the steam reforming of hydrocarbons corollary justify the need for further processes in order to generate a high purity hydrogen stream. The water gas shift reaction (WGS) offers an efficient solution for this concern, as it enables the carbon monoxide conversion to carbon dioxide with the added advantage of further hydrogen production. Two classes of materials are used as catalysts for the WGS reactions in the industry. The first is the iron-based catalyst also called high temperature shift catalyst operating between 320°C and 450°C. Whereas the second class is the copper-based catalyst performing better at lower temperatures with an operating range of 200°C to 250 °C thus it is referred to as the low temperature shift catalyst. A typical composition of this latter includes Cu, Zn, Cr and Al oxides. Copper is more sensitive to catalyst thermal sintering and should not be operated at higher temperatures.

The water gas shift is an exothermic reaction and thus the high and low temperature WGS reactions are governed by chemical kinetics and thermodynamic equilibrium. At low temperature the thermodynamics are favorable for the reaction however kinetics constrain the reaction rate hence requiring a highly active catalysts to attain adequate activity (Jacobsa, et al., 2005); whereas at high temperatures, thermodynamics limit the conversion equilibrium. This phenomenon can be explained by the Arrhenius law of kinetics, expressed by Eq.(3.9), which shows the effect of temperature on the reaction rate. This latter actually increases with temperature. However according to Le Châtelier principle when the temperature of an exothermic system is increased, it consumes some of the heat by shifting the reaction thereby decreasing its equilibrium conversion. Therefore the optimal operating point of a WGS is a tradeoff between kinetics and equilibrium driving forces.

$$k = k_0 \times \exp(-\frac{e_a}{RT}) \tag{3.9}$$

The use of hydrogen selective membrane in the WGS reactors provides an effective solution in one step (Piemonte, et al., 2010). Actually in the resulting membrane reactor both reaction and separation can be carried out simultaneously. This enables the carbon monoxide conversion reaction to overcome the thermodynamic equilibrium limit of a conventional fixed bed reactor, through hydrogen extraction, thereby decreasing the products concentration and promoting the chemical reaction. When employing a highly selective membrane for the desired product, this latter could be recovered directly during its formation thus requiring no downstream separation unit (Criscuolia, et al., 2001).

3.3.3.2. Water Gas-Shift membrane reactor model

The Water Gas Shift membrane reactor consists of a catalytic bed where the chemical reaction takes place and another channel wherein the hydrogen is sucked by vacuum effect through a membrane made of a palladium rich alloy (Pd−Ag), Figure 3.15. In the bed channel, the carbon monoxide reacts with steam to produce a mixture of hydrogen and carbon dioxide: $CO + H_2O \rightarrow CO_2 + H_2$. Due to vacuum in the non-reaction channel, the membrane selectivity enables the hydrogen separation progressively as its production in the mixture. The hydrogen partial pressures in the catalytic bed and in the non-reaction channel are respectively $P_{H_2}^{high}$ and $P_{H_2}^{low}$.

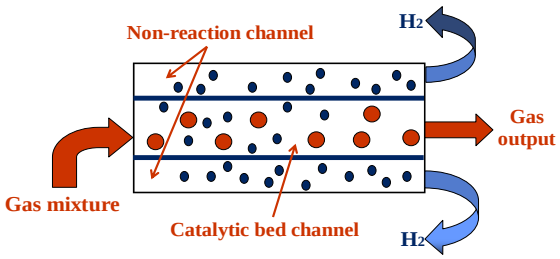


Figure 3.15. Water Gas-Shift membrane reactor

Since the membrane surface is defined as a parameter of a constant value, the main variable affecting the hydrogen separation in the WGS membrane reactor is the partial pressure of the channel where the hydrogen is extracted $P_{H_2}^{low}$. The hydrogen permeability N_{H2} through the selective membrane of a δ_{H_2} thickness is calculated according to Eq.(3.10). The apparent activation energy E_A and the pre-exponential factor P_m have the values of 29.73 kJ/mol and 7.71×10^{-4} mol.m / (s.m^2 bar$^{0.5}$) respectively (Feng, et al., 2007). Note that the membrane temperature T_m is supposed to be the average temperature between the two sides.

$$N_{H2} = \frac{P_m e^{\frac{-E_A}{RT_m}}}{\delta_{H_2}} \left(\sqrt{P_{H_2}^{high}} - \sqrt{P_{H_2}^{low}} \right) \tag{3.10}$$

The kinetic models of both high and low temperature WGS reactions are listed in

Table 3.9. The employed HWGS reaction kinetic was proposed by Bohlbro (Bohlbro, 1969) and proved its good accuracy at atmospheric pressure within the temperature range of 330 to 500°C with the parameters k_0 and e_a respectively equal to $e^{16.68}$ and 114.6 kJ/mol. As for the LWGS reaction kinetic, it is that proposed by Amadeo, et al. (Amadeo & Laborde, 1995). This reaction kinetic is valid on different pressure levels and is manifested by the variation of φ according to Eq.(3.11).

$$\varphi = \begin{cases} 0.86 + 0.14P & P \leq 24.8 \text{ bar} \\ 4.33 & P > 24.8 \text{ bar} \end{cases} \tag{3.11}$$

Table 3.9. Kinetic models of both high and low temperature water gas-shift reactions

Reaction type	Reaction kinetic (mol.kg^{-1}.s^{-1})
High temperature Water Gas shift (HWGS)	$-r_{co} = k\,(P_{CO})^{0.9}(P_{H_2O})^{0.25}(P_{CO_2})^{-0.6}\left(1-\frac{P_{CO_2}P_{H_2}}{P_{CO}P_{H_2O}K_{eq}}\right)$ with $k = k_0 e^{\frac{-e_a}{RT}}$
Low temperature Water Gas shift (LWGS)	$-r_{co} = \frac{0.92e^{\frac{-454.3}{T}} - P_{H_2O}\left(1-\frac{P_{CO_2}P_{H_2}}{P_{CO}P_{H_2O}K_{eq}}\right)\varphi}{(1+2.2e^{\frac{101,5}{T}}P_{CO} + 0.4e^{\frac{158,3}{T}}P_{H_2O} + 0.0047e^{\frac{2737.9}{T}}P_{CO_2} + 0.05e^{\frac{1596.1}{T}}P_{H_2})^2}$

Molar and energy balances are established for the WGS membrane reactor assuming a plug flow reactor for the catalytic bed channel where the WGS reaction takes place. The reactor is represented in a one dimensional model where its temperature and concentration vary along its axial length. The model molar and energy balances are written based on the weight of the catalyst (W) since the reaction kinetics are a function of this parameter. Table 3.10 describes the model for the two channels of the reactor: the catalytic bed and the non-reacting channel. When the two channels present a temperature difference, a conductive heat flux (q) is transferred throughout the membrane which has a thermal conductivity k_m and a surface per meter of a_{H2}.

Table 3.10. Molar and Energy balance of the WGS membrane reactor

Catalytic bed channel	$\frac{dF_i}{dw} = \upsilon_i(-r_{co}) - j.a_{H_2}N_{H2}\left(\frac{L}{W}\right)$, with $j=\begin{cases}1, & i=H_2\\ 0, & i\neq H_2\end{cases}$ $\frac{dT_r}{dw} = \frac{-\Delta H(-r_{co}) - a_{H_2}N_{H2}\Delta H_{H_2}\left(\frac{L}{W}\right) - q\left(\frac{L}{W}\right)}{\sum_{i=1}^{R}(-F_iC_{p_i})}$
Non-reaction channel	$\frac{dG_{H_2}}{dw} = a_{H_2}N_{H2}\left(\frac{L}{W}\right)$ $\frac{dT_{nr}}{dw} = \frac{a_{H_2}N_{H2}\Delta H_2\left(\frac{L}{W}\right) + q\left(\frac{L}{W}\right)}{\sum_{i=1}^{R}(-G_iC_{p_i})}$, with $q=a_{H_2}\times\frac{k_m}{\delta_{H_2}}\times(T_r - T_{nr})$

The model validation of the WGS membrane reactor is conducted in two steps. The first compares the results of the conventional HWGS reactor and LWGS reactor respectively with Feng, et al. (Feng, et al., 2007) and González-Velasco, et al. (González-Velasco, et al., 1992). In the second step, the WGS membrane reactor comparison with the results of Ji, et al. (Ji, et al., 2009) was carried out. The first part of Table 3.11 shows the results of the HWGS model, considering a catalyst mass W of 3 g deposited in the reactor operating under a pressure of 15 bar. The aforementioned part of the table lists the inlet flow composition and the outlet content for both the developed model and the results of Feng, et al. (Feng, et al., 2007). For these simulations, the total molar flow rate at the reactor inlet is of 7.4 mol/h.

Table 3.11. HWGS and LWGS developed models validation

		HWGS			LWGS		
		Input	Feng, et al.	Model	Input	González-Velasco, et al.	Model
Molar composition (%)	H_2	0.42	0.48	0.481	76.8	77.42	77.43
	CO	0.09	0.03	0.028	3.2	0.43	0.40
	CO_2	0.04	0.10	0.101	18.16	20.36	20.38
	CH_4	0.01	0.01	0.01	1.84	1.79	1.79
Temperature (K)		720	787	786	480	505	501

The second part of Table 3.11 shows the simulation outcome of a LWGS reactor compared to industrial data for a reactor operating at a pressure of 17 bar with 1.5 kg of a copper-based catalyst (González-Velasco, et al., 1992). The reactor inlet flow rate is of 0.339 mol/s on a dry basis and that of the steam is of 0.208 mol/s. The results shown in Table 3.11 prove that the developed WGS model is in good agreement with literature. After validating the kinetic model of a conventional WGS, the hydrogen membrane reactor is compared with the work of Ji, et al. (Ji, et al., 2009) to ensure the proper simulation results. An iron-based catalyst is used since the operating temperature is of 720 K. This type of WGS catalyst was chosen by the authors since the permeability of the hydrogen membrane increases with temperature. Its density is 10% that of iron which is 7874 kg/m^3. The operating and design parameters employed to simulate the membrane reactor model are listed in Table 3.12. The membrane thickness is assumed to be 5 μm and its thermal conductivity is 0.15 W.m^{-1}.K^{-1}. The outlet molar composition from the catalytic bed channel of the developed model shows a good consistency with the results obtained by Ji, et al. (Ji, et al., 2009), as illustrated in Table 3.13. The hydrogen concentration increases at the entrance of the catalytic bed due to the carbon monoxide conversion then it decreases because of the hydrogen passage throughout the selective H_2 membrane.

Table 3.12. Operating and design parameters

Parameter	Value
$P_{coté\ membrane}$ (bar)	0.09
$P_{coté\ lit\ catalytique}$ (bar)	1.103
$T_{0\ entrée}$ (K)	720
F_0 (mol/s)	0.0774
L (m)	1
d (m)	0.07

Table 3.13. WGS membrane reactor validation

Parameter	Input	Ji, et al.	Model
CO_2 % $_{dry\ basis}$	7	73	73.16
CO % $_{dry\ basis}$	35	3	3.61
H_2 % $_{dry\ basis}$	57	23	21.40

3.3.4. Combustion chamber model

The exiting gas from the catalytic bed channel of the WGS membrane reactor has a residual significant heating value. To take advantage of this feature, it is burned in a combustion chamber with 100% pure oxygen as oxidizer to benefit from having only water vapor and carbon dioxide at the outlet of the reactor. Table 3.14 lists the exothermic combustion reactions that each of the combustible components of the gas mixture undergoes in this reactor. This process is formulated using a thermo-chemical equilibrium model (Trambouze, et al., 1984) which is based on the chemical equilibrium of the process.

Table 3.14. The gas mixture combustion reactions

Component which undergo the combustion	Combustion reaction
Phenol C_6H_6O	$C_6H_6O + 7O_2 \rightarrow 3H_2O + 6CO_2$
Benzene C_6H_6	$C_6H_6 + 7.5O_2 \rightarrow 3H_2O + 6CO_2$
Naphthalene $C_{10}H_8$	$C_{10}H_8 + 12O_2 \rightarrow 4H_2O + 10CO_2$
Methane CH_4	$CH_4 + 2O_2 \rightarrow 2H_2O + CO_2$
Hydrogen H_2	$H_2 + 0.5O_2 \rightarrow H_2O$
Carbon monoxide CO	$CO + 0.5\ O_2 \rightarrow CO_2$

First, the equilibrium constant $K_{eq\ k}$ of each reaction k are evaluated according to Eq.(3.12). The Gibbs free energy for reaction k at temperature T and pressure P can be determined by Eq.(3.13) as a function of the enthalpy and entropy of reaction.

$$K_{eq_k} = \exp(-\Delta G_k / RT) \tag{3.12}$$

$$\Delta G_k = \Delta H_k(T) - T \times \Delta S_k(T,P) \tag{3.13}$$

Then, using this thermodynamic quantity that characterizes the system equilibrium $K_{eq\ k}$, the extent of reaction ξ_k of each reaction k are determined in order to find the equilibrium composition of the ideal-gas mixture. This is accomplished by expressing the components partial pressures in terms of their molar fraction x_i and thus solving the system of equations described by Eq.(3.14). P_{P_i} and P_{R_i} denote respectively the partial pressures of the products and those of the reactants. Because the number of moles of a reactant decreases as the reaction progresses, a minus sign is added to the $\upsilon_{ik}\xi_k$ term to find the output flow rate F_i for such component. The changes in the components number of moles is proportional to the stoichiometric coefficients υ_{ik} evaluated from the specified reactions.

$$\begin{cases} K_{eq_k} = \dfrac{\prod_i P_{P_i}^{\upsilon_{ik}}}{\prod_i P_{R_i}^{\upsilon_{ik}}} \\ P_i = x_i\, P \\ x_i = F_i / \sum_{i=1}^{N} F_i \\ F_i = F_{i0} \pm \sum_{k=1}^{N_R} \upsilon_{ik}\, \xi_k \end{cases} \tag{3.14}$$

The combustion chamber is assumed adiabatic, thus evacuating a null heat flow Q. The energy balance of this reactor is thus evaluated according to Eq.(3.15) and it serves in finding the flue gas outlet temperature T_{out}. Noting that the total enthalpy of the reactions ΔH_R is the sum of the product of each reaction's enthalpy and the components flow rates that undergo this reaction.

$$\sum_{i=1}^{N} F_{out_i} h_{out_i}(T_{out}) - F_{fuel} h_{fuel}(T_{fuel}) - F_{O_2} h_{O_2}(T_{O_2}) - (-\Delta H_R) = Q \tag{3.15}$$

The simulation results obtained from the gas combustion model designed on Dymola® are compared with those of an RStoic reactor on Aspen Plus® for adiabatic combustion with oxygen under atmospheric pressure. Aspen Plus® is a well-known process simulation software whose interface of the assembled system is shown in Figure 3.16. Table 3.15 shows the good agreement of the model results with a maximum error of 1.12% for the temperature. This may be due to the use of different enthalpy and entropy models in Dymola® and Aspen Plus®. The lower calorific value (PCI) of the fuel calculated by both models seems equivalent. Since the combustion is performed with pure oxygen, the flue gas leaving the combustion chamber consist mainly of carbon dioxide and water molecules, as shown by the results of the simulations in Table 3.15. In this case, recovery of carbon dioxide by condensation of water will be interesting to evoke.

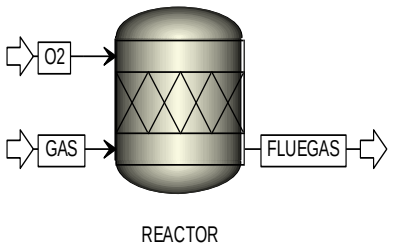


Figure 3.16. Combustion chamber on Aspen Plus®

Table 3.15. Dymola® model results comparison with Aspen's

Parameter	Input	Dymola Results	Aspen Results
CH_4 (mol%)	0.65	0	0
H_2 (mol%)	8.97	0	0
CO (mol%)	1.13	0	0
CO_2 (mol%)	58.80	72.74	72.74
H_2O (mol%)	24.11	27.26	27.26
O_2 (mol%)	6.35	0	0
Flow rate $_{total}$ (mol/s)	399.81	379.62	379.62
T (°C)	558.37	1259	1245
LHV (MW)	–	12.196	12.197

3.3.5. Water separation model

This separation step is accomplished first by cooling the flue gases to a temperature below the water saturation point. This temperature decrease promotes the water passage from the gas to the liquid phase upon reaching its condensation temperature. Then the liquid-vapor mixture passes

through a flash drum where the gas exits from the top and the liquid from the bottom of the drum due to density difference, Figure 3.17. The degree of separation is considered to be such that 99% of the initial water molar flow rate is recovered in liquid form.

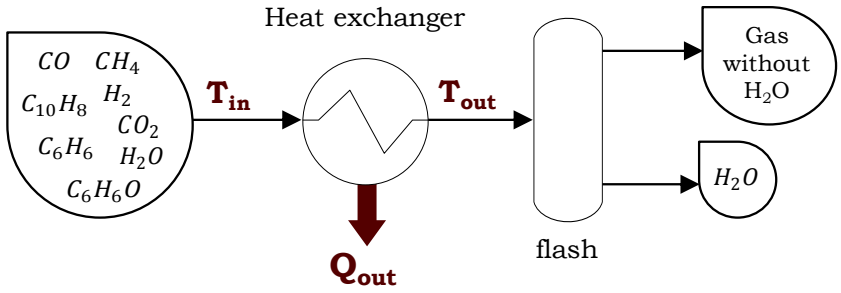


Figure 3.17. Water separation unit

The energy balance established for the separation unit, according to Eq. (3.16) enables the evaluation of the removed heat, Q_{out}, by defining the flash exiting temperature T_{out}. The mass flow rate at the unit entrance is the sum of that of the exiting condensed water and the flow rate of the rest of the exiting mixture containing 1% of water vapor, Eq.(3.17).

$$Q_{out}=F_{gas_{out}}h_{gas_{out}}(T_{out}) + F_{H_2O}h_{H_2O}(T_{out}) - F_{in}h_{in}(T_{in}) \quad (3.16)$$

$$\rho_{out}F_{out} = \rho_{H_2O}F_{H_2O} + \rho_{gas_{out}}F_{gas_{out}} \quad (3.17)$$

The obtained simulation results of the condenser thermodynamic model are compared to the results obtained from Aspen Plus® by coupling a heat exchanger and a flash unit, Figure 3.18. The combustion flue gas composition resulted in Table 3.15 of the previous section is considered as the input mixture of the separation unit. Table 3.16 lists the output results of the separation unit obtained from the simulation of the developed model on Dymola® and that assembled on Aspen Plus®. The recovery of the water stream in the condenser is considered to be of 100% purity (by neglecting the gas dissolution), hence the zero molar flow rate of the other components in the liquid water outlet of the Dymola® results. This hypothesis presents the largest difference between the two software results and is however considered to be a negligible variation considering the aim of this model.

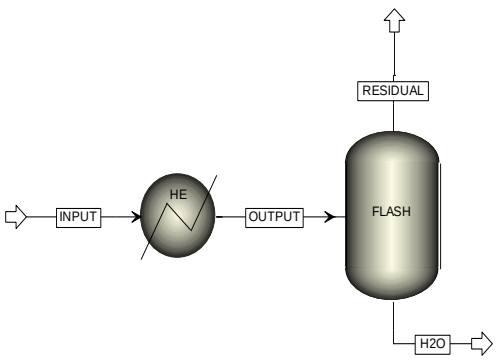


Figure 3.18. Separation unit on Aspen plus®

Table 3.16. Dymola® model results comparison with Aspen Plus® results

	Liquid H_2O		Residual mixture	
Molar flow rate (mol/s)	Dymola Results	Aspen Results	Dymola Results	Aspen Results
CH_4	0	0	0	0
H_2	0	0	0	0
CO	0	0	0	0
CO_2	0	4.17	103.48	99.31
H_2O	273.37	272.93	2.76	3.20
O_2	0	0	0	0

3.4. Wood to methane conversion system

The second possible valorization path is the wood conversion to methane whose main unit is that of the methanation which ensures the generation of methane. Nonetheless, a thermo-chemical gasification is also essential to this path given the need of converting biomass into a gas mixture before its introduction into the methanation unit. Figure 3.19 represents the block flow diagram of wood to methane conversion system. The biomass gasification with steam generates a mixture rich in hydrogen as mentioned earlier. The passage of the latter in the methanation unit increases its methane content. However to achieve a high purity methane, first the water is condensed by cooling the gas and then the mixture is compressed for eventually separating carbon dioxide via a selective membrane.

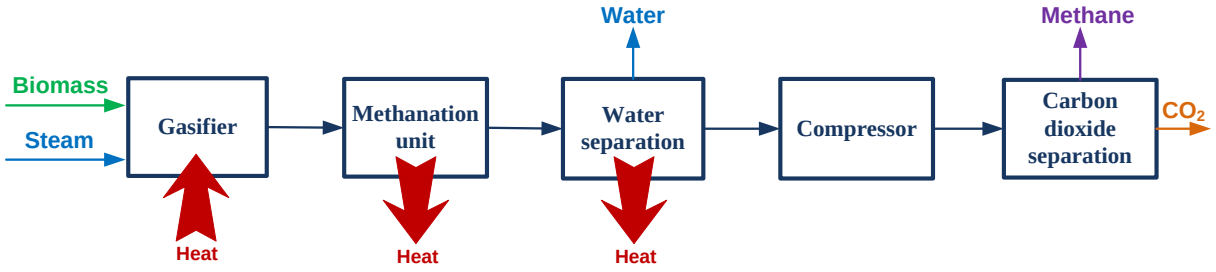


Figure 3.19. Block flow diagram of wood waste conversion to methane

The gasifier model described in the previous section of the hydrogen production pathway is used for this conversion pathway as well, since it is the same reactor for gasifying biomass by water vapor. Similarly for the water separation unit, it is the same for both conversion systems. Hence the units that will be modeled in the following section are that of the methanation, the compressor and the carbon dioxide separator.

3.4.1. Methanation unit

3.4.1.1. Methanation overview

Methanation is a heterogeneous catalytic reaction. It has two main industrial uses: Removal of CO traces from process gases (i.e., for ammonia production) and conversion of synthesis gas into methane-rich gas (Ryi, et al., 2012). It thus plays a key role in creating substitute natural gas (SNG) from the product gas of wood or coal gasification. This reaction was carried out on various catalysts Ru, Rh Pt, Fe and Co. Yet, Nickel remains the most relevant catalyst given its low price, its selectivity and its very interesting activity. The methanation reaction occurs chiefly through the hydrogenation of carbon monoxide. When the reaction stoichiometry encompasses hydrogen at least three times as carbon monoxide, this latter reacts with hydrogen to produce methane and water. However, a feed with an hydrogen to carbon dioxide ratio less than three, engenders low conversion rates and lead to reducing the life of the catalyst. The first commercial plant was developed in the United States (North Dakota) in 1984. It is still operational and enables the production of 1.53 billion Nm3/year SNG (GPGP, 2006). The high exothermicity of methanation can limit its commercial deployment. The thermal runaway in fixed bed reactors can be avoided through either deploying multiple stages of adiabatic reactors with partial recycling (e.g., the TREMP^{TM} technology developed in 2009 by Haldor Topsoe in Denmark) or using an isothermal bed with integrated tubes to extract heat by producing steam (e.g., the Linde process in Germany developed in 1970).

3.4.1.2. Methanation modeling and validation

The hydrogen contained in the gasification output gas reacts with carbon monoxide over a metal based catalyst to produce methane and steam. This highly exothermic reaction occurs in the methanation unit simultaneously with a side reaction of water gas shift, Figure 3.20.

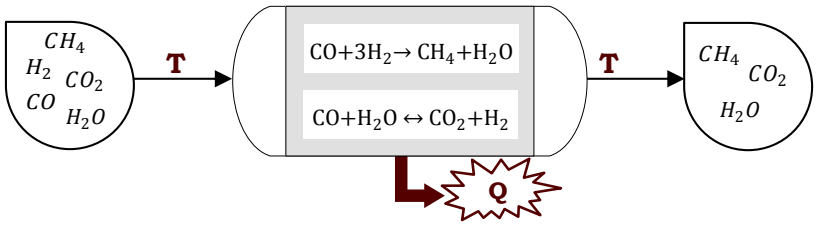


Figure 3.20. Methanation unit

The kinetic model of this unit is formulated as a plug flow reactor assuming a catalytic fixed bed in steady state conditions. The continuity equation represented in Eq.(3.18) by the molar flow variation with respect to the reactor axial coordinate, takes into account the chemical conversion of component i produced or consumed through reaction k.

$$\frac{dF_i}{dz} = a_r \rho_s \sum_{k=1}^{N_R} \nu_{ik} r_k \tag{3.18}$$

Considering an isothermal process, the energy evacuation of the reactor is equal to that generated by the chemical reaction taking place within. Eq. (3.19) shows the energy balance of a one-dimensional catalytic bed.

$$\frac{dT}{dz} = \frac{a_r \rho_s \sum_{k=1}^{N_R} (-\Delta H_k r_k) - q}{\sum_{i=1}^{R} (-F_i C_{p_i})} \tag{3.19}$$

The kinetics of the reactions occurring in the methanation unit on the Ni/Al_2O_3 catalyst are described in Table 3.17 (Er-rbib & Bouallou, 2014). The operating temperature range of the aforementioned catalyst varies between 200°C and 400°C.

Table 3.17. Methanation unit kinetic model

Chemical reaction	Reaction Kinetic ($mol.m^{-3}.s^{-1}$)
$CO+3H_2 \rightarrow CH_4+H_2O$	$r_1 = \frac{k_1 K_C P_{CO}^{0.5} P_{H_2}^{0.5}}{\left(1+K_C P_{CO}^{0.5}+K_{OH} P_{H_2O} P_{H_2}^{-0.5}\right)^2}$
$CO+H_2O \leftrightarrow CO_2+H_2$	$r_2 = \frac{k_2 \left(K_\alpha P_{CO} P_{H_2O} - \frac{P_{CO_2} P_{H_2}}{K_{eq}}\right)}{P_{H_2}^{0.5}\left(1+K_C P_{CO}^{0.5}+K_{OH} P_{H_2O} P_{H_2}^{-0.5}\right)^2}$

The coefficients of the methanation reactions rate and adsorption are dependent on the reactor temperature and are defined respectively according to Arrhenius equation $k_i = k_{0i} \exp\left(\frac{-E_{ai}}{RT}\right)$ and that of Vant Hoff: $K_j = K_{0j} \exp\left(\frac{-\Delta H_{Rj}}{RT}\right)$. Those parameters are presented in Table 3.18.

Table 3.18. Coefficients of the methanation kinetic model

	k_1	k_2		K_C	K_α	K_{OH}
k_{0i}	3.34×10^{6}	9.62×10^{14}	K_{0j}	8.1×10^{-6}	9.3×10^{-2}	3.97×10^{-7}
E_{ai}	-74000	-161740	ΔH_{Rj}	61200	6500	72650

Figure 3.21 shows the developed methanation model results of the gas molar composition represented by lines and those of the experimental data depicted as symbols (Kopyscinski, 2010). The operating and design parameters for this latter are listed in Table 3.19, for a catalytic bed on Ni/Al_2O_3 with a density of 3120 kg/m^3. The predicted model results are in very good agreement with experimental data thus the developed methanation unit model is supposed to be valid.

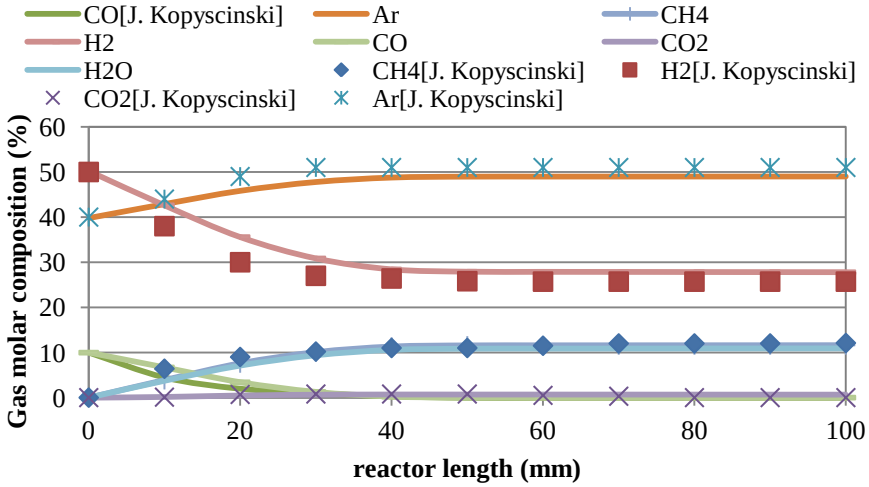


Figure 3.21. Gas composition profile in the methanation unit

Table 3.19. Operating and design parameters

Parameter	Value
P	2 bar
$T_{entrée}$	320°C
ρ_s	3120 kg/m^3
Input total flow rate	0.3 l_N/min
L	0.1 m
d	0.001 m

3.4.2. Compressor model

As shown in the block flow diagram of Figure 3.19, a compressor is needed before the carbon dioxide separation since the employed technology for this purpose requires a pressurized flow stream. The compressor is modeled with an isentropic efficiency of η_{is} by its mass and energy balances in which the enthalpies of each component at different states are calculated using the correlations embedded in Dymola®. The isentropic work of the compressor is expressed by Eq.(3.20).

$$W_{is} = F_{total} M_{m_{total}} (h_{out_{is}} - h_{in}) \tag{3.20}$$

The gas mixture maintains a constant molar flow rate and composition during the compression process since no chemical reaction takes place. Therefore the variable outputs of this model are the gas output temperature and the actual required compressor work. Setting the isentropic efficiency as a parameter of the model, the actual output enthalpy of the gas can be found using Eq. (3.21) and thus the temperature could be deduced. Whereas the second output is evaluated according to Eq.(3.22).

$$\eta_{is} = \frac{h_{out_{is}} - h_{in}}{h_{out_{actual}} - h_{in}} \tag{3.21}$$

$$W_{actual} = \frac{W_{is}}{\eta_{is}} \tag{3.22}$$

The results generated from the compressor model developed on Modelica® and simulated in Dymola® are compared with a compressor on Aspen Plus® with an isentropic efficiency of 0.85 and whose input composition and operating parameters are listed in Table 3.20. A good consistency is observed between the results obtained from both models with a maximum deviation of 0.17%, Table 3.21. This error may be due to the difference in the enthalpy correlations used in each software.

Table 3.20. Operating parameters

Parameter	Value
CH_4 (%)	0.48
H_2 (%)	0.02
CO (%)	0.02
CO_2 (%)	0.42
H_2O (%)	0.06
Flow rate $_{total}$ (mol/s)	500
T (°C)	200
Pressure (bar)	1

Table 3.21. Dymola® model results comparison with Aspen Plus® results for the compressor

Parameter	Dymola Results	Aspen Results	Error (%)
Isentropic temperature (°C)	433.47	434	0.12
Real temperature (°C)	470.57	471.36	0.17
Work W_{real} (MW)	6.58	6.59	0.16
Pressure (bar)	10	10	0

3.4.3. Carbon dioxide separation model

After collecting H_2O from the output methanation gas, CO_2 remains the only component to be eliminated for reaching highly rich-methane stream adapted to the gas network specifications. Carbon dioxide capture technologies can be classified into four categories: absorption, adsorption, membranes and cryogenic separations. The application of each method depends mainly on the gas mixture that contains the CO_2 to be separated. Its composition, temperature, pressure, CO_2 concentration and the amount of CO_2 to be eliminated are the main criteria for choosing the method to be used.

Absorption is carried out with chemical or physical solvents. Chemical absorption is the preferred method of CO_2 capture for low CO_2 concentrations. In the absorption column, the CO_2 reacts with the solvent to form new water-soluble components. The CO_2-rich solvent is then fed to a regeneration column in which the thermal energy is supplied in order to reverse the reaction and recover CO_2. Physical absorption in the other hand is employed when dealing with high carbon dioxide concentrations with fractions greater than 15 vol%. This technique consumes less energy for the regeneration than chemical absorption.

The adsorption method is more suitable for high-pressure and low-temperature CO_2 capture. The CO_2 in the gas mixture is selectively adsorbed by contacting the gas with the packed column which contains the adsorbent. The regeneration is carried out by either reducing pressure (PSA-Pressure Swing Adsorption) or by increasing temperature (TSA-Temperature Swing Adsorption).

Cryogenic separation is feasible for systems with very high CO_2 concentrations. It consists on separating CO_2 through cooling and condensation process which requires great amounts of energy.

Capturing carbon dioxide using membranes avoids the operation problems tied to direct gas-liquid contact such as: engorgement and foaming. Membranes are used industrially in biogas purification processes. A membrane is a selective physical barrier of a few hundred nanometers to a few millimeters thick, which under the effect of a transfer force (pressure gradient or concentration) enable or not the passage of certain components between the two channels which it separates.

The last described technique was selected for CO_2 capture in the wood to methane conversion process. The employed permeable membrane allows the diffusion of the steam leftovers in the mixture with 97% of carbon dioxide, 95% of carbon monoxide and 5% of methane while the rest of the mixture can be collected from the other side of the membrane. The employed diffusion percentages are used from the intervals given in the technical review of Bio-methane conducted by Vienna University of Technology (Vienna university of Technology, 2012).

3.5. Wood to electricity and heat conversion system

The conversion of wood to energy is the third investigated valorization pathway. Actually, the exothermic combustion of biomass releases heat which can be absorbed by water either during phase change or for a temperature gradient in a heat exchanger. By adding a simple steam cycle after the biomass furnace, electricity is produced by the expansion of the steam in the turbine and the latent heat stored within can be released through the condenser. By splitting the flow before it enters the turbine, the heat can be recovered on two different temperature levels as shown in Figure 3.22. Noting that depending on the selected fraction allowed to pass through the heat path loop, the amount of electricity generated changes and thus the released energy at the condensers.

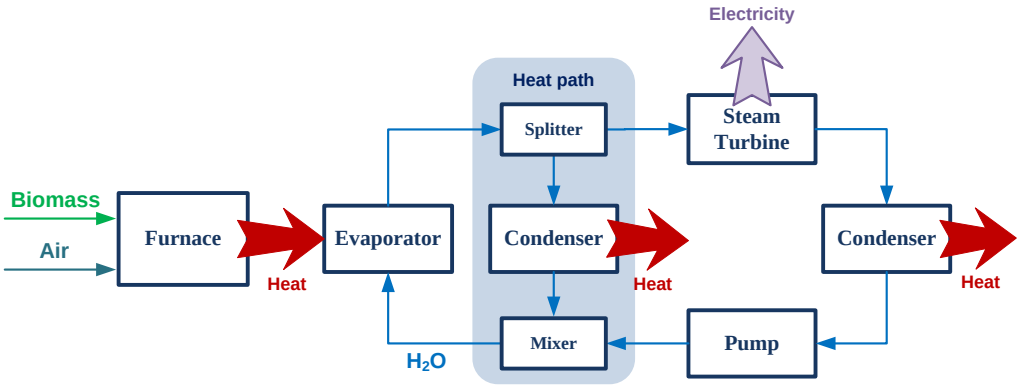


Figure 3.22. Block flow diagram of wood waste conversion to electricity and heat

The modeling of the furnace, the steam turbine, the splitter and mixer are mandatory to being able to assemble and evaluate the conversion of wood to electricity and heat. Therefore in the following sections the aforementioned units will be described and modeled.

3.5.1. Furnace model

The adiabatic furnace model is formed by the combustion chamber described in §3.3.4 with two additional steps to convert the biomass to a gas mixture, Figure 3.23. Upon entering the furnace the biomass is instantaneously converted into gas, tar and coke, under the heat effect, by the primary pyrolysis reaction (cf. §3.3.1). At 300°C, the tar cracking or the secondary pyrolysis is assumed to start, Table 3.22. This step is formulated as a thermo-chemical equilibrium model. The air is then introduced to the furnace which is at 600°C to trigger the combustion. The inlet air temperature is defined as a parameter of the model. The energy needed to heat the introduced air to 600°C and the required heat by the endothermic pyrolysis is covered by a part of the energy produced by the exothermic combustion, thus the heat flow Q in Eq.(3.15) is not null in this system and is equal to this transferred energy. Therefore the flue gas temperature is evaluated once Q is determined.

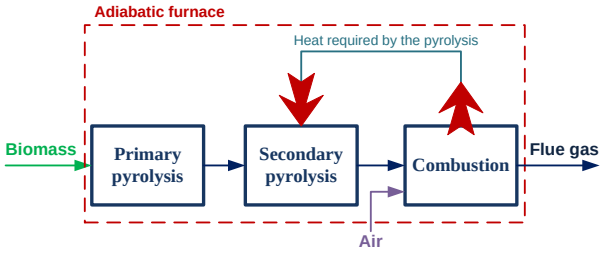


Figure 3.23. Adiabatic furnace block diagram

Table 3.22. Biomass secondary pyrolysis reactions

Chemical reactions
$C_6H_6O \rightarrow CO + 0{,}4C_{10}H_8 + 0{,}15C_6H_6 + 0{,}1CH_4 + 0{,}75H_2$
$C_6H_6O + 3H_2O \rightarrow 4CO + 2CH_4 + 2H_2$
$C_{10}H_8 \rightarrow 7{,}38C + 0{,}275C_6H_6 + 0{,}97CH_4 + 1{,}235H_2$
$C_6H_6 + 2H_2O \rightarrow 1{,}5C + 2{,}5CH_4 + 2CO$

To ensure the validity of the above described model, a furnace assembly was put together in Aspen Plus®. The secondary pyrolysis reactions were inputted in an equilibrium reactor from Aspen Plus® based on stoichiometric approach. This reactor has the product of the primary pyrolysis as its inlet flow whose composition is listed in Table 3.23. This composition is generated from the pyrolysis of 12 t/hr of woody biomass. The equilibrium reactor is connected to an RStoic of Aspen Plus® which generates the combustion reactions with the introduced air at 25°C. A heat transfer between the two reactors is enabled via a heat flow; this simulates the use of some of the combustion released heat to cover the endothermic pyrolysis. In the model established in Modelica®, this is achieved by adding a connector that transmits the required heat flux from the combustion model to the pyrolysis block. The inlet air composition is evaluated in Dymola® and then inserted in Aspen Plus®. The O_2 molar flow rate is assessed according to Eq.(3.23) with the excess air percentage set as a parameter and the N_2 flow rate is considered to be 3.76 that of O_2. According to the results displayed in Table 3.23 the developed model shows a very good agreement with the one assembled in Aspen Plus®.

$$F_{O_2} = (1 + \text{excess air } \%) \times \sum_{k=1}^{N_R} \upsilon_{O_2 k}\, \xi_k \tag{3.23}$$

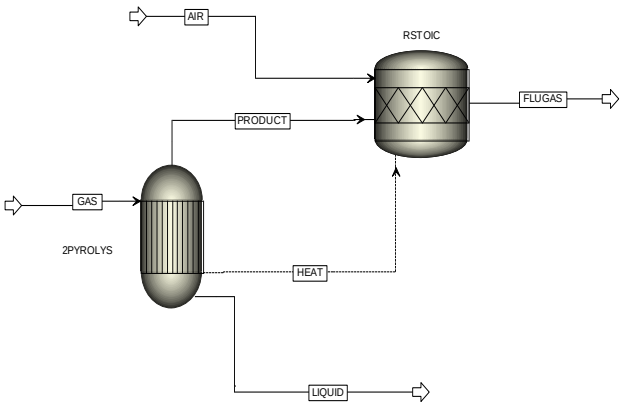


Figure 3.24. Furnace assembly on Aspen plus®

Table 3.23. Comparison of Dymola® model results with those of Aspen Plus®

	Input	Dymola Results	Aspen Results
C_6H_6O (mol/s)	17.482	0	0
CH_4 (mol/s)	5.021	0	0
H_2 (mol/s)	2.667	0	0
CO (mol/s)	25.762	0	0
CO_2 (mol/s)	2.33	138.01	138.007
H_2O (mol/s)	14.889	80.044	80.044
O_2 (mol/s)	0	293.264	293.264
N_2 (mol/s)	0	1654	1654
$T_{\text{flue gas}}$ (°C)	-	941.3	943.3
Q (MW)	-	3.639	3.417

3.5.2. Steam turbine model

The transferred thermal energy to the steam flow from the flue gas is converted to mechanical work by the turbine through depressurizing the superheated steam. Assuming an isentropic efficiency of η_{is} the generated work is evaluated according Eq.(3.24). The actual enthalpy of the exiting stream can be evaluated from the actual outlet enthalpy found by (3.25).

$$W_{elec} = F_{total} M_{m_{total}} (h_{out_{is}} - h_{in}) \times \eta_{is} \tag{3.24}$$

$$\eta_{is} = \frac{h_{out_{actual}} - h_{in}}{h_{out_{is}} - h_{in}} \tag{3.25}$$

The simulation results of a steam turbine operating at the listed parameters in Table 3.24 is compared with the result obtained when simulating a pressure changer with an isentropic efficiency of 0.85 in Aspen Plus®. Table 3.25 shows the consistency between both results illustrated by the very low relative error which does not surpass 0.6%.

Table 3.24. Operating parameters

Parameter	Value
CH_4 (%)	0
H_2 (%)	0
CO (%)	0
CO_2 (%)	0
H_2O (%)	1
Flow rate $_{total}$ (mol/s)	500
T (°C)	600
Pressure (bar)	10

Table 3.25. Dymola® model results comparison with Aspen Plus® results for the steam turbine

Parameter	Dymola Results	Aspen Results	Error (%)
Isentropic temperature (°C)	249.05	249.66	0.24
Real temperature (°C)	303.47	304.75	0.42
Work W_{real} (MW)	5.55	5.58	0.54
Pressure (bar)	1	1	0

3.5.3. Splitter and mixer models

To enable the heat recovery at two temperatures in the conversion system of wood to heat and electricity, a stream splitter is employed, Figure 3.25.(a). This component enables the flow division into two streams. The first one goes through the turbine with a fraction x of the inlet flow rate, and the rest of the flow (1-x) circulates in the heat path loop where the heat is recovered at high temperature (cf. Figure 3.22).



(a) (b)

Figure 3.25. (a) Splitter unit, (b) mixer unit

After its expansion in the turbine the latent heat released from its cooling can be recovered on a temperature lower than the one in the heat loop path, thus the two temperature levels. To close the cycle a mixer (Figure 3.25.b) is added after pumping the water of the low temperature stream to meet the same pressure of the high temperature flow. According to the energy balance in Eq.(3.26), the outlet temperature of the mix is identified from the enthalpy of the water, knowing that the outlet mass flow rate is the sum of that of the two inlets of the mixer.

$$\dot{m}_{out} h_{out} = \dot{m}_{in1} h_{in1} + \dot{m}_{in2} h_{in2} \quad (3.26)$$

3.6. Process scale up

The design of the conversion system is directly impacted by the supplied quantities of raw material and the desired yield of products. The modeling process was conducted according to literature studies which supposed certain reactors design. Consequently, scale up procedure is required to adapt the reactors' volume to the adequate sizes for the case study. This is carried out considering a constant

space velocity in the reactors which is defined by the ratio of the volumetric flow rate to the catalytic bed's volume (Trambouze, et al., 1984). Having an incompressible flow, the new reactor's volume is the old one multiplied by the scaling factor X which is the ratio of the new to the old mass flow rate, Eq.(3.27). Thus the diameter of the scaled up reactor is determined according to Eq.(3.28); wherein the vessel's volume is considered to be that of a cylindrical reactor and is computed using Eq.(3.29). However by maintaining a constant length to diameter ratio, k, the new length can be evaluated by Eq.(3.30). Once the reactor's volume is assessed, the catalyst mass could be evaluated by multiplying the new reactor's volume V_{new} by the catalyst density. For the membrane scale up the ratio of the membrane surface to the reactor volume is maintained fixed. Thus for the same thickness, the new membrane surface is the old one times the scale factor X.

$$\frac{\dot{m}_{new}}{V_{new}} = \frac{\dot{m}_{old}}{V_{old}} \rightarrow V_{new} = V_{old} \times \frac{\dot{m}_{new}}{\dot{m}_{old}} \rightarrow V_{new} = V_{old} \times X \tag{3.27}$$

$$D_{new} = \left(\frac{4\,X \times V_{old}}{\pi k}\right)^{1/3} \tag{3.28}$$

$$V_{old} = \frac{\pi d_{old}^2}{4} L_{old} \tag{3.29}$$

$$L_{new} = k\, D_{new} \tag{3.30}$$

3.7. Conversion System Economic model

The economic model of each of the conversion systems is formulated by their fixed and variable costs. The fixed cost of a process is actually formed by the investment needed to install each of its units. As for the variable cost of the process, it consists of the operating cost of which the avoided cost and revenues are deduced. The system operating cost is the expenses associated with the required raw material that ensures the efficient operation of the conversion system. While the avoided costs are ensued by the avoided charges of the carbon dioxide tax, the revenues are generated from selling the type of by-products that are not required in the park (i.e., electricity and natural gas).

3.7.1. Conversion System Fixed Cost

As described earlier, the wood to hydrogen conversion system mainly consists of a gasifier a steam methane reformer, a water gas shift membrane reactor and a combustion chamber. The first three reactors are or have a catalytic bed, whereas the combustion chamber is not. Thus this latter was not taken into account in the investment cost considering that the catalyst cost surpasses the tank investment. Thereby, the investment cost of the wood to hydrogen conversion system consists of that of the three catalytic reactors. For the methane production system from wood, the investment expenses are due to the gasifier, methanation unit, carbon dioxide separation and compressor costs. Each unit investment cost (I) is calculated according to the actual capacity (Size), reference size ($Size_0$) and reference investment cost (I_0) by Eq.(3.26); where F denotes the overall installation factor. These parameters are listed in Table 3.26 for the aforementioned units.

$$I = I_0 \left(\frac{Size}{Size_0}\right)^n \times F \tag{3.31}$$

Table 3.26. Reference investment cost of the conversion system units

Component	Reference Size ($Size_0$)	Size unit	Investment I_0 (€)	Scale factor (n)	F	Ref.
Gasifier	220	$Kg_{biomass}/hr$	0.3×10^6 (2011)	0.75	1.86	(Andersson, et al., 2014)
Steam Reformer	10	Kg_{H2}/s	251×10^6 (2011)	0.67	1	(Berghout, et al., 2015)
Methanation unit	1770	MW_{HHV}	82.5×10^6 (2012)	0.65	1	(De Saint Jean, et al., 2015)
CO_2 Separation	100	$m^3_{methane}/hr$	750 (2012)	0.6	1	(Vienna university of Technology, 2012)
Compressor	445	kW_{elc}	267×10^3 (2012)	0,67	1	(De Saint Jean, et al., 2015)

Since the WGS reactor differs from the other units by an additional membrane, its investment cost is correlated in function of not only the used catalyst but also of its membrane cost according to Eq. (3.32) (Van Der Sluijs, et al., 1992), where Pa refers to the palladium of which the membrane is mainly made of. The exchange rate of 1.1 EUR/US$ was used for monetary conversion.

$$I_{WGS\ reactor}=\left(\$_{Pa}/kg_{Pa}\right)\times\left(\rho_{Pa}\times V_{membrane}\right)+\left(\$_{catalyst}/kg_{catalyst}\right)\times\left(W_{catalyst}\right) \quad (3.32)$$

The capital cost of the wood to electricity and heat conversion system consists of the furnace, pump and steam turbine investment. Each of these units cost is formulated according to the correlation in Eq. (3.33), where the coefficients a and b are evaluated on the basis of experimental and literature data (Caputo, et al., 2005). As seen in Table 3.27, both the steam turbine and pump have the net electric power of the system as their investment characteristic parameter (S). As for the boiler's cost, it is correlated as a function of the power generated by a typical steam cycle placed downstream of the furnace having a 23% electric efficiency (the choice of this value depends on the plant size which is fixed by the biomass supply).

$$I = a \times S^b \quad (3.33)$$

Table 3.27. Correlation coefficients for the investment of the cogeneration units

Component	Characteristic parameter (S)	Parameter unit	Coefficient a (€)	Coefficient (b)
Furnace	Combustion electric energy	MW	1.34×10^6 (2005)	0.694
Steam Turbine	Net electric power	MW	633×10^3 (2005)	0.398
Pump	Net electric power	MW	280×10^3 (2005)	0.5575

In order to convert the investment cost to the price level of 2014, Eq.(3.34) was employed to take into account the price and service inflation. It consists on multiplying the investment cost of the reference year ($I_{year\ x}$) by the ratio between the Chemical Engineering's Plant Index of the year 2014 ($CEPI_{current\ year}$) and the one of the year the reference investment was made ($CEPI_{year\ x}$).

$$I_{current\ year}=I_{year\ x}\left(\frac{CEPI_{current\ year}}{CEPI_{year\ x}}\right) \quad (3.34)$$

3.7.2. Conversion System Variable Cost

The variable cost of the conversion system consists of its operating cost from which the avoided cost and revenues are deduced. The operating cost of the wood conversion system is the cost of resources used in order to maintain its operation. The annual cost of raw material is computed by multiplying the feed rate of the process by the appropriate price per volume or mass. Consequently, the hydrogen production system inputs are biomass, steam and oxygen, while that of methane production is biomass, steam and electricity. However the route for energy production has only biomass demand. This latter is considered wood waste to be recovered and thus its price directly depends on the economic scheme governing the studied park, it is evaluated correspondingly in the case study. In the oxy-combustion of the hydrogen production system, the oxygen is supposed to be entirely bought from an external source.

As for steam flow, the wood to hydrogen system has two intakes: the first to the gasifier and the second is before the steam methane reformer; whilst the methane production pathway has only the need for steam at the gasifier inlet. Moreover, for both of these conversion systems, a part of the water is recovered from the flue gases through condensation. Therefore the required water resource amount is the difference between the system water intake and the recovered quantity. This material integration is so obvious owing to the singularity of the water source and which is also considered to meet the quality standard of the water sinks.

The time of operation is supposed to be 6000 hours per year accounting for annual maintenance shutdown. The prices of the detected resources are: 3.09 €/m^3 for water (ein, 2009) and 30 €/ton for pure oxygen. The price of this latter is estimated from the investment and operating costs of an air separation unit (ASU) assuming 10€ per ton of oxygen for other charges and profit. Actually having a specific power demand of 240 kWh per ton of oxygen (Gale, et al., 2009) with the MWh of electricity at 55 €, the operating cost share of the oxygen price is around 14 €/ton. The investment of an ASU is 30 M€ for an annual capacity of 518000 ton of O_2 (Amarkhail, 2010). With a 10 year period of operation, 6 € is approximately the investment share per ton of oxygen.

The avoided cost is engendered by the carbon dioxide capture leading to avert from the carbon tax which levies a fee on the production of fuels based on how much carbon their combustion emits. The avoided tax value is considered to be 50 €/ton for an optimistic carbon dioxide capture reward.

Since the only required material by the industrial actors of the territory is hydrogen, the other types of commodities have no integration opportunities. Subsequently, the produced electricity and methane are supposed to be sold to the power and gas companies supplying the territory. The generated electricity from the wood conversion is directly injected into the grid or auto-consumed by the park for 55.3 €/MWh. Similarly for the methane due to its high purity it is supplied to the grid with a generated revenue equivalent to the gas market price (the reference scenario considers 30 €/MWh). The reason behind the selection of this value is furtherly discussed in the following chapter. Table 3.28 summarizes the adopted prices of the conversion systems' resources and the potential revenues from the generated commodities per type of material. The hypothesis for the heat cost will also be explored in the case study application and which will vary according to the governance scheme of the territory.

Table 3.28. Price of the conversion systems resources and products

	Water	Oxygen	Carbon dioxide	Methane	Electricity
Price/Revenue	3.09 €/m^3	30 €/ton	50 €/ton	30 €/MWh	55.3 €/MWh

3.8. Conclusions

The case study on which both proposed methodological frameworks will be demonstrated was presented in this chapter. The preliminary study of the studied industrial park evinced the missed opportunities for the discharged wood waste to be recovered in the territory due to the lack of such demand. In the aim of enhancing resources management through circular economy, the conversion of the wood was proposed to alter the initial form of this non-usable stream into interesting commodities for the territory. Consequently the main thermodynamic reacting systems for woody biomass were explored. Those were classified in two main categories: the biochemical conversion and the thermo-chemical conversion. The first's product being essentially ethanol, it was not adopted as a possible conversion pathway for the wood in the studied territory by dint of the non-existing potential reuse. However three wood conversion routes, which fall under the thermo-chemical category, were judged to be in accordance with the park resources demand.

The transformation of wood to hydrogen, the conversion route towards methane production and the conversion pathway of wood into energy were the three selected systems to be investigated. The process units forming each of these pathways were identified and then modeled by physical models based on their energy and material balances while accounting for the chemical reaction occurring in the reactors. The set hypotheses were explored and the developed models were validated or compared to literature results and thus proved to be reliable. Economical models were also proposed based on the unit capacities with the view of accounting for the design parameters alteration impact when comparing different conversion processes sizing scenarios. The models actually serve to simulate multiple sets of operating parameters and evaluate the ensuing process flowsheets from which the energy and material streams will be extracted to conduct the integration according to the territory economical scheme.

In the following chapter the developed wood conversion systems will be employed as a database for both cooperative and non-cooperative frameworks applications. These latter will be demonstrated on the explored industrial park with the purpose of designing an optimal EIP configuration and identifying the synergy patterns to be implemented.

Chapitre 4 (résumé)

Application des cadres méthodologiques pour l'intégration des procédés de conversion dans un territoire

Le scénario de référence qui sera utilisé pour évaluer les résultats coopératifs et non-coopératifs était considéré le cas où chaque site industriel du territoire agit comme s'il ne faisait pas partie du territoire; ce qui signifie en tant qu'acteur isolé. Par conséquent, chaque site réalise son intégration locale de matière et d'énergie en essayant d'établir des synergies sur site entre ses unités pour profiter autant que possible de ses flux et réduire ses besoins en ressources et en chaleur.

Comme on l'a vu au chapitre 3, trois voies de conversion ont été jugées intéressants à évaluer et à mettre en concurrence en considérant les demandes du territoire étudié. Ces voies sont la production d'hydrogène à partir du bois, la conversion du bois en méthane et la troisième est la voie de la cogénération. Pour ces trois systèmes de conversion, leurs unités ont étaient d'abord dimensionnées pour la prise de la totalité de la biomasse. Ensuite, leur flow-sheet étaient établie pour extraire les flux d'énergie et de matière qui serviront comme les entrées pour les problèmes d'intégration. Le degré de liberté de chaque route était ensuite identifié en fonction du nombre de paramètres des systèmes potentiellement manipulable qui constituent les variables souveraines du problème. Grâce à l'altération de ces variables, plusieurs ensembles de configurations de procédé étaient établis. Dans le cadre méthodologique proposé d'un territoire à schéma coopératif, ces ensembles sont utilisés pour générer les scénarios prospectifs du territoire à analyser. Cependant, dans le schéma non-coopératif, les différents ensembles de configurations de paramètres sont utilisés par les agents potentiels pour générer leurs sous-agents.

Intégration des procédés de conversion dans un territoire avec un régime de gouvernance coopératif

Le parc étudié est formé par trois acteurs industriels prêts à collaborer pour l'amélioration de l'économie circulaire du territoire afin de diminuer la consommation globale de ressources et de rejets de déchets. Ils échangent ainsi leurs flux d'énergie et de matières gratuitement tout en partageant les dépenses d'investissement nécessaires à la mise en œuvre des synergies identifiées et les éventuelles gains. Le problème est alors formulé pour un territoire coopératif en utilisant le cadre méthodologique attribué. Les évaluations préliminaires du parc de l'intégration d'énergie et de matière ont montré que le bois déchargé O_1^{wood} présente des possibilités de récupération limitées dans sa forme initiale.

Par conséquence, il est identifié comme le flux déchets du territoire provenant du Site1 et est désigné par W_1^{wood}. Néanmoins, sa conversion en hydrogène, méthane ou électricité et chaleur stimule l'économie circulaire du parc en créant une nouvelle valorisation potentielle pour W_1^{wood}. L'ensemble des systèmes de conversion étudiés est formé par les trois voies conduisant à la production des produits précités: $CS = \{CS_1^{wood}, CS_2^{wood}, CS_3^{wood}\}$. Leurs variables souveraines $SV = \{SV_1^{wood}, SV_2^{wood}, SV_3^{wood}\}$ préalablement établies forment avec l'ensemble CS la superstructure du problème maître des voies de conversion.

Cette superstructure est utilisée pour générer les scénarios prospectifs du territoire en ajoutant dans chaque scénario une route de conversion du bois à partir de CS avec un ensemble correspondant q de SV; de ce fait, un nouvel acteur industriel $CS_{k,\,set\,q}^{wood}$ qui va modifier la forme du flux non utilisable est ajouté au parc et l'ensemble Territoire devient $\{Site_1, Site_2, Site_3, CS_{k,\,set\,q}^{wood}\}$.

Les résultats générés par le cadre méthodologique pour l'intégration des procédés de conversion dans un territoire à régime coopératif sont exprimés par les coûts fixes et variables du parc induits après l'établissement des échanges optimaux de matière et d'énergie parmi les éléments du Territoire. Les statuts économiques des scénario de chaque voie de conversion étaient évalués individuellement afin d'évaluer l'impact des variables souveraines sur les synergies établies. Les scénarios générant la plus grande amélioration de la gestion des flux du territoire par rapport au scénario de référence étaient identifiés pour étudier l'effet des fluctuations du prix du gaz et leur sensibilité sur la valeur monétaire de W_1^{wood}. L'afflux net annuel C_t résultant de la mise en œuvre d'un scénario prospectif par rapport au scénario de référence est la différence entre leurs coûts variables totaux, alors que la différence de leurs coûts fixes totaux sont les investissements supplémentaires C_0. Ces variables sont utilisées pour évaluer la valeur actuelle nette (VAN) d'un scénario prospectif comparé au scénario de référence afin d'étudier la rentabilité de sa structure selon l'Eq.1.

$$VAN = \sum_{t=1}^{T} \frac{C_t}{(1+r)^t} - C_0 \qquad \text{(Eq.1)}$$

L'implémentation du procédé de conversion du bois en hydrogène dans le parc était évaluer en premier. Étant donné que l'hydrogène possède une valeur plus élevée que la chaleur et donc plus coûteux d'obtenir d'une source externe, le coût variable total le plus bas du territoire est engendré avec la configuration des variable souveraines qui génère le plus haut rendement d'hydrogène. Sans surprise, la meilleur configuration $CS_{1,\,set10}^{wood}$ se compose du SB_{ratio} le plus bas et du plus haut $T_{gasifier}$ et T_{SMR}, maximisant ainsi la production d'hydrogène. Si la voie de conversion du bois en méthane est choisie comme voie de valorisation du bois non utilisable, $CS_{2,\,set\,5}^{wood}$ devrait être intégré dans le territoire pour atteindre le profit le plus élevé. À partir de l'ensemble des configurations évaluées des variables souveraines pour CS_3^{wood}, l'équilibre le plus rentable entre production de chaleur et d'électricité pour le parc opérant sous gouvernance coopérative est celui de l'ensemble 20. Ce dernier consiste de la cogénération ayant la moitié de la vapeur circulant traversant la turbine et fonctionnant à des températures élevées et basses à 280 °C et 180 °C respectivement.

Chaque voie de conversion a été étudiée individuellement pour déterminer les options techniques et les paramètres de fonctionnement des unités du procédé de conversion qui engendrent la plus grande rentabilité. Cependant, pour sélectionner la route de conversion du bois la plus rentable à mettre en œuvre sur le territoire, une analyse combinée des trois voies de valorisation était obligatoire.

L'ensemble des scénarios induits par l'analyse des trois voies de conversion est représenté sur la Fig. 6 en termes des coûts totaux fixes et annuels variables du territoire, avec le scénario de référence et les scénarios jugés comme étant les meilleurs de chaque route. Le premier aspect remarquable de ce graphique est que, indépendamment du chemin de conversion choisie, les opportunités de valorisation créées à partir de la transformation du bois non utilisable en sa forme initiale améliore considérablement le coût variable du territoire à un niveau bas qui serait autrement inaccessible.

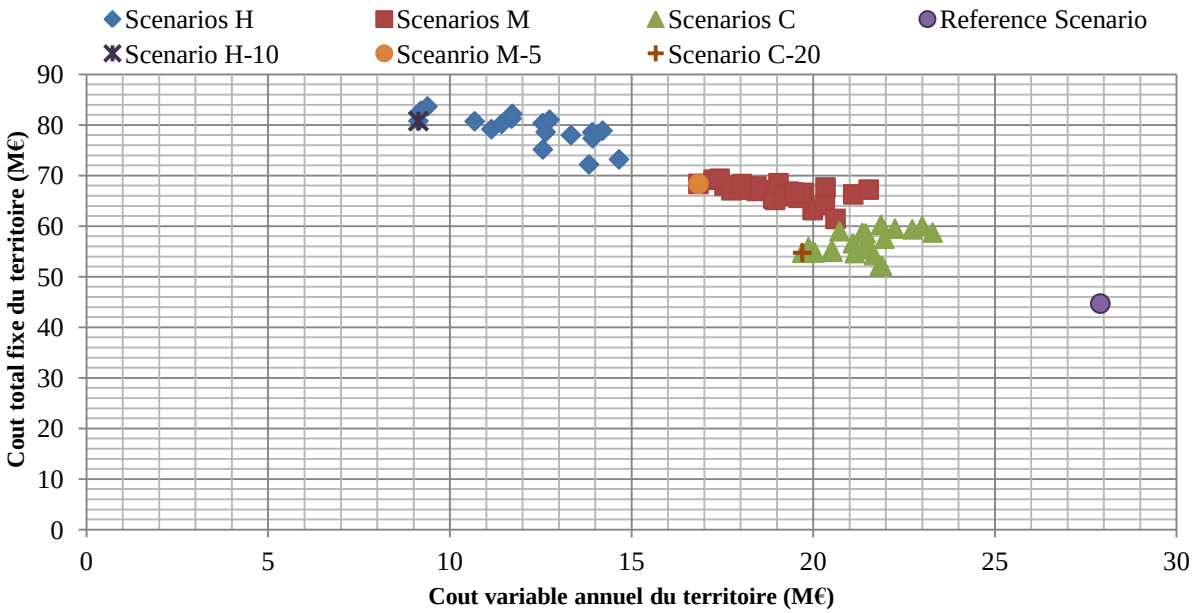


Fig. 6. Statuts économiques des trois voies étudiées de conversion du bois

On peut également déduire de ce graphique que la production d'hydrogène est la voie de conversion générant le coût variable le plus bas; Cependant, cette route exige le plus de fonds pour mettre en place la topologie de l'éco-parc industriel évalué. Cela peut s'expliquer par la demande d'hydrogène du parc qui est plus chère à acheter auprès d'une source externe que de payer pour la demande de chaleur. Ce fait souligne l'importance de prendre en compte la demande du territoire lors de l'étude préliminaire des système de valorisation des flux non utilisables afin de sélectionner celles qui doivent être étudiées profondément et potentiellement être mise en œuvre.

Une étude de sensibilité était réalisée pour les scénarios jugés comme étant les plus rentables pour chaque voie de conversion dans le but de détecter la stratégie de collaboration à exécuter pour les meilleures synergies sur site et entre-sites. Les statuts économiques de ces scénarios sont listés dans le Tableau 1.

Tableau 1. Statuts économiques du territoire pour les meilleurs scénarios

Scenario	Coût fixe (M€)	Coût variable annuel (M€)
Scenario de référence	*44.67*	*27.90*
Scenario H-10	80.77	9.16
Scenario M-5	68.34	16.84
Scenario C-20	54.72	19.70

Les valeurs actuelles nettes du Scénario H-10, Scénario M-5 et le Scénario C-20 étaient évaluées sur une période de dix ans en fonction du Scénario de référence afin d'évaluer et comparer

leur rentabilité respective, Fig. 7. La voie de cogénération a le retour sur investissement le plus rapide. L'implémentation de ce chemin commence à engendrer des profits à partir de la deuxième année de la mise en œuvre de la topologie de l'éco-parc. En ce qui concerne les deux autres voies de conversion, ce n'est pas avant l'année d'après qu'elles ont une VAN positive. Par conséquent, la période de temps que les décideurs sont prêts à attendre pour obtenir le remboursement intégral de leur investissement joue un rôle majeur dans la sélection de la route de conversion à établir dans le territoire étudié. Néanmoins, cette sélection devrait également tenir compte de la différence de gain entre les routes de conversion sur l'horizon d'exploitation du parc. Après dix années d'exploitation, le scénario de conversion du bois en hydrogène entraîne plus du double des bénéfices qui pourraient être générés par la mise en œuvre de la cogénération à partir du bois. Et enfin, avec un retour sur investissement à peu près similaire, la conversion du bois en méthane est moins intéressante par rapport à la route du bois à l'hydrogène en raison de la rentabilité plus élevée que le second induit.

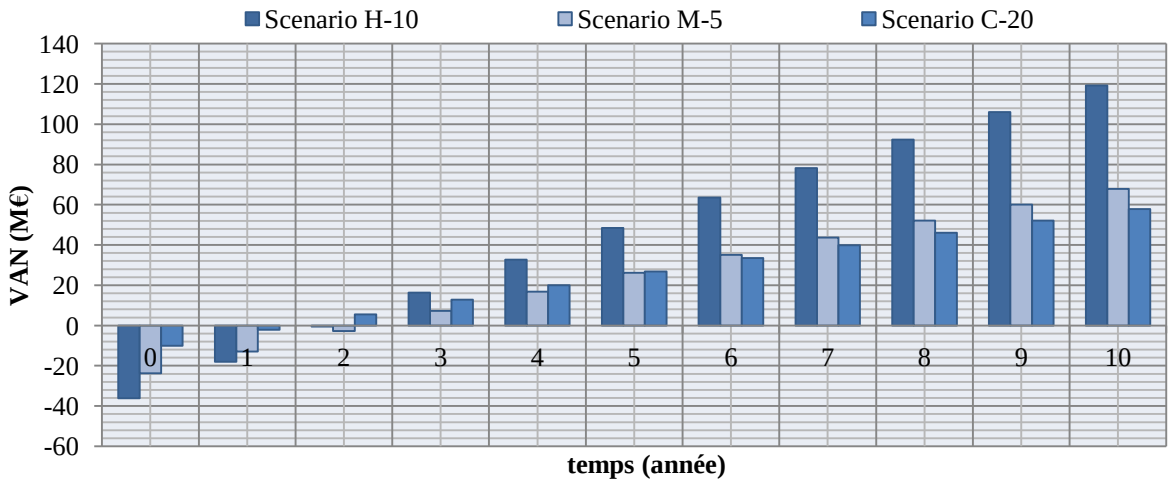


Fig. 7. Comparaison des VAN sur dix ans pour le meilleur scénario de chaque voie

Que la sélection tombe sur CS_1^{wood}, CS_2^{wood}or CS_3^{wood}, il est apparent que la conversion des flux identifiés comme non-utilisables dans le territoire en des produits de plus grande valeur s'avère toujours lucrative avec un temps de retour sur investissement variable. Cette déclaration est vraie pour les déchets n'ayant aucune valeur; Cependant, quand ils ont une valeur monétaire, cela pourrait ne pas être toujours le cas. Le problème devrait donc déterminer s'il est plus avantageux d'investir dans un système de conversion pour récupérer les déchets en interne et changer leurs formes initiales ou bien de les vendre à des clients externes pour leur valeur. En plus, les principaux produits auxquels le bois était converti sont l'hydrogène, le méthane et la chaleur. Les prix de ces trois sont supposés être corrélés avec le prix fluctuant du marché du gaz. Par conséquent, des études de sensibilité étaient menées visant à évaluer la variation de la rentabilité et le temps de retour avec la fluctuation du prix du gaz (§ 4.4.6.1 et § 4.4.6.2 présentent respectivement l'étude de l'impact de la valeur du bois et de la variation du prix du gaz sur la sélection de la meilleure route). L'intégration d'un système de conversion dans un territoire était constatée d'être fortement influencée par les besoins en ressources du parc étudié. Un autre facteur intéressant a été trouvé d'avoir un grand poids dans la prise de décision, celui-ci est le temps de retour sur investissement désiré. Néanmoins, cela pourrait conduire à des choix biaisés vers certains systèmes de conversion qui pourront éventuellement être moins lucratifs que d'autres routes. Par conséquent, une vue globale devrait être prise sur la durée de vie du parc afin d'évaluer si les décideurs devraient être plus flexibles sur le temps de retour sur leurs investissements en vue d'une plus grande rentabilité dans les années à venir.

La meilleure voie de conversion qui subit le moins de dégâts avec les fluctuations du marché du gaz ou de la valeur monétaire des déchets non-utilisables s'avère être la conversion du bois en hydrogène. En particulier, ce procédés de conversion devraient avoir la $10^{ème}$ configuration de l'ensemble étudié des variables souveraines: $(SB_{ratio}, T_{gasifier}, T_{SMR}) = (0.5, 850, 850)$. La topologie des synergies induite avec l'intégration du $CS^{wood}_{1,\ set\ 10}$ dans le territoire étudié est illustrée à la Fig. 8.

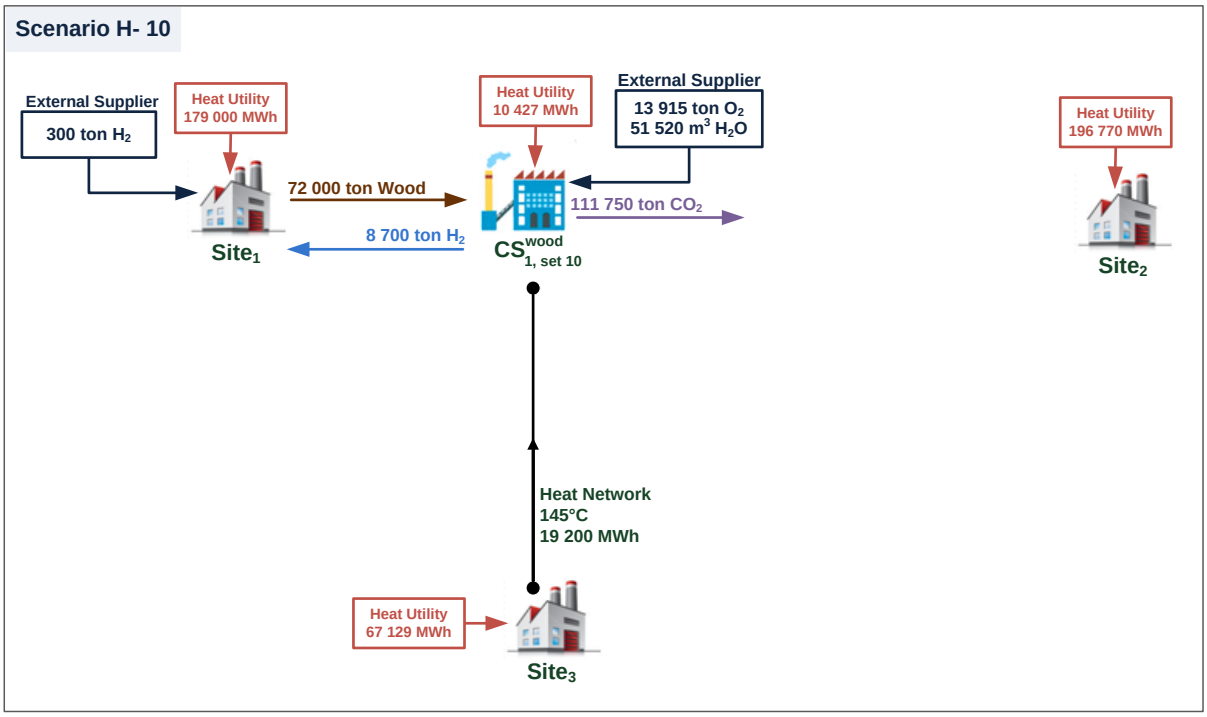


Fig. 8. Configuration de l'éco-parc pour le meilleur scénario du territoire en gouvernance coopérative

La configuration d'éco-parc industriel induite à partir de l'intégration de $CS^{wood}_{1,\ set\ 10}$ dans le territoire étudié assure le *social welfare* du territoire considérant ses sites industriels comme une entité économique unique dans laquelle les flux d'énergie et de matière sont librement échangés. Néanmoins, dans des circonstances plus réalistes, les industries cherchent leurs propre avantage et n'agissent donc que dans l'intérêt de leur bien-être individuel. Par conséquent, ils vont probablement mettre un prix sur les produits sortants ou même les déchets qu'ils allouent pour établir une synergie avec un autre acteur industriel aussi cherchant son propre intérêt. Cela aura un impact important sur la configuration des synergies du territoire qui en résultera et pourrait également changer la meilleure route de conversion du bois. Par conséquent, dans la section suivante, la topologie de l'eco-parc industriel avec une gouvernance non coopérative sera examinée pour déterminer les transactions d'achat et de vente optimales pour les flux d'énergie et de matière circulant entre sites.

Intégration des procédés de conversion dans un territoire avec un régime de gouvernance non-coopératif

Les trois sites industriels situés dans les limites prédéfinies du territoire étudié sont maintenant supposés être motivés par l'augmentation de leurs avantages individuels sans tenir compte de l'amélioration du fonctionnement global du parc. Les gains induits de l'échange de leurs flux sont leur seule stimulation pour participer à l'établissement de synergies. Dans le but de trouver les accords

conjoints qui sont lucratifs pour chaque partie participante du parc, le cadre méthodologique proposé pour l'intégration des procédés de conversion dans un territoire régi par une gouvernance non-coopératif était employé. Le problème est donc formulé comme un système multi-agent dans lequel l'ensemble d'agents industriels IA se compose des trois sites du parc, $IA = \{IA_1, IA_2, IA_3\}$. Ceux-ci transmettent leurs besoins et leurs rejets d'énergie et de matière à la tierce-partie qui intervient exclusivement dans l'évaluation des synergies potentielles entre-sites basées sur une optimisation purement exergétique pour l'intégration énergétique et consistant en la minimisation de la source fraîche pour le problème de matière.

À partir du "Material Message" vide que IA_1 reçoit de la tierce-partie après l'analyse des flux matière, il dérive que son rejet de bois n'a aucune possibilité de récupération dans le territoire sous sa forme existante et définit ainsi ses 72 000 tonnes de bois rejetés annuellement comme ses déchets W_1^{wood}. Dans le but d'augmenter ses gains, IA_1 lance une vente aux enchères sur W_1^{wood} pour des investisseurs potentiels avec un prix de départ C_0 de 10 € pour la tonne de biomasse; Il pourrait ainsi augmenter son chiffre d'affaires annuel d'au moins 0,72 M€ de la vente de ses déchets. Bien évidement, un participant aux enchères voudra investir dans un système de procédé exigeant que le W_1^{wood} vendu aux enchères soit utilisé comme ressource pour générer des produits qui peuvent ensuite être revendus à d'autres agents industriels du parc dans lequel il sera implémenté. Par conséquent, les enchérisseurs qui composent les agents potentiels PA du problème sont identifiés à partir de la base de données de systèmes de conversion CS. Ce dernier est formé par les trois voies de conversion du bois qui permettent respectivement la génération d'hydrogène, de méthane et d'énergie, ainsi: $CS = \{CS_1^{wood}, CS_2^{wood}, CS_3^{wood}\}$ and $PA = \{PA_{1,1}, PA_{1,2}, PA_{1,3}\}$.

Chaque élément de PA génère sa sous-population à partir des ensembles de variables souveraines identifiés correspondant à chaque route de conversion; donc un agent sous-potentiel de $PA_{1,1}$ avec l'ensemble q de SV est noté $PA_{1,1,set\,q}$. De sa population crée, un agent potentiel k sélectionne son sous-agent ayant le plus haut potentiel d'enchères $PA_{1,k,set\,q_\beta kmax}$ pour entrer avec lui dans la vente aux enchères. Cependant, pour réduire le fardeau du temps de calcul, les configurations défavorables des variables souveraines ont été éliminés en fonction des résultats engendrés par l'application de la méthodologie coopérative sur le parc étudié.

L'évaluation de leurs potentiels d'enchères est réalisée en fonction de la stratégie d'investissement qu'ils suivent. De même pour les agents industriels qui évaluent leurs "Trade Messages" commerciaux reçus de la part de Network Investor (NI) en fonction du temps qu'ils sont prêts à attendre avant la génération de leur bénéfice net. En vue d'évaluer éventuellement les résultats du régime non-coopératif avec ceux issus de la méthodologie d'un régime coopératif, la section suivante présentera les résultats induits par l'intégration de procédés de conversion dans un territoire à gouvernance non-coopérative pour le même plan d'investissement de 100 mois que celui pour l'étude précédente. Néanmoins, une analyse de sensibilité a été réalisée sur les stratégies d'investissement choisies dans le but d'évaluer leur impact sur le vainqueur des enchères et les états d'équilibre des transactions ainsi qu'une évaluation de l'effet des fluctuations du prix du marché du gaz sur les configurations de l'éco-parc qui en résultent (§ 4.5.3).

La première vente aux enchères est lancée avec le NI proposant les prix d'achat et de vente de la chaleur respectivement à 10% et 90% du prix du marché. La vente aux enchères se termine par IA_1 attribuant son W_1^{wood} au plus offrant qui était $PA_{1,1}$pour un montant de 85,35 € pour la tonne de bois. L'investisseur du système de conversion du bois en hydrogène est entré dans l'appel d'offres avec son $PA_{1,1,set\,10}$ qui présentait le plus haut potentiel d'enchères parmi ses sous-agents; il aurait pu augmenter son offre pour la tonne de bois jusqu'à son β_k de 193 €.

$PA_{1,1}$ a été confronté par un autre soumissionnaire qui est $PA_{1,2}$ avec son $PA_{1,2,set\ 5}$. Cependant, ce dernier n'a pas pu enchérir plus haut que l'agent vainqueur puisqu'il n'a pas pu augmenter l'offre finale de $0{,}1\beta_{k\ PA_{1,2,set\ 5}}$ équivaut à 8,68 € vu que ça surpasse le coût de la tonne de bois qui lui permet de rembourser son investissement en moins de 100 mois. Quant à la voie de cogénération qui est le troisième agent potentiel $PA_{1,3}$, elle n'entre même pas dans la vente aux enchères à cause de son potentiel d'enchères limité de 2,21 € pour la tonne de bois inférieure à le prix de réservation initial. Par la suite, le gagnant de l'enchère est ajouté aux acteurs industriels et prend part aux négociations pour les échanges de chaleur avec le NI; ainsi $PA_{1,1}$ devient IA_4.

Sur la base de la synthèse exergétique des échangeurs de chaleur territoriale réalisée par tierce-partie avec la liste actualisée des agents industriels, le NI établit ses premiers "Trade Message" spécifiques destiné à chaque IA. Les agents industriels évaluent alors leur TM et envoient un message d'offre au NI. Ceci est répété jusqu'à ce que des accords conjoints soient établis entre tous les agents du territoire définissant un état d'équilibre. Notant que la décision de participer ou non à un accord négocié est basée sur la rationalité de l'agent, car un agent cherchant son propre intérêt ne fera partie d'un accord que s'il obtient des gains plus élevés. À partir de l'état d'équilibre qui en résulte et des messages d'offre reçus, le NI augmente progressivement le prix d'achat ou diminue le prix de vente pour certaines températures de réseaux auxquelles l'agent industriel prévu n'a pas échangé tout son potentiel. Le NI prend cette action dans le but de motiver l'agent industriel à négocier de plus grandes quantités qui pourraient ainsi augmenter son propre bénéfice. Par conséquent, un nouvel état d'équilibre est déterminé pour chaque TM avec les offres modifiées.

Dix états d'équilibre distincts de configurations d'éco-parc ont étaient trouvés pour le territoire étudié. La VAN de chaque agent industriel est évaluée à 100 mois d'opération afin d'examiner la rentabilité de chaque état à la date de leur horizon d'investissement établi en fonction de leur statut économique lorsqu'ils agissent comme des agents isolés. Les graphes de Fig. 9 à la Fig. 13 illustrent les VAN pour les dix états d'équilibre du NI et des quatre agents industriels, le quatrième agent étant l'investisseur du procédé de conversion du bois en hydrogène.

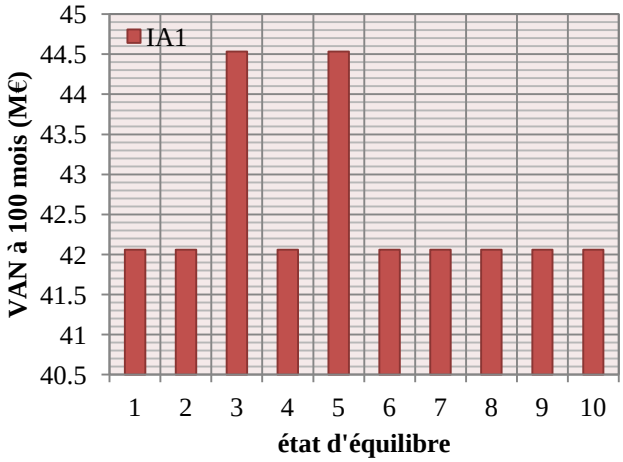


Fig. 9. VAN à 100 mois d'opération de IA_1

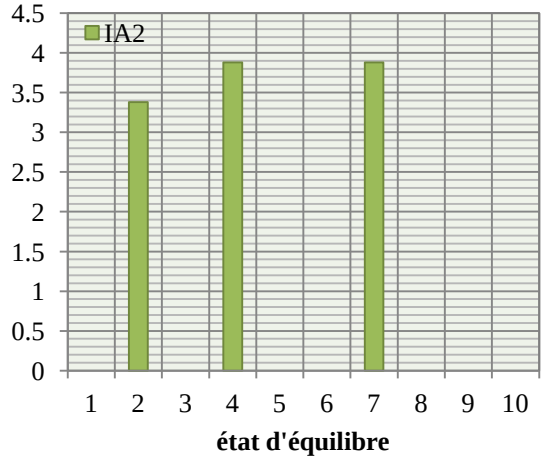


Fig. 10. VAN à 100 mois d'opération de IA_2

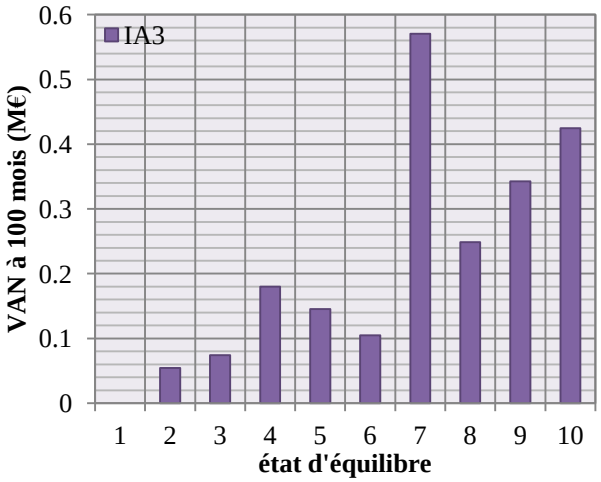


Fig. 11. VAN à 100 mois d'opération de IA_3

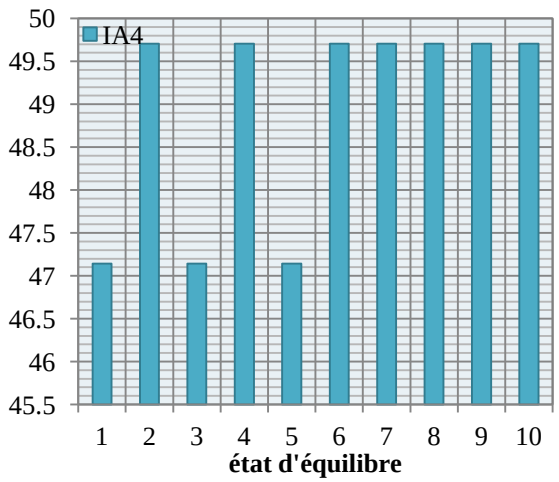


Fig. 12. VAN à 100 mois d'opération de IA_4

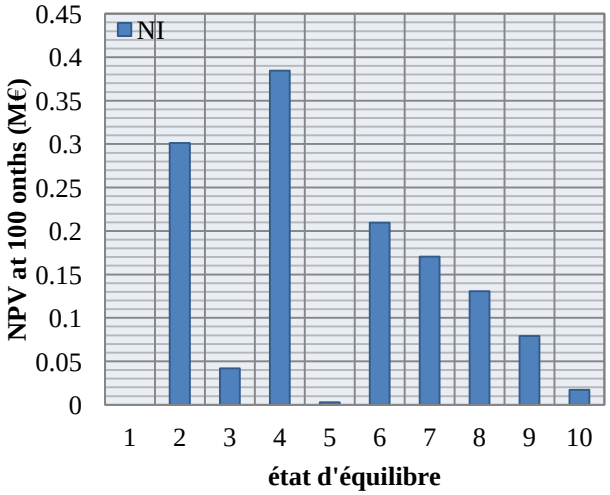


Fig. 13. VAN à 100 mois d'opération du NI

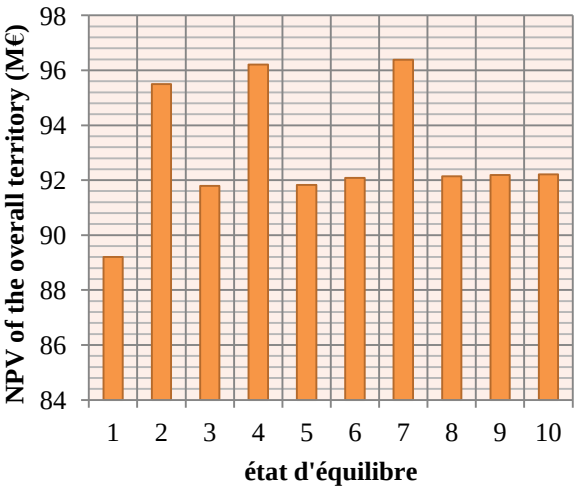


Fig. 14. Le *social welfare* des états d'équilibres

D'après les résultats ci-dessus, on peut noter l'absence de consensus pour un état d'équilibre. Alors que IA_1 trouve que l'état 3 est le plus lucratif, IA_2 génère ses plus hauts gains dans l'état 4. Là encore, pour IA_3, l'état 8 se manifeste comme étant son équilibre stable le plus rentable. Quant à IA_4 il n'a pas un seul favori mais en a plusieurs. Pourtant, le NI a un état préférable, c'est l'état 4.

Par conséquent, pour sélectionner une topologie de transactions pour laquelle tous les agents sont satisfaits de sa mise en œuvre, le critère du *social welfare* était utilisé. Ce dernier est évalué par l'agrégation de la VAN à 100 mois des quatre agents industriels ainsi que celle du NI pour chaque état d'équilibre correspondant puisque le *social welfare* est défini par la somme des gains associés à un accord donné. Comme on peut le voir sur la Fig. 14, les trois états ayant les meilleurs bien-être social sont ceux dans lesquels tout les agents sont impliqués dans une certaine synergie de matière ou de chaleur. De ces trois, l'état 7 induit le bien-être social le plus élevé. Néanmoins, cet état d'équilibre étant instable, du point de vue NI vu qu'il lui génère moins de profits que l'état 4, le deuxième meilleur choix est l'état 4 et, par conséquent, il est considéré comme l'état d'équilibre le plus adéquat à établir.

Il convient de souligner que les états stables ont été évalués en considérant le NI comme étant le seul investisseur de l'infrastructure des réseaux de transport qui achète et vend de la chaleur à travers son réseau construit. Cependant, lorsqu'il existe une concurrence pour l'achat et la vente d'énergie entre

plusieurs agents, le NI devrait évaluer le risque lié à la préférence d'un accord négocié par rapport à un autre qui pourrait influencer la décision de l'agent industriel concerné. Comme par exemple dans les états d'équilibre 4 et 7 où IA_3 préfère l'accord négocié dans l'état 7, tandis que le NI a des gains plus élevés de l'état 4. Par conséquent, avec plusieurs agents impliqués pour acheter la chaleur de IA_3, le NI a intérêt à établir l'accord dans l'état 7 même si c'est à moindre profit afin de s'assurer que IA_3 ne dévie pas vers vendre ses 10.42 MW à un autre acheteur de chaleur avec une meilleure proposition. Dans ce cas d'étude le NI est en effet le seul agent à prendre en charge l'achat et la vente de chaleur et donc l'état 4 est le plus susceptible d'être l'accord établi entre les agents industriels du territoire régi sous une gouvernance non-coopérative. La configuration de l'eco-parc industriel résultant de cet équilibre montre les transactions d'achat et de vente entre les agents du territoire, Fig. 15.

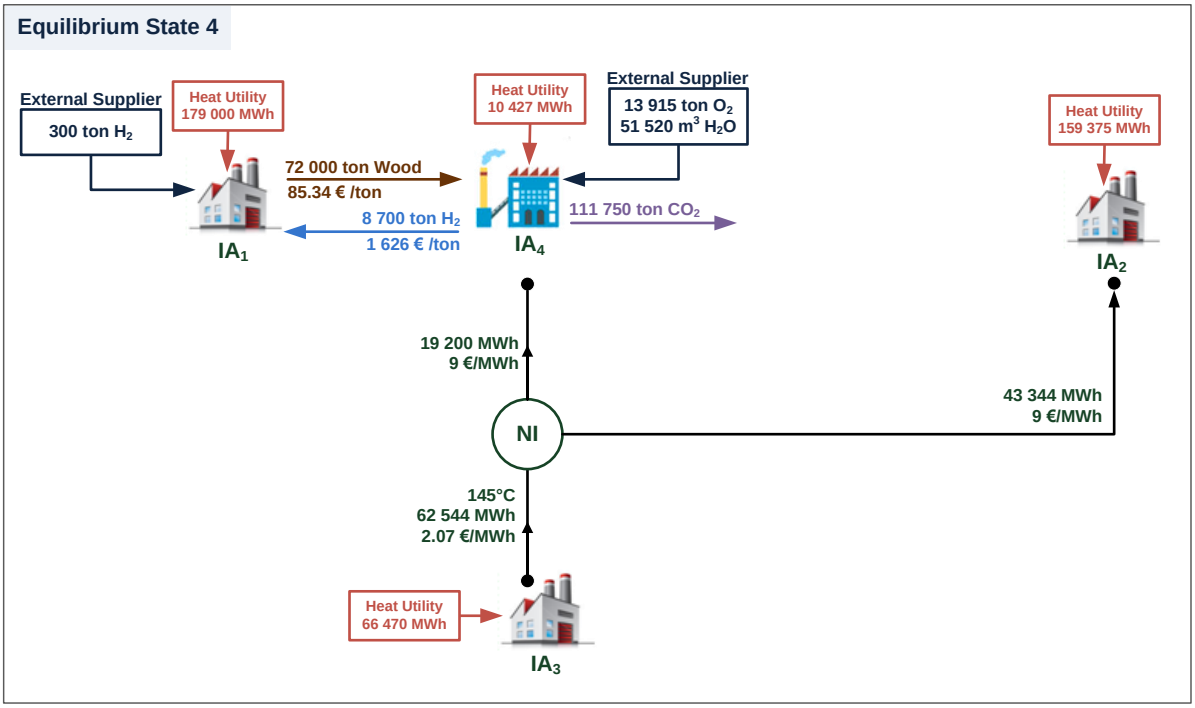


Fig. 15. Configuration de l'éco-parc pour l'état d'équilibre le plus adéquat du schéma non-coopératif

Remarquablement, la chaleur récupérée à travers le réseau est de 62 544 MWh par rapport à une capacité de 19 200 MWh dans le réseau coopératif. Les 43 344 MWh supplémentaires sont également récupérés auprès de IA_3 et vendus à IA_2 qui ne participait pas au réseau pour le modèle coopératif. Par la suite, le *social welfare* du territoire dans le régime non-coopératif de 96,21 M € est supérieur d'environ 4% à la VAN du territoire avec une gouvernance économique coopérative. La raison de ces résultats inattendus pourrait être liée à la méthode séquentielle utilisée dans le schéma coopératif pour concevoir les réseaux de chaleur locaux et territorial dans lesquels les deux problèmes sont itérés pour converger vers un modèle d'éco-parc qui pourrait être le résultat d'une configuration de synergie sous-optimale.

L'adjonction du système de conversion du bois a créé de nouvelles opportunités de synergies pour un territoire plus dynamique. IA_4 est la bio-raffinerie formée par la série des procédés permettant de passer du bois à l'hydrogène et ayant les valeurs de ses variables souveraines de la configuration numéro 10 étudiée. Un autre résultat important est que le système de conversion qui a été trouvé dans l'application du schéma coopératif comme étant le plus intéressant à mettre en œuvre dans le territoire étudié est le même qui a remporté l'enchère pour le bois et a participé aux négociations dans le schéma

non-coopératif. Ceci souligne à nouveau l'importance d'évaluer la demande du parc lors de la sélection des procédés de conversion à être examiner plus en profondeur.

En fait, même en répétant la vente aux enchères de bois avec des Trade Message améliorés comportant des plus bas prix de vente et des prix d'achat plus élevés, l'investisseur du système de conversion du bois en hydrogène remporte chaque fois le même sous-agent $PA_{1,\,1,\,set\,10}$. Notamment, pour les trois investisseurs de chaque voie de conversion, le sous-agent présentant le potentiel d'enchères le plus élevé possède le même ensemble de variables souveraines que CS_k^{wood} des scénarios les mieux jugés à l'issus des résultats coopératifs. Par conséquent, pour une meilleure efficacité de calcul, des sous-agents potentiels défavorables pourraient en effet être exclus sur la base de l'évaluation du parc régi d'une gouvernance coopérative.

À partir des résultats et de l'analyse des évaluations de sensibilité des stratégies d'investissement des agents et du prix du gaz, il été constaté que la conversion du bois en hydrogène est la voie la plus rentable pour investir dans sa mise en œuvre comparée aux deux autres voies étudiées. En effet, $CS_{1,\,set\,10}^{wood}$ résiste aux fluctuations du marché du gaz ainsi qu'aux modifications des plans de remboursement souhaitées par les investissements en conservant son premier rang pour le potentiel d'enchères le plus élevé. Par conséquent, il assure pour l'ensemble des états d'équilibre la conversion du bois en un produit de plus grande valeur et crée ainsi des synergies sans précédent dans le parc qui seraient autrement inaccessibles.

Il a également été noté que les synergies thermiques établies sur le territoire sont fortement impactées par l'objectif fixé pour le retour sur investissement le plus élevé possible dans la mesure où les stratégies d'investissement à court et moyen terme pourraient nuire aux opportunités d'échange de chaleur. La raison derrière cela est la petite période disponible pour le remboursement des investissements versés des échangeurs de chaleur pour les agents industriels ou des pipeline pour l'investisseur du réseau. D'autre part, le prix du marché du gaz joue un rôle majeur dans les prix d'achat et de vente offerts par l'investisseur du réseau NI. Par conséquent, les prix plus élevés du gaz entraînent plus de gains pour les agents industriels, ce qui leur permet d'échanger plus de chaleur augmentant ainsi la capacité du réseau.

Chapter 4

Application of the methodological frameworks for Conversion System integration in a territory

The foregoing chapter presented the case study which consists of an industrial park with three actors on which the demonstration of the proposed methodologies will be carried out. It was inferred from a preliminary assessment of the territory that untapped wood is discharged without any opportunity for recovery. The wood conversion routes to be potentially integrated in the territory were chosen subsequent to an overview of the main conversion categories of woody biomass. Each process unit of the selected conversion pathways was formulated in its physical and economic models.

This chapter focuses on applying the developed methodological frameworks for both cooperative and non-cooperative schemes on the aforementioned park using the developed models of the wood conversion systems. This is conducted in the aim of exhibiting how to implement conversion processes in a territory to reinsert streams judged to be non-recoverable by the conventional on-site and inter-site energy and material integration techniques.

First the reference establishment used for both schemes is carried out considering isolated industrial actors. The developed models in Chapter 3 are then employed to design the reactors of the conversion processes according to their capacity to intake the intended feed. Afterwards, the process flow sheets for the three wood conversion pathways are established to then determine the sovereign variables from the appraisal of the models design and operating parameters. The superstructure of the conversion pathways created from the alteration of the sovereign variables is employed to generate the potential scenarios of the territory with each wood conversion route as the bio-refinery to be implemented.

Subsequently, the computational framework for integrating conversion systems in a territory with cooperative scheme governance is launched. The resulting synergies configuration of the constructed scenarios are evaluated and compared economically in terms of their fixed and variable costs, to eventually pick out the best scenarios of every wood conversion route. Those are further assessed through sensitivity study on the wood waste value and the gas price fluctuations.

The non-cooperative scheme methodological framework is next conducted for the studied park with the conversion systems scenarios being the potential agents of the problem. The generated equilibrium states are explored to determine the best purchase and sale strategies according to each participating industrial agent. Finally sensitivity analysis of the gas price and the investment horizon are carried out to evaluate the impact of these parameters on the agents' strategies.

4.1. Economic data Hypotheses

The economic hypotheses concerning the commodities present in the territory should be set before initiating the methodologies demonstration. Considering the high purity of the produced methane from the conversion system, it is regarded as natural gas. The employed hydrogen price is that generated from a steam methane reformer being the commonly used technology. The ton of hydrogen average price produced from a conventional SMR is actually 1826 € (Mondal & Chandran, 2014) (Laveissiere, 2012). The hydrogen price is thus highly sensitive to methane price which is set by the natural gas market. From the developed relationship of Gray and Tomlinson (Gray & Tomlinson, 2002) between hydrogen and natural gas prices, Eq.(4.2) was deduced to get the values in the desired units; knowing that the high heating value (HHV) of hydrogen is 142.18 MJ/kg which is equivalent to 39.5 kWh/kg and the HHV of methane is considered to be 15.27 kWh/kg.

$$\text{HydrogenPrice } (€/\text{ton}) = 50.2 \times \text{GasPrice } (€/\text{MWh}) + 120 \tag{4.2}$$

The heating price is supposed to be the market price of a heat source produced from a steam generator fueled by natural gas. Subsequently, the heat price tangibly changes with the gas market and it is also supposed to alter according to the temperature at which it is required. The price of natural gas for an average size industrial consumer in the EU is of 34 €/MWh (eurostat, 2016) in the second half of 2015; this price exhibits regular variations by dint of the international market fluctuations. A reference value of 30 €/MWh will be thus considered for the study, while the results sensitivity on its fluctuations will be assessed in both governance schemes.

For a reference gas market price 'GasPrice_0' of 30 €/MWh, the heating cost per kWh is supposed to be at 0.01€ below 150°C and above 300°C the kWh of the heat utility costs 0.03€. Whilst in between these two heat levels, the price has an increasing linear function. Consequently, the heat price relationship in function of methane market price and temperature is expressed as in Eq.(4.3).

$$\text{HeatPrice } (\text{GasPrice}, T) = \left(\frac{\text{GasPrice}}{\text{GasPrice}_0}\right) \times \begin{cases} 0.01 & T<150°C \\ \frac{0.02}{150} \times T - 0.01 & 150<T<300 \\ 0.03 & T>300°C \end{cases} \tag{4.3}$$

The strong assumption intertwining the methane, hydrogen and heat prices entails their simultaneous variation. With the natural gas market fluctuation and to be consistent with the heat price will adopt the price of the reference gas price 'GasPrice_0'. The methane price is hence supposed to be at 30 €/MWh and the evaluation of Eq.(4.2) set the hydrogen ton price at 1626 €. Another worth noting hypothesis lies within the territorial energy integration problem, in which the network is supposed with a monthly discount rate of 0.003%. And unless mentioned otherwise, the investment horizon is fixed to 100 months for the local and territorial HEN synthesis. The heat exchangers investment is supposed to be formed by a fixed cost of 100965 € and a variable cost of 927.25 €/m^2.

4.2. Reference Scenario Establishment

The reference scenario that will be employed to evaluate both cooperative and non-cooperative results is considered as the case in which each industrial site of the territory acts as if it is not a part of the territory; meaning as an isolated actor. Consequently, each site conducts its local material and energy integration trying to establish on-site synergies between its process units to make the best out of its streams and reduce as much as possible its resources demand and heat requirements.

Every site in the park is supposed to have at disposal enough supply to satisfy its heating and cooling demands. Even though cooling utilities are supposed cost free by dint of the relatively high temperatures of the cooling needs compared to the neighboring environment, the heat utilities come at a cost fixed at the heating market price and which is correlated with their temperature level.

Site 1 of the industrial park needs approximately 105 MW of heating utilities to cover its entire heat load demand (cf. § 3.1). With a hot utility at 300°C, the annual operating cost of this industrial site entailing from its energy requirements adds up roughly to 19 M€. However by locally integrating its energy streams, 75 MW in total are recovered through the installation of 19.5M€ worth of heat exchangers and which enable the heat transfer from a stream that needs to be cooled to another that should be heated. This outcome could be perceived by the HEN configuration of Site 1 in Figure 4.1. Each couple of dots connected by a straight line depicts a heat exchanger between a heat source (the blue dot) and a heat sink (the red dot on which the heat capacity is noted).

Site 1 processes also consume 9000 ton of hydrogen per year, which induces approximately 15 M€ of operating expenses. Notably, the hydrogen consumption of Site 1 forms three-fourth of its total variable cost while heat only takes up one-fourth. The wood it discharges has no value and is neither valorized nor recovered. There is no opportunity for mass integration owing to the material difference.

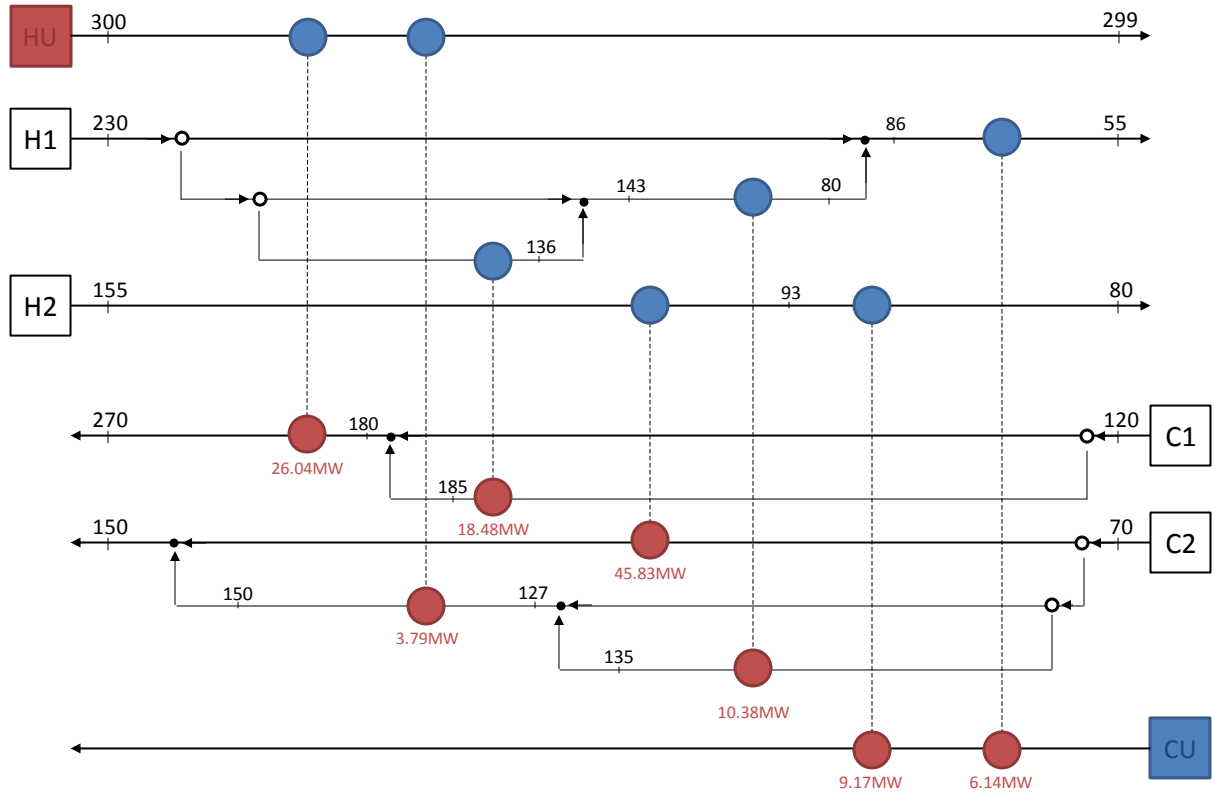


Figure 4.1. HEN of Site 1 as an isolated industrial actor

On the other hand, for Site 2 the streams to be heated require an aggregate heat load of 130 MW that is equivalent to an annual operating cost of 23.4 M€. Acting as an isolated industrial plant, Site 2 searches to decrease its charges via synergies establishment. The resulting HEN synthesis of Site 2 induced from its local integration problem resolution is illustrated in Figure 4.2, wherein HU and CU designate the used hot and cold utilities respectively. The installed heat exchangers lead to the recuperation of 97 MW of thermal potential and redistribute it internally, making up grossly 75% decrease in the hot utility uptake for an overall investment of 15.64M€.

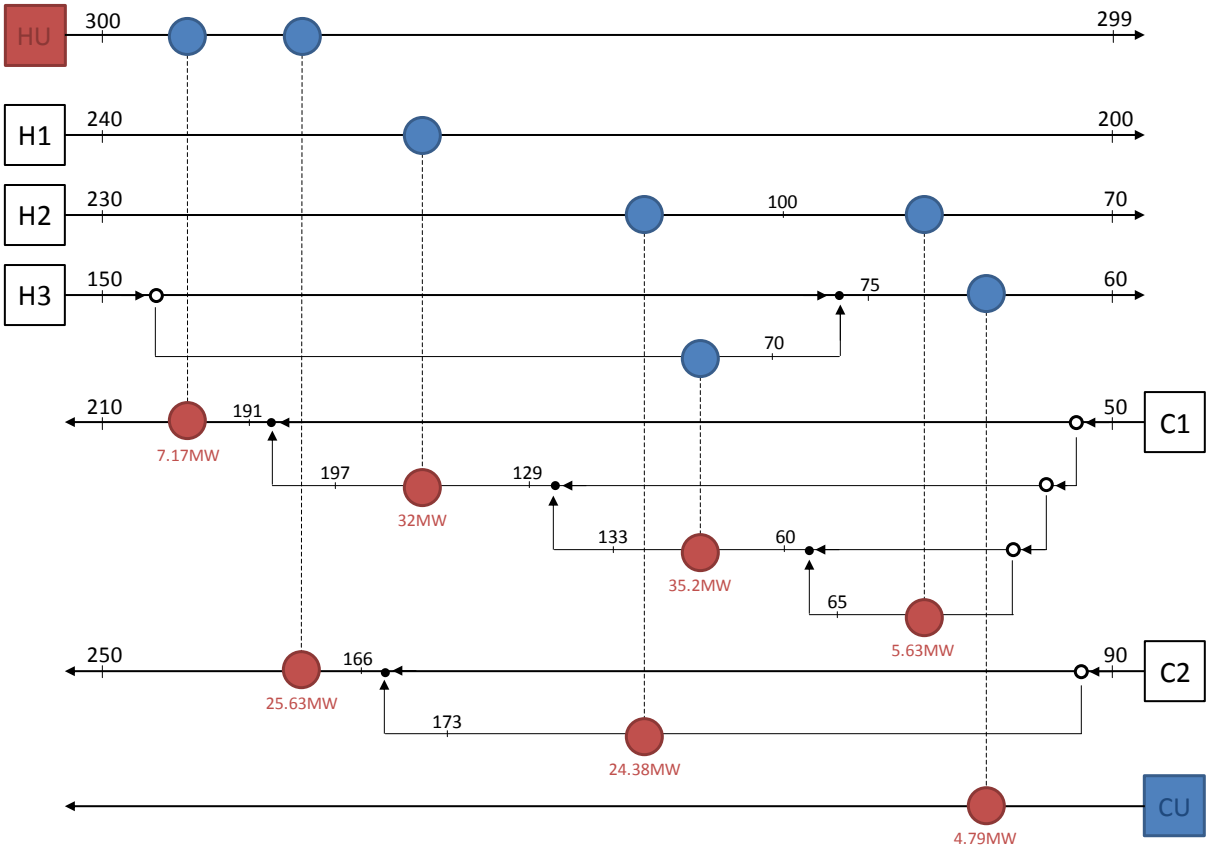


Figure 4.2. HEN of Site 2 as an isolated industrial actor

The third plant of the territory requires a heat subtotal of 43 MW when no integration is performed. However, this is reduced to 11 MW by dint of the established heat synergies through the local HEN synthesis of Site 3, cutting down its annual operating costs from 5.75 to 2 M€. As represented in Figure 4.3, five heat exchangers were installed generating an investment cost of 9.58 M€. Noting that the minimum temperature difference is set to 20 K for the heat exchangers design.

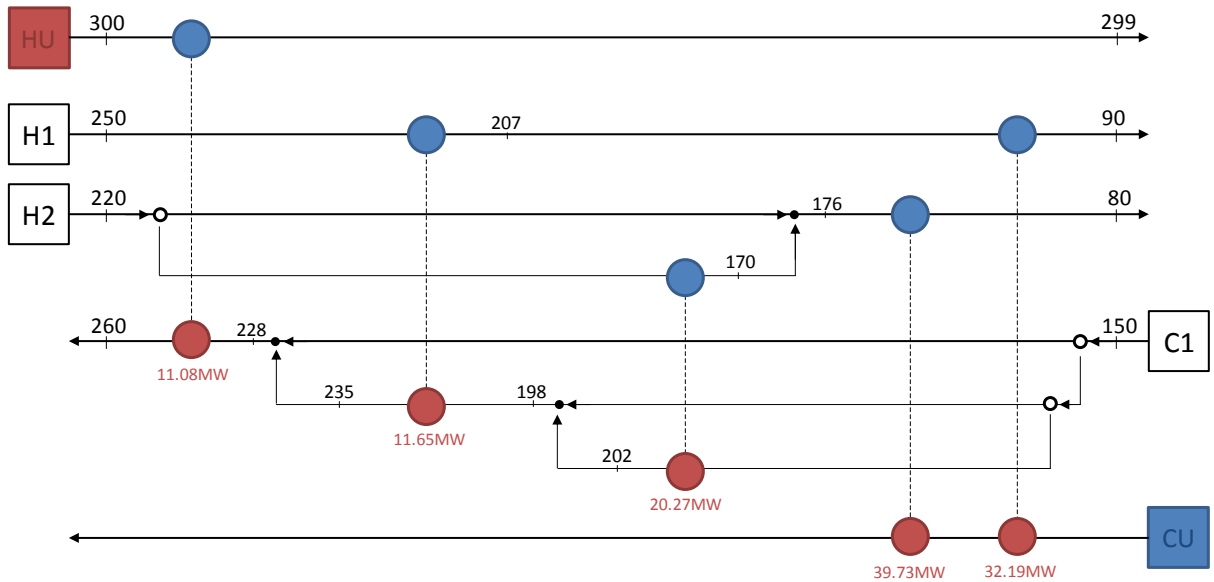


Figure 4.3. HEN of Site 3 as an isolated industrial actor

The economic statuses of the industrial actors of the studied territory when implemented as isolated agents are summarized in Table 4.1. These are employed as being the reference scenarios for comparing the resulting outcome of the methodologies in cooperative and non-cooperative schemes.

Table 4.1. Economic status of the territory's sites as isolated actors

Industrial actor	Fixed Cost (M€)	Variable Cost (M€)
Site 1	19.49	20.00
Site 2	15.59	5.90
Site 3	9.58	2.00

4.3. Conversion routes design and process degree of freedom

The potential conversion processes that make up the bio-refinery to be implemented in the territory for converting the untapped wood discharge into another form of desired commodity were investigated in Chapter 3. Three routes of conversion were judged convenient to assess and put in competition based on the studied territory requirements. Those pathways are the hydrogen production from wood, the wood conversion to methane and the third is the cogeneration pathway. For the three favored wood conversion systems, the process units should be first sized to intake the entire quantity of woody biomass. This is achieved through the process scale-up mechanism detailed in § 3.6 in which the denoted 'old' variables are based on the literature work employed to validate the developed process units. Afterwards their process flow sheet must be established to extract the energy and material streams that will serve as the inputs for the integration problems. A unified hot utility source at 900 °C is available for the cost per kWh of 0.03€ for the bio-refinery no matter what conversion route is implemented. Parenthetically, the prospective position of the wood conversion plant relative to the territory's existing industrial sites is illustrated in Figure 4.4. The selected placement will greatly impact the territorial integration outcome since the networks investments are directly proportional to the distance of the required pipeline to transfer energy or allocate materials from one site to another.

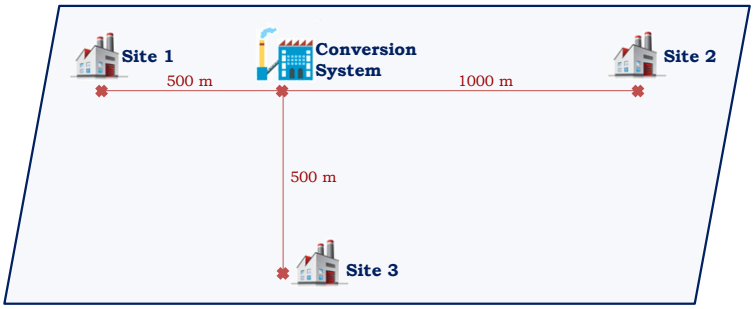


Figure 4.4. Bio-refinery placement relative to the existing industrial actors

The degree of freedom of each route is then identified based on the number of potentially manipulated systems' parameters which form the sovereign variables of the problem. Through the alteration of these variables several sets of process configurations can be established. In the proposed methodological framework of a territory with cooperative scheme, these sets are employed to generate the prospective scenarios of the territory to be analyzed. However in the non-cooperative scheme, the different sets of parameters configurations are used by the Potential Agents to generate their sub-agents. Consequently the current section explores the aforementioned aspects prior to probing the resulting outcomes from the methodologies application later in this chapter.

4.3.1. Wood to hydrogen conversion route

4.3.1.1. Conversion System design to intake intended feed

The first studied valorisation pathway of the 12 t/hr wood waste discharged from the investigated park is its conversion to hydrogen since the territory presents the need for this commodity. As illustrated in Figure 4.5 which represents the process flow sheet of this conversion route, the waste wood to be valorised is first gasified with steam at a variable steam to biomass ratio (SB_{ratio}). This variable steam flow rate generates a changing heat load demand for heating up the gasifying water from 25 to 457°C at which the first pyrolysis reaction takes place. The exiting gaseous mixture from the gasifier is mixed with water to raise the water to carbon ratio and prevent carbon deposit in the downstream units. Then this flow is sent to the steam methane reformer (SMR) where the tar is converted to hydrogen and carbon monoxide. Before entering the water gas-shift membrane reactor the flow temperature is reduced in the aim of maintaining the catalyst activity. For that purpose, it is supposed that the feed temperature of the WGS reactor $T_{WGSinput}$ does not exceed 450 °C and that its outlet temperature $T_{WGSoutput}$ to be limited by an upper bound fixed at 560 °C. The hydrogen is sucked by a vacuum pump through the selective H_2 membrane, hence yielding to a high purity hydrogen stream. The remaining gas mixture is burned in a combustion chamber with pure oxygen in order to limit the flue gases mixture to carbon dioxide and steam. The exiting temperature of the combustion chamber should not surpass 1300 °C for technology reasons. Finally, the flue gas are cooled down and then sent through a separation unit to get recovered water from one side and captured carbon dioxide from the other.

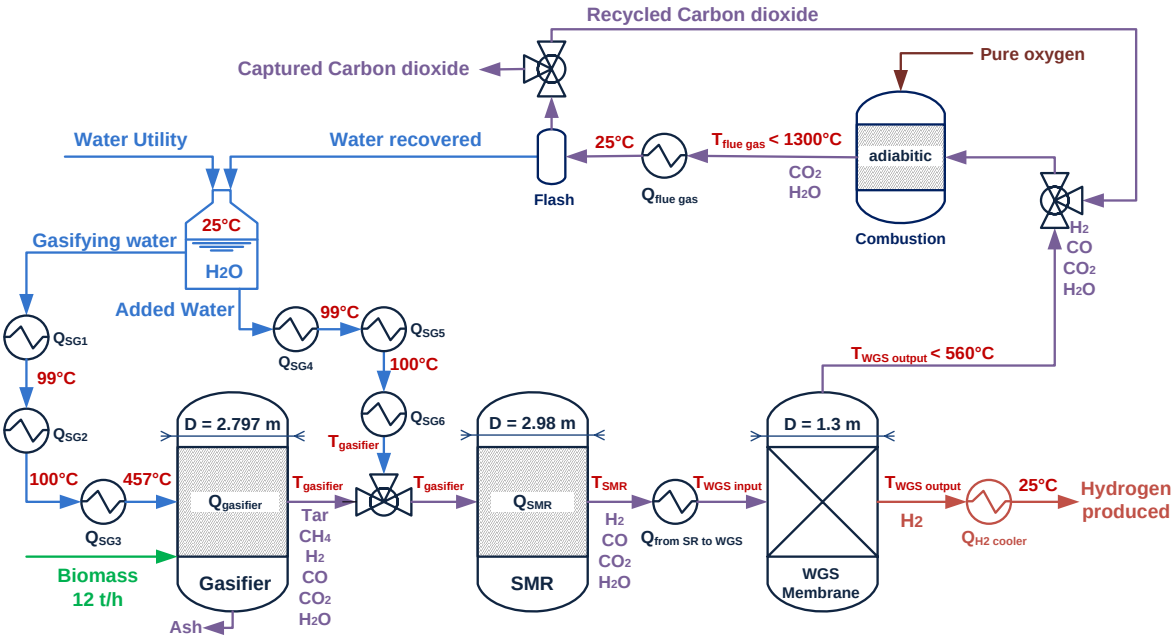


Figure 4.5. Wood to hydrogen conversion process flow sheet

The scale-up of the process reactors to intake the whole intended quantity of the woody biomass entailed the length and diameter computation for the desired reactors capacities. The diameters D of the reactors are indicated on the flow sheet. The gasifier has a total length of 26.11 m with the freeboard making up roughly 71% of it, whereas the SMR and the WGS reactors extend over 18.65 m. The hydrogen selective membrane has a surface area of 810.8 m^2. Remarkably, if the units are positioned parallel to each other, the bio-refinery could spread on nearly a 30x10 m^2 field area.

The heat exchangers depicted in the flow sheet are designed in the local energy integration problem of the wood to hydrogen conversion system; they are illustrated to indicate the presence of heating and cooling requirements. Actually, the process flow sheet allows the extraction of the circulating energy streams to be employed for the HEN synthesis. Seven cold streams and four hot streams are identified by their inlet and outlet temperatures as well as their heat load and are listed in Table 4.2, wherein the notation used is in reference to the above process flow sheet. For every water flow, the stream is partitioned into three in order to account for the latent heat that should be supplied to the water mixture for it to transform into steam. This is mandatory by dint of the temperature vs. enthalpy tendency difference between the steam generator providing the sensible heat for water to its liquid saturation point (Steam Generator 1, Steam Generator 4) or for superheated steam (Steam Generator 3, Steam Generator6) that has linear variations, and that in the generators heating the liquid-vapor mixture from its liquid to its vapor saturation point (Steam Generator 2, Steam Generator 5).

Table 4.2. Heat streams data of the wood to hydrogen conversion system

Stream name	T_{in} (°C)	T_{out} (°C)	Q (MW)
Cold Process Heat Stream			
Steam Generator 1	25	99.9	Q_{SG1}
Steam Generator 2	99.9	100	Q_{SG2}
Steam Generator 3	100	457	Q_{SG3}
Gasifier	457	$T_{gasifier}$	$Q_{gasifier}$
Steam Generator 4	25	99.9	Q_{SG4}
Steam Generator 5	99.9	100	Q_{SG5}
Steam Generator 6	99.9	$T_{gasifier}$	Q_{SG6}
Hot Process Heat Stream			
Seam reformer	$T_{gasifier}$	T_{SMR}	Q_{SMR}
SR to WGS	T_{SMR}	$T_{WGS\ input}$ **<450**	$Q_{from\ SR\ to\ WGS}$
WGS output H2	$T_{WGS\ output}$ **< 560**	25	$Q_{H2\ cooler}$
Condenser	$T_{flue\ gases}$ **<1300**	25	$Q_{flue\ gas}$

4.3.1.2. Sovereign variables of the wood to hydrogen conversion system

From the previously described hydrogen production system, the degree of freedom of this conversion route is found to be equal to three in accordance with the number of workable parameters. Those are the steam to biomass ratio SB_{ratio}, the gasifier output temperature $T_{gasifier}$ and that of the steam methane reformer T_{SMR}. These parameters form the set of sovereign variables SV_1^{wood} of the first wood conversion system CS_1^{wood}. Therefore, a lower and upper bounds should be established for each variable, namely: SV_1^{wood}={(SB_{ratio},0.5,1.5), ($T_{gasifier}$,650,850), (T_{SMR},650,850)}.

However in order to control the constrained temperatures with the variation of the sovereign variables, two parameters are changed depending upon the selected operating conditions. Actually a recycling possibility is added to the combustion chamber (see Figure 4.5), where a percentage of the recovered carbon dioxide is reintroduced in the combustor in order to dilute the flow and decrease the flue gas temperature so it does not exceed the allowable temperature limit. Therefore, the recycling percentage is one of the two manipulated parameters, whereas the other one is the WGS input temperature $T_{WGS\ input}$. Consequently, eighteen sets of parameters are generated by altering the SB_{ratio}, $T_{gasifier}$ and T_{SMR} considering a discontinuous step between the temperature intervals of 100°C and a 0.5 variation pace for the SB_{ratio}. Table 4.3 lists the opted values for the sovereign variables in each set.

Table 4.3. The generated sets of parameters for the hydrogen route

set q	SB_{ratio}	$T_{gasifier}$ (°C)	T_{SMR} (°C)	CO_2 recycling %
set 1	1	750	750	0
set 2	0.5	750	750	0
set 3	1.5	750	750	0
set 4	1	850	750	0
set 5	1	650	750	55
set 6	0.5	850	750	0
set 7	0.5	650	750	50
set 8	1.5	850	750	0
set 9	1.5	650	750	55
set 10	0.5	850	850	0
set 11	1	850	850	0
set 12	1.5	850	850	0
set 13	0.5	650	650	50
set 14	1	650	650	55
set 15	1.5	650	650	55
set 16	0.5	650	850	42
set 17	1	650	850	47
set 18	1.5	650	850	50

4.3.2. Wood to methane conversion route

4.3.2.1. Conversion System design to intake intended feed

The second option for the wood reinsertion in the territory is to convert it into methane since this could be sold to the gas network supposed to be passing through the park. The process flow sheet in Figure 4.6 displays the relationships and circulating flows between the wood to methane main process units which were modeled in the previous chapter. First in this facility, the biomass feedstock is sent to the steam gasifier with a steam to biomass ratio SB_{ratio} that plays a major role in the reactions progress rates. The exiting gas from the gasifier at $T_{gasifier}$ are cleaned from the tar residue and cooled down to the temperature T_{meth}. This latter must be in the range of 200°C to 400°C in order to ensure the appropriate operation of the catalyst in the isothermal methanation unit.

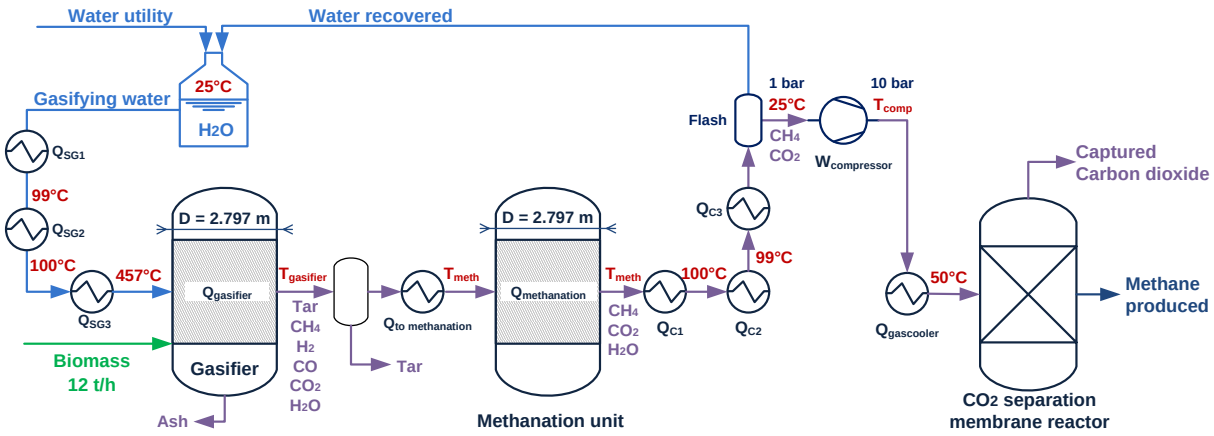


Figure 4.6. Wood to methane conversion process flow sheet

Being highly exothermal, the methanation reactions introduce great synergy opportunities for their released heat in the territory seeing that it matches the heat deficit temperature level in the park. Right after the methanation, a series of heat exchangers are required to cool down the process flow: the first serves for decreasing the stream temperature to the water vapor saturation, then another captures the released latent heat and the third heat exchanger leads to lowering the temperature from the liquid saturation point to 25°C. The condensed water is then collected to compensate a part of the gasifier water demand. This material synergy is readily conspicuous with the singularity of the water sinks and source qualities. At this stage of the process, the gas flow is highly concentrated in methane and carbon dioxide, the remaining step for obtaining a rich-methane stream is hence to eliminate the CO_2. The gas flow is thus compressed to 10 bar then cooled to 50°C prior to entering the separator unit. The latter consists of a permeable membrane through which CO_2 is diffused and then sequestered. Consequently, the rich-methane gas is retrieved from the other channel of the separation unit.

From the assessment of the process flow sheet of the wood to methane conversion system, the energy and material streams details can be extracted. For the energy requirements of this conversion route, four cold streams that need to be heated and six hot streams presenting heat surplus can be identified. The inlet and outlet temperatures and heat load of these streams are listed in Table 4.4. Despite the substantially released heat from the methanation process, the methane from wood pathway is not auto-sufficient in terms of energy by dint of the heat deficit of the gasifier at $T_{gasifier}$ which is greater than the heat excess of the process at T_{meth}. Regarding the material flows, this process has a methane source created from the wood and water sinks that it intakes. Internal water integration is conducted as previously mentioned to reduce the water consumption of the conversion system.

Table 4.4. Heat streams data of the wood to methane conversion system

Stream name	T_{in} (°C)	T_{out} (°C)	Q (MW)
Cold Process Heat Stream			
Steam Generator 1	25	99.9	Q_{SG1}
Steam Generator 2	99.9	100	Q_{SG2}
Steam Generator 3	100	457	Q_{SG3}
Gasifier	457	$T_{gasifier}$	$Q_{gasifier}$
Hot Process Heat Stream			
To methanation	$T_{gasifier}$	T_{meth}	$Q_{to\ methanation}$
Methanation	T_{meth}	T_{meth}	$Q_{methanation}$
Cooler 1	T_{meth}	100	Q_{C1}
Cooler 2	100	99.9	Q_{C2}
Cooler 3	99.9	25	Q_{C3}
Gas Cooler	T_{comp}	50	$Q_{gas\ cooler}$

With a view to evaluate the investment costs of the wood to methane process units in accordance with the system's capacity, the reactors are sized to be capable of processing the entire quantity of the indented feed of woody biomass. The gasifier has the same design as in the previously described conversion pathway, since the feed amount is identical. As for the methanation unit, its scale-up induces a 27.97 m long reactor of a 2.79 m diameter. However, large scale exothermal processes are prone to thermal runaway. This could be controlled by enhancing the cooling rate of the methanation unit. The reactor could for instance be built by a stack of axial tubes of five centimeters in diameter to fill the entire vessel volume to reinforce the circulation of the heat-transfer fluid and thus prevent vicious thermal explosion. Yet, this aspect investigation transcends the scope of this thesis.

4.3.2.2. Sovereign variables of the wood to methane conversion system

From the examination of the formulated models and the established flow sheet of the wood to methane process units, the governing parameters of the yielding amount of methane and hence the system's degree of freedom are reckoned at three. The first being the flow rate of the gasifying agent which is implicitly represented in the steam to biomass ratio SB_{ratio} since the wood flow rate is fixed to the intended treated stream value. It is supposed that this parameter can take the values of 0.5,1 and 1.5 in the aim of limiting the computation time for the entire problem resolution. The gasifier operating temperature $T_{gasifier}$ is adopted as the second changeable parameter, knowing that it highly impacts the gasifier produced gas composition and therefore the methane yield. As for the hydrogen production route, $T_{gasifier}$ is bounded by a lower and an upper limit of 650 °C and 850 °C respectively. The last parameter is the methanation unit temperature T_{meth} which is constrained by the catalyst operating temperature.

The set of sovereign variables SV_2^{wood} of the second wood conversion pathway CS_2^{wood} is defined by these parameters, namely: $SV_2^{wood}=\{(SB_{ratio},0.5,1.5), (T_{gasifier},650,850), (T_{meth},200,400)\}$. The sovereign variables alteration of the methane conversion route begets twenty seven sets of parameters with sporadic values selected amidst their established limits; those are listed in Table 4.5.

Table 4.5. The generated sets of parameters for the methane route

set q	SB_{ratio}	$T_{gasifier}$ (°C)	T_{meth} (°C)
set 1	0.5	650	200
set 2	1	650	200
set 3	1.5	650	200
set 4	0.5	650	300
set 5	1	650	300
set 6	1.5	650	300
set 7	0.5	650	400
set 8	1	650	400
set 9	1.5	650	400
set 10	0.5	750	200
set 11	1	750	200
set 12	1.5	750	200
set 13	0.5	750	300
set 14	1	750	300
set 15	1.5	750	300
set 16	0.5	750	400
set 17	1	750	400
set 18	1.5	750	400
set 19	0.5	850	200
set 20	1	850	200
set 21	1.5	850	200
set 22	0.5	850	300
set 23	1	850	300
set 24	1.5	850	300
set 25	0.5	850	400
set 26	1	850	400
set 27	1.5	850	400

4.3.3. Wood to energy conversion route

4.3.3.1. Conversion System design to intake intended feed

The third investigated conversion pathway is the production of electricity and heat from wood. First the biomass goes through an adiabatic combustion chamber with 90% excess air yielding flue gas at 1363°C which are then cooled down to 300°C. The theoretical air required to complete the 12 t/hr biomass combustion is roughly 72.5 mol/s. The 53 MW released heat from the wood combustion feeds a cogeneration cycle generating steam at two pressure levels and producing electricity by dint of an installed turbine in the midst of these levels which are characterized by their saturation temperatures $T_{out\ high}$ and $T_{out\ low}$. The steam cycle requires pumping power W_{pump}, its net electricity production is therefore the difference between the produced turbine power W_{elec} and W_{pump}. This steam cycle can actually operates in two modes: either only generating steam or producing heat and electricity. This is achieved by twiddling the fraction x that acts on the flow rate of steam going in each path. When closing the valve from the turbine side, x is set to 1. The entire steam flow will go through the heat path and thus recovering the released combustion heat as a steam flow at $T_{out\ high}$. When x is zero, no flow is able cross the high temperature condenser and the entire flow is directed towards the turbine. The inlet temperatures of this latter is typically around 565°C thus $T_{in\ high}$ is set to be at most 500°C.

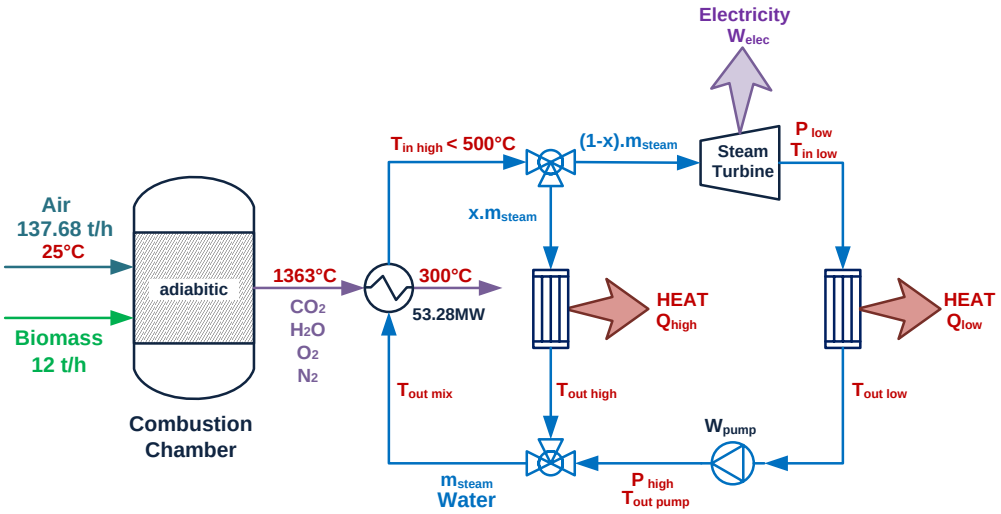


Figure 4.7. Wood cogeneration process flow sheet

From the flow sheet of the wood cogeneration depicted in Figure 4.7, two main heat streams are identified. The energy generated from each of these streams is divided into two: the sensible and the latent heat; thus entailing four hot process streams. With only released heat from the system, this conversion pathway is a heat supplier and might as well in some scenarios produce electricity.

Table 4.6. Heat streams data of the wood to electricity and heat conversion system

Stream name	T_{in} (°C)	T_{out} (°C)	Q (MW)
Hot Process Heat Stream			
Condenser $high_{sensible}$	$T_{in\ high}$ < **500**	$T_{out\ high}$ + 0.5	$Q_{high\ sensible}$
Condenser $high_{latent}$	$T_{out\ high}$ + 0.5	$T_{out\ high}$	$Q_{high\ latent}$
Condenser $low_{sensible}$	$T_{in\ low}$	$T_{out\ low}$ + 0.5	$Q_{low\ sensible}$
Condenser low_{latent}	$T_{out\ low}$ + 0.5	$T_{out\ low}$	$Q_{low\ latent}$

4.3.3.2. Sovereign variables of the wood to energy conversion system

The yield of the woody biomass into heat and electricity conversion pathway is governed by the high and the low condensers temperatures ($T_{out\ high}$ and $T_{out\ low}$ respectively) as well as the fraction x of the flow rate going through the heat path. Consequently, the degree of freedom of this path is set to three since this consists of the number of the system's highly influencer parameters. The set of sovereign variables SV_3^{wood} of the third wood conversion route CS_3^{wood} is made up by these parameters. The temperatures variation ranges are selected based on the territory's heat requirements with a view to raise the integration opportunities for this pathway. As for the flow fraction, it must have a positive value that does not exceed the unit; hence: $SV_3^{wood}=\{(T_{out\ high}, 280, 300), (T_{out\ low}, 150, 200), (x, 0, 1)\}$.

Twenty one sets of parameters are established for the wood cogeneration system, having their sovereign variables established from their allowable value ranges as in Table 4.7. Following the adjustment of the sovereign variables to values meeting the permissible domain, the steam mass flow rate is tuned in the aim of controlling the turbine inlet temperature $T_{in\ high}$ such that it does not protrude the technical temperature bound of 500°C.

Table 4.7. The generated sets of parameters for the cogeneration route

set q	$T_{out\ high}$ (°C)	$T_{out\ low}$ (°C)	x (heat path fraction)	m_{steam} (kg/s)
set 1	300	-	1	26.2
set 2	290	-	1	25.3
set 3	280	-	1	24.6
set 4	300	200	0	21.2
set 5	300	180	0	20.5
set 6	300	150	0	19.5
set 7	290	200	0	21
set 8	290	180	0	20.3
set 9	290	150	0	19.4
set 10	280	200	0	21
set 11	280	180	0	20.2
set 12	280	150	0	19.3
set 13	300	200	0.5	23.5
set 14	300	180	0.5	23
set 15	300	150	0.5	22.3
set 16	290	200	0.5	23
set 17	290	180	0.5	22.5
set 18	290	150	0.5	22
set 19	280	200	0.5	22.6
set 20	280	180	0.5	22.2
set 21	280	150	0.5	21.6

The objective being to explore the proposed methodological frameworks which enable the park's synergy design, the three wood conversion routes explored in this section will be individually integrated in the studied territory for the different established sets of sovereign variables in cooperative scheme governance. Their economic effect on the territory will be investigated and then the pathways will be challenged to examine which of them will stand out. With non-cooperative actors, the conversion pathways will be challenged as being separate entities with individual interests in the aim of determining the best purchase and sale strategies of each industrial participant of the territory.

4.4. CS integration in a territory with cooperative scheme

4.4.1. Problem Statement

The investigated park is formed by three industrial actors willing to collaborate in the search of enhancing the circular economy of the territory to decrease the overall resources consumption and waste discharge. They thus exchange their energy and material streams without any incentives while sharing the investment expenses required for implementing the identified synergies. Consequently, the problem is formulated for a cooperative territory using the attributed methodological framework.

The participating industrial actors of the park form the set Territory = $\{Site_1, Site_2, Site_3\}$. The geographic coordinates of every $Site_i$ in the set Territory are respectively: C_1= (0; 0), C_2= (1500; 0) and C_3= (500;-500). Their energy stream lists E_i are formed by their individual heat streams (cf. § 3.1):

E_1={(230, 55, 35) ; (155, 80, 55) ; (120, 270, 44.5) ; (70, 150, 60)}
E_2={(240, 200, 30) ; (230, 70, 30) ; (150, 60, 40) ; (50, 210, 80) ; (90, 250, 50)}
E_3={(250, 90, 44) ; (220, 80, 60) ; (150, 260, 43)}

Heating and cooling utilities are appropriate for every $Site_i$, however they are similar for the three actors, hence U_1=U_2=U_3. For material data, $Site_1$ is the single actor with material inputs and output. It presents hydrogen demand and discharges woody biomass, therefore M_1={(1.5 t/hr)^{H_2}} and O_1={(12 t/hr)^{wood}}. The preliminary energy and material integration assessments of the park showed that due to the absence of wood material demand, the discharged O_1^{wood} exhibits limiting recovery opportunities in its wood form. Consequently, it is identified as the waste stream of the territory originating from $Site_1$ and is referred to as W_1^{wood}. Nonetheless, its thermodynamic conversion into hydrogen, methane or electricity and heat boost the park's circular economy by creating new potential valorization for W_1^{wood}. The set of the studied conversion systems CS is formed by the three pathways leading to the production of the aforementioned commodities: CS = $\{CS_1^{wood}, CS_2^{wood}, CS_3^{wood}\}$. Their previously established sovereign variables SV = $\{SV_1^{wood}, SV_2^{wood}, SV_3^{wood}\}$ together with the CS set form the Master problem superstructure of the conversion pathways illustrated in Figure 4.8.

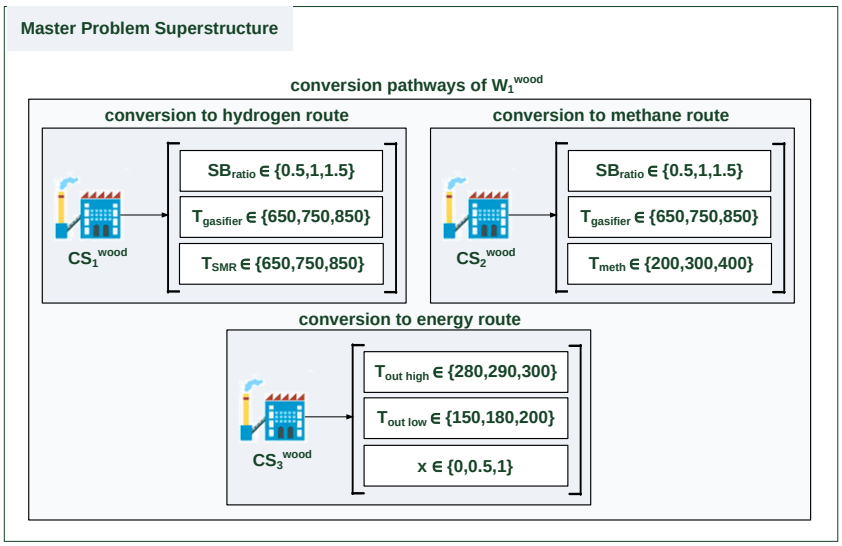


Figure 4.8. Superstructure of W_1^{wood} conversion pathways

This superstructure is employed to generate the prospect scenarios of the territory by appending in each scenario a wood conversion route from CS with a corresponding set q of SV; thereby, a new industrial actor $CS^{wood}_{k,\,set\,q}$ that will alter the form of the non-usable stream is added to the park and the Territory set becomes $\{Site_1, Site_2, Site_3, CS^{wood}_{k,\,set\,q}\}$. The new $Site_4$ is supposed to be placed 500 m to the right of $Site_1$ as depicted in Figure 4.4; its coordinates are thus C_4= (500; 0).

When CS^{wood}_1 is the bio-refinery to be implemented, the W^{wood}_1 are recovered to create a hydrogen source for the territory. The q^{th} scenario of such case is referred to as Scenario H-q. Every scenario in which CS^{wood}_2 intakes the wood waste to convert it into methane is denoted by Scenario M-q. Yet, Scenario C-q is utilized in order to refer to a scenario in which wood cogeneration is the appended industrial actor. Figure 4.9 shows a sample of Territory prospective scenarios.

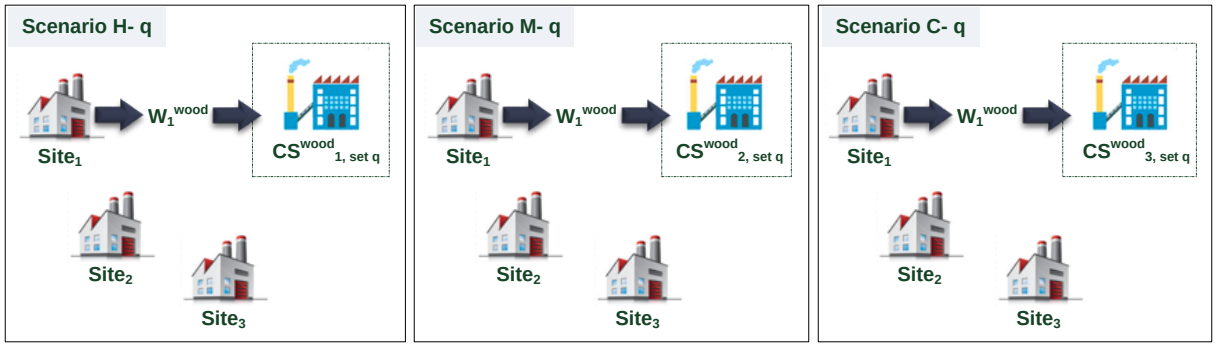


Figure 4.9. Sample of the territory's prospective generated scenarios

The generated outcome of the computational framework for integrating conversion systems in a territory with cooperative scheme are expressed by the fixed and variable costs induced after establishing the optimal material and energy exchanges amongst Territory's elements. The economic statuses for every conversion pathway scenarios are discussed individually, to assess the sovereign variables impact on the established synergies. The scenarios generating the highest enhancement of the territory's streams management compared to the reference case are identified to further investigate the effect of the gas market price fluctuations and their sensitivity on the waste W^{wood}_1 value.

4.4.2. Results of CS^{wood}_1 implementation in the territory

Without any opportunities for reuse or recovery in its initial form, the woody biomass having no monetary value is sent to a bio-refinery formed by CS^{wood}_1 processes. In cooperative governance, the hydrogen yield from this wood conversion system is allocated for no charges to the hydrogen sink of the park which is $Site_1$. This material synergy reduces the territory's resource consumption leading to its operating costs cut down. Moreover in some scenarios, CS^{wood}_1 generates heat surplus that could be recovered by the network to be then redistributed to the deficit industrial sites, thus decreasing the park's heat utility demand. Nonetheless, investment expenses arise from the conversion system units' costs. Therefore, the scenarios' economic assessment must account for both fixed and variable costs. The former consists of the investment of the energy and hydrogen transport networks, that of the heat exchangers and the bio-refinery implementation; while the latter is induced from the heat utilities, the water and oxygen required by CS^{wood}_1 and also from the rest of the hydrogen demand imported from an external supplier to maintain the park's operation. The sequestered CO_2 in the conversion process enables avoiding the CO_2 levies which is deduced from the variable cost of the territory.

The resulting economic status of the territory for the optimally computed EIP configurations of the eighteen scenarios in which CS_1^{wood} is integrated are presented in Figure 4.10 by the total fixed and annual variable costs of the park. The undermost curve is formed by connecting Scenario H-10, Scenario H-18 and Scenario H-13; the whole above scenarios are hence less interesting.

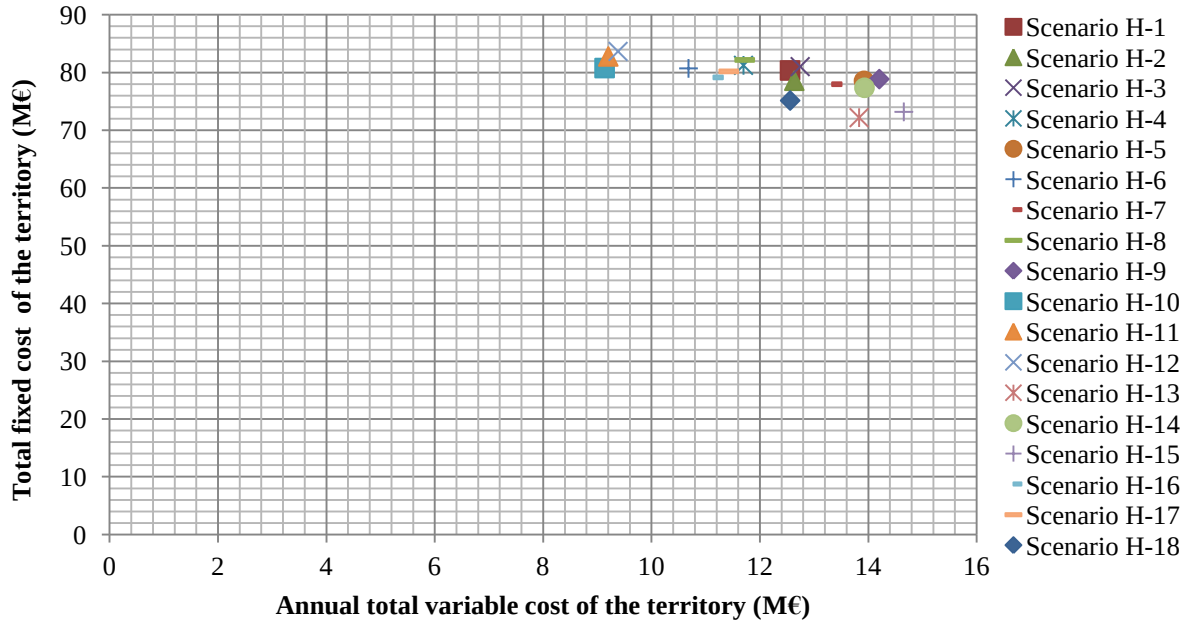


Figure 4.10. Economic statuses of the EIP configurations induced from integrating CS_1^{wood} in the park

In the aim of comparing these scenarios with the reference case, the aggregate variable and fixed costs of the territory are reckoned from the sum of the isolated industrial actors' economic status (expressed in Table 4.1) and are thus respectively 27.90 M€ and 44.67 M€. The annual net inflow C_t induced from implementing the established EIP pattern in each prospective scenario incorporating CS_1^{wood} is the difference between the reference scenario variable costs and that of the Scenario H-q, Eq.(4.4); whereas the additional entailing investments C_0 compared to the reference scenario are the difference of the total fixed costs as expressed in Eq.(4.5).

$$C_t = \text{Variable Cost}_{\text{reference Scenario}} - \text{Variable Cost}_{\text{Scenario H-q}} \quad (4.4)$$

$$C_0 = \text{Fixed Cost}_{\text{Scenario H-q}} - \text{FixedCost}_{\text{reference Scenario}} \quad (4.5)$$

To analyze the profitability of establishing any prospective scenario, the above introduced variables are employed to evaluate its net present value according to Eq.(4.6) supposing a monthly discount rate r of 0.003%. A positive NPV value indicates that the investment to be made for implementing the identified EIP configuration is lucrative regarding its generated inflows. However a negative NPV at an investment horizon T will drive a net loss. Consequently when the net inflows are equal to the required costs, the NPV is null and the year T is the time of return on investment.

$$NPV = \sum_{t=1}^{T} \frac{C_t}{(1+r)^t} - C_0 \quad (4.6)$$

Figure 4.11 illustrates the NPV over a period of ten years for the scenarios judged to be most interesting. The returns on investment for the three scenarios are roughly equivalent and are sparsely above two years of operation. Though their profitability varies and Scenario H-10 stands out for becoming the option with the highest NPV just after three years of operation by dint of its lowest total variable cost of 9.16 M€. When Scenario H-10, Scenario H-18 and Scenario H-13 become lucrative to implement, Scenario H-10 profitability surpasses the other two gains. Consequently, it only makes sense to consider Scenario H-10 as being the best between the investigated scenarios and thus the sovereign variables set 10 are the most adequate for integrating CS_1^{wood} in the studied territory.

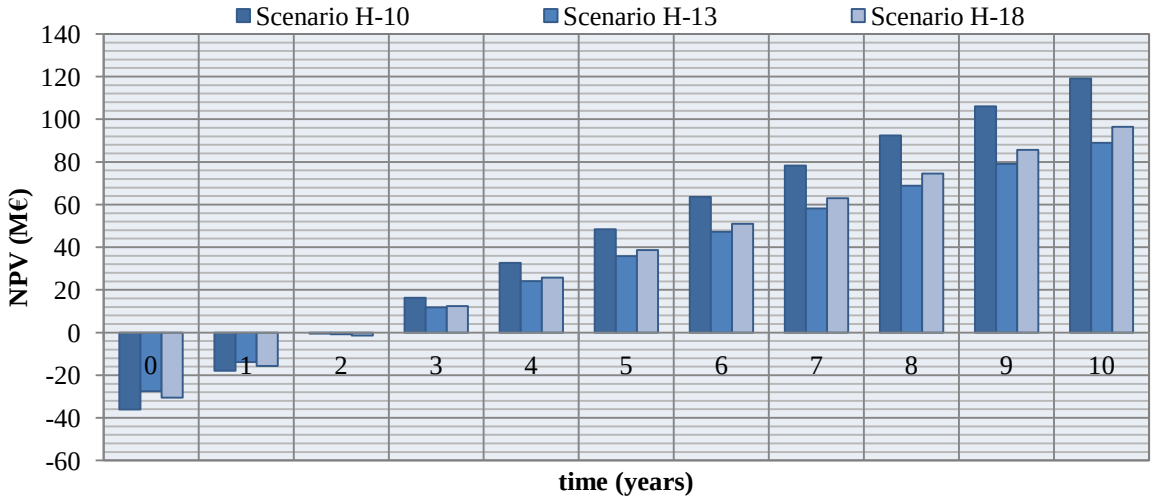


Figure 4.11. The net present values over ten years of selected scenarios integrating CS_1^{wood} in the park

But why did this set of sovereign variables induce the highest NPV even though it is one of the scenarios with the upmost fixed costs being 88.77 M€? To answer this question the hydrogen yield (Figure 4.12) from CS_1^{wood} of the eighteen studied scenarios and their minimum energy required for heating MER_{hot} and for cooling MER_{cold} (Figure 4.13) are examined to understand the influence of the sovereign variables alteration.

By comparing the studied scenarios with only the SB_{ratio} being the varying parameter of the conversion system, such those integrating $CS_{1,\,set13}^{wood}$, $CS_{1,\,set14}^{wood}$ or $CS_{1,\,set15}^{wood}$, it is noted that while the surplus heat grows simultaneously with the increasing SB_{ratio}, the hydrogen production goes in the opposite direction despite the increase of the gasifier and SMR hydrogen yields. Actually the higher concentration of H_2 in the exiting flow from the SMR reactor results in lower WGS reaction rate thus generating less hydrogen compared to an input flow with low H_2 concentration. As for heat, the necessary added water to raise the water to carbon ratio upstream of the SMR decreases with the increase of the SB_{ratio} thus leading to the reduction of the required heat Q_{SG4}, Q_{SG5} and Q_{SG6} to generate steam and to elevate the water temperature to T_{SMR}. Moreover, with less hydrogen being produced for a higher SB_{ratio}, the heating value of the stream passing through the combustion chamber intensifies. These lead to greater excess heat to be valorized in the park, hence demanding less heat utility but more hydrogen from external suppliers.

The evaluation of $T_{gasifier}$ shows that higher gasifier temperatures lead to more hydrogen production by dint of the advanced reaction rates, however require further heating load to reach and maintain the operating temperature. The steam reformer temperature, T_{SMR}, presents similar effect. Even though the increase of either $T_{gasifier}$ or T_{SMR} entails greater heat utilities, the higher allocated amount of hydrogen brings about the purchase of less external raw material.

Since hydrogen is more valuable than heat and thus more expensive to get from an external source, the lowest total variable cost of the territory is engendered from the sovereign variable arrangement that generates the greatest hydrogen yield. Unsurprisingly, the set of $CS^{wood}_{1,\,set10}$ consists of the lowest SB_{ratio} and the highest $T_{gasifier}$ and T_{SMR}, thus maximizing hydrogen production and having the greatest heat demand MER_{hot} and the least MER_{cold}. On the other hand, $CS^{wood}_{1,\,set15}$ manifests as having the biggest heat surplus and the lowest hydrogen yield. Therefore when integrated in the territory, Scenario H-15, it arise the highest total variable cost. Predictably its sovereign variables consist of the highest SB_{ratio} value coupled with the lowest $T_{gasifier}$ and T_{SMR}.

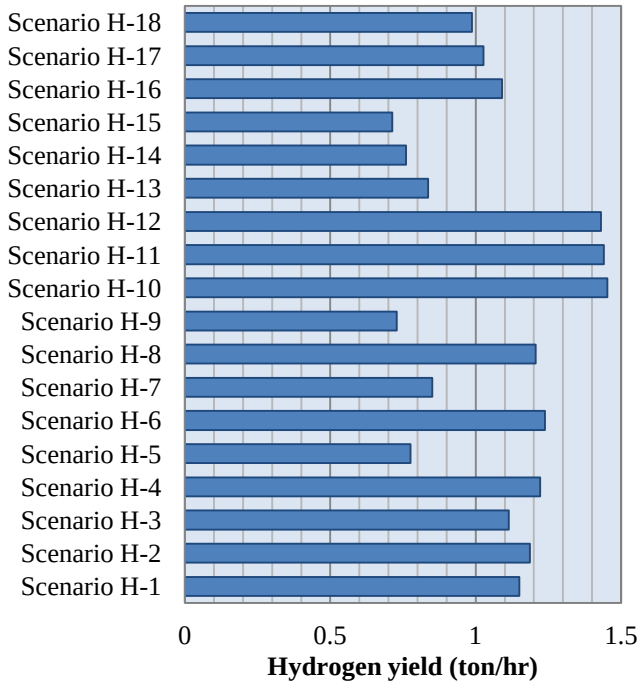


Figure 4.12. Hydrogen yield from $CS^{wood}_{1,\,set\,q}$

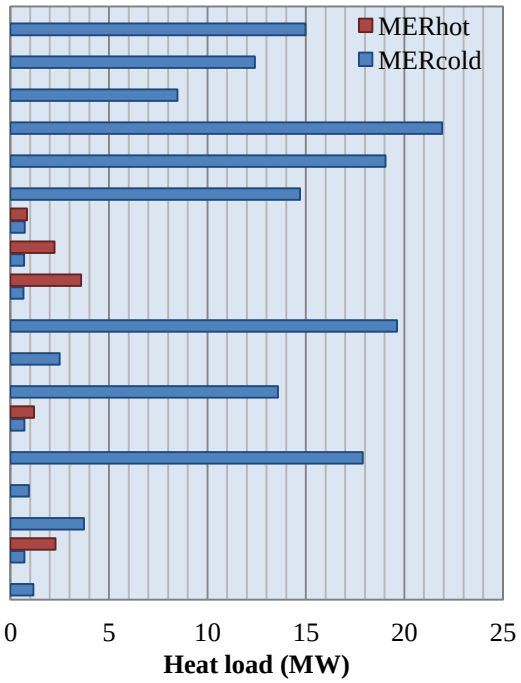


Figure 4.13. MER_{hot} and MER_{cold} of $CS^{wood}_{1,\,set\,q}$

4.4.3. Results of CS^{wood}_{2} implementation in the territory

When the wood to methane conversion system is implemented in the territory which actors' collaborate to nourish the circular economy, the non-usable wood is transferred to the bio-refinery for zero charges to be treated and converted to new commodities. Due to its high purity, the main product of CS^{wood}_{2} is sold to the national gas network that has a passing pipeline in the park; hence inducing sales income for the territory and reducing its total variable cost. The captured carbon dioxide in this conversion pathway avoids the imposed tax on its emission inducing cut downs in the territory's variable cost. This latter consists of the water and electricity power requisite by CS^{wood}_{2} in addition to the hydrogen and heat utility charges. At the energy, this route has heating demands MER_{hot} at relatively high temperature mainly for the gasifier requiring heat utility to meet this need entailing an elevation in the operating expenses. However it presents heat surplus MER_{cold} at the exothermic methanation unit temperature which range variation matches the heat requirements of the park. Consequently, the excess heat could be transferred to the energy network to be then transported towards the deficit sites of the territory reducing through these synergies the operating costs brought about from the heat utility charges.

Though the implementation of the bio-refinery yield to better variable cost for the territory, it comes at a price ensued from its process units' investment which adds up to the heat exchangers and the transport network investment. Figure 4.14 illustrates the economic status consisting of the total fixed and variable costs of territory which are generated for the twenty seven prospect scenario each integrating CS_2^{wood} with a different set of sovereign variables. By examining the plotted graph, Scenario M-5, Scenario M-25, Scenario M-7, Scenario M-3 and Scenario M-19 are found to be of most interest. Actually Scenario M-19 presents the lowest total fixed cost of 61.41 M€ and Scenario M-5 has the lowest variable cost of 16.84 M€. As for the reason behind the selection of the other three scenarios, it is because they lie on the established curve connecting Scenario M-5 and Scenario M-19.

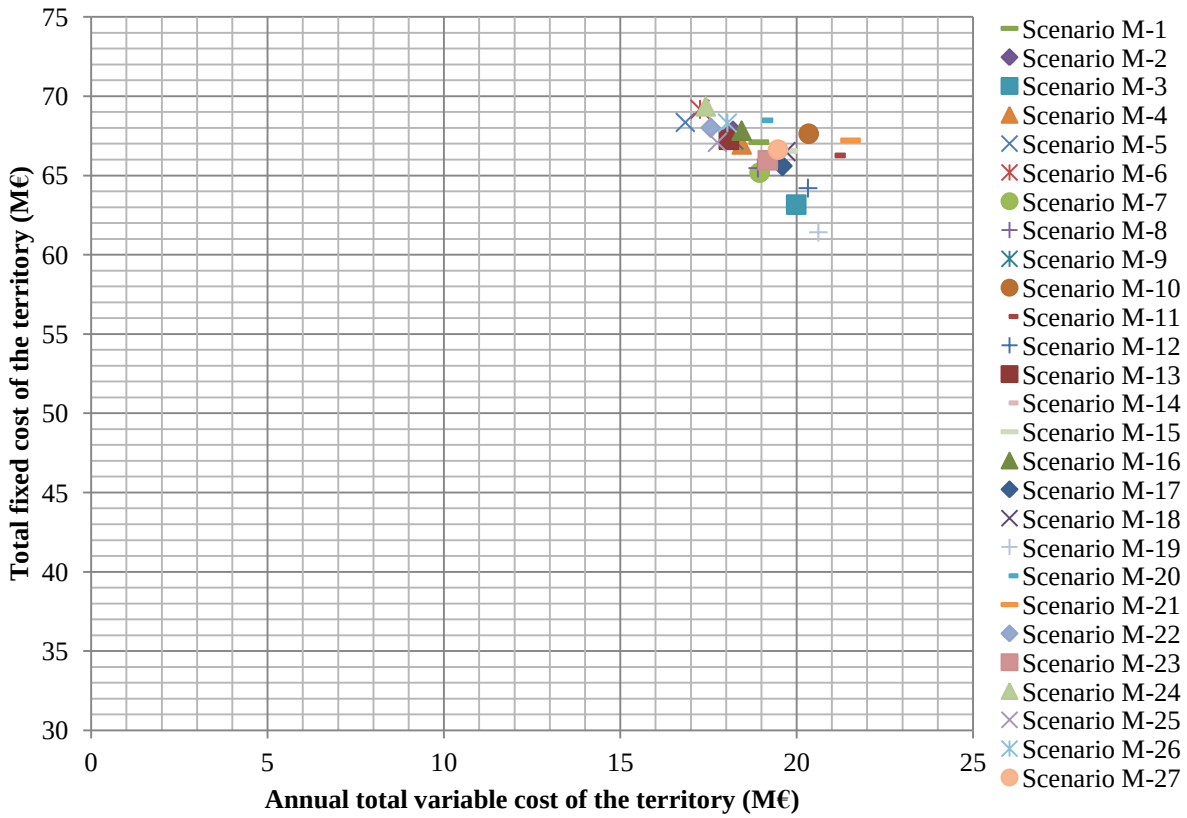


Figure 4.14. Economic statuses of the EIP configurations induced from integrating CS_2^{wood} in the park

Subsequently, the NPV of Scenario M-5, Scenario M-25, Scenario M-7, Scenario M-3 and Scenario M-19 are assessed to compare them in terms of their implementation profitability based on the reference scenario. The NPV of these five scenarios over a ten year period are presented in Figure 4.15 following an ascending order from the scenario generating the least variable cost to the one engendering the highest. Few months after the second year of operation, the generated inflows compensate the investment made for the establishment of the EIP synergy pattern of the five studied scenarios. However the brought about profitability from implementing one of the evaluated scenarios varies. Following the year at which the return on investment occurs, it actually increases from the scenario with the highest variable cost (Scenario M-19) to the one presenting the lowest (Scenario M-5). Consequently, the latter stands out as the scenario inducing the greatest profit for the territory. Therefore, when integrating a wood to methane conversion system for recovering the non-usable wood of the territory functioning under cooperative governance, $CS_{2,\,set\,5}^{wood}$ manifests as having the best adequate set of sovereign variables from the twenty seven investigated configurations of CS_2^{wood}.

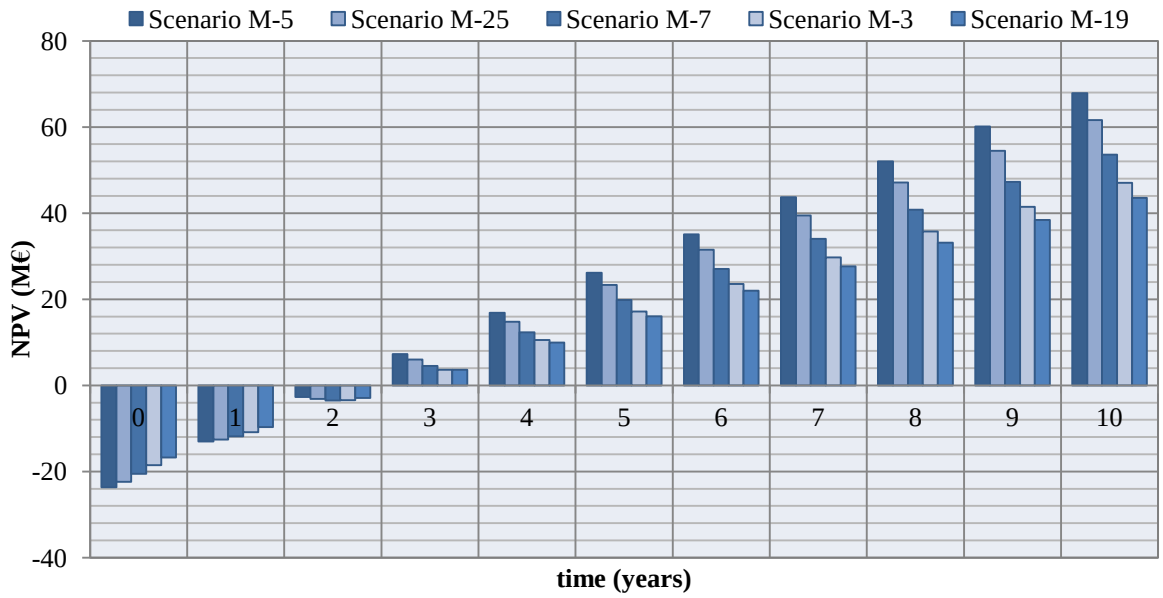


Figure 4.15. The net present values over ten years of selected scenarios integrating CS_2^{wood} in the park

In the aim of understanding the impact of the sovereign variables selection on the formerly explored results, a closer examination is carried out on the CS_2^{wood} engendered outcome from varying these variables. For the twenty seven scenarios, Figure 4.16 and Figure 4.17 illustrate respectively the methane yield from the conversion system and its energy requirements for heating and cooling.

The assessment of the above charts ensues the following inferences about SV_2^{wood}. Raising the gasifier operating temperature $T_{gasifier}$ slightly increases the process methane yield since a higher temperature enhances the reaction rates for the hydrogen production in the gasifier, but strongly impacts the heat utility requirements of the territory. It actually entails higher energy supply to attain the gasifier fixed temperature of operation.

The increase of the methanation operating temperature T_{meth} favors the prime chemical reaction in this unit which is $CO+3H_2 \rightarrow CH_4+H_2O$; thus driving greater methane generation. This can be perceived for instance in the outcomes of $CS_{2,\,set\,2}^{wood}$, $CS_{2,\,set\,5}^{wood}$ and $CS_{2,\,set\,8}^{wood}$. Notably, the greatest methane yield variation manifests between the first two since at 300°C the limiting reactant which is the carbon monoxide is almost used up. Consequently, even by increasing T_{meth} no further methane production could occur when no reactants are left to be converted. The increased methane production entails more released heat to maintain the isothermal operation of the methanation unit leading to higher MER_{cold} and hence less MER_{hot} by dint of the internal energy recovery.

In spite of the higher amount of heat required by the steam generators to increase the water feed for a bigger SB_{ratio}, the surplus energy induced from the hot process streams are more important due to the circulating flow greater H_2O content; hence the resulting MER_{hot} is less for a higher SB_{ratio}. An interesting event happens at the methanation level when increasing the SB_{ratio}. The side WGS reaction $CO+H_2O \leftrightarrow CO_2+H_2$ is promoted owing to the additional quantity of steam entering the conversion system. The steam thus reacts with carbon monoxide and generates hydrogen and carbon dioxide consuming by that the mandatory carbon monoxide for producing methane through the main unit's reaction. Therefore between $CS_{2,\,set\,1}^{wood}$, $CS_{2,\,set\,2}^{wood}$ and $CS_{2,\,set\,3}^{wood}$, the highest methane yield is induced by $CS_{2,\,set\,2}^{wood}$ having a SB_{ratio} equal to a unit because in $CS_{2,\,set\,3}^{wood}$ the great amount of steam that boosts the WGS leads to less methane production.

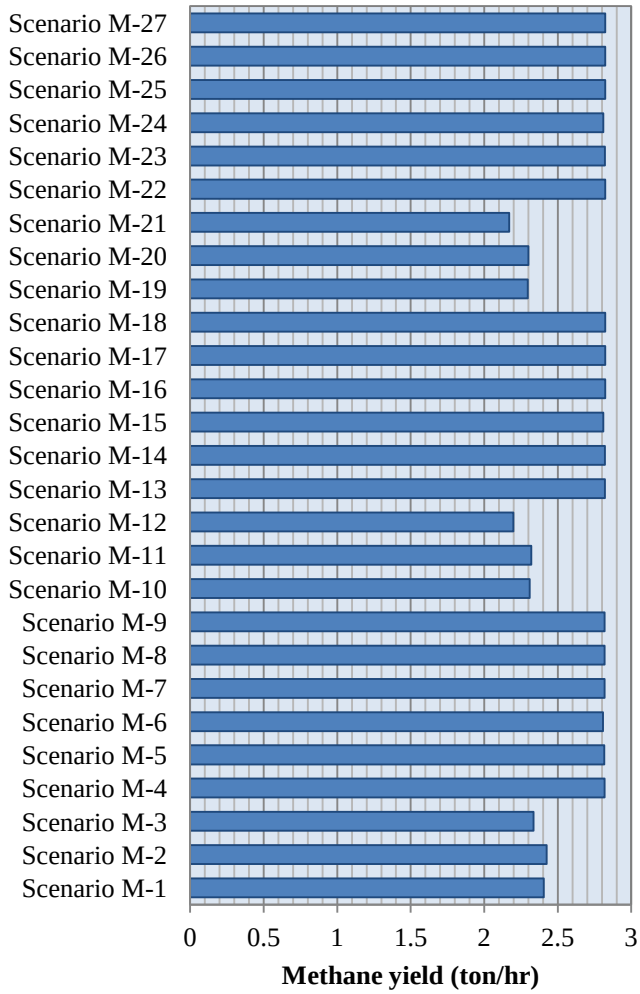


Figure 4.16. Methane yield from $CS^{wood}_{2,\ set\ q}$

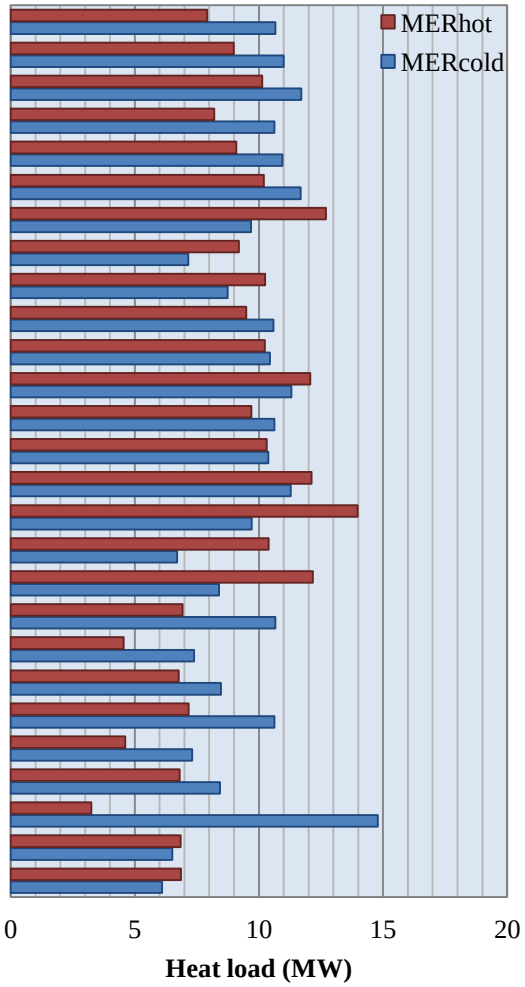


Figure 4.17. MER_{hot} and MER_{cold} of $CS^{wood}_{2,\ set\ q}$

Methane being the main commodity of the CS^{wood}_{2}, the sovereign variables set in favor of its generation results in the lowest total variable cost of the territory. Based on the aforementioned analysis, this set should be formed by the lowest $T_{gasifier}$ and the highest T_{meth} of the possible value ranges with a SB_{ratio} fixed at one; thereby they must be appointed the values of 650 °C and 400 °C and 1 respectively. Even though according to the variables description set 8 should be forming the wood to methane conversion system inducing the smallest variable cost, it is in fact $CS^{wood}_{2,\ set\ 5}$ that does.

The reason for this result is because no heat network was constructed when implementing $CS^{wood}_{2,\ set\ 8}$ in the territory. Despite the fact that the exergy analysis showed promising integration opportunities, economically the network was not lucrative to invest in thus resulting in higher energy utility expenses to cover the necessary need of each industrial actor which adds up to the park's variable costs. Nonetheless, in Scenario M-5 a heat network was installed at 160°C to retrieve the excess heat of $Site_3$ from which 9.37 MW are redirected to $Site_2$ and 4.65 MW sent to $Site_1$. Interestingly in this scenario, the bio-refinery does not participate in the heat network. This is due to the fact that the heat exchangers are less expensive when installed at the low cold utility temperature than when connected to the network due to the greater heat exchangers' sizes. Therefore if the wood to methane conversion pathway is chosen as the valorization route for the non-usable wood, $CS^{wood}_{2,\ set\ 5}$ should be integrated in the territory to attain the uppermost profit.

4.4.4. Results of CS_3^{wood} implementation in the territory

For the third investigated wood conversion route CS_3^{wood}, the woody biomass having no worth in the form it is found in, is fed to a bio-refinery installed in the territory to convert its initial form through a series of processes into high temperature steam and electric power. Consequently, the investment that must be put in return for the process units could be regained from the inflow that might be engendered from the more valuable produced commodities. The generated electricity from CS_3^{wood} could actually be sold to the power grid at the market worth ensuing a revenue for the territory operating with cooperative governance. The begotten steam could be employed for heat generation by transferring its heat content to the deficit industrial participants of the park through the energy network resulting in less heat utility purchase. With a view to examine the best balance between heat and electricity production inducing the highest profitability from the investment made for establishing the bio-refinery, the resulting economic statuses from the optimal on-site and inter-sites synergy patterns including the CS_3^{wood} for several set of sovereign variables are explored. Figure 4.18 displays the relationship between the total fixed and annual variable costs of the territory for the twenty one studied variables configurations of the wood to energy conversion system.

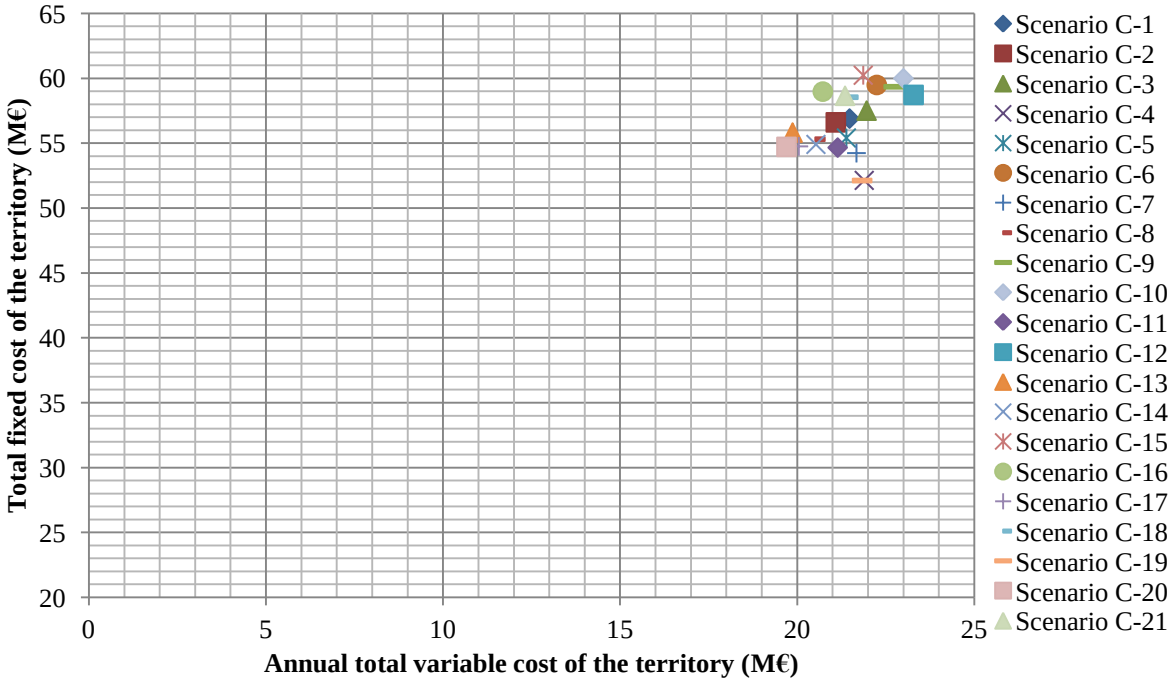


Figure 4.18. Economic statuses of the EIP configurations induced from integrating CS_3^{wood} in the park

From the obtained results Scenario C-19 and Scenario C-20 emerge. The former entails the lowest investment of 52.13 M€ for the heat exchangers, transport network and bio-refinery implementation, while the latter integrates $CS_{3,\,set\,20}^{wood}$ with the set of sovereign variables that induces the optimal EIP pattern with the least variable cost of 19.70 M€. Nonetheless, the configuration generating the smallest variable expenses demands more investment to build the synergies behind the decrease of resources and energy consumption. Actually, Scenario C-20 has a fixed cost of only 5% higher than Scenario C-19. Therefore in order to assess the weight of the additional costs on the territory's profitability, the NPV of both of these scenarios are examined. The NPV over a ten year period of Scenario C-19 and Scenario C-20 are illustrated in Figure 4.19.

Even though the starting year the former has the smaller NPV by dint of its lower investment expenses, it does not take too long before the latter becomes more profitable. Scenario C-20 succeeds in compensating the 5% difference in the annual fixed cost by its 10% lower variable cost compared to Scenario C-19. Following ten years of operation, the established EIP pattern in Scenario C-20 generates 15 M€ more than the one implemented with $CS^{wood}_{3,\ set\ 19}$. Consequently with both scenarios' return on investment being couple of months after one year of operation, the most profitable sovereign variables to opt for when integrating CS^{wood}_{3} for the non-usable wood conversion is the set 20.

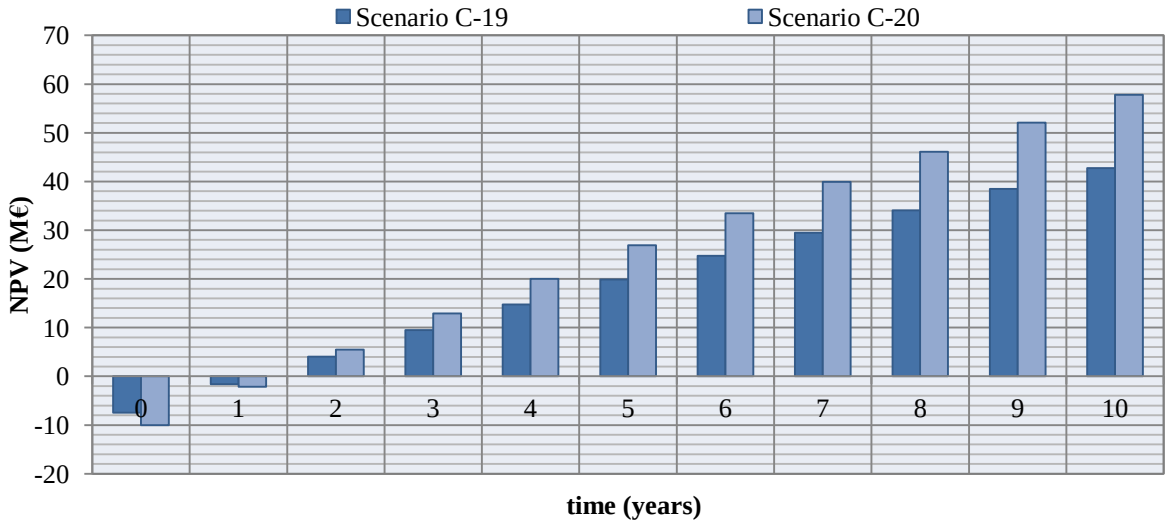


Figure 4.19. The net present values over ten years of selected scenarios integrating CS^{wood}_{3} in the park

In the aim of further assessing the physical modifications in the conversion system related to the alteration of CS^{wood}_{3} sovereign variables, the power and heat generation are explored for the twenty one studied set of configurations and are respectively illustrated in Figure 4.20 and Figure 4.21.

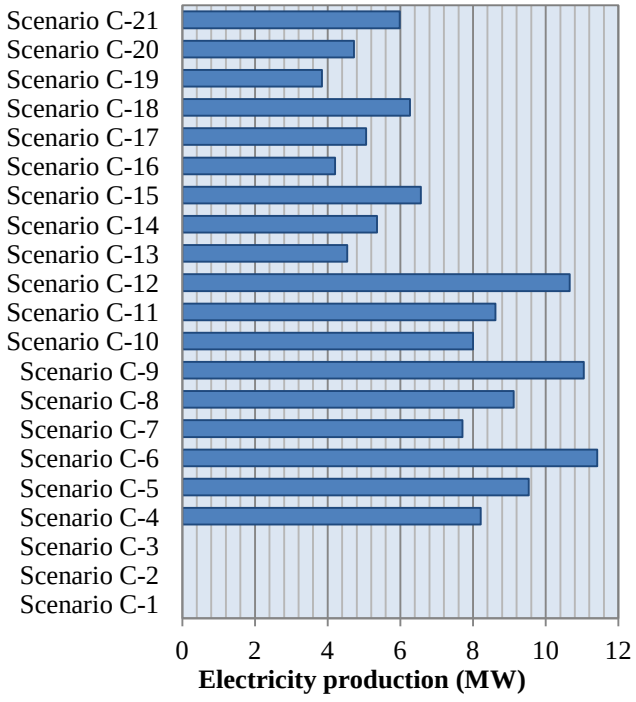


Figure 4.20. Electric power generation from $CS^{wood}_{3,\ set\ q}$

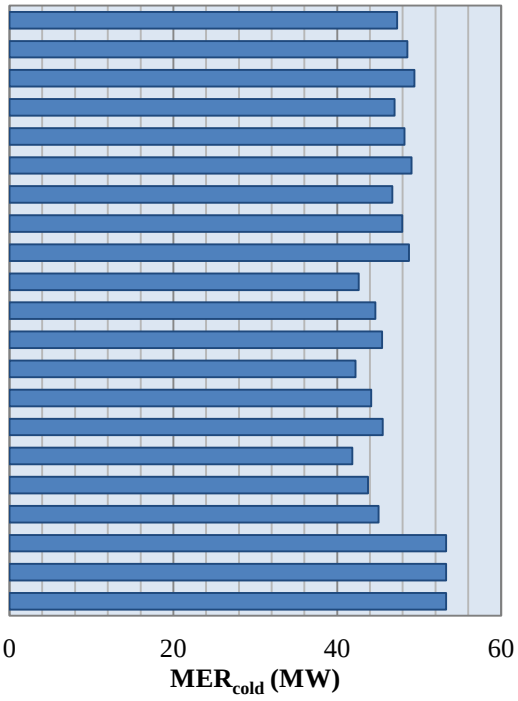


Figure 4.21. Heat generation of $CS^{wood}_{3,\ set\ q}$

First the fraction of steam x that goes through the high pressure condenser is examined. The collection of $CS^{wood}_{3,\,set\,4}$, $CS^{wood}_{3,\,set\,13}$ and $CS^{wood}_{3,\,set\,1}$ are taken as an example for three scenarios in which only x varies from zero meaning only power is generated to 0.5 and the third have its x set to 1 so that the conversion system only produces high pressure steam. Unsurprisingly by shifting from exclusively converting the biomass into electric power to a cogeneration transformation and then to only heat production, less electricity is produced and more steam is generated. Even though the conversion system investment decreases when the turbine size is reduced, the total fixed cost of the territory might increase by dint of the pipeline and heat exchangers costs required to transfer the produced steam; as opposed to electricity generation that only results in sales income for the park.

When altering the high pressure condenser operation to lower $T_{out\,high}$ for a fixed $T_{out\,low}$, or by changing the low pressure condenser operation by increasing $T_{out\,low}$ for a fixed $T_{out\,high}$ similar effects are encountered. Actually, the pressure difference between the high and low sides of the steam cycle decreases. Consequently, the generated turbine power goes low leading to less electricity accompanied by an increase in the steam production by dint of the additional released heat at the low pressure condenser. These effects could be discerned for instance by examining the heat and electric power outcomes of $CS^{wood}_{3,\,set\,14}$, $CS^{wood}_{3,\,set\,17}$ and $CS^{wood}_{3,\,set\,20}$ with the single difference in their sovereign variables being $T_{out\,high}$ which is set respectively at 300°C, 290°C and 280°C; or those of $CS^{wood}_{3,\,set\,15}$, $CS^{wood}_{3,\,set\,14}$ and $CS^{wood}_{3,\,set\,13}$ having $T_{out\,low}$ fixed respectively at 150°C, 180°C and 200°C.

From the evaluated set of sovereign variables for CS^{wood}_{3}, the most profitable balance between heat and electricity production for the territory operating under cooperative governance is found to be that of set 20. This latter consists of wood cogeneration having half of the circulating steam going through the turbine and operating with high and low temperatures at 280°C and 180°C respectively.

4.4.5. Comparison of the three wood conversion pathways

Each conversion pathway was investigated individually to determine the technical options and operating parameters of the conversion process units which engenders the greatest profitability. However to select the most cost-effective wood conversion route to be implemented in the territory, a combined analysis for the three valorization pathways is mandatory to be carried out.

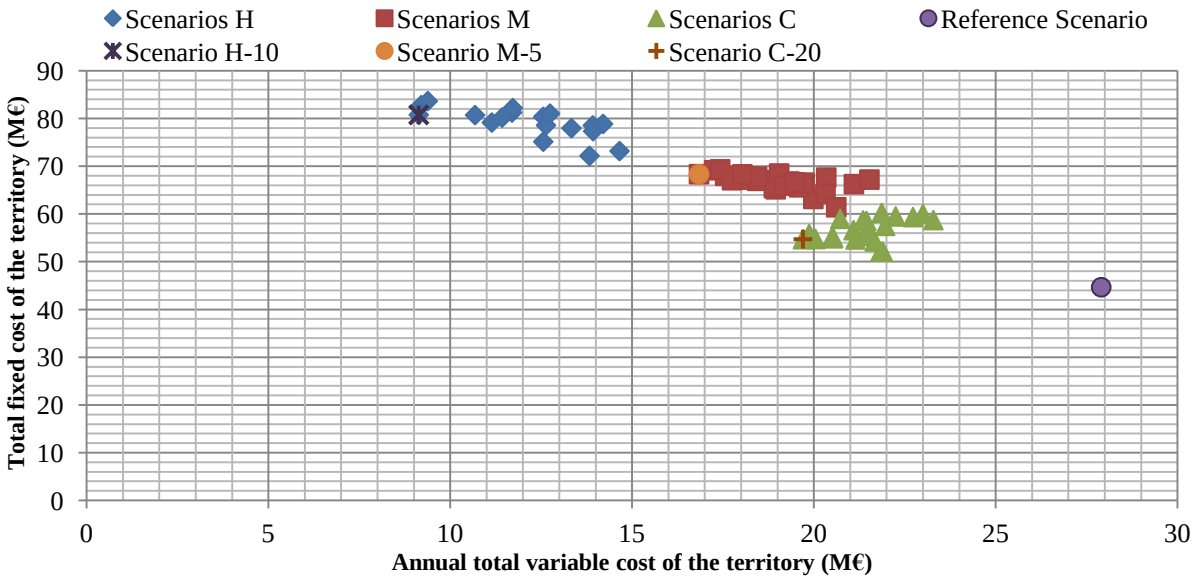


Figure 4.22. Economic status for the three investigated wood conversion routes combined

The entire collection of scenarios induced from the preceding analysis of the three conversion routes is represented in Figure 4.22 in terms of the total fixed and annual variable costs of the territory, together with the reference scenario and the best judged scenarios of each pathway. The first remarkable aspect of this graph is that irrelevantly from the selected conversion route, the created valorization opportunities from the transformation of the non-usable wood substantially enhance the variable cost of the territory to a low level which is otherwise unattainable.

It can also be deduced from this chart that the hydrogen production is the conversion route generating by far the lowest variable cost; however it demands the most funds to install the computed EIP pattern. This can be explained by the park's demand of hydrogen which is more expensive to be purchased from an external source than to pay for heat utilities. This fact highlights the importance of considering the territory's demand when scouting the non-usable streams valorization system to select the ones to be further investigated and potentially implemented.

Even though the wood cogeneration requires the least investment to put in place the induced EIP configuration, it results in the highest variable cost compared to the other two conversion routes. Nonetheless, certain methane generation scenarios align with the cogeneration pathway and are slightly above. Actually, with identical variable expenses the project with the least payments to be made for establishing the synergies is obviously better. Consequently, the configurations of the methane pathway engendering a variable total cost higher than 20 M€ will always be surmounted by a better cogeneration scenario.

4.4.6. Further assessment of the best Scenarios

The adjudicated scenarios as being the greatest cost-effective for each conversion pathway are further explored in the aim of detecting the collaborative strategy to be executed for the best on-site and inter-sites synergies. Their economic statuses are listed in Table 4.8.

Table 4.8. Economic status of the territory for best judged prospect scenarios

Scenario	Fixed Cost (M€)	Annual Variable Cost (M€)
Reference Scenario	*44.67*	*27.90*
Scenario H-10	80.77	9.16
Scenario M-5	68.34	16.84
Scenario C-20	54.72	19.70

Subsequently, the NPV of Scenario H-10, Scenario M-5 and Scenario C-20 are evaluated over a ten year period based on the reference scenario to assess their respective profitability, Figure 4.23. The wood cogeneration has the fastest return on investment. It starts engendering profits as from the second year of the implemented EIP operation. As for the two other conversion pathways, it is not before the year after for them to have a positive NPV. Consequently, the time period the decision makers are willing to wait for to having their full investment reimbursed, plays a major role in the selection of the conversion route to be set up in the intended territory.

Nonetheless, this selection should also be sensitive to the gain difference between conversion routes over the park’s operation horizon. Following ten years of operation, the wood to hydrogen conversion scenario ensues more than double the profits that could be generated from implementing the wood cogeneration. And finally, with roughly similar return on investment period, converting wood into methane is less interesting compared to the wood to hydrogen route by dint of the higher profitability the second induces.

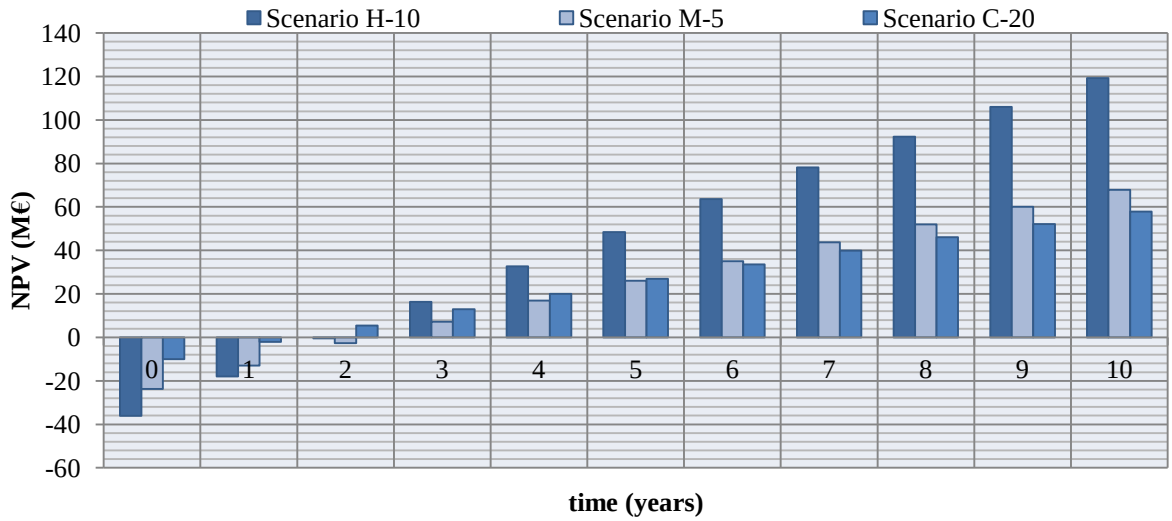


Figure 4.23. Comparison of the NPV over ten year period for the best scenario of each pathway

Whether the selection falls on CS_1^{wood}, CS_2^{wood}or CS_3^{wood}, it is apparent that the conversion of the identified non-usable streams of the territory into more valuable commodities always turns out to be lucrative with a varying time of return on investment. The aforementioned statement is true for waste having no value; however when it does have a monetary worth, that might not be always the case. The problem should therefore assess whether it is more beneficial to invest in a conversion system to recover the waste internally or sell the waste to external clients for its value.

Moreover, the main commodities to which the wood is converted into are hydrogen, methane and heat. The prices of those three are correlated with the fluctuating gas market. Therefore a study to assess the profitability variation and time of return examination for altering gas market price should be carried out. Subsequently, the next two sections present respectively the study of the wood value impact and the sensitivity of the changing gas price on the best route selection carried out for the best judged scenarios of each conversion system.

4.4.6.1. Wood value sensitivity analysis

In the previous evaluations the non-usable woody biomass whose thermo-chemical conversion pathways were investigated, was supposed having no value. Nonetheless the wood market worth might change over time or even in some occasions or locations for instance wood scarcity in some regions. The non-usable wood of the territory turns out to becoming a valuable commodity. It could therefore be sold at its market worth to external buyers and thereby engendering sales revenue to the territory. Consequently, when assessing the profitability and the time of return on investment of the potential conversion routes of the wood commodity the reference scenario changes. This latter consists of the isolated agents with the exact same territory's annual total fixed cost. However the variable cost of the reference scenario is amended by the new wood sales revenue which is deduced from the operating expenses of territory.

With a view to study the impact of such event, a sensitivity analysis on the wood market worth is conducted to evaluate the profitability alteration of the best judged scenarios for each conversion pathway. This is achieved for several wood values per ton ranging from 20€ to the price of wood at which wood conversion routes are no longer lucrative to be implemented in the territory. The total variable and fixed costs for the several reference scenarios generated from the assessed wood market prices are presented in Figure 4.24 together with the best scenarios of the three conversion route.

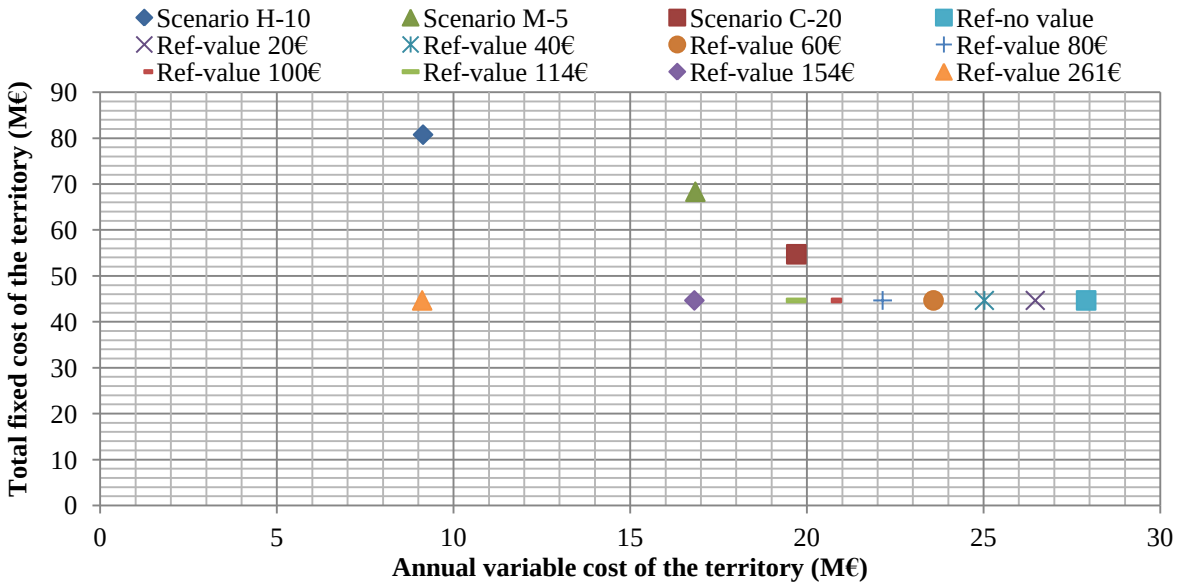


Figure 4.24. Economic statuses of the best scenarios for each pathway with a varying reference

These latter have unchanged economic statuses by dint of the non-interference of the wood value in their economic balance for a territory with cooperative scheme. As for the reference scenario, when the wood sales income increases for a higher market worth it is shifted horizontally towards lower total variable cost since the fixed cost of the park is not impacted by the wood value existence. The variable cost shift is roughly around 11 M€ from the scenario in which wood has no value to the one with a market worth of 154 € the ton. It can be foreseen from the graph that for a ton of wood market value above 114€, the cogeneration pathway is no longer beneficial to implement since it requires 20% higher investment than the reference scenario for that value. Similar analysis can be carried out for the methane production scenario which is aligned with the reference having a wood ton value of 154 €; hence starting from this wood market worth the hydrogen generation route is the only prospect scenario with lucrative potential compared to selling the wood to external buyers. Scenario H-10 maintains its position until the market value for the ton of wood reaches 261€.

The NPV for the three wood conversion scenarios are established based on the reference scenarios induced for every market value in the aim of examining the profitability variation as well as the impact on the payback time of investment. They are illustrated from Figure 4.25 till Figure 4.30.

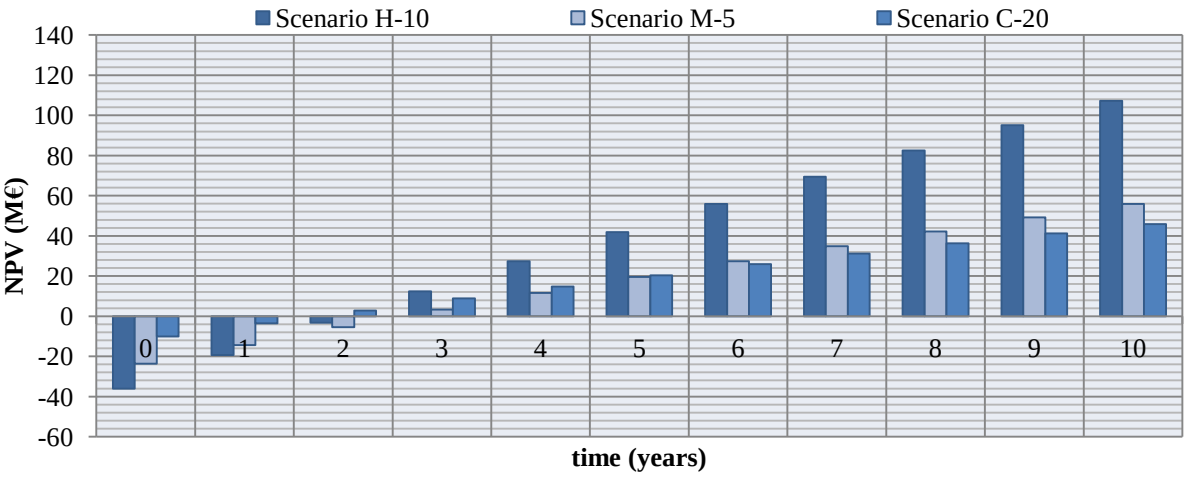


Figure 4.25. NPV over ten years for the best scenario of each pathway with 20€ the ton of wood

For a wood ton value of twenty Euros (Figure 4.25), the return on investment is barely impacted for the three scenarios. Nonetheless their net profits at the tenth year of operation is reduced by approximately 12M€ compared to the scenarios in which wood has no monetary worth.

Up until a value of forty Euros for the ton of wood (Figure 4.26), the cogeneration and hydrogen production routes are slightly impacted in their investment payback time with their gain generation starting respectively the second and the third year of operation; though the return on investment for the wood to methane conversion pathway increases by a whole running year in reference to the lower wood value.

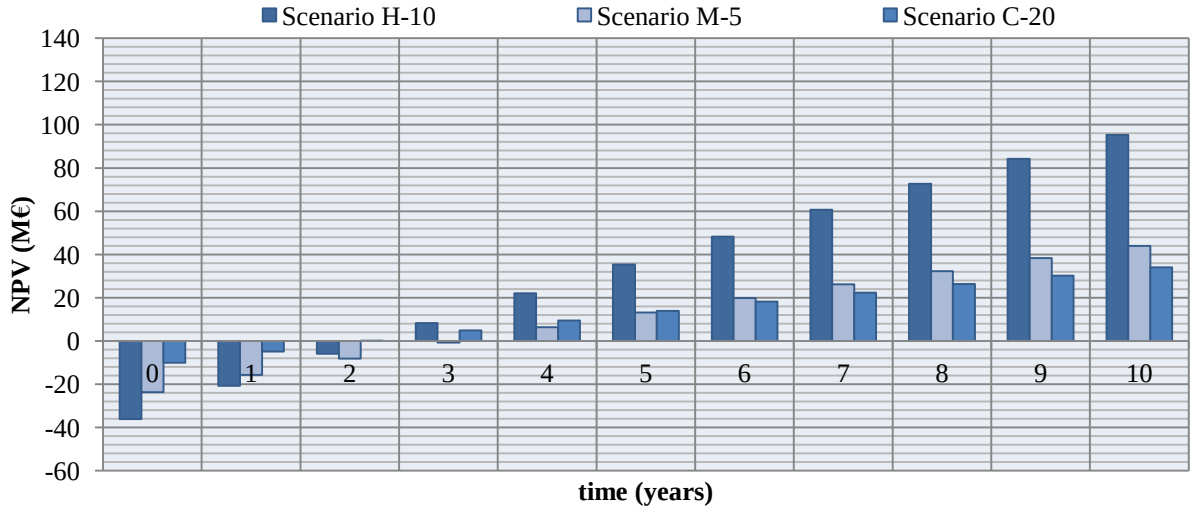


Figure 4.26. NPV over ten years for the best scenario of each pathway with 40€ the ton of wood

However above a ton wood worth of forty Euros (Figure 4.27), the ultimate EIP configuration for the studied territory is the scenario implementing $CS^{wood}_{1,\,set10}$ if the investment reimbursement time is set to more than two years. This is because Scenario H-10 and Scenario C-20 have identical payback time but the former generates 65% higher gains than the latter at the tenth anniversary of the EIP configuration was set up.

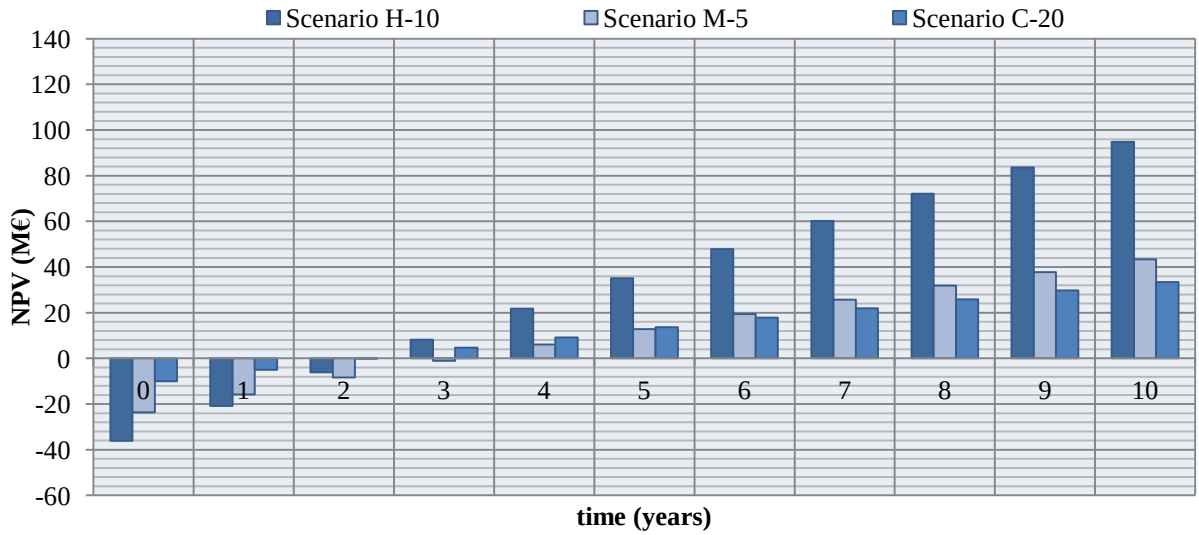


Figure 4.27. NPV over ten years for the best scenario of each pathway with 41€ the ton of wood

When the ton of wood could be sold at eighty Euros (Figure 4.28), the return on investment goes up to the fifth year of operation for methane production and cogeneration. Thereby with double the profits at the tenth year, Scenario M-5 is definitely better to be established than Scenario C-20. Yet, Scenario H-10 net income starts flowing the third year of implementation and presents 70% greater payoffs at year ten than Scenario M-5 does.

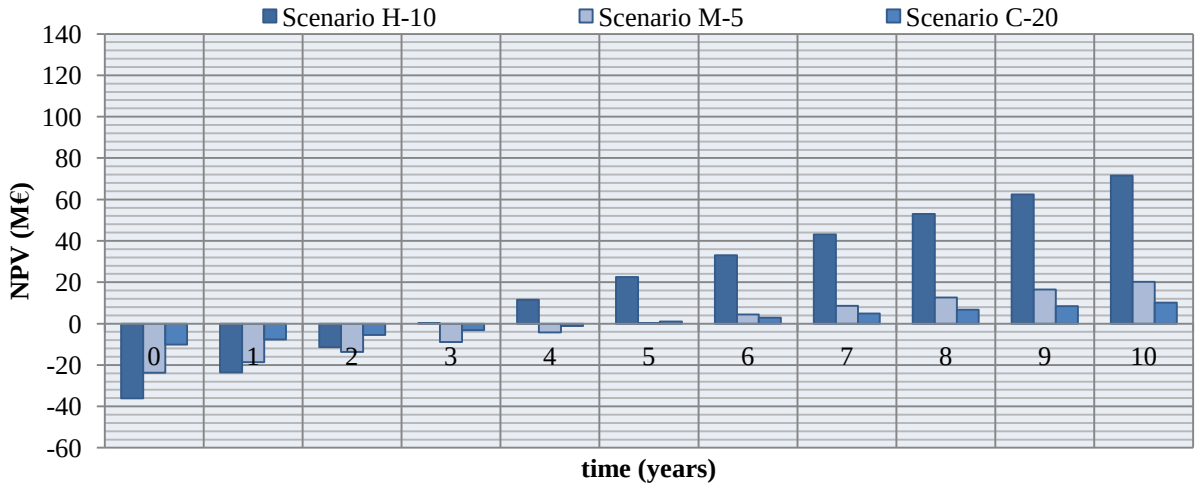


Figure 4.28. NPV over ten years for the best scenario of each pathway with 80€ the ton of wood

Scenario H-10 loses a year in payback time when the ton of wood is one hundred Euros of value (Figure 4.29). While Scenario M-5 return on investment is not until the eighth year of operation, the inflow of Scenario C-20 are not enough to reimburse its investment not even in ten years.

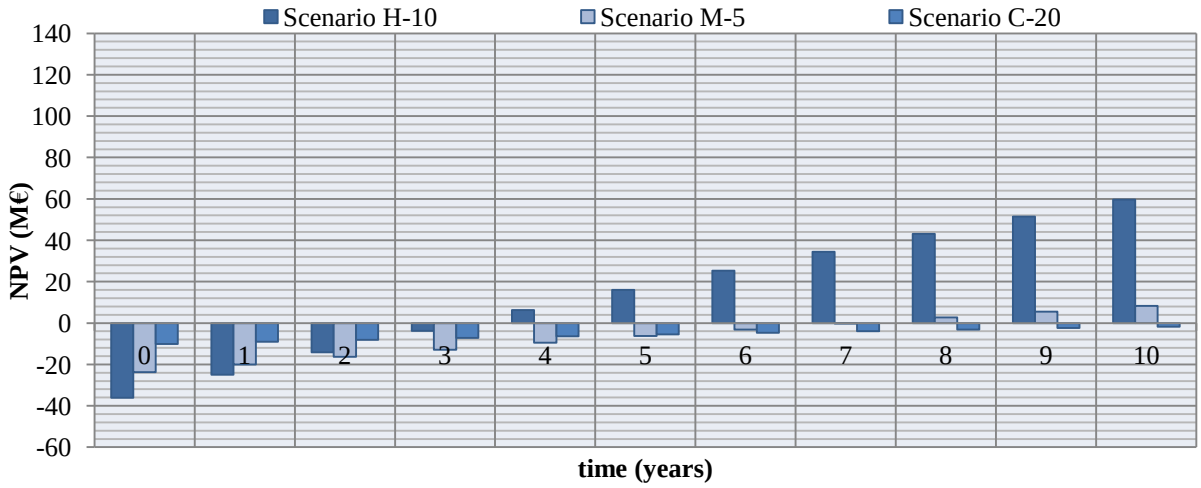


Figure 4.29. NPV over ten years for the best scenario of each pathway with 100€ the ton of wood

At the wood market worth of 154€ per ton (Figure 4.30), neither installing a cogeneration system nor a wood to methane conversion process are feasible, they never come to repay their initial investments. As to Scenario H-10, it begins to gain from its investment six years after the installation of the EIP pattern incorporating $CS^{wood}_{1,\,set10}$ and reaches a net profit of 27 M€ the tenth year which is only one-fourth the payoff it has when no value is associated for the non-usable wood. The time wood value per ton attains 210 €, Scenario H-10 puts more than ten years to reimburse its investment; and above 261€ the ton of wood it is no longer lucrative to implement any of the wood conversion routes.

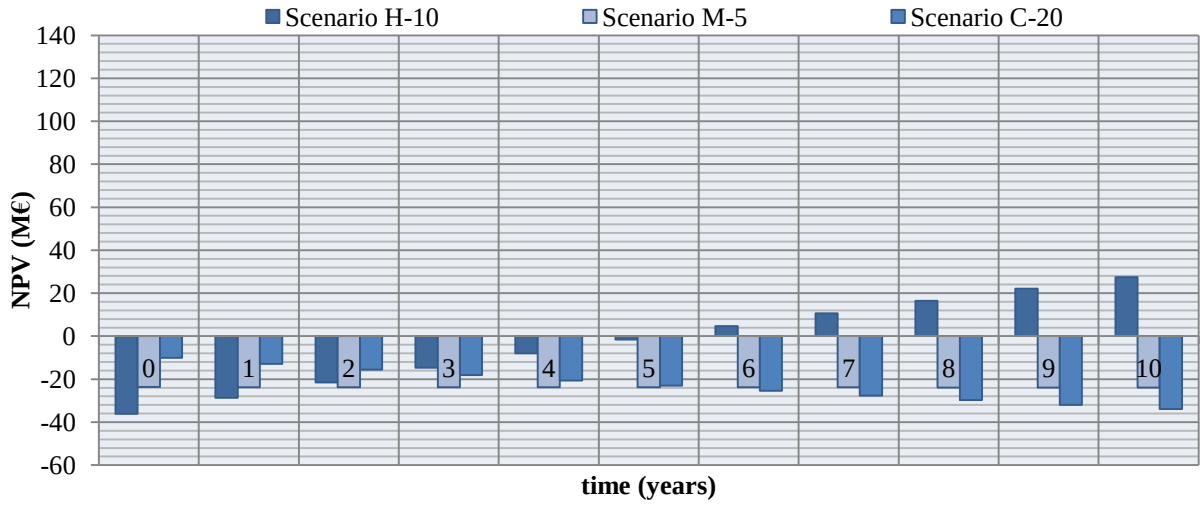


Figure 4.30. NPV over ten years for the best scenario of each pathway with 154€ the ton of wood

4.4.6.2. Fluctuating Gas market price sensitivity analysis

A strong assumption of the correlated relationships between heat, methane and hydrogen prices with the gas market price was established at the beginning of the current chapter. Based on this statement, the prior economic evaluations of the wood conversion system integration in the territory were conducted for a gas market price of 30 € the MWh. Consequently, the fluctuating gas market has a direct impact on the prices of the investigated territory main commodities. In the aim of assessing the weight of this impact on the synergies establishment for the three best wood conversion configurations and the effect it might carry on the ability for each scenario to produce higher value for its investment, a sensitivity analysis is carried out for a low market price of 20€/MWh, a high market price of 40€/MWh and the previously employed gas price of 30€/MWh.

The economic status of the reference scenario differs for each gas market price; since the synergy patterns, an industrial site invests in, are related to the utility costs it is avoiding when implementing the internal recovery. Subsequently, the overall fixed and annual variable costs of the reference scenario for each of the evaluated gas prices are listed in Table 4.9.

Table 4.9. Economic status of the reference scenario for each gas market price

Reference Scenario	Fixed Cost (M€)	Annual variable Cost (M€)
For Gas Price 20€/MWh	20.10	33.61
For Gas Price 30€/MWh	44.67	27.90
For Gas Price 40€/MWh	46.42	36.59

For a relatively low natural gas price, the heating utilities might be less expensive to utilize instead of installing heat exchangers to internally transfer energy. As opposed to high price gas situations in which it could eventually be more lucrative to invest in heat exchangers to create on-site synergies than to pay for utilities. These events are exhibited in the above listed economic status in which the fixed cost increases with the augmentation of the natural gas market price by dint of the expansion of either the number of installed heat exchangers or their energy transfer surface area. The variable cost has however less predictable variation since it is simultaneously reliant on the established synergies and on the induced costs from the employed amount of heating utilities.

The net present values over a ten year period are established for the studied market gas prices based on the appropriate economic data of the reference scenario. Figure 4.31 and Figure 4.32 illustrate the resulting NPV respectively for a low gas market price and for a high market price. For the previously employed gas price of 30€/MWh, the NPV for the three best scenarios were displayed in Figure 4.23. From the corresponding chart of the low gas price, it is noticed that the NPV of the three conversion pathways become positive at the second year of operation. Therefore the prospect scenario engendering the highest profit presents the ultimate EIP to be implemented. Even though the generated profits of the wood to hydrogen conversion route are only of 50% higher by comparison to the scenario in which the MWh of the natural gas is at 30€ and those of Scenario M-5 and Scenario C-20 have doubled, it still is Scenario H-10 that have the greatest payoff.

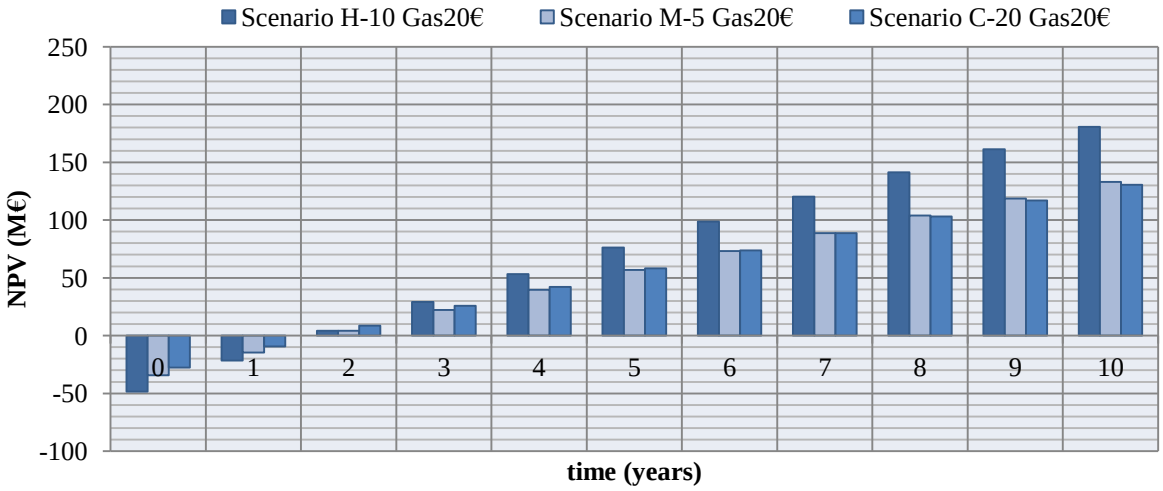


Figure 4.31. NPV over ten years for the best scenario of each pathway with a low gas market price

For the high gas market price, the return on investment is roughly similar for the three pathways with couple of month difference. Their initial net profits are set off at the second anniversary of the EIP implementation. Compared to the 30€/MWh case, the on-site and inter-sites synergies are increased in such that less is paid for the utilities generating higher profits. Those are increased at the tenth year by 30% for each of Scenario M-5 and Scenario H-10 and by 24% in the Scenario C-20.

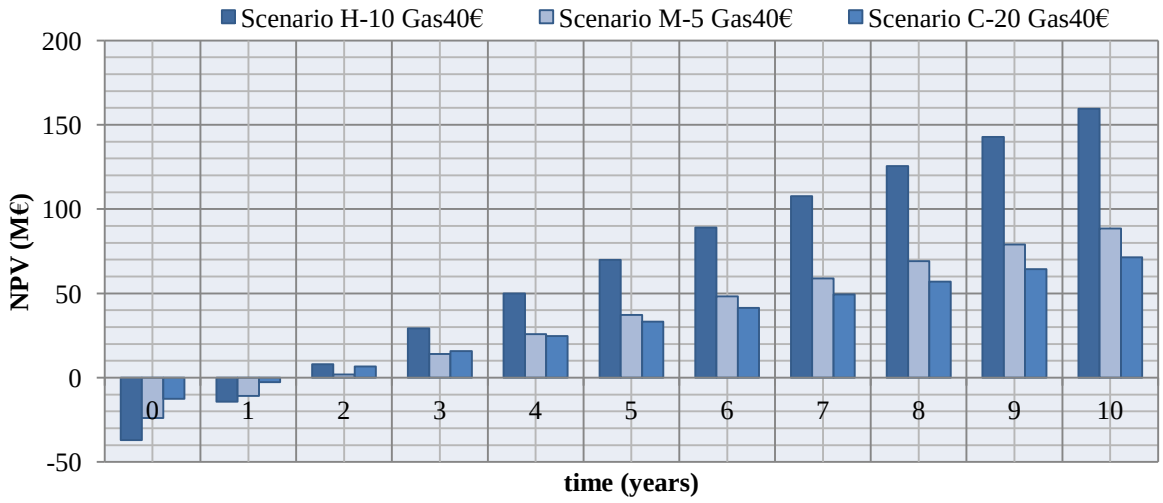


Figure 4.32. NPV over ten years for the best scenario of each pathway with a high gas market price

4.4.7. EIP configuration of the best adjudicated Scenario

Based on the previous results and analysis it is found that the integration of a conversion system in a territory is highly impacted by the resources requirements of the intended park. Another interesting factor was found to have a big weight in the decision making is the desired time of return on investment. Nonetheless this could lead to biased choices towards certain conversion system that could eventually be less lucrative than other routes. Therefore a global view should be taken on the operation life time of the park to evaluate whether or not the decision makers should be more flexible on their investment reimbursement time with a view to greater profitability in the upcoming years.

Consequently the best conversion pathway that undertakes the least damage with the gas market fluctuations or with the non-usable waste earning monetary worth turns out to be the wood conversion into hydrogen. In particular, its conversion processes should have the 10th studied set of sovereign variables: $(SB_{ratio}, T_{gasifier}, T_{SMR}) = (0.5, 850, 850)$.

The induced EIP configuration from the integration of $CS^{wood}_{1,\,set\,10}$ in the studied territory is depicted in Figure 4.33. In this EIP, $Site_3$ gets its 67 129 MWh high level annual heat demand from a utility source and transfers 19 200 MWh of its untapped low temperature energy through a steam network at 145 °C to the appended bio-refinery. This latter gets its wood feed from $Site_1$ for no charge. The formerly non-usable 72 000 ton of woody biomass are converted in the bio-refinery into 8 700 ton of hydrogen which are allocated to $Site_1$ while annually consuming 13 915 ton of pure oxygen, 51 520 m^3 of water and 10 427 MWh of heating utility. In the process of hydrogen production, 111 750 ton of carbon dioxide are sequestered. $Site_1$ purchases from external suppliers 300 ton of hydrogen yearly to cover its remaining resource requirements and for energy demand it intakes 179 000 MWh per year of heating utilities. As for $Site_2$ it satisfies its annual needs via 196 770 MWh of heating utility. This EIP configuration ensures the *social welfare* of the territory considering the industrial sites established in its boundaries as a single economic entity in which energy and material are freely exchanged.

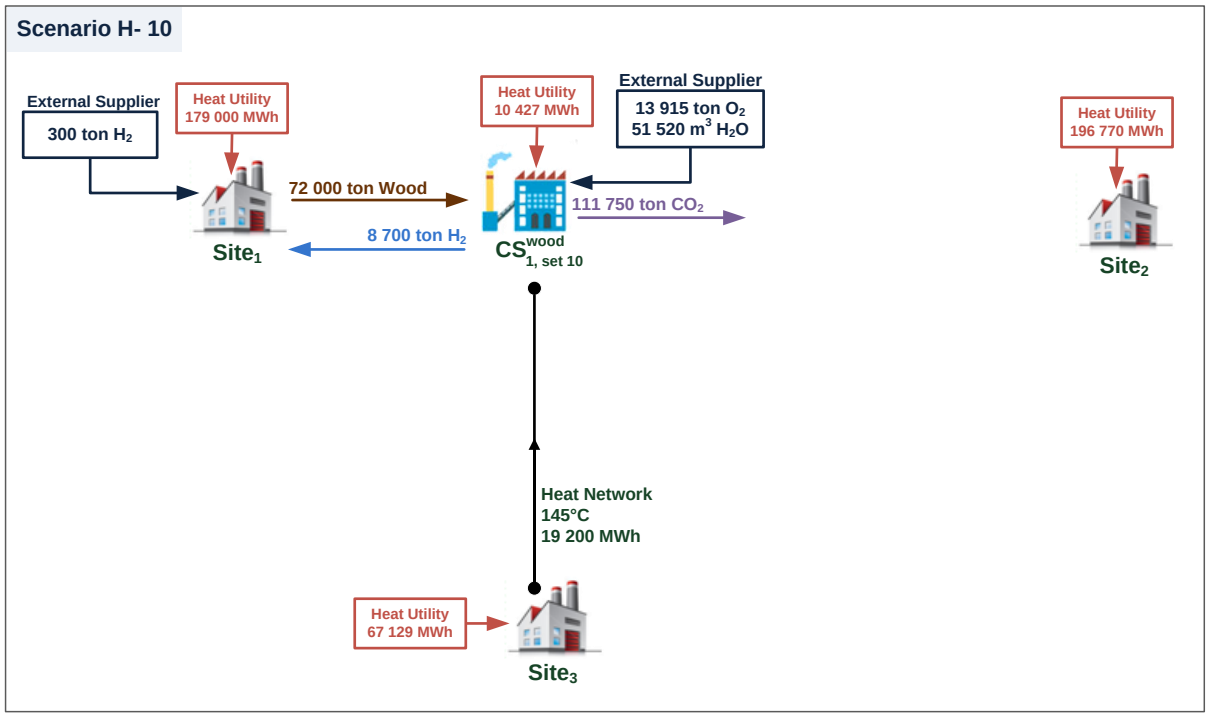


Figure 4.33. EIP configuration of the best adjudicated scenario in cooperative scheme

Nonetheless in more realistic circumstances, industries are self-interested and thus only act in the furtherance of their individual welfare. Therefore they will most likely put a price on the outgoing commodities or even waste that they allocate to establish a potential synergy with another also self-interested industrial actor. This will highly impact the resulting EIP configuration and might as well alter the best wood conversion route. Consequently in the following section, the optimal EIP pattern of the studied park with non-cooperative governance will be investigated in the aim of determining the optimal purchase and selling transactions for the inter-sites circulating energy and material flows.

4.5. CS integration in a territory with non-cooperative Scheme

4.5.1. Problem Statement

The three industrial sites within the predefined boundaries of the studied territory are now assumed to be motivated by their individual advantage increase with no regard to the global enhancement of the park's operation. Wherefore the induced payoffs from trading their untapped streams are the only stimulation for them to participate in synergies establishment. In the aim of finding the joint trading agreements which are lucrative for every participating party of the park, the proposed methodological framework for integrating conversion systems in a territory with non-cooperative scheme is employed. The problem is therefore formulated as a MAS in which the industrial agents set IA consists of the three sites of the park, $IA = \{IA_1, IA_2, IA_3\}$. Those transmit their energy and material requirements and discharges to the third party which exclusively intervenes in the potential assessment of inter-sites synergies based on purely exergy base optimization for the energy integration and consisting of the fresh resource minimizing for the material problem.

From the empty Material Message IA_1 receives from the third party subsequent to the material flows analysis, it derives that his wood discharge has no recovery opportunities in the territory in its existing form and thus defines its 72 000 annual wood discharge as its waste W_1^{wood}. With a view to increase its payoff, IA_1 launches an auction on W_1^{wood} for potential investors with a starting price C_0 of 10 € for the ton of biomass; thereby it could raise its yearly revenue by at least 0.72 M€ from selling its waste. Obviously an auction participant will want to invest in a system of processes requiring the auctioned W_1^{wood} as resource to generate commodities that can be then resold to other industrial agents of the park in which it is going to be implemented. Consequently the auction bidders which compose the potential agents PA of the problem are identified from the conversion systems database CS. This latter is formed by the three wood conversion pathways that enable respectively hydrogen, methane and energy generation, thus: $CS = \{CS_1^{wood}, CS_2^{wood}, CS_3^{wood}\}$ and $PA = \{PA_{1,1}, PA_{1,2}, PA_{1,3}\}$.

Each element in PA generates its sub-population from the identified sets of sovereign variables corresponding to every conversion route (cf. §4.3); hence a sub-potential agent of $PA_{1,1}$ with set q of SV is denoted as $PA_{1,1,\text{set q}}$. From its created population, a potential agent k selects the sub-agent having the highest bidding potential $PA_{1,k,\text{set q_}\beta k\max}$ to enter the auction with. However to lower the *computational time* burden, unfavorable sets were eliminated based upon the begat outcomes of the cooperative methodology application on the studied park. The potential agents' sets are therefore:

$PA_{1,1} = \{PA_{1,1,\text{set 10}}, PA_{1,1,\text{set 13}}, PA_{1,1,\text{set 18}}\}$
$PA_{1,2} = \{PA_{1,2,\text{set 3}}, PA_{1,2,\text{set 5}}, PA_{1,2,\text{set 7}}, PA_{1,2,\text{set 19}}, PA_{1,2,\text{set 25}}\}$
$PA_{1,3} = \{PA_{1,3,\text{set 19}}, PA_{1,3,\text{set 20}}\}$

The evaluation of their bidding potentials are conducted according to the investment strategy they follow. Similarly for the industrial agents that evaluate their received Trade Messages from the Network Investor (NI) based on the time they are willing to wait for prior to their net profit generation. With a view to eventually evaluate the results of the non-cooperative scheme with those generated from the methodology of a cooperative scheme, the following section will present the outcomes induced from integrating conversion systems in a territory with non-cooperative governance for the same 100 months long term investment plan set for the prior study. Nonetheless, a sensitivity analysis was carried out on the chosen investment strategies in the aim of assessing their impact on the auction winner and the trading equilibrium states. The aforementioned study will be subsequently explored as well as an evaluation of the gas market price fluctuations effect on the resulting EIP configurations.

4.5.2. Results for long term investment strategies

The first auction is launched with the NI proposing the buying and selling prices of heat respectively at 10% and 90% of the heat utility market price when the MWh of natural gas is at 30€. The auction ends by IA_1 allocating its W_1^{wood} to the highest bidder which was $PA_{1,1}$ for the amount of 85.35€ for the ton of wood. The wood to hydrogen conversion system investor actually entered the bidding with its $PA_{1,1,set\,10}$ that exhibited the highest bidding potential amongst its sub-agents; it could have raised its bid for the ton of wood up until its β_k of 193 €. $PA_{1,1}$was faced by another bidder that is $PA_{1,2}$ with its $PA_{1,2,set\,5}$. However the latter could not bid higher than the winning agent since it was unable to raise the final bid by $0.1\beta_{k\,PA_{1,2,set\,5}}$ which is equivalent to 8.68 € since it surpasses the cost for the ton of wood it could afford to reimburse its investment in less than 100 months. As for the cogeneration pathway that is the third potential agent $PA_{1,3}$, it does not even enter the auction by dint of its limited bidding potential β_k of 2.21 € for the ton of wood which is less than the initial reservation price of 10€ per ton. Subsequently, the auction winner is appended to the industrial actors and takes part in the negotiations for heat trading with the NI; thereby $PA_{1,1}$ becomes IA_4.

On the basis of the exergy based territorial HEN synthesis conducted by the third party with the updated industrial agents list, the NI establishes its first specific Trade Message destined to each IA. Those are expressed below in degree Celsius for the network temperatures in MW for the heat load and in Euros per MWh the buying and selling prices.

$TM_1 = [\{T_1,T_2\},\{Q_{11},Q_{21}\},\{P_1^s,P_2^s\}]_1 = [\{155,150\}\ ,\ \{4.23,1.70\ \},\{9.6\ ,\ 9\}]$

$TM_2 = [\{T_1,T_2,T_3\},\{Q_{12},Q_{22},,Q_{32}\},\{P_1^s,P_2^s,P_3^s\}]_2 = [\{155,\ 150,\ 145\}\ ,\ \{3.13,\ 3.13,\ 7.22\ \},\{9.6\ ,\ 9,\ 9\}]$

$TM_3 = [\{T_1,T_2,T_3\},\{Q_{13},Q_{23},,Q_{33}\},\{P_1^b,P_2^b,P_3^b\}]_3 = [\{155,\ 150,\ 145\}\ ,\ \{7.36,4.83,10.42\ \},\{1.07\ ,\ 1,\ 1\}]$

$TM_4 = [\{T_3\},\{Q_{34}\},\{P_3^s\}]_4 = [\{145\}\ ,\ \{3.20\},\{9\}]$

The industrial agents then evaluate their TM and send back an offer message to the NI. This is repeated until joint agreements are established between the entire agents of the territory which defines an equilibrium state. Noting that the decision of participating or not in a negotiated agreement is based on the agent *rationality* since a self-interested agent will only be part of an agreement if it gets him higher payoffs. From the resulting equilibrium state and based on the offer messages it received, the NI gradually increases the buying price or decreases the selling price for certain networks' temperatures at which the intended industrial agent did not exchange its full potential. The NI takes this action in the aim of motivating the industrial agent to trade greater amounts which might increase its own profit. Consequently, a new equilibrium state is determined for each TM with amended offers.

Ten distinct equilibrium states of EIP configurations are actually found for the studied territory. The NPV of each industrial agent are evaluated at the 100 months of operation to examine the profitability of each state at the date of their established investment horizon in reference to their economic statuses when acting as isolated agents. Figure 4.34 till Figure 4.38 illustrate the NPV for the ten given equilibrium states of the NI and of the four industrial agents, the fourth agent being the wood to hydrogen conversion system investor. By examining the outcomes of the first industrial agent, Figure 4.34, it can be noticed that IA_1 presents in the ten states consistent annual profits of 6.14 M€ generated from selling its 72 000 ton of wood waste to IA_4. It does not however participate in the heat network except in two equilibrium states 3 and 5 which induces a 6% raise in its profitability. This increase is due to the saved amount from buying 3.9 MW of heat at a 10% lower price than the market. It should be noted that even when trading heat with the NI the heat exchangers costs are still taken in charge by the industrial agent. For the similar reasons related to the energy exchange with the NI, IA_2 has an income in the equilibrium states 2, 4 and 7 being the only three in which it buys heat from the NI. Nonetheless in both states 4 and 7, IA_2 generates the same profits by dint of the identical amount of 7.22 MW of heat that it purchases at the same price from IA.

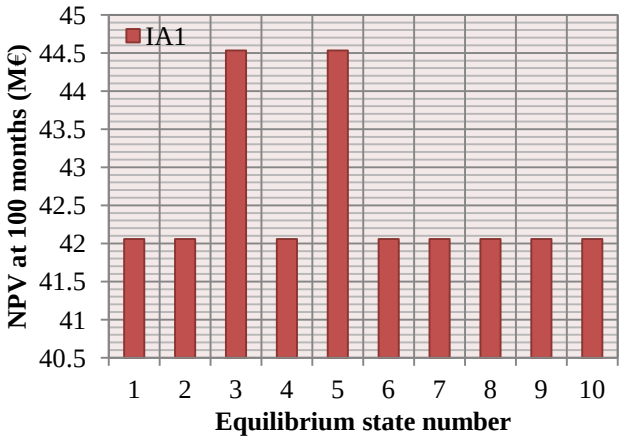


Figure 4.34. NPV at 100 months of operation of IA_1

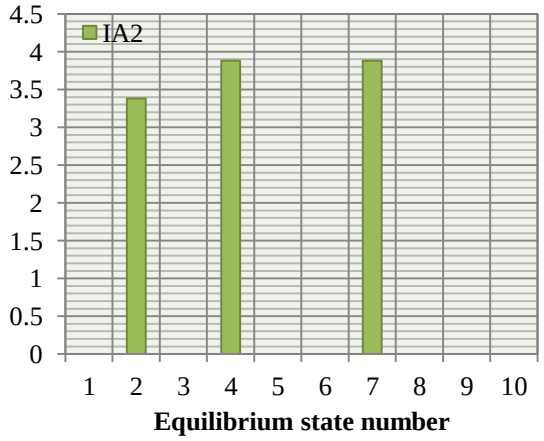


Figure 4.35. NPV at 100 months of IA_2

The only heat seller between the territory's agents and thus the main contributor is IA_3; hence it generates gains by trading its untapped heat surplus to the NI. From its NPV at 100 months of operation, Figure 4.36, it can be induced that the most lucrative state for IA_3 is state 7. Nonetheless through comparing the HEN configurations ensued from state 4 and state 7, it is perceived that both heat streams circulating patterns are identical except for the buying price the NI offers for the 10.42 MW of IA_3 at 145°C which is 44% higher in state 7. Therefore state 4 and 7 are with similar benefice for IA_2 while the latter results in greater payoffs than the former state for IA_3. Consequently, with the same quantities being sold to the NI by IA_3, the buyer will definitely get the lower price. Therefore state 7 is not *stable* in the presence of equilibrium state 4 since the NI decision weighs the most in the network construction and it will deviate from the established agreement towards the state that will add an incentive to its profit.

With the same reasoning another equilibrium state could as well be eliminated between state 3 and state 5 which results in the highest profitability for IA_1. In both equilibriums, the NI buys 3.91 MW of heat at 155 °C from IA_3 and then resells it for IA_1. Nevertheless, the heat purchase transactions from IA_3 are different. The NI pays 20% less in state 3 than it does in state 5 for getting the same amount of energy; the NI will favor the lower suggested buying value from the industrial agent when getting the exact product and hence the equilibrium state 3 is more *stable* than state 5.

Moreover, the EIP configuration in the equilibrium states 8, 9 and 10 only have one distinction being the heat buying price the NI pays to get 3.2 MW at 145 °C from IA_3. Between the three states the NI increases by 20% the buying price it offers for IA_3 with the aim of pushing this latter to sell more heat since its potential at this temperature is of 10.42 MW. However IA_3 trade exclusively 3.2 MW in this equilibrium states. Consequently, state 8 manifests as being of higher *stability* compared to the other two and hence it is, among the *stable* states, the most profitable one for IA_3.

The forth industrial agent IA_4 is the bio-refinery that buys the wood from IA_1 and converts it mainly into hydrogen which it sells back to IA_1. It thus has a substantial trading income from its annual 8 700 ton of hydrogen sold at the market price. As it can be seen from the NPV chart in Figure 4.37, IA_4 generates the highest gains in most of the equilibrium states except in states 1, 3 and 5 since in these latter states either no network is constructed (state 1) or the IA_4 is not offered to participate in it (state 3 and 5). Actually, IA_4 has to purchase its 3.2 MW heat demand at the market price when it does not buy its heat from the NI.

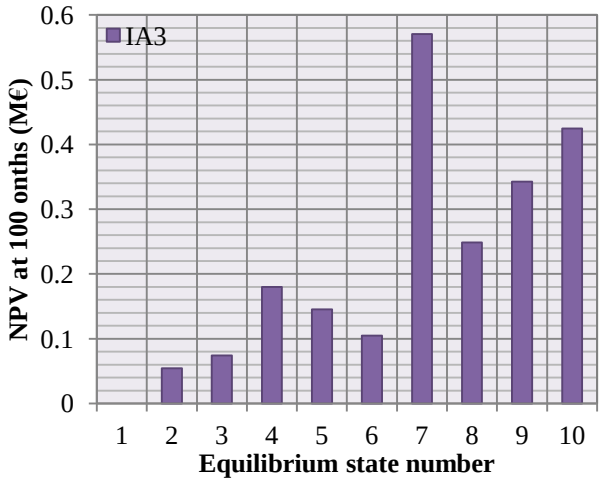


Figure 4.36. NPV at 100 months of operation of IA_3

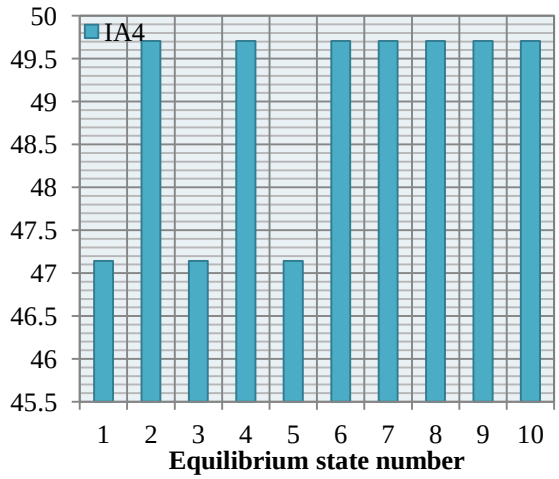


Figure 4.37. NPV at 100 months of IA_4

This latter generates the most profits in the equilibrium state number 4 in which the entire industrial agents of the territory except IA_1 take part in exchanging heat through the suggested network at 145°C. Those also participate in the heat synergies in the equilibrium states 2 and 7.

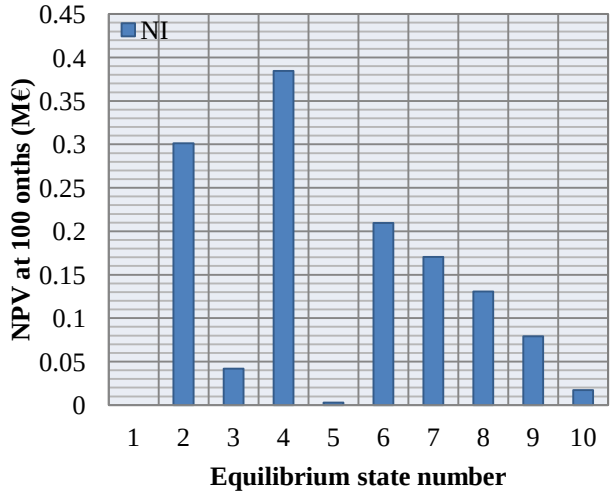


Figure 4.38. NPV at 100 months of the NI

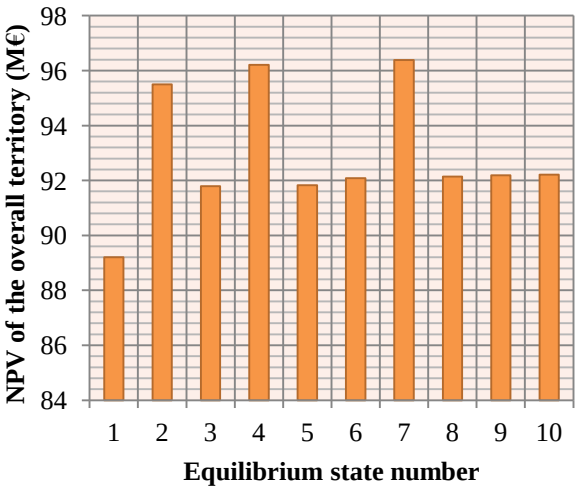


Figure 4.39.The equilibrium states social welfare

From the above results it can be noted the absence of a consensus for one equilibrium state. While IA_1 finds state 3 to be most lucrative, IA_2 generates its highest gains in state 4. Then again for IA_3 state 8 manifests as being its greatest profitable *stable* equilibrium. As for IA_4 it does not have a single favorite but instead has several. Yet, the NI does have a preferable state, this is state 4.

Consequently to select an EIP configuration for which the whole agents are satisfied from its implementation, the criterion of *social welfare* is employed. It is evaluated by the aggregation of the NPV at 100 months of the four industrial agents as well as that of the NI for each corresponding equilibrium state since the *social welfare* is defined by the sum of payoffs associated to a given agreement. As it can be seen from Figure 4.39, the three uppermost states are those in which the entire agents are involved in a certain material or heat synergy. From these three, state 7 induces the highest *social welfare*. Nonetheless as discussed earlier, this equilibrium state being unstable, from the NI perspective, the second best choice is state 4 and therefore it is considered as the most adequate equilibrium to be established.

It should be pointed out that the stable states were assessed considering the NI as being the single investor in the transport networks infrastructure which buys and sells heat through its constructed network. However, when competition does exist for buying and selling energy between multiple agents, the NI should assess the risk related to favoring a negotiated agreement over another which might influence the decision of the involved industrial agent. As for instance in equilibrium states 4 and 7 in which IA_3 prefers the negotiated agreement in state 7, whereas the NI has higher gains from state 4. Therefore with several involved agents for buying the heat from IA_3, the NI has interest in establishing the agreement in state 7 even if it is for less profit in order to ensure that IA_3 will not deviate towards selling its 10.42 MW to another heat buyer with a better proposal. In this case study the NI is indeed the only agent taking in charge the heat purchase and sales and thus state 4 is most likely to be the established agreement between the industrial agents of the territory in non-cooperative governance. The EIP configuration resulting from this equilibrium is depicted in Figure 4.40 which shows the purchase and sales transaction between the agents of the territory.

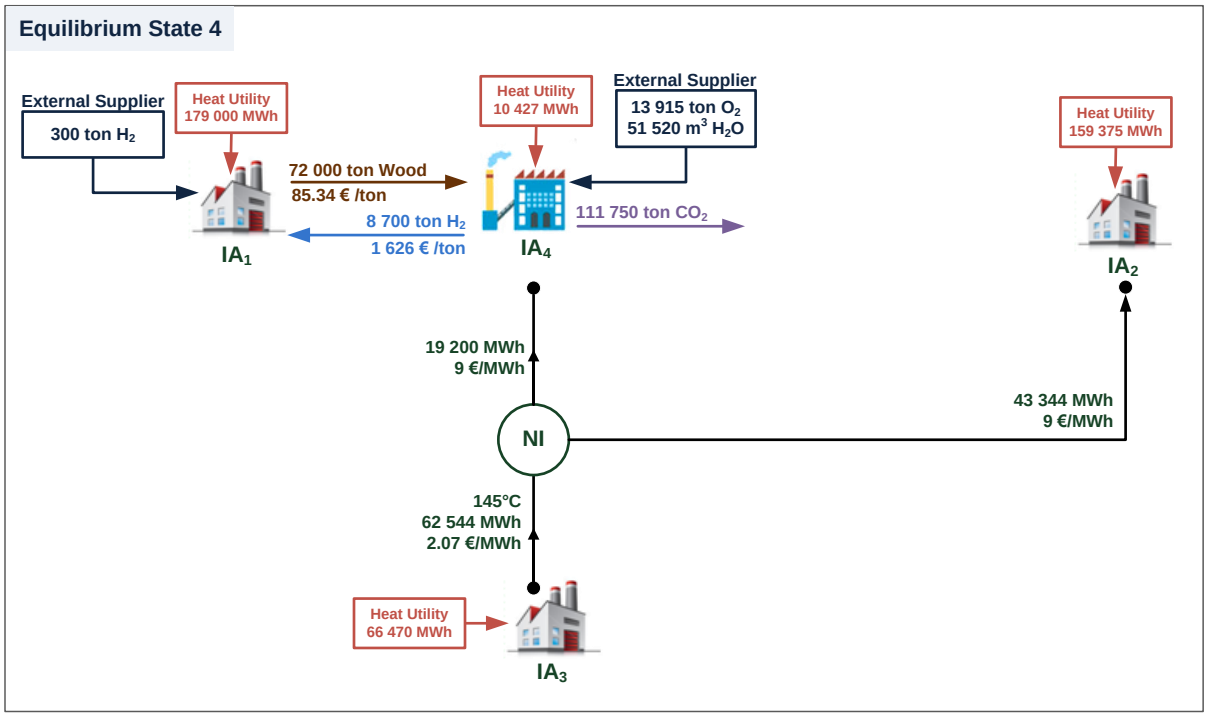


Figure 4.40. EIP configuration of the most adequate equilibrium state in non-cooperative scheme

Remarkably, the recovered heat through the network is 62 544 MWh versus a network capacity of 19 200 MWh in the cooperative scheme. The additional 43 344 MWh are as well recovered from IA_3 and sold to IA_2 which was not participating in the network for the cooperative pattern. Subsequently, the *social welfare* of the territory in the non-cooperative scheme of 96.21 M€ is roughly 4% higher than the NPV of the territory with a cooperative economic governance. The reason for these unexpected outcomes might be related to the sequential method employed in the cooperative scheme to design the local and territorial heat networks in which the two problems are iterated to converge towards an EIP pattern which could be the result of a sub-optimal synergy configuration.

The adjunction of the wood conversion system created new synergies opportunities for a more dynamic territory. IA_4 is the bio-refinery formed by the series of the wood to hydrogen processes with the set 10 of sovereign variables. Another prominent result is that the conversion system that was found in the cooperative scheme application to be the most interesting to implement in the studied territory is the same that won the auction for wood and participates in the non-cooperative negotiations. This again emphasizes on the importance of assessing the required resource of the park when selecting the conversion systems to be further investigated.

In fact even by repeating the wood auction with enhanced trade messages of lower selling and higher buying prices, the wood to hydrogen conversion system investor wins every time with the same sub-agent $PA_{1,\,1,\,set\,10}$. The bidding potential of the potential agents' population are exhibited in the charts of Figure 4.41, Figure 4.42 and Figure 4.43 for a pace increase of 10% for the heat buying price and 10% decrease for the selling price. Despite the slight increase $PA_{1,\,1,\,set\,13}$and $PA_{1,\,1,\,set\,18}$ exhibit from the growth of the offered heat buying price, $PA_{1,\,1,\,set\,10}$still has 30% higher bidding potential compared to the former sub-agent and roughly 60% more than the latter.

The wood cogeneration investor in the other hand, will always select to enter the auction with its sub-agent $PA_{1,3,\,set\,20}$ with the proposed heat offers. However it could not compete with the hydrogen production investor by dint of its relatively low bidding potential in comparison to $PA_{1,1}$.

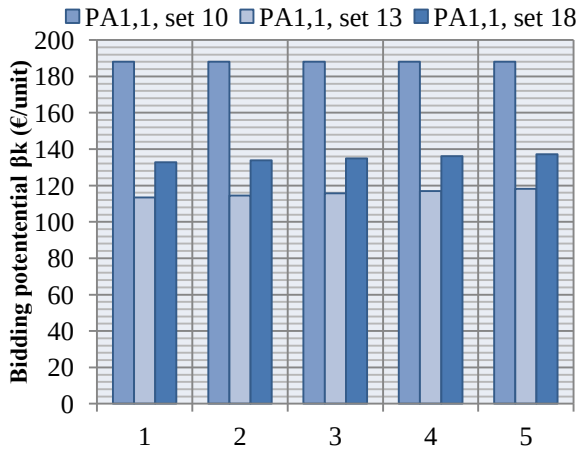


Figure 4.41. Bidding potentials of $PA_{1,1}$ population

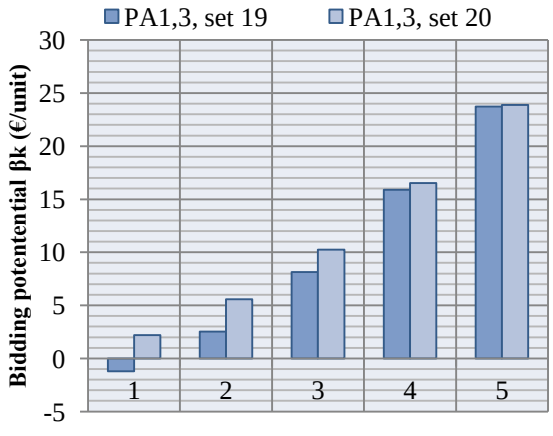


Figure 4.42. $PA_{1,3}$ population bidding potentials

Yet, $PA_{1,2}$ manages to challenge $PA_{1,1}$ to a certain point at which it could not exceed the placed bid by the wood to hydrogen investor, ensuing the raise of the final bid from the low initial reservation price of wood. $PA_{1,2}$ actually chooses to take part in the auction with its sub potential agent having the studied set of sovereign variables for methane production number 5 due to its upmost bidding potential that comes to surpass the slender increase in the other agents bidding capacities.

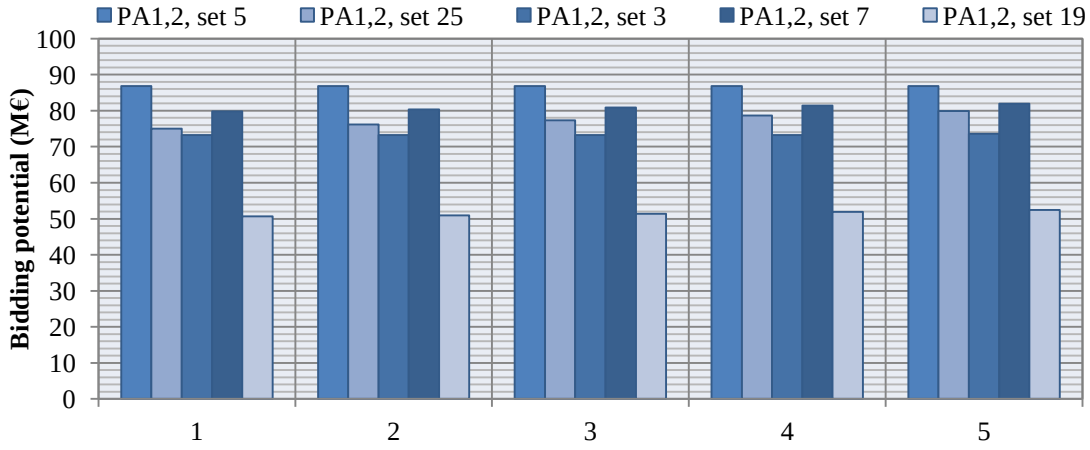


Figure 4.43. $PA_{1,2}$ population's bidding potentials

Notably, for each of the three conversion pathway investors the sub-agent presenting the highest bidding potential has the identical set of sovereign variables as CS_k^{wood} of the best judged scenarios ensued from the cooperative results. Consequently, for better *computational efficiency* unfavorable sub potential agents could indeed be ruled out based on the park's cooperative assessment.

4.5.3. Sensitivity Analysis

The equilibrium states of the negotiations between the agents of the territory are highly dependent on the strategy an agent has set for its investment to start inducing profits. The previous transactions pattern resulted from long term investment strategies in which the corresponding agents would not mind their gain to be initiated 100 months after the installation of the negotiated EIP configuration. With a view to evaluate the agents alterations of profitability as well as the impact on the energy and material equilibrium transactions, a sensitivity analysis for short and medium term investment strategies is explored in the following section. Further analyses are as well carried out to investigate the gas market fluctuations effect on the auction winner and the induced states equilibrium.

4.5.3.1. Time of investment strategies

The basis of a *rational* self-interested agent decision to consent a trading agreement is whether the payoffs it gets from participating in the negotiated trade are greater than if it does not take part of it. Consequently when the payback time is of medium or short term, the pipelines investment that the NI might have to bear manifests fewer chances to be compensated with the gain it generates from buying heat at low cost and then selling it for a higher price. Even for the main heat synergy contributor IA_3, the additional heat exchanger costs that it has to afford when exchanging its heat surplus with the NI could be non-redeemable in the fixed short period of time with its induced profits from trading with the NI.

This fact could actually be exhibited in the results from integrating wood conversion systems in the studied territory with self-interested agents first as having a short investment plan of 25 months and then for a medium term investment of 50 months. Unsurprisingly for both short and medium term strategies, the only resulting equilibrium state is that with no network being constructed since the exchanged heat through the network are not enough for the NI to get its investment reimbursed at the desired time horizon due to the lower heat quantities IA_3 proposes to sell to the NI. Therefore with a negative NPV the NI is better off without making any trading with the industrial agents and thus it does not implement any network base on its *rational* assessment.

As for the potential agents, $PA_{1,1}$ and $PA_{1,2}$ still find it lucrative to invest in a wood conversion system due to the higher values of methane and hydrogen compared to heat. These two agents compete to place higher bids for the 72 000 ton of wood auctioned by IA_1. Nonetheless, in both short and medium term investment strategies the wood to hydrogen conversion system investor takes over the auction by its higher bidding potential as was also the case for the long term investment plan.

The bidding potential alterations for the three potential agents winning sub-agents investment strategies are presented in Figure 4.44. Predictably, the bidding capacities grow with the desired year of return on investment increase. The potential agents are hence able to pay additional cost for the wood by dint of the longer time they can put to reimburse their investments. The negative values $PA_{1,3}$ exhibits point out its incapability to bid on the wood in the corresponding auction. Apparently, the wood cogeneration is not profitable when an external investor wants to invest in due its low generated inflow in comparison to its required investment.

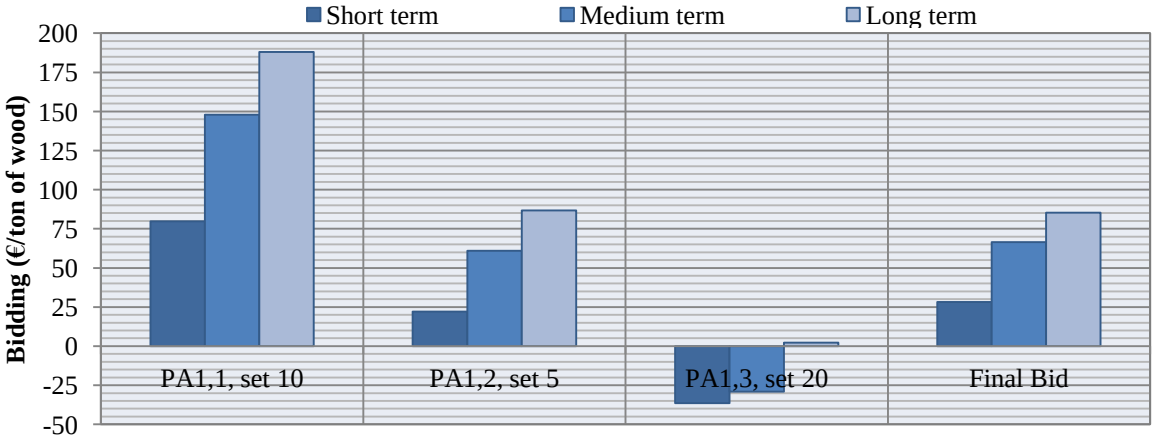


Figure 4.44. Bidding potential and final bid variation with the investment strategy

The final bid variation increases following the same pace as the bidding potential since it is directly related to the ability of the potential agents to raise the previous bid. For the three evaluated investment strategies, IA_1 rewards the auctioned commodity to the wood to hydrogen system investor which places the highest bid for the ton of wood of respectively from the lower to the higher desired time of return 28.14 €, 66.56 € and 85.35€. Consequently for the single equilibrium state ensued from the short term strategy and the one resulting from the medium term plan, two material synergies are established. The first is the 72 000 ton of wood allocation from IA_1 to IA_4 (i.e., the winning potential agent) and the second is the 9 000 ton of hydrogen exchange between the same agents which induces an annual gain of 14.63 M€ for IA_4 in both of the investment strategies. The wood sales income reduces the variable cost of IA_1 by roughly 2 M€ for a potential agent with a short term investment plan and cut it down by 4.8 M€ when the uttermost desired payback time set by IA_4 is of 50 months.

4.5.3.2. Gas Market fluctuations impact

With the self-interested agents of the studied territory, the gas market fluctuations could be a detriment for the synergies establishment of the lower value exchanged commodity that is heat. This latter is directly correlated to the gas price and thus follows its identical decrease pace. Actually for low gas market price, the industrial agents will favor releasing their excess heat to low temperature cold utilities even for no monetary benefits instead of investing in additional heat exchangers to trade their surplus energy with the NI due to the low heat buying price the latter can afford to propose.

Nonetheless when the market alters towards higher gas prices, the NI have to offer greater heat buying price thus motivating the industrial agents to install further heat exchangers to sell their surplus heat to the NI since they could redeem the investment they make faster. The analysis of the market fluctuation impact is based on the ensued outcomes from the non-cooperative methodological framework with a long term investment strategy for a low gas market price of 20€ the MWh, the current gas price per MWh of 30€ and a high market price of 40 € the MWh. The results from the gas price at 30 € per MWh were examined in section 4.5.2 and those from the low and high gas market prices are discussed in the following paragraphs.

Similarly to all the previous auctions, the wood to hydrogen conversion system investor is again the winner of the auctions with both low and high gas price. While IA_1 allocates its auctioned waste to the potential agent $PA_{1,\,1}$ for a ton of wood of 61.38 € when the gas price is 20€ the MWh, it is paid 107.12 € for the ton of wood by $PA_{1,\,1}$ with the high market gas price. This great difference is related to the increase of the hydrogen value with that of the natural gas since the former market worth is supposed intertwined to the fluctuations of the latter's. The bidding potential actually exhibits similar variations tendency as the listed results in Table 4.10 display.

Table 4.10. Bidding potential of the three PA for the investigated gas market prices

Potential agent	$PA_{1,\,1,\,set\,10}$	$PA_{1,\,2,\,set\,5}$	$PA_{1,\,3,\,set\,20}$
Low gas market price	134.72 €/ton	54.82 €/ton	1.17 €/ton
Medium market gas price	193.25 €/ton	86.82 €/ton	2.21 €/ton
High market gas price	244.52 €/ton	118.81 €/ton	3.33 €/ton

Merely three distinct equilibrium states are induced for the low gas price in which the latterly appended IA_4 trades hydrogen and wood with IA_1. Two of the equilibrium states include heat synergy through the constructed pipelines by the NI. In both states the NI buys 3.2 MW at 145 °C from IA_3 and resells it to IA_4 for 6 €/MWh. While in state 3 the NI offers to get the MWh from IA_3 for 2 €, in state 2 it just proposes 1.66 € for the MWh. Consequently, IA1 and IA4 generate the same gains in both of the equilibrium states but IA_3 gets the highest profits in state 3. Nonetheless state 2 is the most profitable for the NI thus it seems that it is more stable considering the monopolistic position of the network investor which will deviate towards its more lucrative state for similar heat synergy patterns.

On the other hand, with the high gas market price thirteen different equilibrium states were induced since the greater profits generated from the higher heat price motivate IA_3 to sell more of its heat to the NI. The NPV at 100 months of operation are established for the thirteen states and are represented for each agent of the territory from Figure 4.45 to Figure 4.49.

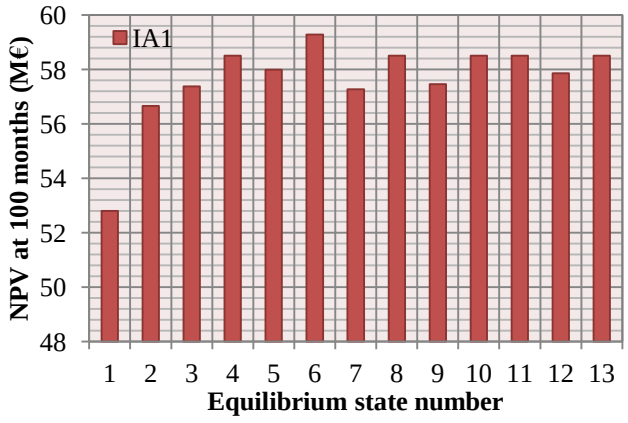


Figure 4.45. NPV at 100 months of IA_1

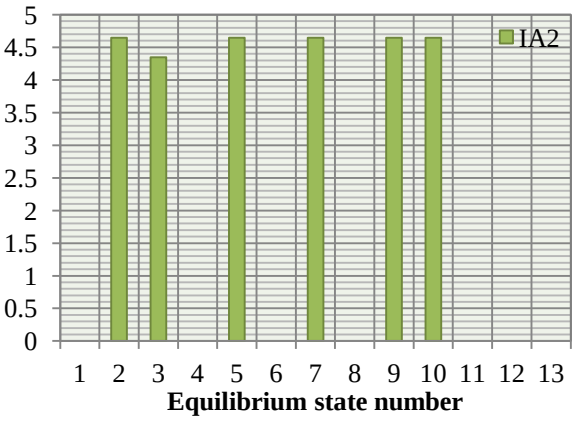


Figure 4.46. NPV at 100 months of IA_2

IA_1 presents a consistent profit of 53 M€ from its wood sales income. It gains even more when it gets a part of its heat utility from the NI for lower cost than the heat market price. From Figure 4.45, it can be deduced that IA_1 takes part in the inter-sites heat exchange in the entire equilibrium states except in the first where no network is even constructed. However, the most profitable trading agreements for IA_1 manifests in equilibrium state 6 in which it buys from the NI at 90% the market heat price the highest amount of 8.87 MW at 165 °C compared to the other states.

The profits of the second industrial agent IA_2 compared to being an isolated agent are only induced from its purchase of heat from the NI. Yet, it does not always participate in the network as it is read from the chart in Figure 4.46. But when it does, it buys the identical amount of 5.93 MW at 145°C and thus generates similar gains except in state 3 in which the NI proposes 7% less heat being the only amount it buys from IA_3 at this temperature.

IA_3 is actually the exclusive heat provider to the NI since no other industrial agent presents heat excess at the required temperatures. The most profitable equilibrium for it is thus when the NI offers to buy its excess heat at the highest price in comparison to the other states proposal prices. In state 13, the NI buys 7.64 MW of heat at 165°C from IA_3 at more than 50% of the heat utility market cost and hence inducing the highest NPV at 100 months for IA_3, Figure 4.47. The second best state for IA_3 is state 10 in which it sells the biggest amount of its excess heat.

The potential agent that won the auctioned wood IA_4 converts it mainly into hydrogen which makes up the biggest part of its revenues since IA_4 sells it to IA_1 at the hydrogen market price of 2 128€ the ton for a 40 € the MWh of natural gas. Yet IA_4 does not take part in the heat synergies and thus preserves consistent gains in the entire equilibrium states.

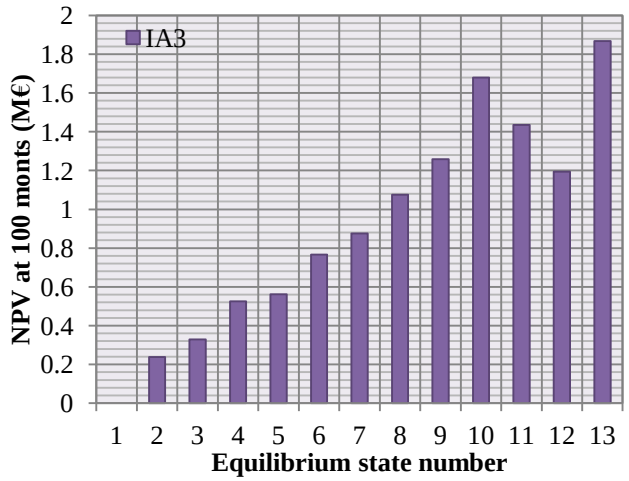


Figure 4.47. NPV at 100 months of IA_3

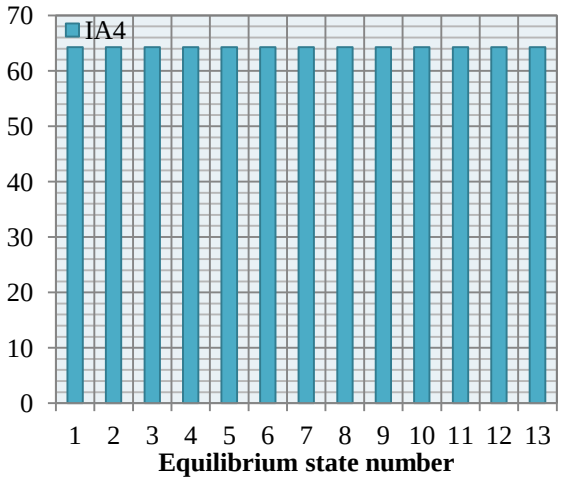


Figure 4.48. NPV at 100 months of IA_4

The equilibrium state 6 manifests to being the most lucrative for the NI, Figure 4.49. This is due to the established agreements consisting of the highest energy exchange for a single pipeline investment. The NI buys the MWh of the 8.87 MW of heat at 165°C from IA_3 at 4.77 € which is 30% the market heat price and resells the same amount for roughly three times more to IA_1.

Even though the equilibrium state 6 is the most lucrative to both the NI and IA_1, IA_3 performs economically better in state 13. And while IA_2 does not have a preference between states 2, 5, 7, 9 and 10, IA_4 do not take part in the heat synergy in none of the joint agreements. Consequently, with no single equilibrium state in which the entire agents will have maximum profits the *social welfare* is again employed to determine the most probable heat transactions to take place. Figure 4.50 illustrates the social welfare of the territory for the thirteen equilibriums induced from the high gas market price.

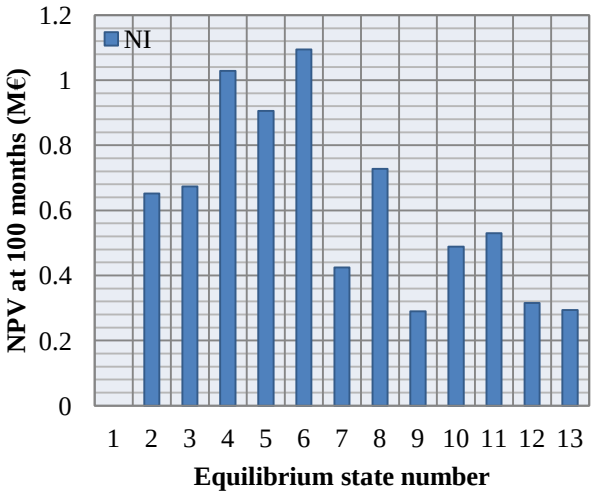


Figure 4.49. NPV at 100 months of the NI

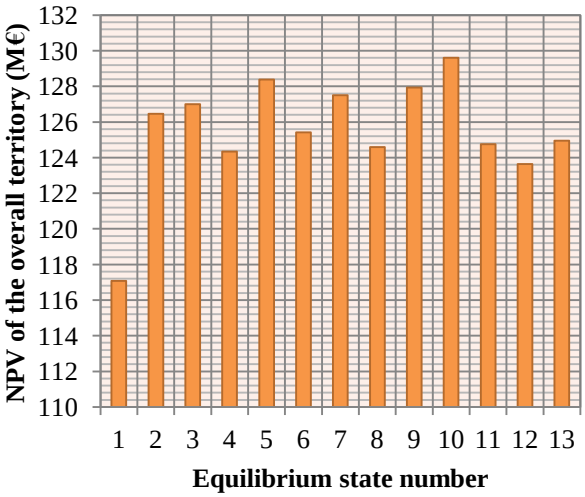


Figure 4.50.The equilibrium states social welfare

Notably the heat exchange joint agreements between the industrial agents and the NI in state 10 ensue the highest combined gains with the uppermost *social welfare* of 129.6 M€; showing again that the non-cooperative scheme welfare is 3% higher than the one engendered from the cooperative governance. The resulting energy and material transactions between the agents of the studied territory are depicted in the EIP pattern of Figure 4.51 for the equilibrium state 10. The NI constructs two networks at 165° C and at 145 °C with a heat capacity of respectively 7.64 and 5.93 MW. It buys the heat at the high temperature from IA_3 for a MWh of 6.88 € and transfers it through the pipeline to IA_1 for 14.4 € the MWh, whereas at the low temperature it gets the heat from IA_3 as well at roughly 4 € the MWh and sells it to IA_2 for triple the price. The remaining heat requirements are purchased from the heat utilities available for each agent. For the material synergies, IA_1 allocates its wood for 7.71 M€ to IA_4 which sells back the hydrogen it produces from the wood conversion to IA_1.

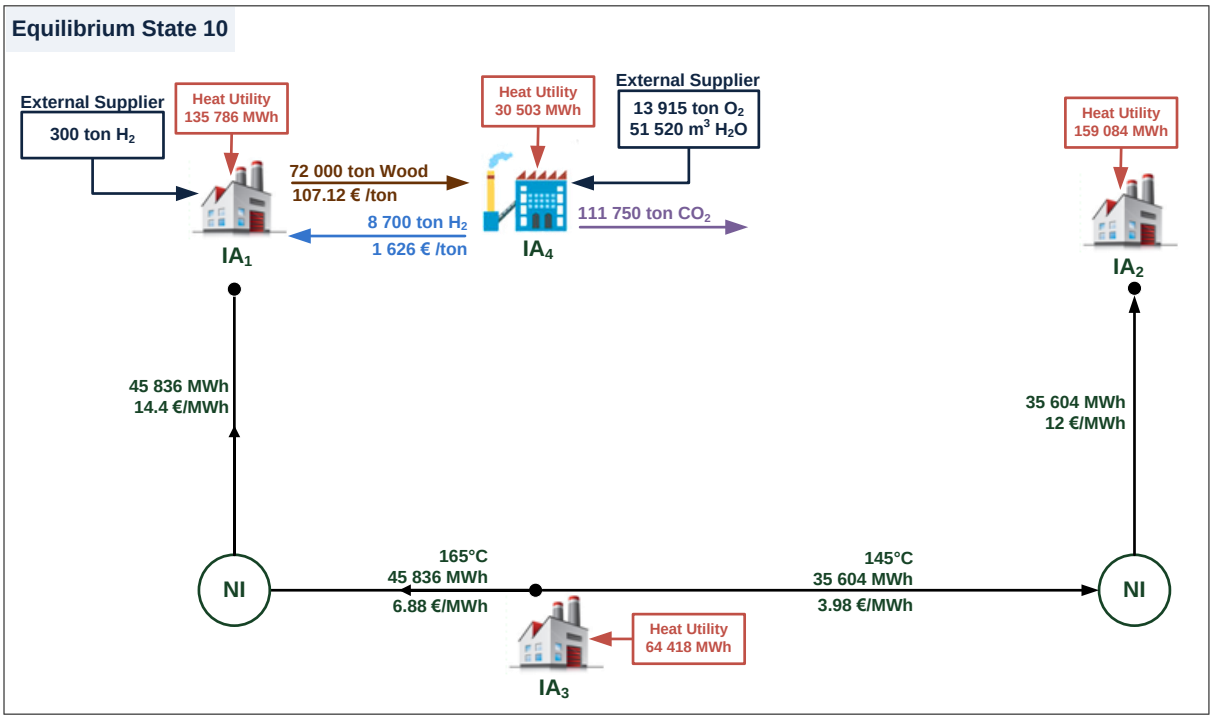


Figure 4.51. EIP configuration of the upmost welfare equilibrium state for the high gas market price

The above described state with the highest *social welfare* is noticed to be as well the state in which the greatest heat synergies of 13.57 MW are established. Actually when IA_1, IA_2 and IA_3 are involved in the heat transactions, the heat network capacity is above 10 MW, whereas when just IA_1 and IA_3 trade with the NI its highest is 8.87 MW. The heat network capacity for each established equilibrium state of the investigated low, medium and high gas market prices are illustrated in the charts of Figure 4.52 in which the null values indicate that for the corresponding equilibrium state no network was installed. As expected, comparing the heat synergies magnitudes reveals that greater heat amounts are exchanged through the network with the alteration of the gas market price towards higher values. This mainly due to the fact that heat will become more expensive forcing the NI to offer higher buying prices for the IA_3 thus giving sense to this latter investment in bigger heat exchangers to transfer its surplus to the proposed steam network.

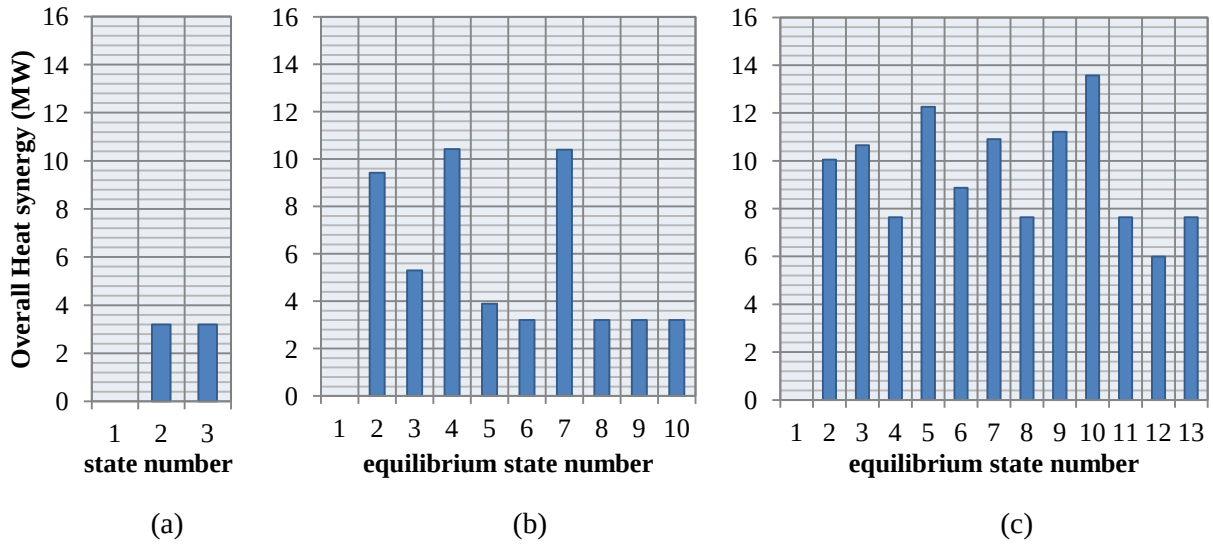


Figure 4.52. Overall heat synergies for the studied gas market prices: (a) low, (b) medium, (c) high

From the results and analysis of the sensitivity assessments over the agents' investment strategies and the gas market price it can be stated that the wood to hydrogen conversion is the most profitable wood pathway to invest in its implementation in the investigated park compared to the wood to methane or wood cogeneration routes. Indeed, $CS^{wood}_{1,\,set\,10}$ withstands the gas market fluctuations as well as the desired investment reimbursement plans alterations by preserving its first ranking for the highest bidding potential. Therefore it ensures for the entire collection of equilibrium states the upgrade of the previously non-usable wood into a commodity of higher value and thus creating unprecedented synergies in the park which are otherwise unattainable.

It was also noted that the established heat synergies in the territory are highly impacted by the set target for the uttermost allowable return on investment to the extent where short and medium term investment strategies could be the detriment for heat trading opportunities. The reason behind this is the small disposable period to assert the investment reimbursement of the larger heat exchangers for the industrial agents or of the pipeline for the network investor. On the other hand, the gas market price plays a major role in the offered buying and selling prices by the network investor. Therefore higher gas prices entail more gains for the industrial agents thus they exchange more heat which results in greater network capacities.

4.6. Conclusions

This chapter served as an application platform for the two proposed methodological frameworks for conversion systems integration in an industrial territory with both cooperative and non-cooperative governances. The studied territory had wood as the non-usable stream to be converted and presented heat and hydrogen demands. Therefore three conversion pathways were challenged in both economic schemes. Those were the wood conversion to hydrogen, to methane and to energy.

In the cooperative scheme, the industrial actors were supposed to freely exchange their energy and material streams to ensure the most profitable EIP configuration for the territory of which they share the investment and the engendered gains. On the other hand in non-cooperative governance, the agents of the park are *rational* and self-interested they thus act upon their payoffs from engaging in a negotiated agreement for energy and material trading; each agent has its individual economic status. The prime inferences ensued from the application of the proposed methodologies are classified into five major categories according to the governing scheme and depending on the specificity of the conclusion to the wood conversion system integration in the studied park.

Specific conclusions entailed from the cooperative scheme application:

- The most suitable set of sovereign variables of the wood to hydrogen conversion process to be integrated in the park was found to be $CS^{wood}_{1,\,set10}$ which consists of the lowest SB_{ratio} and the highest $T_{gasifier}$ and T_{SMR} that result in the greatest hydrogen yield.
- For the valorization route of the non-usable wood through its conversion to methane, $CS^{wood}_{2,\,set\,5}$ should be integrated in the studied territory to attain the uppermost profit.
- The most profitable balance between heat and electricity production for the territory operating under cooperative governance is found to be that entailed from $CS^{wood}_{3,\,set\,20}$.
- The hydrogen production is the conversion route that results by far in the lowest variable cost; however it demands the most funds to install the computed EIP pattern.
- The wood cogeneration requires the least investment to put in place the induced EIP configuration; yet it results in the highest variable cost compared to the other two conversion routes.
- Neither installing a cogeneration system nor a wood to methane conversion process come to reimburse their initial investments at the wood market worth of 154€ per ton. Above 261€ the value of the wood ton, it is no longer lucrative to implement any of the wood conversion routes. Both values are relatively high; they are used to point out the distant scenario of not integrating a reacting wood conversion system in the park.
- The conversion pathway that undertakes the least damages with the gas market fluctuations and with the non-usable waste earning monetary value was found to be the wood conversion into hydrogen $CS^{wood}_{1,\,set10}$.

Specific conclusions entailed from the non-cooperative scheme application:

- Even though for the same conversion pathway some sets of sovereign variables might advance on others in terms of their bidding potential, for the studied wood conversion systems the similar sub potential agent kept on winning.

- The wood to hydrogen conversion system investor manages to place the highest bid in the wood auction with the same sub-agent $PA_{1,\,1,\,set\,10}$. It is thus the most profitable wood pathway to invest in its implementation in the investigated park.
- $CS^{wood}_{1,\,set\,10}$ withstands the gas market fluctuations as well as the desired investment reimbursement plans alterations by preserving its first ranking for the highest bidding potential amongst the other two conversion routes.

Global conclusions entailed from the cooperative scheme application:

- An overall view on the operation life time of the territory is mandatory to assess the flexibility of the decision makers' position on their investment reimbursement time with a view to greater profitability in the upcoming years.
- The sequential method employed in the cooperative scheme for the design of the local and territorial HEN in which the two problems are iterated to converge towards an EIP configuration might be the result of a sub-optimal synergy pattern.

Global conclusions entailed from the non-cooperative scheme application:

- The monopolistic position of a single network investor might lead to higher risk for industrial agents breaking a joint agreement for another more lucrative forthcoming offer. The NI should therefore carry out risk assessment and consider lowering its payoff for the benefit of the industrial agents by for instance opting for the equilibrium state inducing the highest *social welfare* that could considerably lower its risks.
- Short and medium term investment strategies could lead to limited heat recovery opportunities due to the transport network and heat exchanger substantial costs.
- The increase in natural gas market price stimulate self-interested agents to bear the additional investment expenses to trade their surplus heat with the network investor by dint of the greater profits induced from the higher heat price.

Global conclusions from both cooperative and non-cooperative scheme applications:

- The integration of reacting conversion systems in a territory to upgrade non-usable streams into another form of greater opportunities for reuse in the park entails major enhancement in the energy and material synergy patterns.
- The outcome of the most profitable conversion system is highly impacted by two main factors; the first being the resources requirements of the park in which it is going to be implemented and the second is the upgraded new product value.
- The conversion pathway that scores the best results when integrated in the cooperative scheme will most probably have the highest bidding potential in the non-cooperative scheme and hence win the auction for the non-usable stream to be converted.
- To reduce the *computational* burden of the non-cooperative framework, unfavorable sub potential agents could be ruled out based on the outcome from integrating the investigated conversion pathways in the territory using the cooperative methodology.

Conclusions and Perspectives

In recent years, industries search for cost-effective technical solutions enhancing their resource management to comply with the current and upcoming restrictive ecological regulations has never ceased to increase. Many literature studies were conducted to assess the feasibility of heating networks based on industrial heat recovery and similarly for material reuse and recycling aiming to propose technical options for better energy efficiency and resource use. However reacting conversion systems create new valorisation opportunities for the energy or material streams, adjudicated as non-usable by conventional process integration techniques, through converting them into new recoverable products and thus reintroducing them back into the production cycle.

In this perspective, the objective of this doctoral work was to develop a methodology to generate optimal synergy topology for an EIP encompassing the form alteration of unrecoverable waste via conversion systems. EIP with two economic governance were evoked for this purpose. The first is a territory governed by cooperative scheme wherein industrial actors are supposed to share costs and gains as a single entity collaborating to establish inter-sites synergies by exchanging their energy and material streams for free to ensure the most profitable EIP configuration. The second is an EIP functioning under non-cooperative governance in which industrial participants are self-interested acting upon their payoffs from engaging in a negotiated agreement for energy and material trading which are accomplished through purchase and selling transactions.

Consequently, two novel conceptual frameworks, for incorporating reacting thermodynamic conversion systems to the material and energy integration problems in both cooperative and non-cooperative schemes, were proposed in this doctoral dissertation. State of the art models were employed for the methodological bricks of the energy and material integration served for the construction of the proposed frameworks.

The proposed methodology for a cooperative governance was formulated as a Master-slave problem, in which the Master problem creates the potential territory's scenarios by manipulating the sovereign variables of the non-usable identified streams' conversion processes which are established in the conversion pathways' superstructure. The two slave problems that acts according to the sovereign variables of the Master problem are the MILP models of the local and territorial integration. This methodological framework enables the identification of the best design and technical specs of the non-usable streams conversion scenarios which are put in competition with other alternative conversion routes.

The second methodological framework was proposed for designing EIP with non-cooperative governance in which actors search to maximize their individual interests. Formulating the problem

using centralized mechanism with a single objective was found to be complex considering the non-linearity of the actors' aggregate activities. Therefore the problem was formulated using agent-based modeling enabling to account for several heterogeneous agents each with its own objective function and that acts and reacts to each other's behavior.

The interaction between agents was established using the negotiation mechanisms to ensure the coordination between their actions. Three types of agents were defined: network investor agent, industrial agent, potential agent. The NI is supposed to negotiate with the other agents to trade energy and material streams through bilateral bargaining following the alternating offers protocol. The territorial heat integration problem, being the NI core, was modified to account for the buying and selling prices of energy. For each non-usable waste an industrial agent discharges, a single sided auction based on the English Auction is held with the industrial agent being the auctioneer and the potential agents as the collection of bidders in the aim of allocating the waste to the bidder with the highest bid. The potential agents refer to the possible reacting thermodynamic systems which can change the initial composition of waste streams and convert them into new products that it could sell to other industrial actors. The proposed methodology enables the establishment of the strategic decisions to be implemented by each self-interested agent in a territory with non-cooperative governance by identifying the equilibrium prices for the purchase and sale flows between agents.

Both proposed methodological frameworks were demonstrated on an industrial activity zone consisting of three sites presenting hydrogen and heat demand. The preliminary study of the studied industrial park evinced the missed opportunities for the discharged wood waste to be recovered in the territory due to the lack of such demand. The conversion of the non-usable wood was proposed to alter its initial form into more interesting commodities for the territory. Consequently, the transformation of wood to hydrogen, the conversion route towards methane production and the conversion pathway of wood into energy were the three selected reacting conversion systems to be investigated. The process units forming each of these pathways were identified and then modeled by their economic and physical models based on their energy and material balances while accounting for the chemical reaction occurring within the reactors. The developed models were validated or compared to literature results and thus proved to be reliable to be employed as a database for both cooperative and non-cooperative frameworks application.

The application of the proposed methodological frameworks on a realistic industrial park demonstrated how to implement conversion processes in a territory that reinsert streams judged to be non-recoverable by conventional on-site and inter-site energy and material integration techniques ensuing substantial operating costs savings and enhancing the park's circular economy. It was inferred that the most profitable conversion system is highly impacted by two main factors; the first being the resources requirements of the park in which it is going to be implemented and the second is the upgraded new product value. In the non-cooperative framework, the computational burden is advised to be reduced by ruling out unfavorable sub-potential agents based on the outcome from integrating the investigated conversion pathways in the territory using the cooperative methodology.

Therefore, this demonstration study proved the capabilities of the novel developed methodologies that enable going further towards closing the energy and material loops. They serve as decision support tools for neighboring industries searching to evolve towards becoming an EIP by proposing strongly viable EIP topology including the best design and technical options of the non-usable streams conversion systems. Nonetheless some limitations still need to be addressed to strengthen their potential outcomes.

For instance, the sequential method employed in the cooperative scheme for the design of the local and territorial HEN in which the two problems are iterated to converge towards an EIP configuration might be the result of sub-optimal synergy pattern. To surpass this limitation and reach optimal synergy topology, simultaneous local and territorial energy integration optimization could be developed for the cooperative problem. Nonetheless the feasibility of such approach should be assessed considering the numerical burden which might encounter from the problem complexity.

Moreover, the selection of the sovereign variables to be altered strongly impact the best operating and design parameters of the conversion system and thus the most profitable conversion route to be implemented. Therefore a methodology should be developed to properly select these variables by assessing the most influential parameters on an exergy basis on the process outcomes.

In the non-cooperative scheme, the monopolistic position of a single network investor might lead to higher risk for industrial agents breaking a negotiated agreement for another more lucrative forthcoming offer. To prevent such situations, the methodology for a territory with self-interested actors could be extended to include several network investors that compete to transfer resources and energy through their constructed transport network. The industrial agents thus receive multiple offers from which to choose ensuing energy and material transactions patterns of higher stability.

The work initiated in this thesis is not limited to a complex problem but form a part of a moving reflection to enable migrating from the extractive linear model towards sustainability through circular economy. Further research developments could therefore be interesting to conduct to push along this transition.

For instance, the impact of data uncertainties on the resulting EIP topology robustness is still to be assessed before implementing the energy and material synergies. This could be carried out by fluctuating the process parameters to evaluate if any operation limitation for the proposed design does exist. Moreover, the models of HEN and MAN designs employed in the developed frameworks in this thesis are contend to continuous operating mode. Although substantial number of industrial processes do operate in such mode, others run in batch. Therefore, to account for both type of processes, the network design models should be extended to subjoin the time dimension.

References

Amadeo, N. & Laborde, M., 1995. Hydrogen production from the low-temperature water-gas shift reaction: Kinetics and simulation of the industrial reactor. *International Journal of Hydrogen Energy,* 20(12), pp. 949-956.

Amarkhail, S. s., 2010. *Air Separation.* Bratislava: s.n.

Andersson, J., Lundgren, J. & Marklund, M., 2014. Methanol production via pressurized entrained flow biomass gasification -Techno-economic comparison of integrated vs. stand-alone production. *Biomass and Bioenergy,* Volume 64, pp. 256-268.

Bagajewicz, M. & Rodera, H., 2002. Multiple Plant Heat Integration in a Total Site. *AIChE Journal,* 48(10), pp. 2255-2270.

Berghout, N., Kuramochi, T., van den Broek, M. & Faaij, A., 2015. Techno-economic performance and spatial footprint of infrastructure configurations for large scale CO2 capture in industrial zones A case study for the Rotterdam Botlek area (part A). *International Journal of Greenhouse Gas Control,* Volume 39, pp. 256-284.

Bingyan, X. et al., 1994. Circulating fluidized bed gasifier for biomass. *INTEGRATED ENERGY SYSTEMS IN CHINA - THE COLD NORTHEASTERN REGION EXPERIENCE.*

Bohlbro, H., 1969. *an investigation on the kinetics of the conversion of carbon monoxide with water vapor over Iron oxide based catalysts. 2nd Edition,* Gjellerup, Denmark: Copenhagen.

Bridgwater, A., 1995. The technical and economic feasibility of biomass gasification for power generation. *Fuel,* 74(5), pp. 631-653.

Caballero, M. A. et al., 1997. Commercial Steam Reforming Catalysts To Improve Biomass Gasification with Steam−Oxygen Mixtures. 1. Hot Gas Upgrading by the Catalytic Reactor. *Ind. Eng. Chem. Res,* 36(12), pp. 5227-5239.

Caputo, A. C., Palumbo, M., Pelagagge, P. M. & Scacchia, F., 2005. Economics of biomass energy utilization in combustion and gasification plants: effects of logistic variables. *Biomass and Bioenergy,* 28(1), pp. 35-51.

Chertow, M. R., 2000. Industrial symbiosis: literature and taxonomy. *Annual Review of Energy and the Environment,* Volume 25, pp. 313-337.

Criscuolia, A., Basilea, A., Driolia, E. & Loiaconoc, O., 2001. An economic feasibility study for water gas shift membrane reactor. *Journal of Membrane Science,* 181(1), pp. 21-27.

De Saint Jean, M., Baurens, P., Bouallou, C. & Couturier, K., 2015. Economic assessment of a power-to-substitute-natural-gas process including high-temperature steam electrolysis. *International Journal of Hydrogen Energy,* 40(20), pp. 6487-6500.

Dhole, V. R. & Linnhoff, B., 1993. Total site targets for fuel, co-generation, emissions, and cooling. *Computers & Chemical Engineering,* 17, Supplement 1(0), pp. S101 - S109.

Dhole, V. R., Ramchandani, N., Tainsh, R. A. & Wasilewski, M., 1996. Make your process water pay for itself. *Chemical Engineering,* Volume 103, pp. 100-103.

eia, 2016. *International Energy Outlook* , Washington, DC: U.S. Energy Information Administration.
ein, 2009. Prix de l'eau : la France reste bien placée en Europe. *La revue l'Eau, l'Industrie, les Nuisances,* Issue 326.

El-Halwagi, M. M., 2012. *Sustainable Design through process integration.* Waltham, USA: ELSEVIER.

El-Halwagi, M. M., Gabriel, F. & Harell, D., 2003. Rigorous Graphical Targeting for Resource Conservation via Material Recycle/Reuse Networks. *Ind. Eng. Chem. Res,* 42(19), pp. 4319-4328.

El-Halwagi, M. M., Glasgow, I. M., Qin, X. & Eden, M. R., 2004. Property integration: Componentless design techniques and visualization tools. *AIChE Journal,* 50(8), p. 1854–1869.

El-Halwagi, M. M. & Manousiouthakis, V., 1989. Synthesis of mass exchange networks. *AIChE Journal,* 35(8), pp. 1233--1244.

El-Halwagi, M. M. & Spriggs, H. D., 1998. Solve design puzzles with mass integration. *Chem Eng Prog,* 94(8), pp. 25-44.

Er-rbib, H. & Bouallou, C., 2014. Methanation catalytic reactor. *Comptes Rendus Chimie,* 17(7-8), pp. 701-706.

European Commission, 2017. *The implementation of the Circular Economy Action Plan,* Brussels: European Commission.

eurostat, 2016. *Energy price statistics.* [Online] Available at: http://ec.europa.eu/eurostat/statistics-explained/index.php/Energy_price_statistics [Accessed 2016].

Farhat, A., Zoughaib, A. & El Khoury, K., 2014. *Etude de l'extension de la méthode d'intégration énergétique de l'échelle locale à l'échelle territoriale.* Lyon France, Congres Français de Thermique 2014: Approches Multi-Échelle.

Farhat, A., Zoughaib, A. & El Khoury, K., 2015. *Heating and cooling networks design algorithm for site wide energy integration.* Pau- France, ECOS 2015 - The 28th international conference.

Fazlollahi, S. & Maréchal, F., 2013. Multi-objective, multi-period optimization of biomass conversion technologies using evolutionary algorithms and mixed integer linear programming (MILP). *Applied Thermal Engineering ,* 50(2), pp. 1504 - 1513.

Feng, W., Ji, P. & Tan, T., 2007. Efficiency penalty analysis for pure H2 production processes with CO2 capture. *AIChE Journal,* 53(1), pp. 249-261.

Floudas, C. A., Ciric, A. R. & Grossmann, I. E., 1986. Automatic synthesis of optimum heat exchanger network configurations. *AIChE Journal,* 32(2), pp. 276-290.

Floudas, C. A. & Grossmann, I. E., 1986. Synthesis of flexible heat exchanger networks for multiperiod operation. *Computers & Chemical Engineering ,* 10(2), pp. 153 - 168.

Gale, J., Herzog, H., Imo Pfaff, ,. J. B. & Kather, A., 2009. Greenhouse Gas Control Technologies 9Comparative thermodynamic analysis and integration issues of CCS steam power plants based on oxy-combustion with cryogenic or membrane based air separation. *Energy Procedia,* 1(1), pp. 495-502.

Gassner, M. & Maréchal, F., 2009. Methodology for the optimal thermo-economic, multi-objective design of thermochemical fuel production from biomass. *Computers & Chemical Engineering ,* 33(3), pp. 769-781.

Gerber, L., Fazlollahi, S. & Maréchal, F., 2013. A systematic methodology for the environomic design and synthesis of energy systems combining process integration, Life Cycle Assessment and industrial ecology. *Computers & Chemical Engineering ,* 59(0), pp. 2 - 16.

Gerber, L., Gassner, M. & Maréchal, F., 2011. Systematic integration of LCA in process systems design: Application to combined fuel and electricity production from lignocellulosic biomass. *Computers & Chemical Engineering,* 35(7), pp. 1265 - 1280.

Ghazouani, S., Zoughaib, ,. A. & Pelloux-Prayer, S., 2015. *Coupled heat and resource allocation network design considering multi-contaminants, properties and non-isothermal mixing.* Pau - France, ECOS 2015 - The 28th international conference.

González-Velasco, J. R. et al., 1992. Optimal inlet temperature trajectories for adiabatic packed reactors with catalyst decay. *Chemical Engineering Science* , 47(6), pp. 1495 - 1501.

Guana, G., Kaewpanhab, M., Haoc, X. & Abudula, A., 2016. Catalytic steam reforming of biomass tar: Prospects and challenges. *Renewable and Sustainable Energy Reviews,* Volume 58, p. 450–461.

Gundersen, T., 2013. *Heat integration: targets and heat exchanger network design, Chapitre 4. Handbook of process integration (IP): Minimisation of energy and water use, waste emissions.*. United Kingdom: Woodhead Publishing, Cambridge.

Gundersen, T., 2013. *What is Process Integration?*. Gothenburg,Sweden, International Process Integration.

Han, J. & Kim, H., 2008. The reduction and control technology of tar during biomass/pyrolysis: an overview. *Renewable and Sustainable Energy Reviews,* 12(2), p. 397–416.

Herguido, J., Corella, J. & Gonzalez-Saiz, J., 1992. Steam gasification of lgnocellulosic residues in a fluidized bed at a small pilot scale. Effect of the type of feedstock.. *Ind. Eng. Chem. Res.*, 31(5), pp. 1274-1282.

Hugo, A. & Pistikopoulos, E., 2005. Environmentally conscious long-range planning and design of supply chain networks. *Journal of Cleaner Production,* 13(15), pp. 1471 - 1491.

IEA, 2016. *Energy efficiency Market report,* Paris: International Energy Agency.

IEA, 2016. *Key world enrgy statistics*, s.l.: International Energy Agency.

IEA, I. E. A., 2015. *World Energy Outlook Special Report: Energy and Climate Change,* Paris, France: Directory of Global Energy Economics.

Jacobsa, G. et al., 2005. Low-temperature water–gas shift: impact of Pt promoter loading on the partial reduction of ceria and consequences for catalyst design. *Journal of Catalysis,* 229(2), pp. 499-512.

Jess, A., 1996. Catalytic upgrading of tarry fuel gases: A kinetic study with model components. *Chemical Engineering and Processing: Process Intensification,* 35(6), pp. 487 - 494.

Jiménez-Gutiérrez, A., Sandate-Trejo, M. d. C. & El-Halwagi, M. M., 2014. An MINLP Model that Includes the Effect of Temperature and Composition on Property Balances for Mass Integration Networks. *Processes,* 2(3), pp. 675-693.

Ji, P., Feng, W. & Chen, B., 2009. Comprehensive Simulation of an Intensified Process for H2 Production from Steam Gasification of Biomass. *Industrial & Engineering Chemistry Research,* 48(8), pp. 3909-3920.

Kazantzi, V. & El-Halwagi, M., 2005. Targeting material reuse via property integration. *Chem. Eng. Prog.*, 8(101), pp. 28-37.

Kemp, I. C., 2007. *Pinch analysis and process integration.* s.l.:ELSEVIER.

Klemeš, J. J., Varbanov, P. S. & Kravanja, Z., 2013. Recent developments in Process Integration. *Chemical Engineering Research and Design,* 91(10), pp. 2037 - 2053.

Kopyscinski, J., 2010. *Production of synthetic natural gas in a fluidized bed reactor: Understanding the hydrodynamic, mass transfer, and kinetic effects, Ph.D,* Villigen, Switzerland: Paul Scherrer institute.

Kotjabasakis, E. & Linhoff, B., 1986. Sensitivity tables for the design of flexible processes (1) — How much contingency in heat exchanger networks is cost-effective?. *Chemical Engineering Research & Design,* 64(3), pp. 197-211.

Laveissiere, S., 2012. *Les technologies de l'hydrogène au CEA,* Saclay: CEA.

Li, C. & Suzuki, K., 2009. Tar property, analysis, reforming mechanism and model for biomass gasification—An overview. *Renewable and Sustainable Energy Reviews,* 13(3), p. 594–604.

Linnhoff, B. & Flower, J. R., 1978. ynthesis of heat exchanger networks: II. Evolutionary generation of networks with various criteria of optimality. *AIChE Journal,* 24(4), pp. 642-654.

Lowe, E., 2001. *Eco-industrial Park Handbook for Asian Developing Countries,* Oakland, CA: Indigo Development.

Maréchal, F. & Kalitventzeff, B., 1998. Energy integration of industrial sites: tools, methodology and application. *Applied Thermal Engineering,* 18(11), pp. 921-933.

Milne, T. & Evans, R., 1998. *Biomass gasifier ''tars'': their nature, formation, and conversion,* Golden, Colorado, USA: National Renewable Energy Laboratory.

Molinoa, A., Chianese, S. & Musmarra, D., 2016. Biomass gasification technology: The state of the art overview. *Journal of Energy Chemistry,* 25(1), pp. 10-25.

Mondal, K. C. & Chandran, S. R., 2014. Evaluation of the economic impact of hydrogen production by methane decomposition with steam reforming of methane process. *International Journal of Hydrogen Energy,* 39(18), pp. 9670-9674.

Morar, M. & Agachi, P. S., 2010. Review: Important contributions in development and improvement of the heat integration techniques. *Computers and Chemical Engineering,* 34(8), pp. 1171-1179.
Nemet, A., Klemeš, J. J. & Kravanja, Z., 2012. Minimisation of a heat exchanger networks' cost over its lifetime. *Energy,* 45(1), pp. 264 - 276.

Noichi, H., Uddin, A. & Sasaoka, E., 2010. Steam reforming of naphthalene as model biomass tar over iron–aluminum and iron–zirconium oxide catalyst catalysts. *Fuel Processing Technology,* 91(11), p. 1609–1616.

OECD, 2015. *National Accounts at a Glance 2015,* s.l.: OECD Publishing.

Palazzi, F., Autissier, N., Marechal, F. M. & Favrat, D., 2007. A methodology for thermo-economic modeling and optimization of solid oxide fuel cell systems. *Applied Thermal Engineering ,* 27(16), pp. 2703 - 2712.

Papoulias, S. A. & Grossmann, I. E., 1983a. A structural optimization approach in process synthesis—I: Utility systems. *Computers & Chemical Engineering,* 7(6), pp. 695 - 706.

Papoulias, S. A. & Grossmann, I. E., 1983b. A structural optimization approach in process synthesis—II: Heat recovery networks. *Computers & Chemical Engineering,* 7(6), pp. 707 - 721.

Piemonte, V., De Falco, M., Favetta, B. & Basile, A., 2010. Counter-current membrane reactor for WGS process: Membrane design. *International Journal of Hydrogen Energy,* 35(22), pp. 12609 - 12617.

Ponce-Ortega, J. M., Hortua, A. C., El-Halwagi, M. & Jiménez-Gutiérrez, A., 2009. A property-based optimization of direct recycle networks and wastewater treatment processes. *AIChE Journal,* 55(9), pp. 2329-2344.

Savelski, M. J. & Bagajewicz, M. J., 2001. Algorithmic procedure to design water utilization systems featuring a single contaminant in process plants. *Chemical Engineering Science ,* 56(5), pp. 1897 - 1911.

Shelley, M. D. & M. El-Halwagi, M., 2000. Component-less design of recovery and allocation systems: a functionality-based clustering approach. *Computers & Chemical Engineering ,* 24(9-10), pp. 2081 - 2091.

Shi, H., Chertow, M. & Song, Y., 2009. Developing country experience with eco-industrial parks: a case study of the Tianjin. *Journal of Cleaner Production,* 18(3), pp. 191-199.
Stahl, R. et al., 2004. *Definition of a standard biomass,* Germany: Forschungszentzrum Karlsruhe GmbH.

Sutton, D., Kelleher, B. & Ross, J., 2001. Review of literature on catalysts for biomass gasification. *Fuel Processing Technology,* Volume 73, pp. 155-173.

Taylor, R., Howes, J. & Bauen, A., 2009. *Review of Technologies for Gasification of Biomass and Wastes, Final report,* London, UK: NNFCC, E4Tech.

Townsend, D. W. & Linnhoff, B., 1983. Heat and power networks in process design. Part II: Design procedure for equipment selection and process matching. *AIChE Journal,* 29(5), pp. 748-771.

Trambouze, P., Van Landeghem, H. & Wauquier, J. P., 1984. *Les réacteurs chimiques.* Paris: Techinp.
Trambouze, P., Vanlandeghem, H. & Wauquier, J. L., 1984. *Les réacteurs chimiques [Book]*. Paris: Technip.

UN, U. N., 2017. *World Population Prospects,* New York: Department of Economic and Social Affairs.

Van Der Sluijs, J., Hendriks, C. & Blok, K., 1992. Feasibility of polymer membranes for carbon dioxide recovery from flue gases. *Energy Conversion and Management,* 33(5-8), pp. 429-436.

Vienna university of Technology, 2012. *Du Biogaz au biomethane,* Austria: Bio-methane regions.
Vivanpatarakij, S., Rulerkb, D. & Assabumrungrat, S., 2014. Removal of Tar from Biomass Gasification Process by Steam Reforming over Nickel Catalysts. *CHEMICAL ENGINEERING TRANSACTIONS,* Volume 37, pp. 2283-9216.

Wang, Y. & Smith, R., 1994. Wastewater minimisation. *Chemical Engineering Science,* 49(7), pp. 981 - 1006.

Xu, C., Donald, J., Byambajav, E. & Ohtsuka, Y., 2010. Recent advances in catalysts for hot-gas removal of tar and NH3 from biomass gasification. *Fuel,* 89(8), p. 1784–1795.

Résumé

L'objectif principal de ce travail de thèse est d'aider les industries géographiquement voisines à évoluer vers un éco-parc industriel. En effet, l'économie circulaire, qui est régénératrice par conception par opposition au modèle linéaire extractif dominant, prend de l'ampleur comme un de moyens pour la migration vers un paradigme de développement durable. De nombreux travaux ont été menés pour évaluer la faisabilité des réseaux de chauffage basés sur la récupération de chaleur industrielle et de manière similaire pour la réutilisation et le recyclage de la matière afin de proposer des options techniques pour une meilleure efficacité énergétique et de gestion de ressources que ce soit à l'échelle de procédé ou au niveau territorial. Cependant, les procédés de conversion créent de nouvelles opportunités de valorisation pour les flux d'énergie ou de matière, jugés non-utilisables, tel qu'ils existent, par les techniques actuelles d'intégration de procédé. En effet, en les transformant en nouveaux produits récupérables ils peuvent être réintroduits dans le cycle de production.

Dans cette perspective, deux nouveaux cadres méthodologiques, pour intégrer les procédés de conversion aux problèmes d'intégration matière et énergie dans des territoires à gouvernance coopératives et non coopératives, ont été proposés dans cette thèse. L'application des méthodologies proposées conduit sur un parc industriel réaliste à démontrer des économies substantielles de coûts d'exploitation tout en améliorant l'économie circulaire du parc. Le flux non-utilisable du parc étudié est le bois déchet pour lequel trois voies de conversion ont été mis en compétition: la conversion du bois en hydrogène, en méthane et la cogénération.

Mots Clés

Ecologie industrielle, Eco-parc industriel, Intégration des procédés, Conception des procédés, Systèmes multi-agents, Procédé de conversion.

Abstract

The prime objective of this doctoral work is to assist geographically neighboring industries to evolve towards becoming an eco-industrial park (EIP). Indeed, circular economy, which is regenerative by design as opposed to the prevailing extractive linear model, is gaining momentum as an answer for migrating towards a sustainable paradigm. Many literature studies were conducted to assess the feasibility of heating networks based on industrial heat recovery and similarly for material reuse and recycling aiming to propose technical options for better energy efficiency and resource use whether on the process scale or on a larger inter-sites level. However reacting conversion systems create new valorization opportunities for the energy or material streams, adjudicated as non-usable by conventional process integration techniques, through converting them into new recoverable products and thus reintroducing them back into the production cycle.

In this perspective, two novel conceptual frameworks, for incorporating reacting thermodynamic conversion systems to the material and energy integration problems in both cooperative and non-cooperative schemes, were proposed in this doctoral dissertation. The application of the proposed methodological frameworks on a realistic industrial park demonstrated how to implement conversion processes in a territory that reinsert streams judged to be non-recoverable by conventional on-site and inter-site energy and material integration techniques ensuing substantial operating costs savings and enhancing the park's circular economy. The non-usable stream in the investigated park is woody biomass for which three conversion routes were challenged being the wood to hydrogen, methane production and cogeneration.

Keywords

Industrial Ecology, Eco-Industrial Park, Process Integration, Process Design, Multi-agent systems, Reacting Conversion Systems